COMPARISON AND CHARACTERISATION OF RIBOZYME DELIVERY IN CULTURED GLIAL AND NEURONAL CELLS *IN VIVO* AND *IN VITRO*

QAMAR NAWAZ

Doctor of Philosophy

ASTON UNIVERSITY

APRIL 2003

ASTON UNIVERSITY

COMPARISON AND CHARACTERISATION OF FREE AND POLYMER ENTRAPPED RIBOZYME DELIVERY IN CULTURED GLIAL AND NEURONAL CELLS *IN VITRO* AND *IN VIVO*

QAMAR NAWAZ

2003

SUMMARY

Ribozymes are short strands of RNA that possess a huge potential as biological tools for studying gene expression and as therapeutic agents to down-regulate undesirable gene expression. Successful application of ribozymes requires delivery to the target site in sufficient amounts for an adequate duration. However, due to their large size and polyanionic character ribozymes are not amenable to transport across biological membranes. In this study a chemically modified ribozyme with enhanced biological stability, targeted against the EGFR mRNA has been evaluated for cellular delivery to cultured glial and neuronal cells with a view to developing treatments for brain tumours.

Cellular delivery of free ribozyme was characterised in cultured glial and neuronal cells from the human and rat. Delivery was very limited and time dependent with no consistent difference observed between glial and neuronal cells in both species. Cellular association was largely temperature and energy-dependent with a small component of non-energy dependent association. Further studies showed that ribozyme cellular association was inhibited with self and cross competition with nucleic and non-nucleic acid polyanions indicating the presence of cell surface ribozyme-binding molecules. Trypsin washing experiments further implied that the ribozyme binding surface molecules were protein by nature. Dependence of cellular association on pH indicated that interaction of ribozyme with cell surface molecules was based on ionic interactions. Fluoresence studies indicated that, post cell association, ribozymes were sequestered in sub-cellular vesicles. South-Western blots identified several cell surface proteins which bind to ribozymes and could facilitate cellular association.

The limited cellular association observed with free ribozyme required the development and evaluation of polylactide-co-glycolide microspheres incorporating ribozyme for enhanced cellular delivery. Characterisation of microsphere mediated delivery of ribozyme in cultured glial and neuronal cells showed that association increased by 18 to 27-fold in all cell types with no differences observed between cell lines and species. Microsphere mediated delivery was temperature and energy dependent and independent of pH.

In order to assess the potential of PLGA microspheres for the CNS delivery of ribozyme the distribution of ribozyme entrapping microspheres was investigated in rat CNS after intracerebroventricular injection. Distribution studies demonstrated that after 24 hours there was no free ribozyme present in the brain parenchyma, however microsphere entrapped ribozyme was found in the CNS. Microspheres remained in the ventricular system after deposition and passed from the lateral ventricles to the third and fourth ventricle and in the subarachnoid space. Investigation of the influence of microsphere size on the distribution in CNS demonstrated that particles up to 2.5 and 0.5μm remained in the ventricles around the choroid plexus and ependymal lining.

Key words: hammerhead ribozyme, exogenous delivery, Polylactide-co-glycolide, microspheres, sustained release, CNS delivery.

DEDICATION

To my dear grandmothers,

for always praying for my well being and success.

LIST OF CONTENTS

LIST OF FIGURES

LIST OF TABLES

LIST OF ABBREVIATIONS

A,G,C,T,U	Adenine, Guanine, Cytidine, Thymidine, Uridine
AE	Adsorptive endocytosis
AIDS	Acquired immune deficiency syndrome
ATP	Adenosine triphosphate
BBB	Blood brain barrier
cf	Compared with
CSF	Cerebrospinal fluid
°C	Degrees Celsius
cm, mm, μm	centimetre, millimetre, micrometre
CMV	Cytomegalovirus
CNS	Central nervous system
Cpm	Counts per minute
ddATP	Dideoxy adenosine triphosphate
DEPC	Diethyl pyrocarbonate
DMEM	Dulbecco's modified eagle's medium
DMSO	Dimethyl sulphoxide
DMTT	Dimethoxytrityl
DNA	Deoxyribonucleic acid
DNAse	Deoxyribonuclease
DOPE	Dioelylphosphatidylethanolamine
DTT	Dithiothreitol
EDTA	Ethylenediaminetetraacetate
EGFr	Epidermal growth factor receptor
EVAc	Ethylene-co-vinyl acetate
FBS	Foetal bovine serum
FCS	Foetal calf serum
FDA	Food and Drug Agency
FITC	Fluorescein isothiocyanate
FPE	Fluid phase endocytosis
g, mg, μg	gram, milligram, microgram
HIV	Human immuno-deficiency virus

IC	Intra-cerebral
ICV	intra-cerebroventricular
i.m.	intra-muscular
i.p.	intra-peritoneal
i.v.	intravenous
KCl	Potassium chloride
kDa	Kilo-Daltons
L, mL, μL	Litre, millilitre, microlitre
LSC	Liquid scintillation counting
μCi	Micro Curies
mol, mmol	mole, millimole
μmol, nmol	Micromole, nanomole
M	Molar
mRNA	Messenger-ribonucleic acid
MW	Molecular weight
NGF	Nerve Growth Factor
nmol, pmol	Nanomoles, picomoles
O.D	Optical density
ODN	Oligodeoxynucleotide
PAGE	Polyacrylamide gel electrophoresis
PBS	Phosphate buffered saline
PCL	Poly(ε-caprolactone)
PLGA	Polylactide-co-glycolide
PNK	Polynucleotide kinase
PO	Phosphodiester
PS	Phosphorothioate
PVA	Poly(vinyl alcohol)
RBZ	Ribozyme
RNA	Ribonucleic acid
rpm	Revolutions per minute
s.c.	subcutaneous
SD	Standard deviation
SEM	Scanning electron microscope

TBE	Tris-borate-EDTA buffer
Tris	Tris(hydroxymethyl)amino methane
UV	ultraviolet light
v/v	volume per volume
w/o/w	water-in-oil-in-water
w/v	weight per volume
w/w	weight per weight

CHAPTER ONE

GENERAL INTRODUCTION

1.1. Ribozymes, catalytic ribonucleic acids

During the study of the RNA processing in the early Nineteen eighties it was discovered that RNA along with being a carrier of genetic information also had the capability to cleave RNA strands. Kruger *et al.*, (1982) observed, *in vitro*, that an intron present in the ribosomal RNA precursor from *Tetrahymena thermophila* was capable of excising itself without any energy source or enzyme. This was followed by a second report in which it was shown that the RNA component of RNAase P from *Escherichia coli* was able to process tRNA precursors without any protein factors (Gurerrier-Takada *et al.*, 1983). In order to describe these RNA motifs with catalytic properties the term ribozyme was coined; *ribo* derived from ribonucleic acids and *zyme* from enzyme, which are the two characteristics of these molecules. Ribozymes by definition are short single strands of RNA which posses catalytic activity to cleave or splice a given mRNA (Uhlenbeck, 1987).

These pioneering reports stimulated extensive research in the area of RNA catalysis and to date several different RNA motifs possessing catalytic properties have been discovered. For reviews see Puerta-Fernandez *et al.*, (2003); Phylactou, (2000); Sun *et al.*, (2000); Tanner, (1999) and Rossi, (1998). Initially characterised as *cis-acting* catalytic molecules, it was subsequently shown that ribozymes could be modified to act in *trans*. Haseloff and Gerlach, (1998) demonstrated that the hammerhead ribozyme can be resolved into a substrate and a catalytic strand (ribozyme) which cleaves the substrate. This fundamental observation led to the hope that ribozymes can be potentially used to selectively cleave any target mRNA. Since then ribozymes have been successfully used as biological tools for gene function analysis and as potential targeted therapeutics for the inhibition of undesirable genes.

Ribozymes are categorised into two classes based on their size and reaction mechanisms. The large catalytic RNAs consist of group I, II and RNaseP and mainly carry out self-splicing catalytic reactions. In contrast, small ribozymes consist of hammerhead, hairpin, hepatitis

delta and VS RNA and catalyse self-cleavage reactions. Below is a brief overview of these various motifs with the exception of the hammerhead, which is discussed in depth, as it is the subject of this thesis.

1.1.1. Group I introns.

These motifs range in size from a few hundred nucleotides to around 3000 and are mainly found in fungal, plant mitochondrion, bacteriophages and eukaryotic viruses. These ribozymes are introns, non-coding sequences that interrupt the coding sequences of genes, which have the capability of self-splicing (auto-excision) from the mRNA before translation begins. This auto-excision involves a two-step trans-esterification reaction in the presence of a divalent metal ion. The substrate specificity of group 1 introns is determined by a sequence called the internal guide sequence within the intron, which can be modified to work in trans. A trans acting group 1 intron can be potentially used as a therapeutic molecule for correcting aberrant mRNAs as demonstrated in a study in which a Group I intron was successfully used to correct a truncated LacZ transcript in *Eschericia coli* (Sullenger and Cech, 1994). For a brief review see Phylactou, (2000).

1.1.2. Group II introns

These range in size from several hundred to around 2500 nucleotides and in comparison to group I introns are much less widely distributed (Bonen and Vogel, 2001; Jacquier, 1996; Michel and Ferat, 1995). These occur in mitochondria and chloroplasts of fungal and plant cells. This class of ribozymes are less studied because their mode of action requires non-physiological conditions (100mM $MgCl_2$, 500mM $(NH_4)_2SO_4$ and 45°C). There are no reports in published literature on the use of group II introns in any model system to evaluate their potential as a therapeutic ribozyme. For a review see Fedorova *et al.*, (2002)

1.1.3. RNaseP

Ribonuclease P (RNAase P) is found in all living cells, which process 5' termini of tRNA precursors and is the only ribozyme, which in its unmodified form can act *in trans* on multiple substrates (For reviews see Cobaleda and Sanchez-Garcia, 2001; Kurz and Fierke,

2000; Darr *et al.*, 1992; Altman *et al.*, 1993). Most RNaseP ribozymes exist as a complex with a protein and the presence of this protein component is an essential requirement for the action of this ribozyme *in vivo*. However, the RNA component from RNaseP of certain organisms possesses catalytic activity under high salt conditions without the presence of protein. The exact mechanism of action of these ribozymes is not clear and there seems to be no important primary sequence requirements for the action of RNaseP. The substrate recognition by RNaseP is largely based on tertiary interactions with the substrate. RNaseP has been successfully adapted to inactivate the thymidine kinase mRNA from Herpes simplex virus (Liu and Altman, 1995) and IE1-2 mRNA of human cytomegalovirus (Trang *et al.*, 2002).

1.1.4. Hairpin

Hairpin ribozymes are found in plant pathogenic satellite viruses associated with tobacco ringspot virus, chicory yellow mottle virus and arabis mosaic virus (Walter and Burke, 1998). Due to the three-dimensional arrangement of the stems in this ribozyme motif it is called a hairpin (Fay *et al.*, 2001). The mechanism of action of this motif is still not clear. However, like other catalytic RNAs, hairpin ribozymes can only function in the presence of divalent cation Mg^{2+} (Hampel and Cowan, 1997). The hairpin ribozyme has been successfully adapted to work *in trans* and its potential as an anti-HIV therapeutic agent has been demonstrated *in vitro* (Earnshaw *et al.*, 2001; Feng *et al.*, 2000). A hairpin ribozyme has been recently used as a tool for the identification of novel targets for the treatment of neurodegenerative diseases (Rhoades and Wong-Staal, 2003). For a review see Fedor, (2000).

1.1.5. VS RNA

This motif is found in RNA transcribed from the plasmid of a certain strain of *Neurospora* (Kennell *et al.*, 1995) and compared to all the self-cleaving RNAs the properties of this ribozyme are most poorly understood. As with RNaseP, the ribozyme seems to recognize the structure of the substrate largely as a helical domain without any sequence requirements (Zamel and Collins, 2002) (for a review see Lafontaine *et al.*, 2002). There are no reports of its therapeutic use in the literature.

1.1.6. Hepatitis Delta virus

The hepatitis delta virus (HDV) is a viroid like satellite virus of the hepatitis B virus (Been and Wickham, 1997) and is sometimes referred to as the "axehead" ribozyme. The genomic and anti-genomic, both strands have catalytic domains. HDV has not been studied extensively because of the difficulty in of obtaining high activity with the trans-cleaving forms.

1.2.0. Hammerhead ribozyme

Of all the various motifs of ribozymes the hammerhead is the most well characterised motif possibly due to its common occurrence and small size (Symons, 1994). Its smaller size (40-50 nucleotides in length) also makes it more amenable to mechanistic investigation and synthesis via automated, solid state chemistry (Wincott *et al.*, 1995; Usman and Stinchcomb, 1996). It is named hammerhead because its Australian discoverers found the secondary structure, as originally drawn, to be reminiscent of the head of a hammerhead shark. The hammerhead ribozyme was originally discovered as a self-cleaving RNA molecule in certain plant viroids and satellite RNAs (Symons, 1992) and there are several reviews, which describe the structure, function and potential utility of this RNA molecule (Phylactou, 2000; Fritz *et al.*, 2002; Butcher, 2001; Amarzguioui and Prydz, 1998; Engels *et al.*, 1998; Birikh *et al.*, 1997).

1.2.1. Structure of the hammerhead

Several attempts have been made to determine the overall global conformation and detailed atomic structure of the ribozyme using a variety of experimental techniques. These include electrophoretic mobility (Bassi *et al.*, 1995, 1996), electrical birefringence (Amiri and Hagerman, 1996), fluorescence resonance energy transfer (Tuschl *et al.*, 1995) and X-ray diffraction (Pley *et al.*, 1994). The hammerhead ribozyme, which is composed of a short single strand of RNA, can be described as a molecule, which has three helices (stems I, II and III), a conserved central core and a stem II-loop as shown in figure 1.1. Stems I and III form the hybridising arms of the ribozyme and are essential for substrate recognition whereas Stem II is connected to the catalytic core and has a loop at its terminal end. The 3-D structure of the hammerhead ribozyme can be visualised as a wishbone or Y shape with stems I and II

at the arms and the stem III at the base (Sigurdsson and Eckstein, 1995; Scott and Klug, 1996).

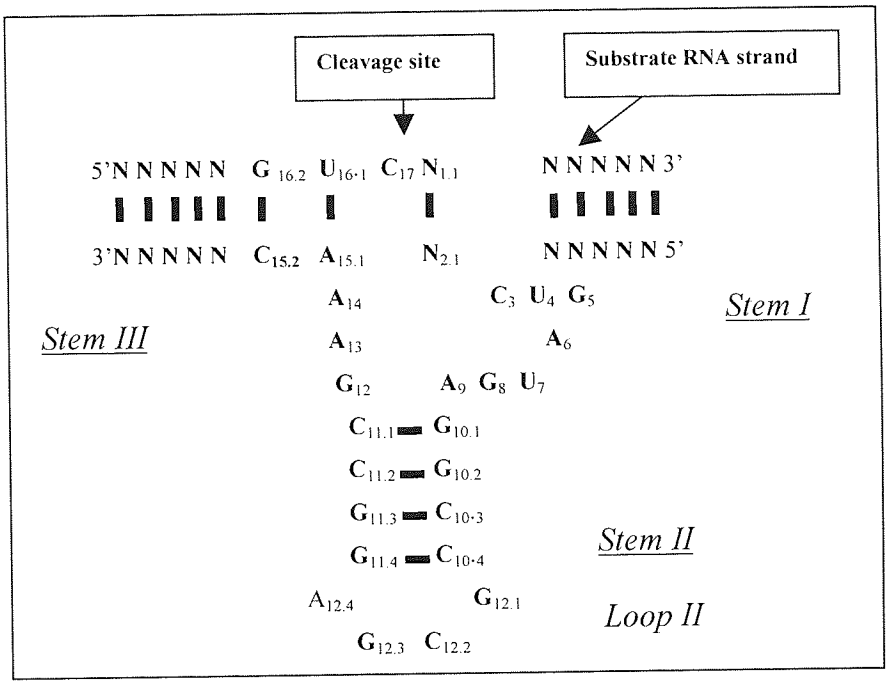

Figure 1.1. *Schematic representation of the hammerhead ribozyme in complex with its complementary substrate. The ribozyme forms helix I with its 5'arm and the substrate, helix III with its 3'arm and the substrate, and helix II with nucleotides joining A_9 and G_{12}. In the ribozymes all the nucleotides except for conserved C_3 to A_9 and G_{12} and $A_{15.1}$ can be chemically modified. A downward arrow shows the site of cleavage. The subscripts next to the letters for the nucleotides denote the standard numbering system introduced by Hertel et al., (1992) for the Haseloff and Gerlach, (1998) classic hammerhead ribozyme.*

In order to facilitate comparison of data from different laboratories, a uniform numbering system for nucleotides was introduced by Hertel *et al.*, (1992) as shown in figure 1.1. In the central core, nucleotides G_5, A_6, G_8, G_{12} and $A_{15.1}$ are deemed conserved nucleotides of the catalytic core and are essential for the catalytic activity of the hammerhead and any change in these nucleotides completely destroys the catalytic activity (Ruffner and Uhlenbeck, 1990). These conserved central bases do not form normal Watson-Crick base pairs but instead form more complex structures, which mediate RNA folding and catalysis.

1.2.2. Divalent ion requirement

Although evidently different in size, structure and mechanism of action, a common feature of all the different ribozyme motifs is that they act as metalloenzymes . Divalent metal ions are considered essential for the functioning of the ribozymes as they not only stabilise the tertiary structure and but also participate in the catalytic reaction mechanism (Hanna and

Doudna, 2000; Bratty *et al.*, 1993). The most commonly used cation is the Mg^{2+} but other ions such as Mn^{2+}, Ca^{2+}, Co^{2+}, and to a lesser degree Sr^{2+} and Ba^{2+} can also support catalysis.

1.2.3. Reaction mechanism

Despite the small size and extensive investigations the exact mechanism of hammerhead catalysis still remains ambigous (for a review see DeRose, 2002). Generally, the hammerhead ribozyme catalyses a trans-esterification reaction by cleaving the 3'-5' phosphodiester bond between adjacent nucleotides, forming a cyclic 2'3' phosphodiester on one nucleotide and free 5' hydroxyl on the other nucleotide (figure 1.2). According to Scott and Klug, (1996), the proposed mechanism of action begins with deprotonation of the 2' sugar at the 3' side of the cleavage site by the magnesium-aqua-hydroxy complex. This results in a nucleophilic attack by the resultant 2'-alkoxide on the adjacent phosphodiester bond and subsequently protonation of the 5'-oxyanion leaving group, generating a 2'3'-cyclic phosphate and a 5'-hydroxyl group.

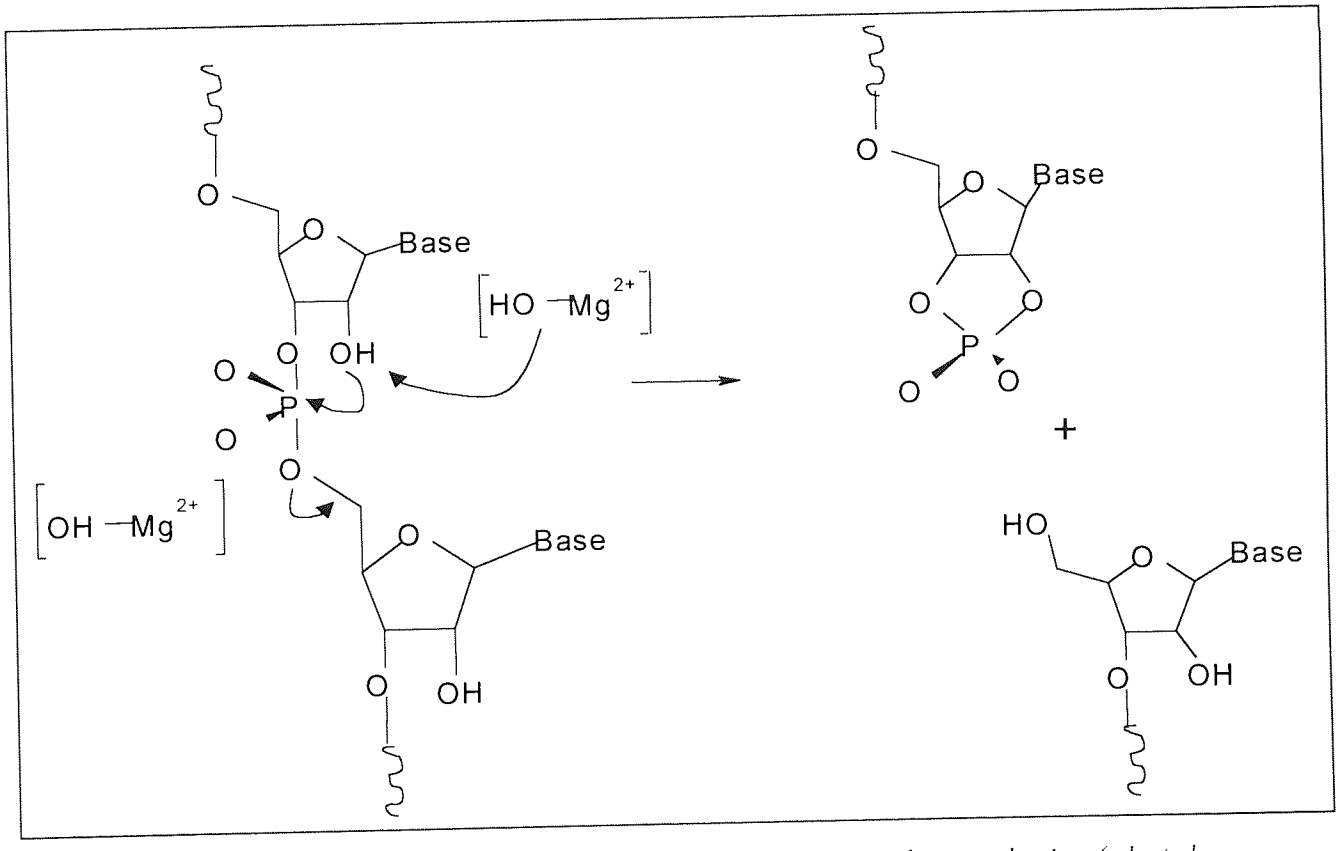

Figure 1.2. *A schematic representation of the hammerhead ribozyme catalytic mechanism (adapted from Dahm et al., 1993).*

1.2.4. Sequence requirements of hammerhead

In order for the ribozyme to function it is a necessary requirement that the substrate possesses a specific triplet in its sequence. Several researchers have reported different cleavage triplets, GUC (Keese *et al.*, 1983), GUA (Miller *et al.*, 1991) with the most commonly found triplet being GUC. These observations led to the NUX rule. In this rule N is any base, U is Uracil and X is any base except G (Zoumadakis and Tabler, 1995). Investigation of the twelve possible combinations of the NUX motifs, showed that the ribozyme has a strong preference for C as the third nucleotide and for A or G as the first nucleotide (Shimaya *et al.*, 1995).

1.2.5. Ribozyme functional strategy

A generalised representation of the ribozyme strategy is given in figure 1.3. As the diagram shows the first step in the action of ribozymes is the co-localisation of the ribozymes with the target mRNA, which is the substrate molecule. Stems I and III of the ribozyme hybridise with the nucleotides on either side of the substrate cleavage site.

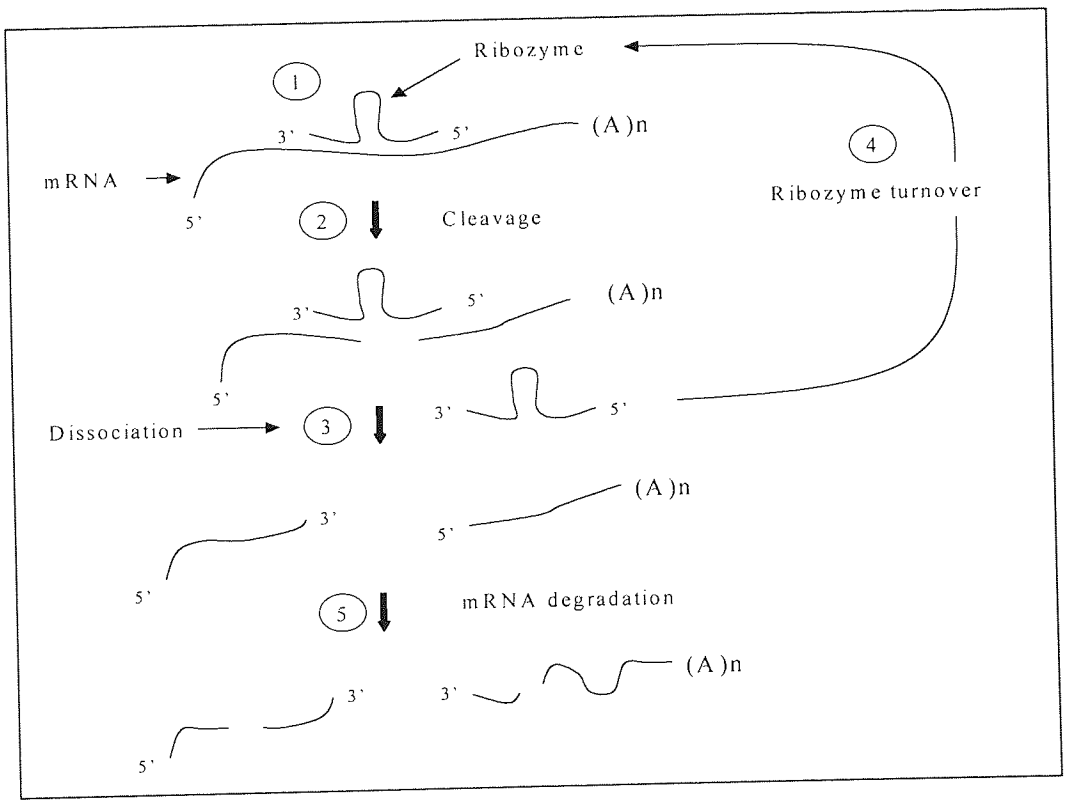

Figure 1.3. *A schematic representation of the hammerhead ribozyme strategy. Adapted from Sioud and Leirdal, (2000).*

In the presence of a divalent metal ion such as magnesium Mg^{2+}, it adopts a reactive conformation and positions itself to cleave the target (step 2) with a reaction mechanism as described in section 1.2.3. In step 3 after the cleavage of the target the ribozyme dissociates itself from the cleaved fragments and ribozyme makes itself available to hybridise with another molecule (step 4). The step 5 shows further degradation of the cleaved fragments by the cellular ribonucleases.

1.3.0. Ribozyme delivery strategies

In order to utilise ribozymes to down-regulate the expression of any gene it is important that the ribozyme is delivered inside the cells to cleave the target mRNA. In this regard, the ribozyme has to permeate through biological membranes such as the cell membrane and endosomal membranes to co-localise with the mRNA. In this section an overview of the various strategies employed for the cellular delivery of ribozymes is presented (for reviews see Hughes *et al.*, 2001; Akhtar *et al.*, 2000). These delivery strategies can be broadly divided in to two principal categories, exogenous and endogenous as schematically described in figure 1.4.

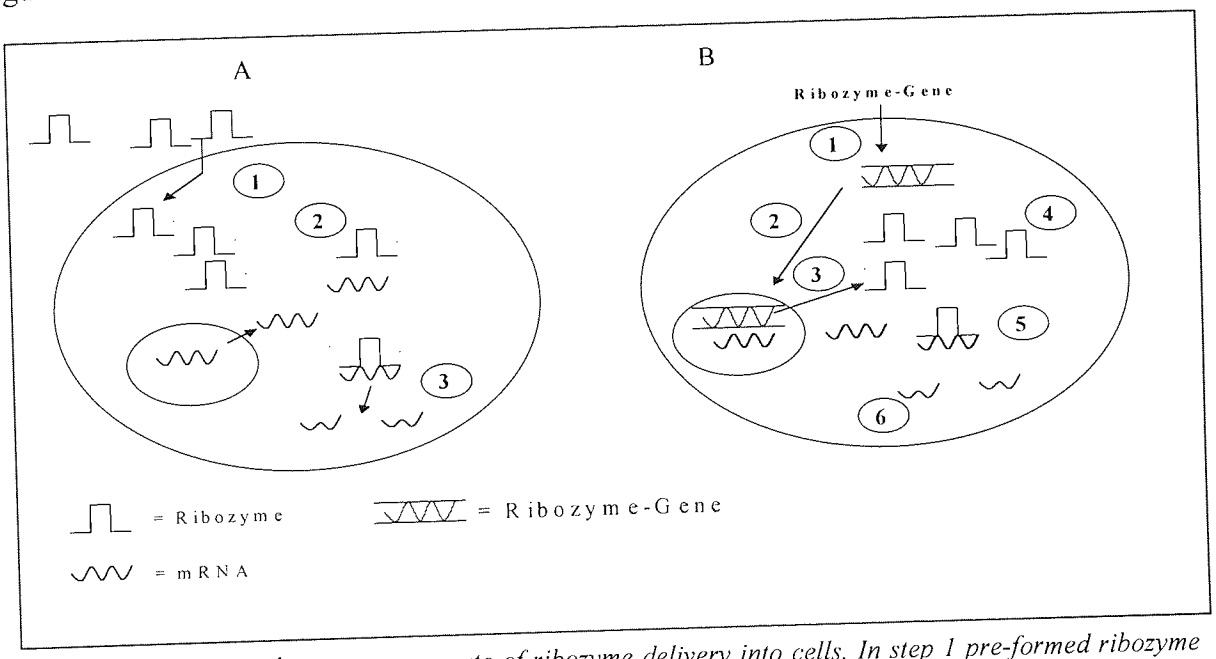

Figure 1.4. *A: shows the exogenous route of ribozyme delivery into cells. In step 1 pre-formed ribozyme enters into the cell, 2 shows binding of ribozyme to mRNA, 3 shows the cleavage step. In the second approach, which is shown in B; shows the endogenous route. In step 1 a vector construct bearing the ribozyme gene is inserted into the cell. In step 2 the gene is integrated into the host genome. In 3 the gene is transcribed which is shown expressed in 4. In 5 the ribozyme hybridises to the target mRNA. Step 6 shows the cleavage.*

1.3.1. Endogenous delivery

In this strategy the ribozyme is produced from within the cell by inserting a gene encoding the ribozyme into the target cell using a vector as shown in figure 1.4B. This vector can either be a plasmid or a virus containing a suitable promoter, which uses the transcriptional machinery of the cell to express the gene in to a ribozyme. The level and duration of ribozyme expression in the cell can be controlled by selecting a suitable promoter and type of vector. To date three types of viral vectors namely retroviruses, adenoviruses and adeno-associated virus have been used in different studies (reviewed by Lorens *et al.*, 2001; Altman, 1993; Sullivan, 1994). Retroviruses and adeno-associated viruses result in stable transfection whereas use of adenoviruses results in transient transfection of the gene. At present retroviral vectors are the most utilized for delivering ribozymes into cells because of high transduction efficiency and stable integration into the host cell genome. A critical limitation is the inability, with the exception of Lentiviruses, to infect non-dividing cells because the pre-integration complex cannot migrate to the nucleus in the absence of mitosis (Bramlage *et al.*, 1998). However, retroviruses have several disadvantages including a limited tropism, low viral titre and the potential generation of replication competent virus during packaging.

Adenoviruses are DNA viruses which exist in the host cell in an extra-chromosomal form and provide only transient transfection of the gene and have been evaluated for the delivery of ribozymes (reviewed by Ali *et al.*, 1994). It is suggested that these viruses should only be used for the treatment of non-life-threatening acute diseases (Birikh *et al.*, 1997). In comparison to the retroviruses the adenoviruses have high transfection efficiency and therefore produce high expression levels of the ribozymes. Adeno-virus vectors are easy to produce in high titre and purity and infect a wide variety of dividing and non-dividing cells (Lewin and Hauswirth, 2001). Nonetheless, recombinant adenovirus provokes both humoral and cell-mediated immune responses that restrict its usefulness for human therapy (Chirmule, 2001). Finally, the endogenous strategy has two disadvantages, firstly, only unmodified ribozyme is produced in the cell and secondly, the integration of the vector into the host genome is a non-specific process raising the possibility of interruption of important gene sequences or activation of oncogenes. For this reason, much research is being undertaken to develop an efficient exogenous delivery system for nuclease stable synthetic ribozymes.

Following is a selective table of recent studies in which ribozymes were delivered endogenously.

Table 1.1. A selective account of endogenous delivery studies.

Ribozyme/ Delivery Vector	**Target mRNA**	***In vitro/vivo.* Disease Model/Biological tool**	**Result**	**Reference:**
Hammerhead Plasmid Electroporation	Caspase-3	*In vitro* Model of Parkinson's Disease	42% reduction in mRNA, protein reduced by 40% compared with control	(Xu *et al.*, 2001)
Hammerhead Plasmid & adenovirus mediated.	Neuronal nitric oxide synthase mRNA	Biological tool for studying neuronal gene expression	50% reduction in endogenous NOS mRNA with adenoviral delivery. Plasmid delivery reduced target by 48-82%.	(Maniotis *et al.*, 2002)
Hammerhead Plasmid/ Lipofection	VEGF 189	*In vitro/ ex-vivo* model of tumorigenesis	mRNA reduced to 9.6% compared with control which was 51.5%. No tumours formed in ribozymes transfected cells compared with controls.	(Oshika *et al.*, 2000)
Hammerhead Plasmid/ Lipofection	VPAC1 (G-Protein coupled receptor)	*In vitro* biological tool	mRNA reduced (qualitatively). 50-75% reduction in ligand binding. VIP induced intracellular signalling suppressed by 75%.	(Jabranne-Ferrat *et al.*, 2000)
Hammerhead Adenovirus	Bcl-2	*In vitro* and in vivo model of smooth muscle hyperplasia	mRNA and protein levels reduced but no quantitative analysis given. Reduced hyperplasia after carotid artery in vivo. Aberrations in cell cycle programme	(Perlman *et al.*, 2000)
Hammerhead Plasmid Transfection with Calcium Phosphate precipitation	Caspase-3	*In vitro* model of neuronal apoptosis	mRNA reduced by 13% compared with control. Caspase-3 protein levels also reduced along with the activity (~67%). Apoptosis was significantly reduced.	(Eldadah *et al.*, 2000)
Hammerhead Plasmid Lipofection	mutant type1 Collagen	*In vitro* model of Osteogenesis imperfecta	mRNA suppressed by ~50%. Mutant collagen was significantly reduced. Transfectant cells had similar growth to the controls.	(Dawson and Marini, 2000)

Hammerhead Plasmid Lipofection	mutant RET	*In vitro* model of Medullary thyroid carcinoma	Significant reduction (83%) in colony formation. 60% reduction in mRNA.	(Parthasarthy *et al.*, 1999)
Hammerhead Plasmid Lipofection	Estrogen Receptor-α	*In vitro* model of Estrogen dependent mammary tumour	80% reduction in mRNA. Progression of quiescent cells was inhibited after exposure to Estrogen by the ribozymes.	(Lavrovsky *et al.*, 1999)
Hammerhead Plasmid Lipofection	Murine Tumour necrosis factor-α	*In vitro* model of inflammatory conditions	Reduction of mRNA and protein levels significantly. No quantitative values given.	(MacKay *et al.*, 1999)
Hammerhead tRNA expression cassette-retrovirus	Neuregulin-1 mRNA (NRG-1)	*In vivo & vivo* model to assess the function of NRG-1	45% inhibition of mRNA. At 90 hours postinjection there was deformation in the heart muscle. Inhibition of development and proliferation of retinal cells.	(Zhao and Lemke, 1998)
Hammerhead Viral vector	N-*ras* mRNA	*In vitro* model for cancer therapeutics	60% inhibition in target mRNA	(Engels *et al.*, 1998)
Hammerhead Adenovirus	c-myb	*In vivo* model of restenosis	Cell proliferation was inhibited twofold compared with control. mRNA level reduced by >90%.	(Macejak *et al.*, 1999)

1.3.2. Exogenous delivery

The second strategy for the cellular delivery of ribozymes is schematically represented in figure 1.4A. In this strategy preformed ribozymes are introduced into cells to specifically cleave target mRNAs. This strategy is far more flexible than the endogenous approach as it has a number of advantages over the endogenous strategy. These include introduction of chemically modified nuclease resistant ribozymes, potential for enhancing cellular association, control of pharmacokinetics and pharmacodynamics, no risk of adverse effect on the genome such as interruption of coding sequences or activation of proto-oncogenes as the ribozymes are not integrated in the genome and can be considered as a form of chemotherapy, low cytotoxicity, low risk of side-effects as ribozymes have high target specificity, option of immediate withdrawal of treatment if severe side-effects develop and finally localised delivery to tissues such as tumours and inflammatory sites.

Hammerhead ribozymes are ideal candidates for exogenous delivery due to their relative smaller size and the recent availability of nuclease resistant ribozymes but in comparison to other conventional drug molecules, ribozymes, which generally are 30 to 40 nucleotides in length are large polyanionic molecules. Their highly polar nature reduces their ability to traverse biological membranes. As a result the delivery of free ribozymes is a highly inefficient process for cellular uptake of ribozymes (Fell *et al.*, 1997; Bramlage *et al.*, 1999). In order to overcome this limitation and improve the uptake of exogenously delivered ribozymes several strategies have been investigated for use in delivering ribozymes. An account of these strategies is given below:

As shown in the section 1.4.1.1 various modifications can be made to the functional groups present on the ribozymes to increase the lipophilicity of these molecules in order to enhance their membrane permeability. In this regard the 2' position on the ribose sugar has been exploited for increasing the lipophilicity of the ribozyme by adding hydrophobic groups such as allyl instead of the hydroxyl group on the ribose sugar (Lyngstadaas *et al.*, 1995). Another option of increasing lipophilicity is the addition of cholesterol at the 3'-end. It is thought that this should result in an increase in uptake as there is an increase in adsorption of the ribozymes via hydrophobic interactions with the cell membrane or mediated via the low density lipoprotein receptor.

Another extensively investigated delivery system is liposomes, which are micron sized small spheres of phospholipid bilayer, which can either encapsulate nucleic acids within the aqueous core or form lipid-nucleic acid complexes protecting them from nuclease attacks. Liposomes are broadly categorised into cationic, neutral and anionic based on the type of lipid used in their formulation. Although anionic and neutral liposomes have been studied for nucleic acid delivery their poor encapsulation efficiencies has prevented their widespread use (for a recent review see Tari, 2000). Cationic liposomes, due to their positive charge have not only high encapsulation efficiencies but also have high affinity for cell membranes that are negatively charged under physiological conditions. As a result cationic liposomes and lipoplexes (cationic lipid-nucleic acid complexes) have shown far greater success in achieving biological effects in cell culture systems. An important prerequisite for the effective utilisation of cationic lipids for nucleic acid delivery is optimisation of the charge ratio between the lipids and the nucleic acids at a given dose.

It is considered that liposomes gain entry into cells via adsorptive endocytosis and the ribozymes remain in endosomal vesicles within the cytoplasm (Prasmickaite *et al.*, 1998), which is not desirable as the ribozyme needs to be localised with the target mRNA in the cytosol. Therefore it is necessary that the ribozymes be released from these endosomal compartments. In order to facilitate this, many commercially available lipoplex transfection agents, such as Transfectin or Cytofectin, contain a helper lipid such as DOPE which is an inverted-cone shaped lipid thought to facilitate cytosolic release through the disruption of the endosomal membrane (Farhood *et al.*, 1992). A variety of novel modifications of liposomes and lipoplexes have been investigated in order to improve the effectiveness of these delivery systems. These include adding polyethylene glycol to avoid phagocytoses by the cells of reticulo-endothelial system when administered *in vivo* (Klibanov, 1990) or pH sensitive chemical moieties to produce pH sensitive fusogenic liposomes to enhance release of nucleic acids from endosomes (DeOliveira, 1998).

There are two main advantages with liposomes and lipoplexes, firstly, the protection of ribozymes from nucleases and secondly, enhanced uptake and localization of ribozymes in the appropriate cellular compartments. Liposomal delivery of ribozymes also ensures that they will not be degraded by lysosomal enzymes, a common problem with delivery of naked DNA oligonucleotides once in the subcellular compartments. The disadvantage of these lipid systems when used systemically is the cytotoxicity due to their overall positive surface

charge which leads to unspecific interactions with cellular blood compartments, vessel endothelia and plasma proteins such as albumin, immunoglobulin and complement factors (Ogris *et al.*, 1999). This cytotoxicity can be improved by rigorous optimisation of the lipid-ribozyme complexes. Certain lipid complexes have been reported as being inactive in serum medium, which is being addressed by developing new formulations of lipids, which are active in serum medium. In terms of amount of ribozyme, taken up by cells with the aid of lipids, there are no reports in the literature but efficacy of down-regulation of the target mRNA and protein has been stated in studies which ranged from 50 to 70% as detailed in table 1.2.

Microinjection is an invasive technique, which has been used for the delivery and evaluation of efficiency of ribozymes *in vitro*. With microinjection the ribozymes can be directly injected into the nucleus or specific compartments of the cytoplasm (Hormes *et al.*, 1997). This method is only experimental and cannot be widely used because of the need for specialised equipment and skills and it can only be used on one cell and therefore ultimately cannot be developed into a clinical grade delivery system.

Another approach for delivering ribozymes into cells, called receptor mediated delivery, utilizes naturally existing transport systems like particular carriers and receptors to deliver to cells. This strategy further allows targeting particular sub-sets of cells or to specific organs. In a receptor mediated delivery model the ribozyme is attached to the ligand for the receptors, which after binding to the receptor is internalised. An example of this is conjugation of ribozyme with transferrin molecules which resulted in a 3-fold increase in uptake mediated by transferrin receptors (Hudson *et al.*, 1999).

The pharmacological effects of ribozymes whether delivered free or via a delivery system are short lived due to metabolism, redistribution and rapid elimination of the ribozyme from the cellular environment. In a pharmacokinetic study of a chemically stabilised ribozyme the elimination half life after intra-venous administration was 28 to 40 minutes (Sandberg *et al.*, 2000). Therefore in order to obtain clinically efficacious down regulation of the target protein, repeated administration is required especially for targets with long half-lives. However, repeated administration is not only undesirable in terms of time, labour and costs but also leads to undesirable side-effects. A possible approach in improving the chemical stability, pharmacokinetics and the pharmacodynamics of ribozymes involves the use of

sustained-release biodegradable polymer formulations. Sustained release of drug molecules from these devices can be suitably controlled by careful selection of formulation parameters like polymer chemistry, co-polymer ratio, shape and size of the device. The most widely used polymers are polylactides and co-polymers of lactic acid and glycolic acid (PLGA). A further extensive account of polymers is given in section 1.5.

The above-mentioned strategies are far from optimal and further studies on their physicochemical and biological properties will provide valuable knowledge to develop highly efficient and sophisticated delivery systems. An account of recent studies is given in the next section in which ribozymes have been delivered exogenously.

Table 1.2. A selective account of various exogenous delivery strategies.

Ribozyme/ Delivery System	**Target mRNA**	**In vitro/vivo/ Disease Model/Biological tool**	**Result**	**Reference:**
2'-modified, phosphorothioated and unmodified hammerheads delivered with liposome (Tfx-50 cationic lipid) & free cholesterolated ribozyme.	Luciferase	*In vitro* experimental model stably expressing luciferase	Both modified, non-modified showed ~50% inhibition of luciferase when delivered with lipids in comparison to controls. Cholesterol moiety did not enhance uptake.	(Bramlage *et al.*, 1999)
Unmodified 37 mer hammerhead complexed with Lipofectin	Human urikinase	*In vitro* model of osteosarcoma	Lipofectin protection from RNases lasted to 22h. Ribozyme was rapidly taken into cells (5min). No figures on the magnitude of uptake given.	(Kariko *et al.*, 1994)
Phosphorothioate DNA-RNA chimeric hammerhead & a wild type ribozyme Transfectam (lipid)	V3 loop of HIV-1	*In-vitro* model of HIV. Envelope gene of HIV-1 carried by Chinese hamster ovary cells.	Both ribozymes were readily delivered to cells with wild type remaining intact for 12h and the chimeric for 24h. Inhibitory effect of chimeric ribozyme was time dependent and showed a maximum of 70% at 72h.	(Zhang *et al.*, 1996)
Chimeric DNA-RNA hammerhead ribozyme Lipofectin mediated transfection	Transforming growth factor β_1	*In vitro* model of arterial proliferative diseases	DNA synthesis and cellular proliferation was significantly inhibited. Target mRNA & protein levels were significantly reduced dose dependently.	(Teng *et al.*, 2000)
Hammerhead Cytofectin-ribozyme complex	Interleukin-6	*In vitro* model of prostate cancer	Lipid-ribozyme complex inhibited protein levels and cell numbers along with the controls reflecting efficient delivery to cells. However in terms of efficacy this was a non-specific toxic effect.	(Freedland *et al.*, 1996)
Hammerhead, chimeric & wild type. Liposome	Porcine Leukocyte type 12 lipoxygenase (LO)	*In vitro* model of arterial proliferative diseases	Liposome prolongs stability to 42 & 60 h. Complete inhibition of mRNA and 50% reduction in levels of LO protein.	(Gu *et al.*, 1997)
Hammerhead & hairpin. Lipofectin-ribozyme complex.	variant transthyretin (TTR)	*In vitro* model of familial amyloidotic polyneuropathy.	TTR protein levels were reduced to 33% after 24h and 26% after 48 h compared to controls.	(Tanaka *et al.*, 2001)
Chimeric DNA-RNA hammerhead ribozyme complexed with Lipofectamine, Lipofectin,	Long terminal repeat of HIV-1	*In vitro* model of HIV Infected monocytic cells & HeLa $CD4^+$ cells	Ribozyme was successfully delivered by cells as shown by different fluorescence patterns with each formulation. However the ribozyme in liposomes were	(Konopka *et al.*, 1998)

DMRIE:DOPE & DRMRIE:DOTAP			not effective in reducing viral proliferation and had non specific toxic effects.	
Phosphorothioated hammerhead ribozyme Hemagglutinating virus of Japan-cationic liposomes	*rex* and *tac* mRNA of human T cell leukaemia virus.	*In vitro* model of virus induced leukaemia	Delivery with cationic liposomes was 15-20 times higher & anionic liposome was 4-5 times higher than naked ribozyme. Target protein was decreased to about 95%.	(Kitajima *et al.*, 1997)
2'-O-allyl modified hammerhead Cationic lipid-ribozyme complex	Mutant ki-*ras* mRNA	*In vitro* model of pancreatic carcinoma cell line.	Active ribozyme was delivered successfully as is was 2 fold more potent in decreasing mRNA levels, inhibiting cell proliferation & colony formation compared to the controls	(Giannini *et al.*, 1999)
2'-O-Methyl modified hammerhead Receptor mediated delivery by conjugation to transferrin receptor antibody (TRA)	c-*erb*B1	*In vitro* study to evaluate delivery strategy	Cell association increased three fold. It was temperature dependent, inhibited by competition with antibodies. Monensin further enhanced TRA-ribozyme mediated delivery.	(Hudson *et al.*, 1999)
Unmodified hammerhead Polymer matrix delivery system	c-*myc* oncogenes mRNA	*In vitro* model to evaluate release characteristics	Biphasic release profile dependent on ribozyme loading, Stability improved to more than 2 weeks with no adverse effect on cleavage efficiency.	(Hudson *et al.*, 1996a)
Chemically modified Hammerhead freely delivered	EGFR mRNA	*In vitro* uptake in glioblastoma cells	Uptake was time, energy and pH dependent, which could be competed with PO, PS ODNs and other polyanions.	(Fell *et al.*, 1997)
2'-O-methyl modified ribozyme delivered in a Carbopol gel formulation.	Mouse eye Cornelium	*In vivo* model to assess ribozyme/Carbopol formulation	Free ribozymes uptake in the eye was limited ≈ 0.5%. The RBZ/carbopol increased RBZ retention by 5-10 fold.	(Ayers *et al.*, 1996)
Chemically modified hammerhead Intra parenchymal injection	Dopamine D_2 receptor	*In vivo* gene function analysis in the brain	Quinpirole induced stereotyped sniffing and locomotor activation was inhibited by the ribozyme significantly.	(Salmi *et al.*, 2000)

1.4.0. Limitations of the hammerhead ribozyme

Despite significant progress in the utilization of ribozymes in various model systems, there is still need for greater optimisation of the structure and activity of ribozymes. Ribozymes due to their large size and polar nature are not amenable for delivery across biological membranes and compartments at the systemic, cellular and subcellular level. At the systemic level any intra-venous or oral delivery results in the rapid degradation and clearance of unmodified ribozymes. At the cellular level the uptake is hampered at the cell membrane barrier, which only allows a poor and limited permeation across it. The final barrier in the chain of delivery is endolysosomal compartments (Fell *et al.*, 1997), which keep the ribozymes sequestered inside and facilitate possible degradation of the ribozymes with the net result of only a fraction of the administered dose reaching the site of action. Any strategies that can address the above mentioned critical areas are likely to lead to successful applications for ribozymes in the clinic. Below is a brief overview of steps taken to improve upon the above-mentioned points.

1.4.1.1. Chemical modifications of the hammerhead ribozyme structure

A major obstacle in the development of ribozymes as therapeutic agents is the instability of ribozymes in the biological milieu due to the destruction of ribozymes by the action of RNases. Studies have shown that unmodified RNA is rapidly degraded by nucleases with a half-life of an unmodified all RNA hammerhead ribozyme in human serum being less than 0.1 minute (Jarvis *et al.*, 1996). For a significant progress in the development of ribozymes as therapeutic agents, it is important that the stability of ribozyme is increased without compromising the catalytic capacity. An increase in the sophistication of RNA synthesis has lead to many novel chemical modifications of the RNA (for a review see Usman and Cedergren, 1992). This new technology allows site-specific chemical modifications in ribozymes and facilitates the study of the effect of these modifications on the stability and catalysis of ribozymes. From a structural point of view the possible chemical modifications which can be made in ribozymes include as shown in Figure 1.4b:-

- Modifications of the sugar moiety.
- Nucleotide base modifications.
- Modification of inter-nucleotide linkages.

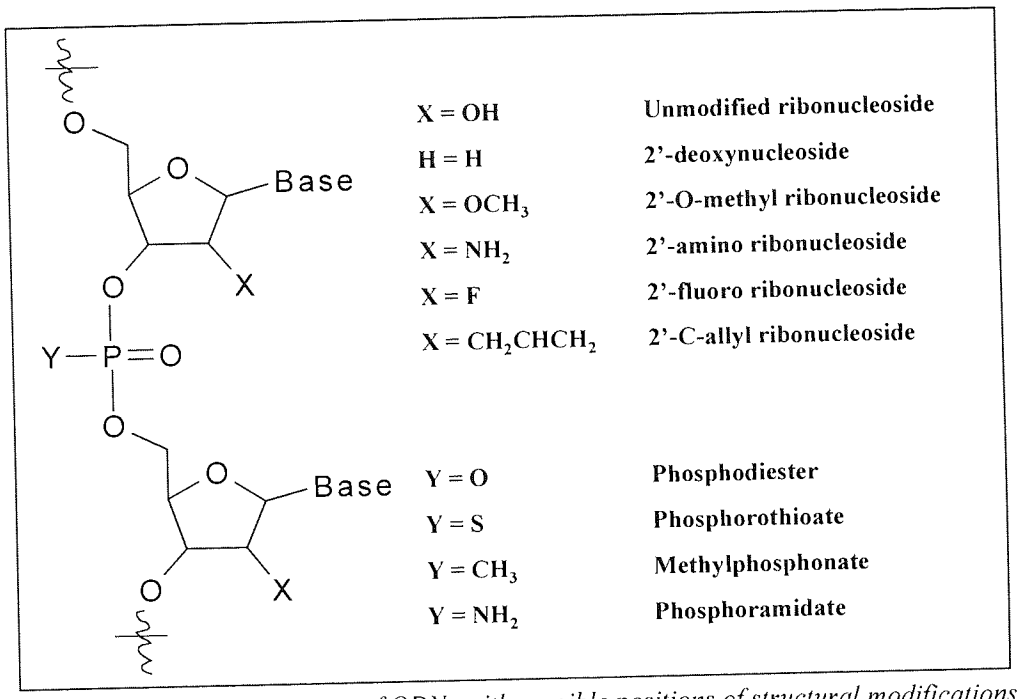

Figure 1.4b *General structure of ODNs with possible positions of structural modifications*

The main source of structural instability in ribozymes is the 2'-OH functional group of the ribose sugars especially of the pyrimidines, which forms the site at which RNases act to cleave the ribozymes. It is thought that any attempt to replace this critical functional group with an analogue would significantly enhance the efficacy of the ribozyme strategy. In this regard many structural modifications of ribozymes have been evaluated in which the 2'-OH group has been replaced with groups like 2'-Dexonucleotides, 2'-O-Methyl, 2'-O-Alkyl, 2'-Amino, 2'-Fluoro and 2'-Uridine at specific positions. In these studies it has been shown that in simple ribozymes these modifications will lead to reduced degradation of ribozymes and consequently improved stability. Taylor *et al.*, (1992) replaced several ribonucleotides of a hammerhead ribozyme by their corresponding 2'-Deoxy analogues in the hybridising arms and observed increased resistance against nuclease digestion and enhanced catalytic activity.

Hendry *et al.*, (1992, 1995) showed that a DNA-modified ribozyme had a higher rate of cleavage and consequently a faster turnover compared to an all-RNA ribozyme. In another study, the 2'-OH group of the ribose sugar was substituted with 2'-O-Methyl nucleotides at all positions in a hammerhead except G_5, G_8, A_9, $A_{15.1}$ and $G_{15.2}$ which resulted in a thousand-fold increase in stability but lowered catalytic activity by a factor of 10^3 (Yang *et al.*, 1992). When nucleotides in stems I and III of the hammerhead were substituted with 2'-O-Methyl nucleotides a four-fold enhanced stability and two-fold higher cleavage efficiency was observed in comparison to an all RNA ribozyme (Goodchild, 1992).

In a study by Paolella *et al.*, (1992), nucleotides were substituted with 2'-O-Allyl analogues except at positions U_4, G_5, A_6, G_8, G_{12}, and $A_{15.1}$ resulting in a 5-fold decrease in catalytic activity of the ribozyme in comparison to an all RNA ribozyme while the stability of this ribozyme in bovine serum was increased substantially with intact ribozyme still present after 2 hours. Pieken *et al.*, (1991) substituted all the pyrimidine nucleotides with 2'-Amino or 2'-Fluoro analogues which resulted in 25-50-fold decrease in activity and a 1200 fold increase in stability in rabbit serum compared to the unmodified ribozyme. Modifications at the 2'-OH positions of ribozymes do not provide for adequate stability as they are still susceptible to degradation from the exonucleases and for this purpose another modification has been investigated. This involves introducing phosphorothioate linkages between selective nucleotides or on terminal nucleotides. To address this Shimayama *et al.*, (1993) prepared a chimeric DNA-RNA ribozyme with 21 phosphorothioate substitutions which showed a 100-fold increase in stability relative to the all RNA ribozyme but the catalytic activity of these chimeras were reduced 15 fold compared with the wild type.

A modified ribozyme containing four 3'-terminal phosphorothioates in addition to 2'-modification of all pyrimidines was shown to be stable in undiluted fetal calf serum for at least 24 hours (Heidenreich *et al.*, 1994). Phosphorothioate linkages, which are widely used in typical DNA-based antisense molecules, can promote non-specific binding to cellular proteins and other biomolecules (Henry *et al.*, 1997). However, ribozymes containing a limited number of phosphorothioate linkages are less promiscuous in their interactions (Usman and Blatt, 2000). Other possible additions to the ribozyme structure to protect against 3'-exonucleases has been the addition of hairpin structure at the 3'-end (Sioud *et al.*, 2002) or an inverted thymidine residue at the 3'-end. The inverted thymidine residue is more desirable than the hairpin structure as it greatly reduces the size of the ribozyme (Beigelman *et al.*, 1995a). However the most important work on the modification of ribozymes to optimise nuclease resistance and catalytic activity has been that of Beigelman *et al.*, (1995b). In this investigation a systematic study of selectively modified 36-mer hammerhead ribozymes was carried out.

The researchers identified a generic, catalytically active and nuclease stable ribozyme motif containing 5 ribose residues, 29-30 2'-O-methyl nucleotides, 1-2 other 2'-modified uridine nucleotides at positions U_4 and U_7 and an inverted nucleotide at the 3'-end. These structural modifications without the 3'-end cap retained the catalytic activity and had a serum half-life

of 5 to 8 hours in a variety of biological fluids including human serum. The addition of a 3'-3' nucleotide cap (inverted thymidine) did not affect catalysis but increased the serum half-lives of these ribozymes to greater than 260 hours. The chemistry and structure of ribozyme used in this thesis is based on their conclusions.

1.4.1.2. Optimisation of hammerhead binding arms

A large set of studies has been carried out to optimise the size of the stems and catalytic core of the hammerhead ribozyme as there are several advantages associated with minimising the size of the ribozymes. These include: 1) reduction in the cost of synthesis for exogenously delivered ribozymes, 2) enhanced biological membrane permeability with small sized ribozymes due to reduced number of polar groups, 3) greater substrate turnover rate with smaller ribozymes as the ribozyme-substrate complex dissociation is faster.

However, any steps taken for the optimisation by reducing the number of nucleotides have serious implications for two important parameters of ribozymes, cleavage rate and specificity. Both of parameters are highly dependent on the number of nucleotides on the hybridising stems of the ribozyme. Ribozymes forming a large number of base pairs with the substrate are unlikely to turnover rapidly in comparison to ribozymes with short arms due to strong hybridisation but have greater specificity. In contrast short stem ribozymes have greater turnover but poor specificity. In regard to specificity the number of base pairs formed between the ribozymes and substrate should be large enough to make the target sequence unique but not so large that imperfectly matched substrates form stable complexes (Herschlag, 1991). Statistically about 13 nucleotides are required to uniquely define a particular site in a mRNA pool in a mammalian cell (Hendry *et al.*, 1998).

In terms of optimisation there are two strategies available to optimise the size of the ribozyme. The first involves shortening the hybridising stems (III and I) of the ribozyme, and the second is to reduce stem and loop II. For short substrates less than 20 nucleotides the optimal length of stems I and III seems to be in the range of 6 to 7 nucleotides (Jarvis *et al.*, 1996). In another study a 10-fold increase in cleavage rates was observed by reducing the lengths of hybridising stems by 20 to 12 nucleotides for a ribozyme directed against the HIV-1 virus RNA (Goodchild and Kholi, 1991). In the case of long substrates with extensive secondary structure, it was thought that longer flanking arms are desirable in order to reduce

hybridisation at incorrect sites along the transcript provided that the turnover rate is not adversely affected. However in a study of ribozyme flanking stem lengths for long substrates it was shown by Lieber and Strauss, (1995) that optimal length should be in the range of 6 to 8 nucleotides, the same as short substrates. Hormes *et al.*, (1997) concluded that for efficient association and dissociation *in vitro* the optimal length has been estimated to be 6 to 8 nucleotides on either side of the catalytic domain. However this observation may not hold true in all cases as in one study a conventional ribozyme with symmetrical stems of 8 nucleotides failed to cleave *in vitro* (Tabler *et al.*, 1994).

The use of hybridising stems with unequal number of nucleotides has in cases unexpectedly shown increased turnover. Ribozymes with this design are referred to as asymmetrical ribozymes and the binding with the substrate is controlled by one stem only. Hendry and McCall, (1996) investigated the cleavage rates of a series of ribozymes with asymmetric flanking arms where stems I and III consisted of 5 and 10 nucleotides and found that ribozymes with shorter stem I cleaved their substrates up to 130-fold more rapidly than asymmetric ribozymes with shorter stem III. Tabler *et al.*, (1994) investigated the effect of length of the two stems on the activity of an HIV-1 targeted ribozyme. The length of stem I was systematically decreased while simultaneously increasing the length of stem III. Interestingly, they found a three nucleotide stem I with a stem III of 280 nucleotides to be sufficient for catalytic activity. Along with the size of the flanking arms, specificity may be increased by choosing an A + U-rich recognition sequence as the weaker binding energy of the A-U base pair compared with the G-C base pair is expected to increase dissociation rates (Herschlag, 1991). Helix II that comprises a stem and loop is the only helix in the hammerhead that is not directly involved in substrate binding. The stem and loop of this helix cannot only be minimised but can be totally eliminated.

Tuschl and Eckstein, (1993) performed a systematic study in which the length and base composition of helix II was varied. They ascertained that the minimum length of stem II was two base pairs and there was a requirement for a conserved G-C pair ($G_{10.1}$-$C_{11.1}$) for maximum catalytic activity. Further reduction in length of the stem led to reduced activity. Inversion of the G-C pair also caused loss of activity, even with a 4 base pair stem. The first two base pairs of helix II are essential for catalytic activity as they probably promote folding of the catalytic core and stabilise tertiary structure (Sigurdsson and Eckstein, 1995). In some cases the helix II is completely removed and the conserved nucleotides A_9 and G_{12} are linked

by linkages, whether nucleotides or non-nucleotides and cleavage was still seen. When the linker contained 13 atoms, slow cleavage rate was observed whereas more reasonable rates were seen with linkers containing 25 atoms (Hendry *et al.*, 1994).

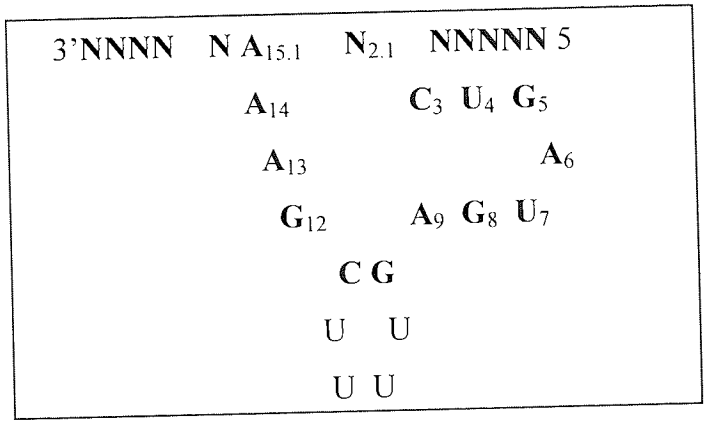

Figure 1.5. *Schematic representation of a miniribozyme, in this structure the helix II is replaced by single GC base pair (Adapted from Hendry et al., 1998).*

Further progress in the attempts to reduce the helix II has been the development of minizymes and mini-ribozymes. Mini-ribozymes are ribozymes in which the helix II is replaced with a sequence 5'rGUUUUC joining A_9 and G_{12} as shown in figure 1.5. A mini-ribozyme with a loop sequence of 5'UUUG was evaluated for cleavage rate constant and was found to have a value of about 10% that of the parent ribozyme (Long and Uhlenbeck, 1994). A ribozyme in which the helix and loop is replaced by a linker that has no Watson-Crick base pairs is called a minizyme. Figure 1.6 is a schematic representation of a minizyme. In this structure the entire helix II is eliminated and the bases G_{12} and A_9 are connected by a linker composed of nucleotides.

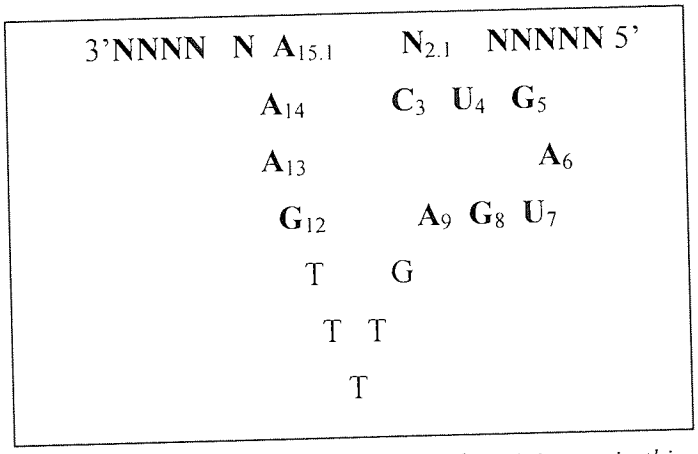

Figure 1.6. *Schematic representation of a minizyme, in this structures the entire helix II is removed (Adapted from Hendry et al., 1998).*

The first minizymes synthesized were about 100 fold less active than analogous standard ribozymes in cleaving short substrates (Tuschl and Eckstein, 1993). However, minizymes like miniribozymes are better than standard ribozymes in cleaving long RNA transcripts (Hendry *et al.*, 1995) *in vitro*. Careful analysis of the various optimisation studies show that the 5'arm of the nucleotide should be approximately 5 to 7 nucleotides long and the 3' arm is not limited in the number of nucleotides but should not be too long to adversely affect the turnover rate by forming stable ribozyme-substrate complex or adopts an unnecessary folded conformation. The optimum helix II must have at least two nucleotides.

1.4.1.3. Target site selection.

A critical step in the design of ribozyme molecules for suppression of gene expression is the identification of sites within the mRNA transcripts, which are accessible for hybridisation by ribozymes. Identification of such accessible sites is difficult because long RNA transcripts and their intracellular protein complexes have extensive secondary and tertiary structures, which may severely limit the accessibility of potential target sites (Xing and Whitton, 1992). This problem is further complicated by the fact that the biophysical principles governing the folding of RNA-protein complexes are not clearly determined. However, despite this there are several methods, which have been used to determine accessible sites with varying degrees of success. These include, computer programmes for predicting RNA secondary structure, the use of DNA oligonucleotides libraries followed by digestion with *Eschericia coli* RNaseH, oligonucleotide scanning arrays and random ribozyme library approaches.

In the first method, site selection is based on secondary structure prediction using RNA folding programmes exemplified by MFOLD (Zuker, 1989a), SAPSSARN (Gaspin and Weshof, 1995) and ESSA (Chetouani *et al.*, 1997). MFOLD (Genetics Computer Group, Madison, WI) is the most widely used from these programmes as it generates several sub-optimal secondary structures which may differ significantly from each other in their folding but differ only slightly in energy (Zuker, 1989b). Analysis of studies using this method shows that this method has not shown any success in predicting accessible or inaccessible sites on mRNA (Ho *et al.*, 1998), (Sohail *et al.*, 1999). This is because of two reasons firstly because the algorithms used in these programmes do not fully predict the tertiary structure of the ribozymes and secondly the RNA-folding programmes do not take into account the

modulating activity of RNA binding proteins (Herschlag *et al.*, 1994; Tsuchihashi *et al.*, 1993).

The second most widely used method is RNaseH mediated assays which are based on the principle that a short strand of DNA which is able to bind to a mRNA transcript can only do so if that site is accessible and this resultant heteroduplex will activate RNaseH which in turn cleaves the RNA part of the heteroduplex and therefore rendering it useless. The cleaved fragment can then be amplified with PCR and separated by polyacrylamide gel electrophoresis and the exact cleaved site can be worked out on the transcript mRNA (Scherr and Rossi, 1998; Scherr *et al.*, 2001; Langlois *et al.*, 2003).

The third method in identifying accessible sites is the use of scanning oligonucleotide approach, in which arrays comprising of large numbers of oligonucleotides, complementary to the regions on the target mRNA, are synthesized in spatially addressed areas on a solid surface like glass. These oligonucleotides are hybridised with radio-labelled transcript and hybridisation patterns obtained by exposure of arrays to an imaging system. Individual oligonucleotides sequences on the scanning array are identified with a computer programme such as XVSEQ (Elder *et al.*, 1999) and oligonucleotides which show strong binding are taken and accessible cleavage sites are detemined. These scanning arrays have been successfully used to design effective ribozymes for targeted RNA inactivation.

The fourth approach is a combinatorial approach in which a library of random sequences of various types of ribozymes have been generated to map accessible sites in a RNA (Pierce and Ruffner, 1998; Yu *et al.*, 1998).

1.4.2. Therapeutic applications of hammerhead ribozymes

Adaptation of ribozymes to act in trans by Haseloff and Gerlach, (1998) to selectively cleave any target mRNA led to the hope that ribozymes can be therapeutically exploited to eliminate the expression of undesirable genes. Since then ribozymes have been used as biological tools for gene function analysis and as potential targeted therapeutics for the inhibition of undesirable genes with varying degrees of success in a variety of organisms including bacteria, yeast, plants, amphibians, flies and mammals (Rossi, 1998). This intense focus on ribozymes as a form of targeted therapeutics arises from the several useful attributes, which ribozyme molecules possess. These include:

1. Target selectivity, based on the Watson-Crick base-pairing of the ribozyme binding arms with sequences on either side of the cleavage site of the substrate. These can be modified to target any mRNA.

2. Specificity of the cleavage site as the ribozyme only cleaves at a site if there is a NUX sequence as described in section 1.2.4.

3. Cleavage of the target mRNA rendering it unsuitable for the translational machinery of the cell.

4. Multiple turnover of substrate. The ribozyme dissociates from the target mRNA after cleavage and hybridises with another molecule therefore exhibiting true enzymatic behaviour by acting on many substrates.

Below is a selective table of various studies in which ribozymes have been used to down-regulate the expression of various genes in various disease model systems in *vitro* and *vivo*.

Table 1.3. A summary of recent therapeutic applications of ribozymes.

Ribozyme/ Delivery System	**Target mRNA**	***In vitro/vivo/* Disease Model**	**Result**	**Reference:**
Hammerhead ribozyme. Liposomal transfection reagent DOTAP mediated exogenous delivery	mRNA of Nucleoplasmin-anaplastic lymphoma kinase	Anaplastic large cell lymphoma *in vitro* model	Ribozyme inhibited target mRNA, with significant inhibition seen with endogenous delivery than in comparison to exogenous delivery.	(Hubinger *et al.*, 2003)
Hammerhead ribozyme, endogenously expressed in the nucleas via tRNA expression cassesette.	Mytonic dystrophy protein kinase mRNA	*In vitro* model of myotonic dystrophy.	Ribozyme was successfully expressed in the nucleus with 63% inhibition in target mRNA and significant reduction in nuclear foci in myoblasts.	(Langlois *et al.*, 2003)
Chimeric DNA-RNA 38mer hammerhead ribozyme delivered exogenously in complex with polyethylenimine	Platelet derived growth factor A chain mRNA	*In vivo* model of neointima formation in rat carotid artery after balloon injury	Ribozyme was delivered to cells until 24 hours after balloon injury. Neointima formation was inibited by 56 and 45% of control levels with 2 and 5μg of ribozyme.	(Kotani *et al.*, 2003)
Hammerhead ribozyme. Delivery mediated by HVJ-liposome complex	MMP-2 mRNA	*In vivo* model of cardiac allograft vasculopathy	Ribozyme significantly inhibited the target mRNA with 50% inhibition in luminal occlusion in comparison to controls.	(Tsukioki *et al.*, 2002)
Hammerhead ribozyme, adenoviral mediated delivery	Human MDR-1 –P-glycoprotein mRNA	*In vitro* model of chemoresistant hepatocellular cancer.	Target mRNA inhibited efficiently and cellular chemosensitivity increased by 30-60 fold.	(Huesker *et al.*, 2002)
Divalent hammerhead ribozyme	Template region of the human telomerase RNA	Endometrial carcinoma cells	Divalent ribozyme (two catalytic cores) was successful in inhibiting telomerase activity. Inhibition was less than the monovalent ribozymes.	(Yokoyama *et al.*, 2002)
Hammerhead ribozyme. Plasmid mediated endogenous delivery	HER-2 mRNA	*In vivo* and *in vitro* model of pancreatic cancer.	*In vitro*, target mRNA and protein were inhibited by 40-50% along with ≈40% inhibition in the proliferation rate. *In vivo* the tumor growth was decreased by 40%.	(Thybusch-Bernhardt *et al.*, 2001)
Hammerhead ribozyme delivered via adenovirus	H-ras mRNA	*In vitro* and *in vivo* model of laryngeal cancer (cultured and nude mice s.c. implanted HEp-2 cells.)	Anti-H-ras ribozyme significantly inhibited target protein expression and tumour growth in comparison to controls. This inhibition was mediated by caspase and mitochondria-dependent pathways.	(Wang *et al.*, 2002)
Hammerhead ribozyme, 38mer , delivered exogenously via Lipofectin	Platelet derived growth factor A chain mRNA	*In vitro* model of cardiovascular proliferative disease.	1 μM dose of ribozyme inhibited the target mRNA by 50% in comparison to mismatch control	(Hu *et al.*, 2001)

Hammerhead, unmodified, FuGene transfection	βAPP^{+} mRNA	*In vitro* model of Alzheimers Disease	Ribozyme inhibited the target mRNA transcript and βAPP protein.	(Dolzhanskaya *et al.*, 2001)
Chemically modified Inosine hammerhead Transfection with DOTAP & Effecten	Mutant Transthyretin mRNA	Hereditary amyloidosis	Target mRNA inhibited by 63 % in comparison to the control.	(Propsting *et al.*, 2000)
Unmodified hammerhead Transient transfection to cells with DOTAP and stable with a plasmid construct.	hTERT catalytic subunit of telomerase	*In vitro* model of endometrial carcinoma cells	Ribozyme inhibited telomerase mRNA and also caused suppression of cellular growth.	(Yokoyama *et al.*, 2000)
Dimeric Maxizyme delivered in a retroviral vector.	BCR-ABL mRNA	*In vivo* murine model of Chronic Myelogenous Leukemia	Mice treated with ribozyme-carrying retrovirus remained healthy despite injection of tumorigenic cells in comparison to mice with control retroviruses.	(Tanabe *et al.*, 2000)
Chimeric DNA-RNA hammerhead ribozyme Lipofection with Lipofectin	TGF-β1	*In vitro* model of arterial proliferative diseases	Ribozyme inhibited cell proliferation. Target mRNA and proteins were reduced significantly.	(Su *et al.*, 2000)
Hammerhead unmodified, plasmid mediated delivery by transfection	γ-glutamylcysteine synthetase mRNA	β-cell line of pancreatic cells. *In vitro* model of insulin secretion.	Ribozyme inhibited target mRNA by almost a half (48-60%). This resulted in a three fold increase in insulin. This was associated with increased intracellular Ca^{2+} concentration.	(Kondo *et al.*, 2000)
Hammerhead Liposome mediated delivery	TNF-∝ mRNA	*In vitro/vivo* murine model	TNF-∝ levels were inhibited in cultured macrophages by 80% in comparison to *in vivo* where inhibition was ~30% after i.p. administration.	(Kisich *et al.*, 1999)
Hammerhead unmodified adenovirally delivered	anti H-*ras*	*In vitro* model of bladder cancer.	Intratumoral injections of ribozyme carrying adenovirus resulted in dose dependent antiproliferative effects with complete regression in some cases.	(Irie *et al.*, 1999)
Unmodified hammerhead ribozyme, delivered via plasmid by electoporation.	c-*kit* mRNA	murine mastocytoma cells. *In vitro* model of mast cell hyperplasia	Temporary inhibition of kit mRNA by ribozyme was observed. Inhibitory efficiency was further improved by co-transfection with green fluorescent protein.	(Shelburne and Huff, 1999)
Unmodified hammerhead ribozyme delivered via a plasmid	Human β-globin mRNA	*In vivo* transgenic model of sickle cell anaemia.	Ribozyme significantly inhibited the target protein by 56% to 60% in young mice.	(Alami *et al.*, 1999)
Unmodified hammerhead ribozyme delivered via a plasmid	k-*ras* oncogenes mRNA	*In vitro* model of human pancreatic carcinoma.	Ribozymes significantly inhibited the target k-ras mRNA compared to controls. Ribozymes also inhibited proliferation of malignant cells.	(Tsuchida *et al.*, 1998)
Chemically modified ribozymes.	*Flt*-1 & KDR mRNA	Human dermal microvascular endothelial cells. For *in vivo*	Both ribozymes inhibited the level of both messages by >50%. This was accompanied by 50-60%	(Parry *et al.*, 1999)

		model of angiogenesis corneal cells were used.	reduction in cellular proliferation.	
Unmodified Hammerhead ribozyme retroviral cellular delivery	HIV tat mRNA	*In vitro* model of AIDS	Target protein activity inhibited by 80%. Cells stably transduced with ribozymes were able to resist HIV infection for 20 days	(Jackson *et al.*, 1998)
Hammerhead endogenous delivery	c-*fos*	*In vitro* and *in vivo* model of chemoresistant tumours	fos mRNA was selectively inhibited in resistant cells *in vitro* and *in vivo*. *In vivo* cellular sensitivity to cisplatin treatment was reversed.	(Funato *et al.*, 1997)
Unmodified hammerhead ribozyme Intrinsically expressed	Bovine ∝-lactalbumin	*In vivo* model of lactation in transgenic animals	Target mRNA levels inhibited by 78, 58 & 50% along with protein levels which were inhibited by 35, 24 & 14%.	(L'Huillier *et al.*, 1996)
Chimeric DNA/RNA hammerhead ribozyme, direct intraartricular space.	Stromelysin mRNA	*In vivo* model of arthritic diseases.	Ribozyme significantly inhibited target mRNA by 40%.	(Flory *et al.*, 1996)
Hammerhead Adenoviral mediated delivery	H-ras	*In vitro* model of bladder carcinoma.	Target mRNA was inhibited in comparison to control with ribozyme significantly suppressed cell growth.	(Feng *et al.*, 1995)

1.4.3. Clinical trials of Ribozymes

There are currently several exogenously delivered ribozymes being investigated in clinical trials. The first is ANGIOZYME™, which was co-developed by Ribozyme Pharmaceuticals, Inc.(RPI) and Chiron Corporation, that inhibits the process of new blood vessel formation (angiogenesis), which is critical for the growth and spread of tumours. ANGIOZYME™ has been designed to specifically cleave the mRNA for the VEGFR-1, a key receptor in tumour angiogenesis. Several studies have been conducted to assess the efficacy of ANGIOZYME™ in animal models of cancer and in these models, ANGIOZYME™, has been shown to inhibit primary tumour growth and metastasis by reducing blood vessels in treated animals. Preliminary data are available from a Phase I/II human clinical trial in which 31 patients were treated with a variety of late stage tumours with once daily dosing for at least 29 days. The ribozyme was well tolerated and it demonstrated that it could be conveniently administered by subcutaneous injection at home by the patient. A phase II trial is now being planned to further assess safety, clinical efficacy and pharmacokinetics of this ribozyme alone and in combination with paclitaxel and carboplatin in patients with breast and metastatic colorectal cancer (www.rpi.com/angiozyme).

The second ribozyme, which is being assessed, is HEPTAZYME™, which is targeted against Hepatitis C virus that causes a chronic infection leading to cirrhosis, liver failure and hepatocellular carcinoma over a period of 10 to 20 years. In the HEPTAZYME™ clinical trial, this ribozyme is being evaluated alone and in combination with interferon alfacon-1 (INFERGEN®), in patients who have not previously had any interferon and/or ribavirin preparation (www.rpi.com/antihcv). Another ribozyme called HERZYME™ is currently in phase I clinical trials after pre-clinical toxicology studies in mice and monkeys have demonstrated extremely safe profiles. This ribozyme is being developed by Medizyme Pharmaceuticals Ltd to target human epidermal growth factor-2 (HER-2) mRNA, which is a key signal pathway receptor over-expressed in several types of cancer cells (www.rpi.com/herzyme).

1.5. POLYMERS

Successful therapeutic application of ribozymes is hampered by poor biological stability, limited cellular uptake and rapid *in vivo* elimination kinetics of ribozymes as described in section 1.3.0. Currently there are several strategies which are being explored to overcome these biopharmaceutical limitations as described in section 1.4.0. In this section a selective account of one of these strategies involving biodegradable polymers, which are being investigated extensively as delivery systems, is presented with a particular focus on PLGA polymers.

Polymers have been studied with great interest over the last twenty years for use as carriers in the drug delivery of a variety of molecules such as proteins (Cohen *et al.*, 1991), nucleic acids (Akhtar and Lewis, 1997) antivirals (Conti *et al.*, 1997) and a wide range of other applications such as implants (Kulkarni *et al.*, 1966), sutures (Cutwright *et al.*, 1971), prosthetics (Hoffman, 1977), orthopaedic repair material (Lenslag *et al.*, 1987)(for reviews see Langer and Pappas, 1981; Holland and Tighe, 1986, Hayashi, 1994; Vert *et al.*, 1994). From drug delivery perspective polymers offer several advantages as enumerated below:

1). Controlled and sustained delivery of biologically labile drug molecules in a physically intact form.
2). Site-specific administration to target organs or sites of disease such as tumours.
3). Reduced utilization of drug in comparison to systemic delivery resulting in minimisation of possible side-effects and enhanced efficacy (Fournier *et al.*, 1991).
4). Systemic administration of polymer microspheres via the intravenous route enables passive targeting to the liver and other reticuloendothelial organs (Davis *et al.*, 1993; Le Ray *et al.*, 1994; Nakada *et al.*, 1996).
5). Elimination of the need for device retrieval after completion of drug release in case of biodegradable polymers.

To date polymers of a large variety of chemistries such as ethylene-vinyl acetate (Langer and Folkman, 1976) polylactic acid, polylactide-co-glycolide, polyhydroxybutyrate, polyanhydrides (Rosen *et al.*, 1983), polyorthoesters (Wuthrich *et al.*, 1992) and polyalkylcyanoacrylates (Couvreveur and Puisieux, 1992) have been evaluated for drug

delivery. In the next section a detailed overview of the delivery systems formulated from the copolymer of lactide with glycolide is presented.

1.5.1. Polylactide-co-glycolide (PLGA)

Polylactide-co-glycolide is a biodegradable copolymer of lactic acid with glycolic acid and is one of the most widely investigated and used polymer as evidenced by its use in a variety of medical and pharmaceutical applications including wound closure, dental repairs, fracture fixation, sutures, ligament reconstruction and drug delivery (for reviews see Lewis, 1990; Okada and Taguchi, 1995). Its long history of use has demonstrated its biocompatibility and degradation to toxicologically acceptable products (Veziers *et al.*, 2001).

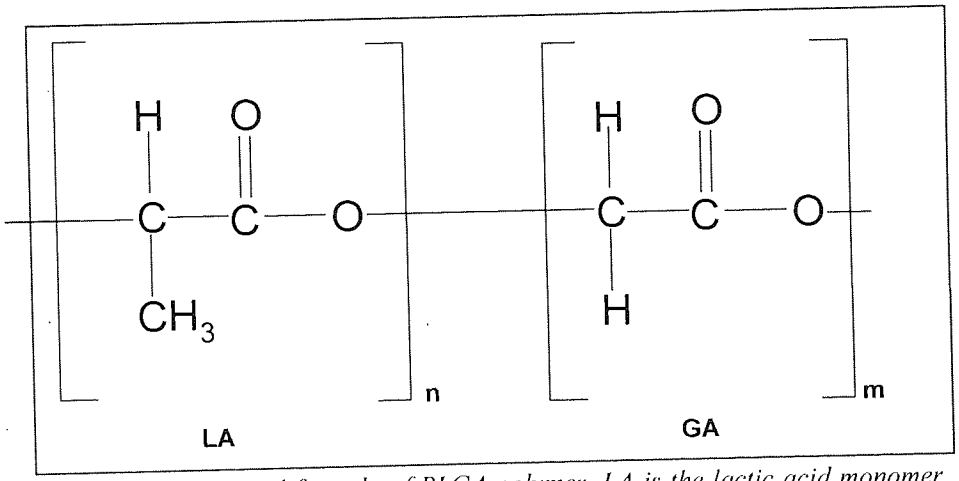

Figure 1.7. *Structural formula of PLGA polymer. LA is the lactic acid monomer and GA is the glycolide monomer. n= number of lactide monomers and m= number of glycolide monomers. Adapted from (Smith, 2000).*

PLGA polymer systems have received FDA approval and are in commercial use for the treatment of advanced prostate cancer and endometriosis. Licensed products containing PLGA include Lupron Depot® (Leuprolide acetate), Zoladex®, Zoladex LA® (Goserelin acetate), Decapeptyl® (Triptorelin), Parlodel LA® (Bromocriptine), Suprefact® (Buserelin) and Prostap® (Leuporelin).

Chemically, PLGA polymers (figure 1.7) are generally classified as aliphatic polyesters, poly(α-hydroxy acids) or polylactones and on the basis of molecular weight can be categorised into low MW polymers (≅ 3,000 Da) and high MW polymers (> 10,000 Da). Low MW polymers are synthesized directly from lactic acid and glycolic acid by condensation polymerisation (Hutchinson *et al.*, 1985) reaction at a high temperature of 130-190°C with Antimony Oxide as a catalyst (Avgoustakis and Nixon, 1991). In contrast for

high molecular weights the preferred method for synthesis is the ring opening polymerisation of the cyclic diesters (lactides and glycolides) using Antimony, Lead or Tin as catalysts (Rak *et al.*, 1985; Marcote and Goosen, 1989). The physicochemical properties of the low MW polymers limit their biomedical applications as their mechanical strength is quite low and they have a rapid degradation rate. These properties make low MW copolymers ideal for formulating drug delivery systems with controllable degradation rates and no requirement of high mechanical strength (Sakakura *et al.*, 1992), (Wada *et al.*, 1991), (Yoshikawa *et al.*, 1998).

1.5.2. Degradation of PLGA

PLGA polymers undergo degradation through hydrolysis of ester linkages in both *in vivo* and *in vitro* environments (Spenlehauer *et al.*, 1989) and the kinetics of hydrolysis are strongly influenced by many factors including MW, pH, temperature, surface structure, crystallinity and the presence of impurities and additives. Biodegradation of the PLGA polymer takes place in four steps (Kumar, 1987). In the first step the polymer absorbs water and undergoes some swelling. The water penetrates in to the amorphous region of the polymer and disrupts secondary and tertiary structures that have been stabilised by Van der Waals forces and hydrogen bonds. In the second step of biodegradation, cleavage of the covalent bonds in the polymer backbone by hydrolysis begins generating soluble monomeric and oligomeric products. These degradation products leave the bulk polymer through the various channels and holes resulting in weight loss of polymer (Hutchinson and Furr, 1985; Vert *et al.*, 1994) further enhancing water uptake and increasing porosity. As hydrolysis proceeds, increasing amounts of carboxylic acid end groups are generated. These free carboxylic groups may autocatalyse the hydrolysis reaction, which accelerates biodegradation. A loss of mechanical strength in polymeric devices is observed at this stage. The third step of biodegradation is characterised by a massive cleavage of the backbone covalent bonds. In the fourth step, the polymer loses mass, which may occur simply by the solubilisation of oligomers in to the surrounding medium. As solubilisation proceeds, the density of the mass decreases until the polymer disappears. Any polymeric fragments that remain are further hydrolysed in to the free acids.

The rate of hydrolysis of the copolymer increases with increasing glycolide content and reaches a maximum when the lactide to glycolide ratio reaches 50:50 (Miller *et al.*, 1977).

The reduction in polymer hydrophobicity when the lactide content is reduced from 100% to 80% results in an increased hydrolysis rate (Floy *et al.*, 1993). Most hydrophobic and crystalline polymers exhibit a relatively slow degradation rate due to the low hydration degree in microspheres (Park, 1994). The hydrophobic nature of LA causes a steric hindrance to attack by water molecules, and thus the LA moieties are less hydrolytically labile than GA moieties, and are therefore degraded slower compared to the latter. Polymer degradation is accelerated in both strongly alkaline and acidic media (Makino *et al.*, 1985; Chu, 1981).

Degradation produces lactic and glycolic acid monomers along with carboxylic acid. The fate of these products *in vivo* is shown in fig 1.8. As LA is a natural metabolic product in all higher animals it enters the tricarboxylic acid cycle, and is metabolised and eliminated from the body as carbon dioxide and water (Wang *et al.*, 1990). GA is a component of several neutral mucopolysaccharides in animal tissues. It can be excreted unchanged by the kidneys or enter the tricarboxylic acid cycle and be eliminated as carbon dioxide and water.

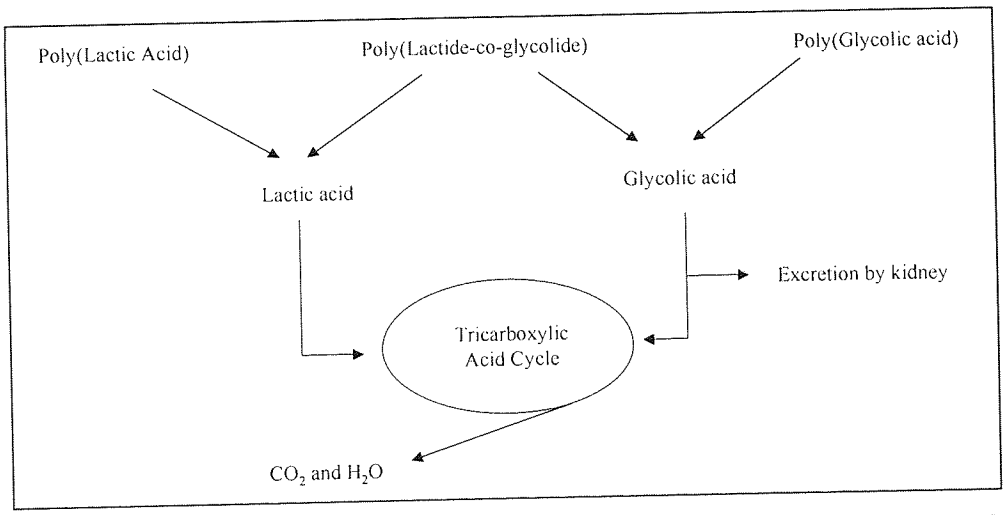

Figure 1.8. *A schematic representation of the metabolism and excretion of biodegradation products of PLGA polymers in vivo. Adapted from Khan, (1999).*

1.5.3. Polymer-mediated CNS delivery

Drug delivery to the CNS remains a challenging area of research as there is still a lack of a robust drug delivery system to deliver molecules to discrete functional regions of the brain at controlled rates (Tamargo and Brem, 1992). As pharmacokinetic studies have demonstrated, large polyanionic molecules like ribozymes have negligible uptake in the central nervous system due to the presence of the formidable blood brain barrier (Pardrige, 2002). It was hoped that strategies involving direct injection of drugs like nucleic acids in the central nervous system may over-come the problems of delivery posed by the BBB. Unfortunately this strategy achieved limited success due to the rapid disappearance of the injected molecule from the target site due to dispersion and diffusion resulting in poor uptake and retention in cells (Morris and Lucion, 1995; Ogawa *et al.*, 1995). In order to overcome this problem several studies have attempted to encapsulate the molecules in biodegradable polymers to obtain controlled and site-specific drug release for a required duration of time. One such attempt, which established the proof of the principle, involved the development of a polyanhydride implant wafer, Gliadel®, composed of the polymers, 1,3-bis (p-carboxyphenoxy) propane (CPP) and sebacic acid (SA).

Gliadel wafer incorporates carmustine (BCNU), which is a potent anti-cancer drug especially effective against glioblastomas (Wang *et al.*, 2002). The polymer in this formulation protects the BCNU from degradation and provides a sustained release up to 2-3 weeks which in free form has a half-life of ≈ 12 min in serum (Brem and Gabikien, 2001). The safety and efficacy of Gliadel has been investigated in several clinical trial studies and has regulatory approval in 22 countries. A study involving 240 patients showed that median survival of patients was 60 weeks in the Gliadel treatment group in comparison to 50 weeks in the placebo group (Westphal *et al.*, 2000). However, a major limitation of this strategy is the risk of development of drug resistance to the chemotherapeutic agent, BCNU.

Another widely studied synthetic polymer, which was investigated in this thesis, for incorporating drugs is PLGA which has been shown to be non-toxic, biocompatible and safe in the central nervous system (Menei *et al.*, 1993). This polymer is formulated as microspheres which are emerging as promising systems for drug delivery to the brain which

due their small size can be easily implanted in discrete, precise and functional areas of the brain without damaging the surrounding tissue by stereotaxy (Menei *et al.*, 1994). This method is far superior to the insertion of large devices such as monolithic implants by open surgery and can be repeated if necessary.

Below is a list of various studies in which neuroactive macromolecules of different classes have been incorporated in various implantable polymeric devices for localised and controlled release site-specific delivery to the central nervous system. Finally the need for a robust delivery system for the central nervous system is becoming more urgent to treat secondary metastatic brain tumours as more and more systemic anticancer therapies become available. As effective systemic therapies will provide complete cancer eradication if the risk of relapse in the central nervous system is reduced.

Table 1.4. A selective account of polymeric delivery to the CNS.

Drug	In vitro/ CNS site	Polymer	Comments	Ref
Nerve Growth Factor	*In vitro* PC12 cells	PLGA PLGA + PCL	NGF encapsulated in all polymers with highest efficiency with PCL. Bioactive NGF was released up to 92 d in a biphasic pattern	(Cao and Shoichet, 1999)
5-Fluorouracil	C6 Glioma bearing rats	PLGA	*In vivo* release profiles were longer than *in vitro*. Slow release microspheres reduced mortality significantly and no toxicity due to polymer reported.	(Menei *et al.*, 1996)
5-Fluorouracil	Humans with glioblastoma	PLGA	Sustained concentrations of 5-FU in the CSF for 1 month. Median survival time was doubled and disease remission achieved with two patients.	(Menei *et al.*, 1999)
Nerve growth factor	Intra-striatal injections	PLGA	Microspheres present in striatum for 2.5 months. Excitotoxic damage was reduced by 40% NGF sustained release cf with controls.	(Menei *et al.*, 2000)
Antisense oligonucleotides	Intrastriatal injection into the Neostriatum	PLGA	Free antisense showed punctate distribution for 24 h whereas polymer loaded microsphere remained until after 48 h and the distribution was diffuse covering both nuclear and cytosolic regions.	(Khan *et al.*, 2000)
Dopamine	Intrastriatal injections in rats with Parkinson disease.	PLGA	Rats displayed an attenuation of the contra-lateral rotational behaviour induced by apomorphine up to 8 weeks postimplantation along with growth of dopamine fibres.	(McRae *et al.*, 1992)
Recombinant nerve growth factor	Intracranial implants in rats	PLGA and EVAc	High levels (60000ng in ≈ 50μL) of growth factor recovered from brain slice after 1,2 and 4 weeks postimplantation indicating successful highly localised delivery in the CNS.	(Saltzman *et al.*, 1999)
Nerve growth factor	Intraseptal stereotaxic implantation	PLGA	PLGA microspheres presented no neurotoxicity and released sufficient amounts of bioactive NGF to significantly promote the survival of axotomized cholinergic neurons.	(Pean *et al.*, 2000)
Nerve growth factor and GM1	Injection into cortical lesions in rats	PLGA	Sustained release from microspheres resulted in effective protection from degenerative changes in lesioned cortex.	(Maysinger *et al.*, 1993)
Dopamine and Norepinepherine	Intrastriatal injection	PLGA	Dopamine and norepinepherine microspheres displayed a 30-50% reduction in rotational behaviour. Implantation of a mixture resulted in 80% decrease in apomorphine induced rotations.	(McRae and Dahlostrum, 1994)

1.6. RIBOZYME RPI.4782.

In this study the ribozyme used is a hammerhead ribozyme designated RPI 4782 (figure 1.9), which was synthesized by Ribozyme Pharmaceuticals Inc, Boulder, Colorado, USA. It is a 37mer hammerhead ribozyme with the following sequence:

5'-UGU GUG UCU GAU GAG GCC GAA AGG CCG AAA CUG AAC T-3'

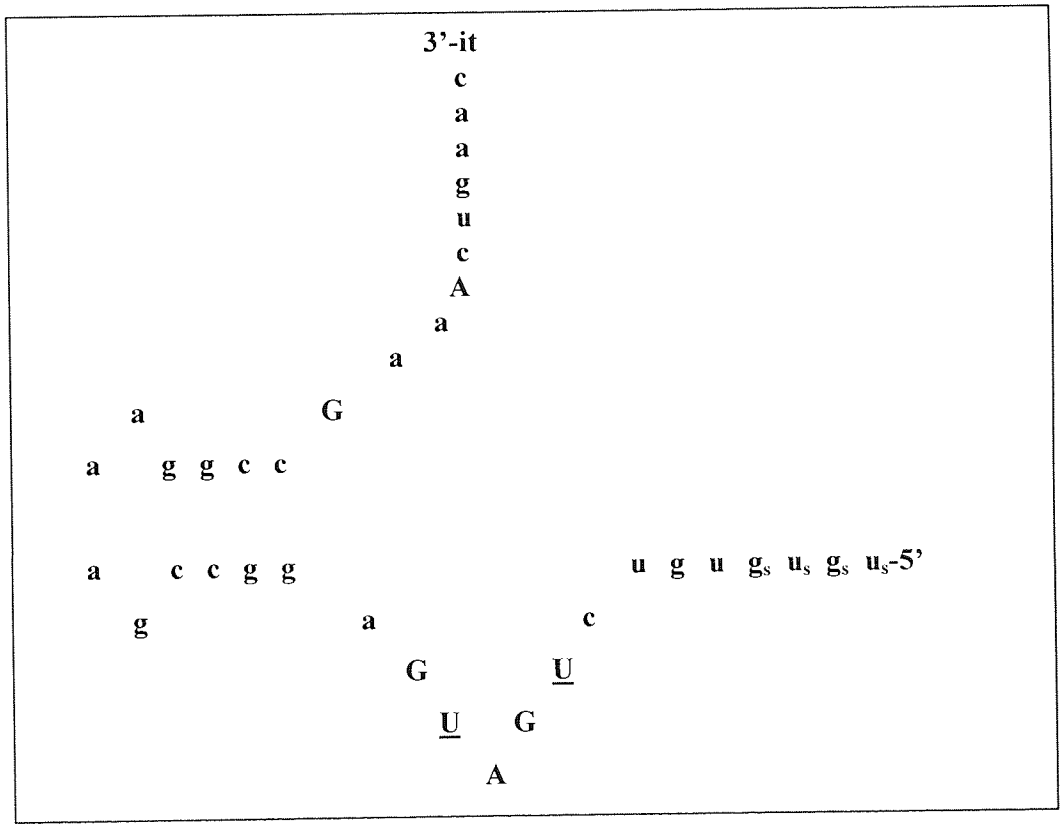

Figure 1.9. *Chemical modifications applied to ribozyme RPI.4782. (1) Uppercase indicates 2'-hydroxyl (ribo) nucleotides. (2) Lowercase indicates 2'-O-Methyl nucleotides. (3) U indicates 2'-amino at positions U4 and U7. (4) it indicates inverted Thymidine. The subscript 's' on the four nucleotides near the 5'-end indicates the phosphorothioate linkages on these nucleotides.*

This ribozyme is designed against the 3' untranslated region of the EGFR mRNA. The First four nucleotides from the 5' side have phosphorothioate internucleotide linkages. All the nucleotides that are shown by lowercase have 2' O-methyl modifications on their bases. The nucleotides, which, are underlined, have 2'-NH_2 modifications. All nucleotides, which are in upper case, are unmodified RNA nucleotides. These modifications are made to increase the stability of the ribozyme. The 'it' at the 3' site shows an inverted thymidine group, which is added to prevent degradation due to 3'exonucleases.

1.7. EPIDERMAL GROWTH FACTOR RECEPTOR

The ribozyme RPI.4782 used in this study targets the 3'untranslated region of the epidermal growth factor receptor mRNA therefore a brief synopsis of the epidermal growth factor receptor (EGFR) is provided below.

The epidermal growth factor receptor (EGFR) is a 170 kDa transmembrane glycoprotein consisting of an extracellular 'ligand' binding domain, a transmembrane region and an intracellular domain with tyrosine kinase activity (Kung *et al.*, 1994). The binding of growth factors to EGFR results in dimeric ligand-receptor complex formation, phosphorylation of the intracellular domain of the receptor and other protein substrates, leading ultimately to DNA synthesis and cell division. The external ligand binding domain is stimulated by epidermal growth factor (EGF) and also by TGFα, Amphiregulin and some viral growth factors (Modjtahedi and Dean, 1994).

EGFR is encoded by the gene c-erbB1, which is located on chromosome 7. Recent studies have shown that the EGFR is over expressed in a number of malignant human tissues when compared to their normal tissue counterparts (Khazaie *et al.*, 1993). An important finding has been the discovery that the gene for the receptor is both amplified and over expressed in a number of cancer cells. Over expression of EGF and TGFα, suggest that an autocrine pathway for control of growth may play a major part in the progression of tumours (Sporn and Robert, 1985). It is now widely believed that this is a mechanism by which tumour cells can escape normal physiological control.

Growth factors and their receptors appear to have an important role in the development of human brain tumours. A high incidence of over expression, over amplification, deletion and structural rearrangement of the gene coding for the EGFR has been found in biopsies of brain tumours (Ostrowski *et al.*, 1994). In fact the amplification the EGFR gene in glioblastoma multiforme tumours is one of the most consistent genetic alterations known, with EGFR being over expressed in approximately 40% of malignant gliomas (Black, 1991). It has also been demonstrated that in 50% of glioblastomas, amplification of the EGFR gene is accompanied by the co-expression of mRNA for at least one or both of the growth factors EGF and TNFα (Ekstrand *et al.*, 1991).

The amplified genes are frequently rearranged and associated with polymorphism leading to abnormal protein products (Wong *et al.*, 1994). The rearrangements that have been characterised usually show deletions of part of the extracellular domain, resulting in the production of an EGFR protein that is smaller in size. Three classes of deletion mutant EGF receptor genes have been identified in glioblastoma tumours. Type I, mutants lack the majority of the external domain, including the ligand binding site, type II, mutants have a deletion in the domain adjacent to the membrane but can still bind ligands and type III, which is the most common and found in 17% of glioblastomas, has a deletion of 267 amino acids spanning domains I and II of the EGFR.

In addition to glioblastomas, abnormal EGFR expression has also been reported in a number of squamous epidermoid cancers and breast cancers (reviewed in Kung *et al.*, 1994). Interestingly, evidence also suggests that many patients with tumours that over express EGFR have a poorer prognosis than those who do not (Khazaie *et al.*, 1993). Consequently, therapeutic strategies, which can potentially inhibit or reduce the aberrant expression of the EGF receptor, are of great interest as potential anti-cancer agents.

1.8. AIMS AND OBJECTIVE

As recounted above ribozymes due to their high molecular weight, polyanionic character and chemistry have poor biological stability, limited cellular uptake and inappropriate subcellular localisation and to become successful therapeutic agents need further development. These limitations of ribozymes are further accentuated when ribozymes are designed against biological and pathological targets in the central nervous system. It was the aim of this report to characterise the extent and mechanism of cellular delivery of ribozymes in cultured neuronal and glial cells from rats and humans and to investigate any potential difference in the uptake characteristics between the two species and type of cells with a view to design polymeric delivery systems to optimise the cellular association of ribozymes. It was further aimed to evaluate the cellular association characteristics after incorporation of ribozymes in polymeric microparticle delivery systems. Finally, it was aimed to evaluate the extent of distribution of ribozyme incorporated in polymeric microspheres after localised injection in comparison to free ribozymes with respect to time and region of the brain, which is the target organ for the glioblastoma or neuroblastoma directed therapies. In order to achieve the above aims following specific objectives were laid out:

1. To investigate the stability of the ribozyme RPI. 4782 *in vitro* and *in vivo* after ICV injection.
2. To characterise the cellular association of ribozyme as a function of time, temperature, pH, metabolic, competitive inhibitors, efflux patterns and intracellular localisation in glial and neuronal cells *in vitro* of human and rat species
3. To identify ribozyme binding cell membrane proteins as potential carriers for mediating cellular uptake of ribozymes.
4. To formulate and characterise a delivery system of PLGA polymer to provide a sustained release of ribozyme and enhanced stability *in vitro* and to study the extent of microsphere entrapped ribozyme uptake in cultured cells with respect to time, temperature, metabolic inhibitors and pH.
5. To evaluate the distribution of the free and polymer entrapped ribozyme after ICV injection in terms of time and space.

CHAPTER TWO

MATERIALS AND GENERAL METHODS

General methods and materials, which were routinely utilized in the experimental work for the preparation of thesis, are described in this chapter. Specific details and variations to the standard procedures are outlined in the relevant chapters.

2.1. MATERIALS

All chemicals used were of the highest grade available from Sigma-Aldrich Company Ltd (Poole Dorset, UK) unless otherwise specified. All reagents were used as received without further purification.

Cell culture reagents and media were purchased from Life Technologies Inc (Paisely, UK). Tissue culture flasks, multi-well tissue culture plates, 15mL and 50mL polypropylene tubes were purchased form Becton Dickinson and Company (Plymouth, UK). Disposable pipettes, microcentrifuge tubes, Finnipipette tubes, Finnipipette tips and 1.5 mL Biofreeze vials were purchased from Sarstedt (Leicester, UK)

The ribozyme used in this study was kindly provided by Ribozyme Pharmaceuticals Inc. (Boulder, Colorado, USA) and was given the number RPI. 4782. It is a 37-mer hammerhead ribozyme with the following sequence:

(5'-UGUGUGUCUGAUGAGGCCGAAAGGCCGAAACUGAACT-3')

2.2. General Methods

2.2.1. Precautions for handling RNA

Once deprotected, RNA is highly susceptible to degradation by the action of 2'-hydroxyl dependent ribonucleases. These ribonucleases (RNases) are present on the surface of the skin and are often present on laboratory glassware and plastic-ware. Stringent aseptic handling is, therefore required to minimise the action of these RNases. As a result, following precautions were taken:

All glassware and plastic-ware was treated with 0.1% (v/v) Diethyl pyrocarbonate (DEPC)–water before use, as DEPC is a strong in-activator of most ribonucleases. The plastics and glassware were soaked in DEPC treated water for at least 4 hours at 37°C, following which they were autoclaved for 15 minutes. RNAase free water was prepared by adding 0.1% DEPC to sterile double distilled water for a period of at least 12 hours and then autoclaved.

Wherever possible, solutions were also treated with 0.1% DEPC in the same manner as above. Solutions containing the buffer, Tris, however, could not be treated with this inhibitor as DEPC reacts readily with amines. In such cases, autoclaved double distilled water was used instead.

Electrophoresis tanks were also stringently cleaned before use with RNA. The tanks were washed with detergent, rinsed with water, dried, treated with ethanol and then filled with a solution of 3% hydrogen peroxide for a period of 10 minutes. Following this treatment they were then thoroughly rinsed with DEPC treated water (Sambrook *et al.*, 2002).

2.2.2. Quantification of ribozymes

The concentration of ribozyme was determined by UV spectroscopy at 260nm. The purine and pyrimidine bases of DNA and RNA strongly absorb light with maximum near 260nm. The absorbance reading can be translated to the concentration according to Beers Law:

$$A=\varepsilon cl$$

where :

A = Absorbance

ε = Molar extinction coefficient

c = Concentration(mg/mL)

1 = path length (typically 1 cm)

The following method converts O.D units into μg units based on the molecular weight of the sequence (Brown and Brown, 1991).

A. Calculation of Molecular weight (MW)

$$MW = (249 \times nA) + (240 \times nT) + (265 \times nG) + (225 \times nC) + (64 \times n-1) + 2$$

Where :-

nA = number of adenine bases, nT =number of thiamine or in the case of RNA Uracil bases, nG =number of guanine bases, nC =number of cytosine bases in the sequence.

n= total number of bases.

(64×n-1) accounts for the molecular weight of the phosphate groups.

A. Calculation of Micromolar Extinction Coefficient, ε, at 260 nm

$$\varepsilon = \{(8.8 \times nT) + (7.3 \times nC) + (11.7 \times nG) + (15.4 \times nA)\} \times 0.9^*$$

nA = number of adenine bases, nT =number of thiamine or in the case of RNA uracil bases, nG =number of guanine bases, nC =number of cytosine bases in the sequence.

* It is necessary to multiply the extinction coefficient of the sum of the individual bases by 0.9 because the base stacking interactions in the single strand suppress the absorbance of DNA.

B. Conversion of OD units to mass of ribozyme (μg)

When the concentration of any nucleic acid is 1mg/mL then the micromolar extinction coefficient is given as

MW/1000=ε

Therefore 1mg=ε

If ε is x OD

Then

1mg = x OD

1OD = 1/x= y mg (eq.1)

From the spectrophotometer, the absorbance reading was taken which shows the OD value. This value was processed using eq.1 to give the mass of ribozyme in mg. This method however does not allow for differences in molecular weight between phosphodiester and phosphorothioate oligoribonucleotides and modified ribozymes. The following adjustments were made to account for these differences.

2.2.3.1. PHOSPHOROTHIOATES

In this case, a Sulphur (MW=32) replaces Oxygen (MW=16) on the phosphodiester side chain. Consequently, an adjustment of +16 is made for n-1 bases.

i.e. MW=(249×nA) + (240×nT) + (265×nG) + (225×nC) + (**80**×n-1) + 2

2.2.3.2. UNMODIFIED RNA

Adjustments are required to account for additional Oxygen (MW=16) on the 2'site of each nucleotide. The adjustment in this case is +16 for each base and an allowance for the difference in MW between Thymine and Uracil.

MW= (**265**×nA) + (**242**×U) + (**281**×nG) + (**241**×nC) + (64×n-1) + 2

2.2.3.3. MODIFIED RIBOZYMES

Adjustments are required to allow for each modification. For example in the case of ribozyme RPI.4782 the following adjustments were made:

4×phosphorothioates	=(4×16)	=+64
5×unmodified RNA	=(5×16)	=+80
29×2'O-methyl	=(29×30)	=+870
2×NH_2	=(2×15)	=+30
Total adjustment		=+ 1044

2.3. Radiolabelling of Nucleic Acids

2.3.1. 5'-end labelling

Synthetic oligonucleotides are synthesized without a phosphate group at their 5'termini and are therefore easily labelled by transfer of the γ^{32} P from [γ-^{32}P] ATP using the enzyme T4 polynucleotide kinase.

The ribozyme used for *in vivo* stability study was 5'end labelled as described below.
Reaction mixture:

RNA substrate		*100 pmole*
T4 Kinase		*1 μL*
*10×reaction buffer**		*1 μL*
γ^{32}P[ATP]		*1 μL*
DEPC ddH_2O	*to*	*10 μL*

*Reaction buffer comprised:
100mM Tris pH7.5, 20mM $MgCl_2$, DTT, 0.2mM Spermidine, 0.2mM EDTA
The reaction mixture was incubated for 45 minutes at 37°C

2.3.2. Internal labelling of ribozyme RPI.4782

5'-end γ^{32}P labels are susceptible to removal by phosphatase enzymes present in serum and cell culture. Ribozyme RPI. 4782 was internally labelled in order to avoid the loss of label through the action of these enzymes. To facilitate this ribozyme RPI.4782 was obtained in

two halves, a donor half and an acceptor half which were then joined together using T4 RNA Ligase. The following two fragment sequences were consequently obtained:

Donor : 5'-gaa agg ccG aaA cug ccc t –3'

Acceptor : 5'-$u_s g_s u_s$ $g_s$ug ucU GAU Gag gcc –3'

T4 RNA Ligase catalyses the formation of phosphodiester bonds between the 5' phosphate of a single stranded donor RNA and the 3' hydroxyl of a single stranded acceptor RNA. Internal labelling was performed in two steps. In the first step, the donor half was labelled with γ^{32}P at the 5' end in the following reaction mixture:-

1st step 5' end labelling:-

Donor half of the ribozyme		*100 pmol*
T4 Kinase buffer		*1μL*
T4 Polynucleotide kinase (Bioline catalogue number M25801b)		*1μL*
γ^{32}P ATP		*1μL*
DEPC treated ddH_2O	*to*	*10μL*

The reaction mixture was incubated at 37°C for 60 minutes. The mixture was then rapidly heated to 65°C for 15 minutes to inactivate the kinase.

2nd step LIGATION.

To ligate the acceptor to the donor T4 RNA Ligase was added to the above in the following scheme:

Acceptor half of the ribozyme		*200pmol*
Ligase buffer		*2μL*
T4 RNA ligase		*1μL*
DEPC treated ddH_2O	*to*	*20μL*

The reaction mixture was then left in the refrigerator for 12 hours at 4°C. Finally, the radio-labelled full length ribozyme was isolated and purified by using polyacrylamide gel electrophoresis (see section 2.3.4).

Sequence of the ligated ribozyme:

5'-$u_s g_s u_s$ $g_s$ug ucU GAU Gag gcc gaa agg ccG aaA cug ccc t –3'

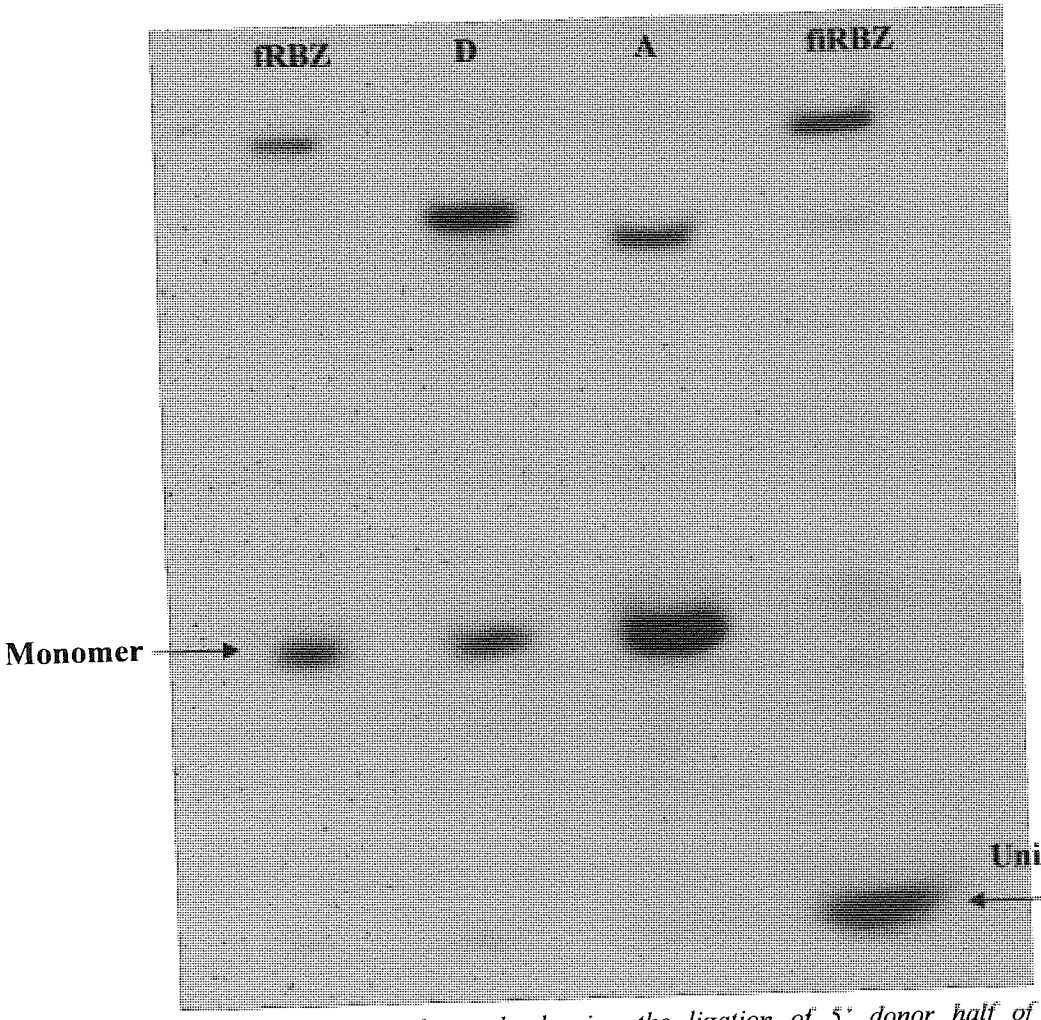

Figure 2.1. *Autoradiograph showing the ligation of 5' donor half of ribozyme (D) to Acceptor half (A) of ribozyme to form a full internally labelled ribozyme (fiRBZ). Lane contains a 5' labelled full ribozyme (fRBZ) which was used as size matched control.*

2.3.3. Purification of radiolabelled ribozyme.

The radio-labelled ribozyme was isolated and purified using the polyacrylamide gel electrophoresis procedure. In electrophoresis, strands of varying lengths of nucleotides are separated based on their charge in an electric field across a polyacrylamide gel.

Polyacrylamide gels are formed by the vinyl polymerisation of acrylamide monomers (CH_2=CH-CO-NH_2) into long random chains of polyacrylamide which are cross-linked by the inclusion into the mixture of small amounts of a co-monomer, N-N'-methylene-bis-acrylamide, commonly known as "*Bis*". The resulting cross linked chains form a gel structure, the pore size of which is determined by the concentrations of both acrylamide and Bis-acrylamide (procedure for setting a gel is described in the next section). As individual strands of nucleic acids have specific charges depending on their chemistry and length of nucleotide sequence, these strands move at different speeds and form separate bands. These bands were then visualised using autoradiography as described in the next section.

2.3.4. Polyacrylamide gel electrophoresis

After the radio-labelling was complete the reaction mixtures were mixed with an equal volume of loading buffer {5% glycerol in 1×TBE(Tris-borate EDTA buffer)} and 1μL of marker dye (Bromophenol blue 100 mg in 20mL of 5%glycerol in 1×TBE). The dye was added to track the progress of sample migration down the gel once the samples were loaded on to the gel. Polyacrylamide gels were set up as described by (Sambrook *et al.*, 2002) using a Protean II electrophoresis apparatus (Bio-Rad). Two glass plates (20cm × 20cm) were clamped together with separators between them and then fitted on the gel stand vertically. To this plate cast 50mL of the gel mixture was added and a comb added to form wells. The polyacrylamide gel mixture was prepared as follows

*20% polyacrylamide gel solution**	*50 mL*
TEMED	*40 μL*
10% Ammonium persulphate	*600 μL*

*The polyacrylamide gel solution had the following composition:

30% polyacrylamide		*333mL*
***Urea*		*420g*
10×TBE		*50mL*
ddwater	*to*	*500mL*

**For native gel, the urea is omitted.

TEMED (N,N,N',N'-trimethylethylenediamine) and Ammonium persulphate were added to activate the polymerisation reaction. The gel was allowed to set for 30 minutes and the combs removed and the wells washed with sterile 1xTBE. Below is the composition of the TBE.

10×Tris borate buffer(TBE)		
Tris base		*54g*
Boric acid		*27.5g*
EDTA(0.5M, pH8)		*20mL*
ddH_2O	*to*	*1000mL*

The electrophoresis was carried out using 20% acrylamide gel (20×20×0.03cm) in sterile 1×TBE buffer at room temperature. The gel was pre-run for 15 minutes at 300mV before loading the samples. The gel was then run at 300mV for 3 hours at which point the samples had migrated to the middle of the gel as seen by the marker dyes. The required bands of the ribozyme were visualized by autoradiography subsequently.

2.3.5. Autoradiography

Following electrophoresis the gel was removed from the glass plates, wrapped in a single layer of Saran wrap and placed in a Hypercassette fitted with an intensifying screen (Amersham, UK). Under dark room conditions a sheet of Kodak HP autoradioraph film was placed on top of the gel and was left to be exposed to the gel. The radiation from the gel causes bands to be formed on the film, which were visualised by developing and fixing the film in Kodak reagents. The processed film was then placed on placed on the gel to identify the ribozyme bands. These bands were then excised and suspended in 3mL DEPC ddH_2O and placed on a mechanical shaker for 3 hours to elute the labelled nucleic acids from the gel fragment. The amount of nucleic acid, which elutes out was then lyophilised in a Savant Speed Vac.

2.3.6. Purification of radiolabelled ribozyme

Pellets of lyophilised radio-labelled ribozyme were reconstituted in 50μL of DEPC treated sterile double distilled water in an eppendorf tube to purify using miniQuick spin columns. Firstly, the column was shaken to re-suspend the matrix and placed in an eppendorf for centrifugation at 1000g in a MSE MicroCentaur centrifuge for 1 minute. This step packs the column and removes the residual buffer. Following this, the column was placed in a new eppendorf tube and the sample was applied to the column bed of the spin column and centrifuged at 1000g for 4 minutes. The resultant eluate left in the eppendorf tube contained the radio-labelled purified ribozyme.

2.3.7. Liquid scintillation counting (LSC)

The activity in cpm of the radio-labelled nucleic acids was determined by LSC. A small volume of the sample was added to 5mL of Optiphase Hi-Safe 3 (Pharmacia Wallace) and counted in a Packard 1900 TR scintillation counter for 5 minutes. Adjustments were automatically made for the background, radioactive decay during the experimental period by entering the half life and reference date of the radioisotope used.

2.4. CELL CULTURE TECHNIQUES

2.4.1. General cell culture maintenance techniques

2.4.2. CELL LINES

Four cell lines were used in this study: U87, C6, GT1 and SY5Y.

The U87-MG cell line was purchased from the European Culture Collection, Porton Down , UK and consist of human glioblastoma astrocytoma cells which were originally derived form a grade 3 malignant glioma by explant technique. The C6 (rat glial cells), SY5Y (human neuroblastoma cells) and GT1 (rat neuroblastoma cells) were kindly provided by Dr. Dawn Smith a researcher at our laboratory.

2.4.3. CELL CULTURE MEDIA

The cells were maintained in different media as previously used in the laboratory and listed in the table below.

Cell Line	Medium
U87	Dulbecco's Modified Eagle Medium HEPES (Gibco)
C6	Dulbecco's Modified Eagle Medium HEPES (Gibco)
SY5Y	50 % Nutrient Ham F-12 (Sigma) + 50% Modified Eagle Medium (Sigma)
GT1	50% Dulbecco's Modified Eagle Medium (Gibco) + 50% Nutrient Ham F-12 (Sigma)

Table 2.1. A table to show the growth media requirements of the different cell lines.

All media were supplemented by 10% v/v foetal bovine serum (FBS), 1% v/v L- Glutamine (2mM) and 1% v/v penicillin/streptomycin. The same media but without the addition of FBS was used for some stability studies.

2.4.4. MAINTENANCE OF STOCK CULTURES

Cells were cultured in 75cm^2 plastic tissue culture flasks (Sarstedt, UK) with 25mL of medium depending on the cell line as in the previous table and were incubated at 37°C in a humidified (95%) atmosphere of 5% CO_2 in air. Stock cultures were passaged when confluent after approximately 4 days. Passaging was carried out using the following procedure:

The medium was aspirated out and the cells were washed with 5mL of sterile PBS. After aspirating out the sterile PBS, 3mL of 1×trypsin solution (0.25% w/v trypsin, 0.2% w/v EDTA in PBS, pH 7.2) was added and the flask was incubated at 37°C for 5 minutes. The flask was tapped to dislodge the cell monolayer from the bottom and 7mL of fresh media was added to neutralise the trypsin, which made the final volume to 10mL. The contents of the flask were mixed well by repeated pippetting to form a cell suspension. From this cell suspension a volume of 3mL was taken and placed in to a new 75cm^2 flask to which 22mL of fresh media had already been added. This resulted in a final volume of 25mL and the flask was returned to the incubator.

2.4.5. LONG TERM STORAGE OF CELLS

For long-term storage of cells, a suspension of cells was prepared according to the following protocol:

A cell suspension was prepared as described in the above section up to a volume of 10mL. This suspension was transferred to a 15mL universal tube (Falcon, UK) and centrifuged for 5 minutes at 1000g (MSE mistral 3000i) to form a pellet of cells. The supernatant was discarded and the pellet was resuspended in freezing medium (10% DMSO in serum medium) to form a concentration of not less than 1 million cells per mL. A volume of 1mL was taken and placed in a 2mL screw capped cryovial (Costar, UK). The vial was then left at -70°C for 24 hours, followed by placement in liquid nitrogen cell bank. When required, cells were brought up from the cell bank. For this a frozen cryovial was rapidly thawed at 37°C and the contents of the vial were gradually diluted with serum medium before seeding in 25cm^2 flasks (Falcon, UK). The medium from this flask was changed after 24 hours to remove the remaining traces of DMSO.

2.4.6. DETERMINATION OF CELL NUMBER/VIABILITY

The viable cell density of stock cultures was measured by haemocytometry using a Trypan Blue exclusion assay test. This assay is based on the principle that the Trypan blue dye is only taken up by dead cells and is used to determine the number of viable cells in a population of cells. For this purpose a 100 μL volume of Trypan Blue (4mg/mL) was mixed with 400μL of cell suspension and 500μL of serum medium to make a final volume of 1mL (2.5×dilution) in an eppendorf tube and mixed well. From this a ≈ 50μL of the Trypan blue cell suspension was transferred to the counting chamber of a Neubauer haemocytometer, with depth of 0.1mm and area 1/400mm^2 (Weber Scientific International Ltd, UK). The non-stained cells were counted in five large squares of the haemocytometer using a light microscope and the cell density was calculated using the following equation:

$$\textit{Cells per mL} = \textit{average count per square} \times 10^4 \times 2.5 \textit{ (dilution factor)}$$

2.5. Cell growth assays

In order to obtain an idea of the growth kinetics of the cell populations, cell growth assays were carried out for all cell lines. In these studies cells were seeded at three densities and their growth followed over a period of five days. The seeding densities used were 0.1×10^5, 0.5×10^5 and 1×10^5 cells per mL. Cells growing in 75cm^2 flasks were trypsinised as described in 2.3 and were counted to obtain their density as in the previous section. From the cell suspension required amounts of the cells were taken to make cell suspensions of the required concentrations to seed on to 24 well plates. The plates were incubated at 37°C for various time points and trypsinised as described in section 2.4.1.3 and counted as described in section 2.4.1.5.

2.6. Ribozyme stability studies

In order to evaluate the structural integrity of the chemically modified RBZ RPI.4782 in different biological milieu, stability studies were carried out. For this purpose the ribozyme was internally labelled as described in section 2.3.2 and incubated in different media over a time course and any degradation was visualized using autoradiography.

2.6.1. Stability in serum and serum free media

The radio-labelled ribozyme (100pmole) was incubated in 200μL of serum and serum free medium at 37°C. Aliquots of 20μL were taken at timed intervals and placed in prefrozen eppendorf tubes, which contained RNAaseIN (Gibco, UK) and held at -70°C freezer until all the samples were taken. These samples were mixed with an equal quantity of loading buffer (1% v/v glycerol in PBS) and then loaded on to a denaturing gel 20%(PAGE + 7M urea) to obtain degradation profiles.

2.6.2. Stability on a cell monolayer

In this experiment cells were seeded at density of 10^5 cells per well in 24 well plates and left to grow for 2 days until a confluent monolayer was achieved inside the wells. The medium was aspirated and the cells were then washed with sterile PBS (Phosphate buffered saline) three times to remove any protein from the serum medium. The monolayer was replenished with 300μL serum free medium, which had been warmed to 37°C. The internally labelled ribozyme was incubated on this monolayer for timed intervals as in the above section. Aliquots of 20μL were taken at required time points and then analysed by electrophoresing on a denaturing gel and visualisation with autoradiography.

2.6.3 Stability of a ribozyme after ICV injection *in vivo*

A male Wistar rat weighing approximately 180-220g was anaesthetised and injected in the lateral ventricle with 100pmole of full ribozyme as described in sections 2.11.1. After 24 hours the rat was sacrificed and the brain was acquired as in section 2.11.2 and the ribozyme recovered using the following protocol.

The brain was homogenised with a pestle gently in 10mL sterile PBS containing 2μl of RNAaseIN (30-40 units). Following this the homogenate was centrifuged at 3000g for 30 minutes at 4°C and the pellet discarded. The supernatant was then divided in 5 eppendorfs and dried to pellets. These were then reconstituted in 100μL of sterile double distilled water with 10μL of DNAse. These eppendorfs were then incubated at 37°C for 30 minutes. To this 250μL of chloroform was added and mixed by vortexing. This mixture was then centrifuged at 13000 rpm for 10 minutes at room temperature. To the upper aqueous layer a further

500μL of chloroform was added and then centrifuged at 13000rpm for another 10 minutes at room temperature. The upper layer was then transferred to a new eppendorf and 150μL of 0.3M sodium acetate was added and the contents were split in to two tubes. To these then 750μL of ice cold ethanol was added and the tubes were then inverted to mix and incubated for 1 hour at -70°C. Centrifugation at 4°C for 15 minutes at a speed of 13000rpm followed this. The supernatant was carefully removed and 100μL of ice-cold ethanol was added without disturbing the pellet. Then, centrifuged for 5 minutes at 4°C. Finally the pellet was air dried for 15 minutes. After recovery the pellet was reconstituted with sterile DEPC treated double distilled water and 5'end labelled (see section 2.3.1). The radio-labelled ribozyme was then electrophoresed in 20% Polyacrylamide and 7M urea gel to determine any degradation of the ribozyme.

2.7. Cell association studies

A series of experiments was conducted to characterise the extent and mechanism of cellular association of the chimeric ribozyme RPI.4782 in the four cell lines. In all these experiments ribozyme RPI.4782 was internally labelled as described in section 2.3.2. and purified by 20% native polyacrylamide gel electrophoresis. Each experiment was carried out in quadruplicate unless otherwise stated. Cells growing in $75cm^3$ tissue culture flasks were trypsinised and the cell number determined using a Neubauer haemocytometer (see section 2.4.1.4). Cell suspensions were diluted, in serum media according to each cell type, to 10^5 cells per mL and then seeded in 24 well plates.

2.7.1. General protocol

Cells were seeded on 24-well plates (Falcon, UK) at a density of 10^5 cells per well. The plates were then placed in an incubator at 37°C which was humidified (95%) in an atmosphere of 5% CO_2 in air and the cells allowed to grow for 2 days to near confluency. Before the start of the experiment cells were counted using the Trypan blue exclusion assay, as the different cell lines have cells which are of different size and shape and which could introduce unnecessary complications in the analysis of the results. Knowledge of the cell numbers is required for calculation and rigorous analysis of the results as the data can then be normalised to cell numbers.

From the experimental wells media was then aspirated and the monolayer carefully washed three times with PBS (37°C) to remove any traces of serum. The washing solution was aspirated and replaced with 200μL of serum free medium containing the radio-labelled ribozyme. The PBS and serum free media were both equilibrated at 37°C for 1 hour in a water bath prior to the experiment. The plates were incubated at 37°C for the duration of the experiment.

Once incubated for the desired period, the apical medium was carefully removed and collected in scintillation vials. The cells were then washed 3 times with ice-cold PBS/ sodium azide (0.05% w/v NaN_3/PBS) to inhibit cellular metabolism and remove any ribozyme loosely associated with the cell surface. These washings were also collected in scintillation vials. Finally the cell monolayers were harvested by solubilisation with 0.5ml of 3% v/v Triton X-100 (Aldrich Chemical company, Gillingham, UK) in distilled water for 1 hour at room temperature. The wells were washed twice more (2×0.5mL) with Triton X-100 to ensure that all cells had been harvested. Once all the cellular fractions were collected in vials their radioactivity content was determined by liquid scintillation counting using a Packard 1900TR scintillation counter. Samples were collected in scintillation vials and 5mL of Optiphase Hi-safe 3 (Pharmacia-Wallace, St Albans,UK) was added. Samples were counted for 5 minutes using the relevant ^{32}P radionuclide programme to account for decay during the experimental period.

2.7.2. Assay to determine optimal number of Sodium-Azide/PBS washes

Following incubation with radio-labelled ribozyme and removal of apical medium, cells were washed with 0.5mL of PBS-azide at increasing number of times, i.e. from 1 wash to 5 washes, or until the monolayer was disturbed. Any such disturbance of the cell monolayer was checked by observation under the microscope after each wash. The radioactivity associated with the apical samples, the individual washes and the cell lysate was quantified using LSC.

2.7.3. Effect of time on cellular association.

Cell monolayers were incubated with equal quantities of ribozyme at 37°C for increasing time periods of 0.5, 1, 2, 4 and 6 hours. To determine if the cells had any intrinsic pinocytic activity, this was determined by investigating the cellular association of the fluid phase marker, [^{14}C] Mannitol, at 37°C over the same time points.

2.7.4. Effect of temperature on cellular association

All cell lines were incubated with equal amount of ribozyme for a period of 4 hour at 37°C or 4°C to determine the effect of temperature on cellular association.

2.7.5. Effect of metabolic inhibitors on cellular association

In order to determine the energy dependence of cellular association of ribozyme, cells were depleted of energy by pre-incubation with metabolic inhibitors 2-deoxyglucose (10mM) and sodium azide (50mM). Cells were seeded and grown as described earlier, followed by washing with PBS and treatment with serum free medium containing the metabolic inhibitors for 1 hour. The medium was then removed and radio-labelled ribozyme in serum free medium containing the inhibitors was added to the wells and thenceforth the standard procedure for uptake was followed.

2.7.6. Disassociation of intracellular ribozyme

To assess the intracellular compartmentalisation of ribozyme following cell association, efflux studies were carried out. Cells were incubated with radio-labelled ribozyme for 4 hours and then the apical medium was removed and placed in scintillation vials. Loosely attached ribozyme was removed with ice cold PBS/azide washes. Following this, 300μL serum free medium was added to cells and incubated for 30 minutes at 37°C. Following this the apical medium was removed and placed in separate scintillation vials. The cells were replenished with fresh serum free medium for another 30 minutes. This procedure was repeated for another 4 hours. Finally cells were solubilised with 3% Triton-X in double distilled water by shaking for 5 minutes on the shaker and placed in vials for LSC along with other fractions.

2.7.7. Effect of self-competition with cold ribozyme

Self-competition study was carried out to determine the specificity of the cellular association process. For this purpose cellular monolayers were incubated with increasing concentrations of non-labelled (cold) ribozymes and cellular uptake was determined as described previously.

2.7.8. Effect of competitive inhibitors on cellular association.

In order to assess whether large polyanionic molecules could compete with the cellular association of ribozyme, a competitive inhibition study was carried out. This experiment involved pre-incubating the cells with heparin (10μM), ATP (5μM), dextran (10μM) and salmon sperm DNA (50μL) and then removing these solutions and washing the cells with serum free medium once to remove loosely attached polyanions. To the wells then the radio-labelled ribozyme in serum free medium was added. This was followed by the normal procedure as shown in section 2.7.1.

2.7.9. Effect of pH on cellular association of ribozyme

Effect of pH on cellular association was carried out by incubating all cell lines in a range of pH values (5 to 8) instead of serum free medium. Incubation solutions of various pH values were prepared as follows: for values 7 and 8, Hanks balanced salt solution (HBSS) containing 5mM D-glucose and buffered with 25mM HEPES [(N-d-hydroxymethylpiperazine)-N'-2-ethanesulfonic acid]. For pH values 5 and 6, HBSS with D-Glucose buffered with MES [2-(N-morpholine)-ethanesulfonic acid] was used. Apart from this modification standard procedure was carried out.

2.7.10. Effect of post-cell association Trypsin washing

In order to further determine the nature of ribozyme binding molecules on cell surface, post-association trypsin washing assay was carried out. Cells were incubated with radio-labelled ribozyme for a period of 2 hours. The apical medium was removed and the loosely attached ribozyme was washed off with sterile ice-cold PBS/Azide. After this the cells were treated with 200μL of trypsin-EDTA until all cells were detached from the wells. To this 1mL of

PBS was added and the cells were recovered by centrifugation at 1000 RPM for 5 minutes. The supernatant was collected and cells were then resuspended in a further 1mL of PBS. The cell-associated radioactivity pertaining to both fractions (washing solution and cell) was determined by LSC.

2.7.11. Sub-cellular localisation of fluorescently labelled ribozyme

Cells of all the cell lines were counted, trypsinised and made into cellular suspensions of 5×10^4 cells/mL as described in sections 2.4.1.3. and 2.4.1.5. and seeded on Labtek chamber slides (Nunc, Gibco, UK.). After seeding, slides were left in the incubator for 24 hours to allow for the cells to grow. Solutions of 30pmol/200μL of ribozyme and 50pmol/μL of dextran-rhodamine 10S (Sigma, UK) in serum free medium were prepared. Cells growing in the chamber slides were washed with pre-warmed (37°C) sterile PBS for three times and then the cells were incubated with the above solutions for 4 hours. After the required time the apical medium was removed and the cells were washed with sterile PBS three times and were incubated with the fixative solution (2% formaldehyde in sterile PBS) for 30 minutes at room temperature. The fixing process protects the monolayer from damage and distortion in further experimental steps. After fixation the cells were washed with sterile PBS and then left to air dry. Once excess moisture was dried up cells were mounted and cover-slipped with Biomedia Gel (EMS, California). Finally cells were observed under a Zeiss microscope fitted with a UV producing mercury lamp and photographed using an Olympus camera with Jenamed adapter and Kodak colour film (ISO 200).

2.8. Identification of ribozyme binding cell surface protein

This experiment was designed to identity putative ribozyme binding cell surface proteins. The experimental procedure involved separation of different cellular fractions and then separating cell membrane proteins on a blotting membrane.

2.8.1. Sub-cellular fractionation

Cells were grown in $75cm^3$ tissue culture flasks and once confluent were trypsinised to harvest the cells. Cells were resuspended in sterile PBS and centrifuged at 1000g for 5

minutes in order to remove the trypsin. The pellet obtained was washed with sterile PBS and resupended in a 1ml volume of sterile PBS in an eppendorf centrifuge tube. Cells were again centrifuged for 5 minutes at 1000g. At this stage the pellet was kept and the supernatant discarded. To the pellet 200μL of nuclear extraction buffer (10 mM Hepes pH 8.0, 1.5mM MgCl, 10mM KCl, 1mM DTT, 10mM EGTA, 2mM EDTA, 1mM PMSF, 100 μM Leupeptin, 2μg/mL Aprotinin) was added and the cells resuspended. This cellular suspension was then left in ice for 15 minutes. This was followed by drawing up the suspension in a 23G needle fitted to a syringe five times in order to shear the cells. This mixture was then centrifuged at 1000g for 1 minute at 4°C. The pellet was discarded as it contains the nuclear proteins and the supernatant was kept as it contains cytosol, membrane and cytoskeletal fractions. This supernatant was then placed in a Beckman plastic tube, which was heat sealed and centrifuged at 100000g (Beckman Ultracentrifuge) at a speed of 57,556 rpm at 4°C for 45 minutes. After centrifugation the supernatant was discarded and to the pellet another 200μL of nuclear extraction buffer was added to which this time 1% Triton-X 100 was added and mixed. This was then left in ice for 30 minutes with occasional vortexing. This was followed by centrifugation at 100000g for 45 minutes at 4°C. The resulting supernatant was the membrane fraction. To this fraction a half volume of sample buffer (2.5mL Glycerol, 1mL 10% SDS, 1mL β-mercaptoethanol, 5mM Tris, 1mg bromophenol blue crystals to a final volume of 5mL) was added and heated to 90°C for 3 minutes and then immediately placed in ice to prevent re-naturation of the proteins and then left for storage in a -70°C freezer.

2.8.2. Estimation of protein content

The protein content of the resulting cell membrane fraction was determined by using a Bio-Rad protein assay. This assay in based on the principle that an indicator dye will change colour in response to various concentrations of protein. The absorbance maximum for an acidic solution of Coumassie Brilliant Blue G-250 shifts from 465nm to 595nm when binding to protein occurs.

Samples of varying concentrations of BSA (0μg/mL-25μg/mL) were prepared for constructing a calibration curve. Cell membrane fractions of unknown concentrations were diluted to obtain a final volume of 800μL. The assay was initiated by adding 200μL of dye

reagent concentrate to each tube of standard and unknown samples and by mixing well before incubating at room temperature for 15 minutes. Absorbance at 595nm was then read using a spectrophotometer (Jenway, UK). A calibration curve was constructed by plotting net absorbance versus the concentration (μg/mL) of the protein standards at 595nm. The calibration curve was then used to determine the amount of protein in the unknown cell membrane fractions.

2.8.3. South-Western blotting protocol

The blotting procedure was carried out using the Bio-Rad mini protean II system using a method described previously by Morton *et al.*, (1995). A 12.5% polyacrylamide gel was set up using the Bio-Rad mini-Protean II system under manufacturer's specifications. The cast was assembled and the resolving gel made up of the following specifications and allowed to set for about 30 minutes [3.2 ml 30% acrylamide, 1.9ml resolving buffer (1.5M Tris-HCl, 0.4% SDS pH 8.8), 2.4mL water, 75μL 10% SDS, 7.5μL TEMED, 1.5μL 10% Ammonium persulphate (AMPS) (freshly made). The resolving gel was then overlaid with a few drops of n-butanol to ensure the surface stayed flat. When the gel was set, the n-butanol was removed and 6% stacking gel [1.25ml 30% acrylamide, 1.56ml stacking buffer (0.5M Tris-HCl, 0.4% SDS pH 6.8), 3.37 mL water; 62.5μL 10% SDS, 6.25μL TEMED, 62.5μL 10% AMPS] was overlaid and the comb inserted. This was allowed to set for 30 minutes and then the comb was removed and the wells were washed in running buffer (6g Tris-HCl, 28.8g Glycine, 1g SDS made up to 1 litre with water). Following this, equal amounts of protein were loaded in to separate wells and the tank was filled with running buffer. The proteins were resolved at 140V for approximately 3 hours. One well was loaded with 5μL of pre-stained molecular weight markers ranging from 27,000-180,000 Da (Sigma, UK).

Once the gel had run far enough, usually determined by the separation of the marker bands, the gel was disassembled and the stacking gel discarded. The gel was then allowed to equilibrate in transfer buffer (3.03 g Tris-HCl, 14.4g Glycine, 2% methanol made up to 1 litre with water) for 15 minutes before being assembled into the Biorad mini-Protean II transfer set-up. The gel was clamped between four sheets of Whatmann 3M filter paper and a piece of Hybond C nitrocellulose cut to the same size. The gel was rolled to release any trapped air bubbles and then put into the transfer clamps. The clamps were inserted into the

apparatus and the tank filled with transfer buffer. The protein was transferred to the nitrocellulose at 250 mA for 80 minutes after which the clamps were disassembled and the gels discarded. A Ponceau (0.1% Ponceau in 1% acetic acid) stain followed by destaining (1% acetic acid in water) detected the protein on the nitrocellulose to show whether equal protein amounts had been loaded. The nitrocellulose was then blocked with 2% BSA solution on the rocking table for 1 hour.

Then the nitrocellulose was washed with binding buffer (2mM HEPES, 75mM NaCl, 0.5M EDTA, 1mM DTT, 5% Glycerol, BSA 25mg/ 500mL) to remove excess BSA. After washing the nitrocellulose was placed in hybridisation bottles with 10ml of binding buffer at 37°C containing radio-labelled ribozyme and placed in a rotator at rate of 4 revolutions per minute for 4 hours. At required time points the nitrocellulose was removed and washed with a strong washing buffer (2mM HEPES, 150mM NaCl, 0.5M EDTA, 1mM DTT, 5% Glycerol, BSA 25mg/ 500 ml) to remove the loosely attached ribozyme. After washing the nitrocellulose it was wrapped in Clingfilm and placed in a hypercassette with a hyperfilm and allowed exposure for 15-20 minutes. After the required time point the film was developed and fixed as described in the section 2.3.5 on autoradiography.

2.9. Formulation and characterisation of PLGA microspheres

Poly lactide-co-glycolide P(LA-GA) co-polymers of three different polymer ratios were used
50:50., i.v. 6.6-8.8 (Medisorb, Alkermes)
80:20., i.v. .0.2 (Park Scientific from Polysciences, UK)
90;10., i.v. 0.22 (Park Scientific from Polysciences, UK)

The 50:50 and 80:20 ratio was supplied as a white odourless powder. Whereas the 90:10 ratio was brown, irregularly shaped solid particles. The polymers were stored in a dessicator at 4°C.

2.9.1. Preparation of large microspheres (10-20μm)

The microspheres were prepared using the double emulsion method. The internal solution was prepared by mixing 10μL of 4% PVA (Polyvinyl alcohol 87-89% hydrolysed, molecular

weight 13,000-23,000) solution and 20μL of ribozyme solution (the quantity of ribozyme solution varies with the concentration of the ribozyme solution) and the final volume made up to 100μL with ddH_2O. This was then added to the polymer solution, which was made by dissolving 500mg of the polymer in 5mL of DCM. This mixture was then vortexed for 5 minutes to generate the primary emulsion. The primary emulsion was added to 160mL of aqueous external phase comprising of 0.9% NaCl and 4% PVA. This mixture was then stirred for three hours at 1000rpm at room temperature using Heidolph stirrers (Labplant , Huddersfield, UK). The revolutions were confirmed by a hand held digital tachometer. The emulsion was then transferred to a magnetic stirrer plate, covered with parafilm and stirred for three hours to allow for complete evaporation of the DCM.

The resulting microspheres were centrifuged at 40000 rpm for 10 minutes (43124-708 rotor, 3000g Mistral 3000 centrifuge MSE Leicester Ltd) and washed three times with distilled water to remove any non-encapsulated ribozyme and emulsifying agent. The resulting microspheres were resuspended in 1ml distilled water, frozen at –70°C and freeze dried over night (Edwards Modolyu, BOC Ltd, Sussex, UK).

2.9.2. Preparation of small microspheres (1-5μM)

A 1-5μm size range of microspheres was also manufactured to assess the effects of microsphere size on ribozyme loading and release profiles.

The microspheres were prepared using the double emulsion method as described in the section above with the volumes being the same but a different mixing method was employed. The primary emulsion was mixed at 4000 rpm using a Silverson homogeniser STD2 (Silverson Machines, Chesham, Bucks, UK) with a 3/8" mini-micro probe (Silverson Machines, Chesham Bucks, UK) for 2 minutes. The resultant emulsion was then further mixed at 6000 rpm using a 1" tubular probe (Silverson Machines, Chesham, Bucks., UK) for 6 minutes. The w/o/w (water-in-oil-in-water) emulsion was stirred on a stirring plate for a minimum of 4 hours to allow the solvent to evaporate and the spheres were centrifuged and freeze dried as before. The resulting spheres were weighed on an electronic balance and stored in a dessicator at room temperature.

2.9.3. Microsphere batch yield determination

The yield of the microspheres was determined using the following formula;

$$\% \text{ Yield} = (\text{weight of microspheres/weight of polymer}) \times 100$$

2.9.4. Microsphere entrapment efficiency and loading

This method involved direct liquid scintillation counting of ribozyme encapsulated microspheres and aqueous solution of ribozyme. 25mg of microspheres were added to 5mL of Optiphase Hi-Safe (Pharmacia-Wallace, St. Albans UK) and counted as in section 2.2.4. Also 5µL of free radio-labelled ribozyme aqueous suspension of known concentration was checked for counts per minute. All samples were assayed in triplicate and results are the mean of three determinations. From these results the % ribozyme encapsulated per dry weight of microspheres could be determined and the encapsulation efficiency calculated.

$$\% \text{ Encapsulation efficiency} = (\text{cpm of RBZ solution used/cpm of microspheres}) \times 100$$

$$\text{Theoretical loading} = (\text{amount of ribozyme/ wt of polymer}) \times 100$$

$$\text{Actual loading} = (\text{amount of ribozyme entrapped/wt of microspheres}) \times 100$$

2.9.5. Microsphere particle size determination

10mg of microspheres were redispersed in double distilled, 0.2µm filtered water and sized by laser diffractometry using a Malvern mastersizer E particle sizer (Malvern Instruments, Malvern, UK). The instrument was fitted with a 45mm angle lens and flow cell. The average size of spheres and size range was plotted using a software package (Malvern, UK).

2.9.6. Scanning electron microscopy

The surface morphology of the microspheres was examined using scanning electron microscopy. Samples were prepared by mounting on aluminium stubs using carbon tape, and coated with gold for 15 minutes under an argon atmosphere (Emsope SC500). Under magnification using a Cambridge Instruments Stereoscan 90B, the surface of particles was studied. Photomicrographs were taken using a Nikon 35mm camera.

2.9.7. Release studies of microspheres *in vitro*

The release of ribozymes from microspheres was performed by incubation of 25mg of spheres in 1.5mL release medium in glass sample tubes. The release medium used was phosphate buffered saline (PBS) (137mM NaCl, 2.7mM KCl and 10mM phosphate buffer pH 7.4). The tubes were incubated at 37°C in a shaking water bath. Release of radio-labelled RBZ was monitored at intervals over a 28 day period. Samples were taken at hourly intervals on the first day for 6 hours, then daily for 7 days and then on 14, 21 and 28 days. At each sampling time the release medium was removed and centrifuged at 13000 rpm for 5 minutes to remove any suspended microspheres. The supernatant was removed for liquid scintillation counting as in section 2.3.7. A 1.5mL aliquot of fresh release medium was added to the microsphere pellet, which was re-suspended and replaced into the release vial.

2.9.8. Stability of polymer entrapped ribozyme

Radiolabelled ribozymes were encapsulated into microspheres as in section 2.9.2. The microspheres were incubated in release medium as detailed in section 2.9.7. The entrapped ribozyme was extracted from the microspheres after a 24 hour period. The extraction of ribozyme from the polymer involved dissolving the microspheres in 2mL chloroform, vortexing with 2mL sterile water for 5 minutes and then centrifuging at 1000g for 1 minute. The aqueous layer containing the ribozyme was removed and concentrated by speed vacuum centrifugation (Savant, UK). The extraction procedure was repeated three times. The stability of these samples was assessed by running down a denaturing 20% polyacrylamide gel as described in section 2.3.4.

2.10. Cellular association of polymer entrapped ribozyme

Before proceeding with microsphere association studies certain optimisation steps were taken and these were to evaluate any negative effect on the growth of cells when incubated with various amounts of microspheres over a time course. Also varying amounts of microspheres were used to evaluate the optimum amount of microspheres required for association studies. Also the optimum number of washes was determined to remove loosely attached microspheres.

2.10.1. Determination of optimum number of Sodium-Azide/PBS washes

The optimum number of washes required to remove loosely attached microspheres without damaging the cell monolayers was carried out using the method described in section 2.7.2 with the exception that the cells were incubated with 0.5mg/mL of microsphere suspension.

2.10.2. Effect of time on cellular association of microspheres

A procedure similar to section 2.7.3 was followed with the exception that the cells were incubated with microspheres instead of free ribozyme.

2.10.3. Effect of temperature on cellular association of microspheres containing ribozymes

Cells were incubated with 500μL of 0.5mg/mL of microsphere suspension solution and the effect of temperature on cellular association of the microspheres was studied by following the procedure in 2.7.4.

2.10.4. Effect of metabolic inhibitors on the cellular association of microspheres

A procedure similar to section 2.7.5. was followed with the exception that the cells were incubated with microspheres instead of free ribozyme.

2.10.5. Effect of pH on cellular association of microspheres

A procedure similar to section 2.7.9 was followed with the exception that the cells were incubated with microspheres instread of free ribozyme.

2.10.6. Effect of post-cell association Trypsin washing

A procedure similar to section 2.7.10. was followed with the exception that the cells were incubated with microspheres instead of free ribozyme.

2.11. *IN VIVO* CNS DELIVERY STUDIES

2.11.1. Animals and treatment

Male Wistar rats (bred at Aston University) weighing 180-220g were maintained under standard 12 hour light/dark cycle (lights on 07:00 hours, 21 ± 1°C and 55% humidity) and allowed free access to food pellets (standard rat diet, Pilsbury Ltd) and water at all times. For surgery rats were anaesthetised with Isoflurane (Vetothane) using a mask (3% for induction and 1.5% for maintenance) in N_2O and O_2 (1:1 ratio) (flow rate set to 0.5 L/min). Once anaesthetised the head of the rats, where the incision was to be made, was shaved and the loose fur was removed with antiseptic swabs and then placed in a Kopf stereotaxic frame with the incisor bar connected to the mouthpiece delivering maintenance anaesthetic. The frame and surrounding area was swabbed down and sprayed with antiseptic spray to minimise risk of infection to the animal during the surgical procedure prior to placing the animal in the frame. The rats were gently wrapped in an insulating bubble wrap to avoid loss of heat by the animal, while being on the frame, and ear bars gently inserted. Under aseptic conditions the skull was exposed and bregma located and using these coordinates the site of injection was identified and a small burr hole was made and the dura was punctured with a 32G needle. The site of injection was the left lateral ventricle at co-ordinates: 0.8mm caudal to bregma, 0.14mm lateral and 0.36mm ventral to bregma (Paxinos and Watson., 1986). Injections were made with a 5μL Hamilton syringe over a 2 minute period and a total volume of 2uL was delivered. The syringe was left in place for a further 2 minute period to reduce any backflow and then slowly withdrawn. The burr hole was sealed with bone wax (HM+S

Derby, UK) and the skin was sutured using sterile Mersilk Ehicon suture (Brosch, UK). The animals were then allowed to recover from the anaesthesia in new pens, which had a heat pad underneath them. Once recovered the rats were placed back in original cages for various time points.

2.11.2. Cryostat sectioning of rat brains

At required time points rats were killed using exposure to rising concentration of CO_2 gas (Animal Scientific Procedures Act, Schedule 1, Appropriate method of humane killing, table A) and killing was completed by confirmation of permanent cessation of circulation. The skin around the upper part of the head was removed and the skull was exposed which was then carefully peeled off by using sharp nose small pliers. Once the actual brain tissue was visible it was removed from the base of the skull by severing the optic and olfactory nerves along with the lower part of the brain stem. This delicate tissue was then immediately frozen to -40°C in isopentane (Sigma, Poole UK). The brain was kept at -70°C until sectioning using a Bright OTF (Bright Instruments Company Ltd., UK) cryostst. The frozen brain was placed on a large droplet of OCT compound (BDH Laboratory Supplies, UK) on an aluminium chuck. After allowing a period of half to one hour for the brain temperature to equalise to the cryostat chamber temperature, sectioning was carried out at a thickness of 30μm. Sequential coronal cryosections were collected on gelatin coated glass microscope slides (Superfrost plus, 25mm x 75mm, BDH Laboratory Supplies) and stored at room temperature for further processing.

2.11.3. Histological evaluation

In order to assess any histological damage, neuronal loss or gliosis, brain cryosections were examined using a Cresyl Fast staining procedure. Without staining the slides can not be viewed at great detail and resolution because of their thickness (30μm). In this procedure sections, as obtained in section 2.7.9.2, were rinsed in sterile double distilled water then stained with Cresyl violet stain (0.5% Cresyl violet, 1M sodium acetate, 1M Acetic acid in double distilled water) for 10 minutes at room temperature. The sections were washed in double distilled water to remove excess stain and then dehydrated through 70%, 95% and

100% ethanol followed by immersion in 100% xylene for 10 minutes. The sections were air dried before being examined on Zeiss microscope for structural changes.

2.11.4. Tissue preparation for fluorescence microscopy

Tissue sections were prepared and mounted on glass microscope slides as described in section 2.7.9.4 and was observed under Zeiss microscope, which was fitted with a high-pressure mercury source. According to the UV emission spectra of fluorescein and rhodamine (Lansing-Taylor and Salman, 1998), a 510nm wavelength blocking filter was used for the detection of fluorescein and FITC (fluorescein isothiocyanate) labelled ribozyme, as such a filter would totally prevent any cross-over excitation from rhodamine. For rhodamine-dextran detection a 590nm wavelength narrow band blocking filter was used (Holz., 1982). Sections showing fluorescence were photographed using an Olympus camera containing Jessops SHR400 colour film, which was attached to the microscope with an adapter.

2.11.5. Preparation of microsphere for ICV injection

Microspheres were prepared and characterised as shown in sections 2.9. Since microspheres are in a dry powder form they were suspended in sterile double distilled water for ease of administration. For this purpose 10mg microspheres were weighed out in eppendorf microtubes and to which 50μL of sterile double distilled water was added immediately before the ICV injection in order to avoid sedimentation of the microspheres. As described earlier a Hamilton syringe was used for the actual injection and a volume of 5μL was drawn up from which only 2μL was injected in to the ventricles.

2.11.6. Animal post-operative well being assessment

Any treatment could potentially have adverse effects on the animal under investigation and in order to assess any such possibility animal post-operative well-being was monitored. The

well being of the animal was assessed, by monitoring the weight, gait, skin condition, muscle tone, posture and locomotion. Any unusual deviation from the normality was noted and this assessment continued at regular intervals until the animal was sacrificed for all time points studied.

2.12. Statistics

Unpaired student's t-test (two sample assuming equal variances) was used to determine whether there were significant differences between mean values of data obtained from different experimental populations. The Microsoft Excel 2000 version was used for this purpose. For studies involving more than two experimental groups one-way ANOVA was used to determine significant differences between groups using the SPSS software package (Version 10.0.7) with different post-hoc tests depending on the design of the experiment.

Low P values indicated that the experimental populations were unlikely to be sampled from populations with equal mean values. Data sets were assumed to be significantly different when P values below 0.05 were calculated. The test assumed that the data were randomly sampled, that each value was obtained independent of the others, that the populations were scattered according to a Gaussian distribution and that the standard deviation (SD) of the two populations were not significantly different. For data sets with unequal variances t-test from the SPSS programme was used.

CHAPTER THREE

CHARACTERISATION OF RIBOZYME CELLULAR ASSOCIATION IN CULTURED GLIAL AND NEURONAL CELLS

3.0. Introduction

Despite significant advances in imaging techniques, neurosurgery, radiation therapy and neuro-oncology there is still no effective cure available to treat primary brain tumours and the prognosis of most patients suffering from these tumours remains dismal. This problem is further compounded by a diagnosis of approximately 13000 new cases of primary malignant brain tumours every year in the United States alone (Parker *et al.*, 1996). For patients suffering from glioblastomas, the median survival is still less than one year after surgical resection and conventional external-beam radiotherapy (Black, 1991). Several strategies have been used to treat these tumours as reviewed in (Gutman *et al.*, 2000).

One of the promising strategies currently being studied extensively is the use of highly selective and target specific ribonucleic acid based molecules, ribozymes, which have been used as biological tools and therapeutic agents as outlined in the introduction. However, there are several problems at the systemic and cellular level, which are hampering the development of exogenously delivered ribozyme therapeutics. These problems include chemical stability, elimination and poor penetration through biological membranes as explained in the introduction (see section 1.4).

With the benefit of advances in nucleic acid chemistry more stable structures of ribozyme have been developed (Beigelman *et al.*, 1995b; Taylor *et al.*, 1992), which has led to an intense investigation of ribozyme in a variety of biological and disease models *in vitro* and *in vivo*. However, despite advances in the successful application of ribozyme in various settings, a survey of published literature reveals that no information is available pertaining to the uptake mechanisms of ribozymes apart from previous work published from our laboratory by (Fell *et al.*, 1997). In this work it was reported that cellular uptake was a function of cell type as different cell lines demonstrated differential uptake of ribozyme.

Moreover, a lead observation was made in another work from the laboratory (Khan *et al.*, 2000) which showed that antisense oligonucleotides entrapped in biodegradable polymers when injected site specifically in the neostriatum of rat brains showed a differential uptake in glial and neuronal cells with neuronal cells taking up antisense molecules more avidly.

In this report it is aimed to further pursue these observations in order to understand and characterise cellular association properties in cultured glial and neuronal cells from human and rat species. It was further aimed to carry out a comparison of the cellular association properties to identify the reasons of differences in mechanisms of cellular association, which give rise to these differences. Information regarding the cellular association mechanism, vesicular transport and intracellular trafficking and hybridisation with target site of ribozymes not only has important implications for the treatment of brain tumours whether glial derived or of neuronal original with chemically stabilised and catalytically competent ribozymes but is also essential for the development of novel and robust delivery systems for these therapeutics to optimise delivery to target sites.

The ribozyme used in this thesis is a 37 mer chemically modified hammerhead ribozyme, which is targeted against the 3'-untranslated region of the epidermal growth factor receptor (EGFr) gene, which is over-expressed in a variety of tumours especially in the central nervous system. The detailed structure of the ribozyme used and an overview of EGFR are provided in the introduction (see section 1.6 and 1.7). The experiments to characterise the cellular association of ribozyme were conducted with cultured glial and neuronal cells, which cells provide an ideal tissue culture model for studying malignancies of the central nervous system as it is the global aim of this laboratory to discover nucleic acid based therapies for the treatment of brain tumours.

In order to obtain valid and rigorous results from the planned experiments on cellular association, the stability of ribozyme was evaluated in different biological media, followed by determination of optimum seeding density for cellular monolayers and optimisation of PBS-azide washes to remove loosely attached ribozymes. A series of experiments have been described in this chapter following the optimisation studies, starting with an investigation of ribozyme cellular association over a time course in all four cell lines simultaneously, to identify the extent and pattern of association. This was followed by investigation of the influence of temperature and metabolic inhibition on cellular association. To further

determine the nature and extent of association of ribozyme it was compared to mannitol, a fluid phase adsorption marker, and ribozyme efflux was investigated. In order to determine the mechanism of cell association, effects of self and cross competition, pH and post-association trypsin washing were evaluated to investigate the possibility of ribozyme binding cell surface molecules, which mediate cellular association of ribozyme. Intracellular distribution was determined by using fluorescein labelled ribozyme and finally South-Western blotting was used to identify ribozyme binding cell surface proteins.

3.1. RESULTS AND DISCUSSION

3.1.1. Stability of chemically modified ribozymes

An important consideration in studying the application of any potential drug molecule, in particular macromolecules such as nucleic acids, is to evaluate its structural stability in all the environments to which it will be exposed to in the course of experiments and eventually in therapeutic settings. This is due to the fact that maintenance of structural integrity is an essential condition of successful delivery and main determinant of efficacy of the administered molecule. Potential therapeutic molecules such as ribozymes are biologically labile molecules and are particularly unstable due to their susceptibility to degradation by ribonucleases. Ribonucleases which are abundantly present in biological environments causing unmodified ribozyme molecules to degrade within 0.1 minutes (Jarvis *et al.*, 1996), which results in poor cellular uptake and intracellular availability (Elkins and Rossi, 1995) (Heidenreich *et al.*, 1994). For a successful application of ribozymes it is imperative to enhance the structural stability of ribozyme in biological media. In this regard several chemical modifications have been investigated as described in section 1.4.1. The ribozyme used in this study has been chemically modified as described by (Beigelman *et al.*, 1995b) to improve its resistance to nucleases and structural integrity (see section 1.6). In the following section the chemical stability of the ribozyme used in this study has been evaluated after exposure to serum, serum free medium and cellular monolayers of cultured glial and neuronal cells.

This assessment is essential to determine a time-frame in which the ribozyme is stable for conducting the cellular association studies to obtain valid and rigorous results from the cellular association studies of the intact ribozyme and not of degraded fragments. As described in section 2.3, autoradiography and electrophoresis were used to assess the stability of the internally labelled ribozyme. Samples exposed to various biological media were electrophoresed on a 20% acrylamide/7M urea gel for 1.5 hours at 10-20 watts to separate fragments of different sizes, which had been produced by the degradation of ribozyme as result of nuclease activity.

3.1.1.1. Stability of ribozyme in serum medium

The stability of internally labelled ribozyme was investigated over a time course as described in section 2.6.1 in serum containing medium. Serum medium, which is constituted of DMEM supplemented with 10% foetal bovine serum (FBS), provides a model for stability studies as serum possesses significant nuclease activity (Hudson *et al.*, 1996b). In the antisense field, stability of nucleic acid molecules in serum medium is generally regarded as being equivalent to stability of nucleic acids in the extra-cellular environment *in vivo*. Although the nuclease activity of sera derived from different species may vary, the nuclease activity of FBS is greater than human and mouse serum (Crooke, 1992). Figure 3.1 shows the stability profile of ribozyme over a time course starting from 0 to 24 hours in serum medium. In the diagram upper bands, which are annotated, represent intact ribozyme at various time intervals with C as a control ribozyme and FL stands for free label.

The control band represents ribozyme which has been unexposed to serum medium and the band labelled FL was free label which represents unincorporated radiolabel γ^{32}P-ATP, which was radioactive marker used to internally label the ribozyme. The bands present on subsequent rows under different time points represent degradation products produced by the action of nucleases. As the diagram in figure 3.1 shows that between the time points 0 h (minimum exposure to the medium) to 1 hour degradation products were not visible suggesting that the ribozyme was stable up to this point. In contrast at time point 2 hours to 24 hours degradation bands were visible below the main band for each time points reflecting the activity of nucleases on the ribozyme with the highest degradation observed at the 24 hour time point.

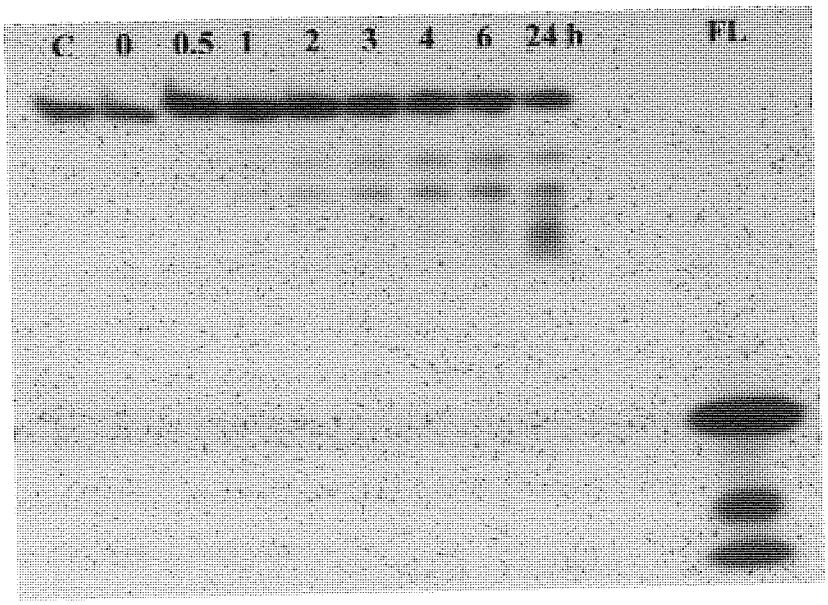

Figure 3.1. *Autoradioradiograph showing stability of ribozyme over a time course. The numbers over the bands indicate the time points starting from zero hours to 24 hours and the abbreviation FL indicates free label and C represents control ribozyme which was intact ribozyme in sterile water. Ribozyme was exposed to the medium at 37℃ for various time intervals and analysed on 20% PAGE (7M urea) gel for degradation products.*

Analysis of the degradation pattern shows that there was a progressive increase in the number of bands indicating a progressive shortening of the ribozyme with increasing time. This progressive shortening was not likely to be from the 3'-end of the molecule as it was protected at that terminal with an inverted thymidine, which confers resistance to the molecule from exonucleases. A possible explanation is that the ribozyme is cleaved into two halves by an endonuclease at the ribose (unmodified) residue sites on the molecule producing a non-inverted t chain, which was then subsequently degraded progressively by exonucleases. However, despite significant degradation of the ribozyme a large proportion of the ribozyme remains intact even after exposure to the serum medium as shown by the presence of a relatively intense band in the 24-hour column.

As the stability in serum medium showed ribozyme was not fully stable for time points above 1 hour and therefore does not form a valid model for *in vitro* cell association studies of ribozyme. As a result the stability of ribozyme was evaluated in serum free medium next to identify a suitable medium to conduct cell association experiments.

3.1.1.2. Stability of ribozyme in serum free medium

The stability of ribozyme was studied in serum free medium as described in section 2.6.1. Serum free medium was identical to the serum medium except that it was not supplemented with fetal bovine serum and therefore had no nuclease activity. Figure 3.2 shows the stability profile of the ribozyme over a time course starting from 0 hours to 24 hours along with a control ribozyme in serum free medium. The first lane shows the free label, which was included to identify if any free label had been removed from the ribozyme at different time points. The second lane shows the control band, which shows the original ribozyme not exposed to the biological medium under investigation. The lanes subsequent to these were bands showing ribozyme exposed to serum free medium for time points 0, 0.5, 1, 2, 4, 6, and 24 hours. Figure 3.2. shows there were no degradation bands visible which could demonstrate the fragmentation of the ribozyme.

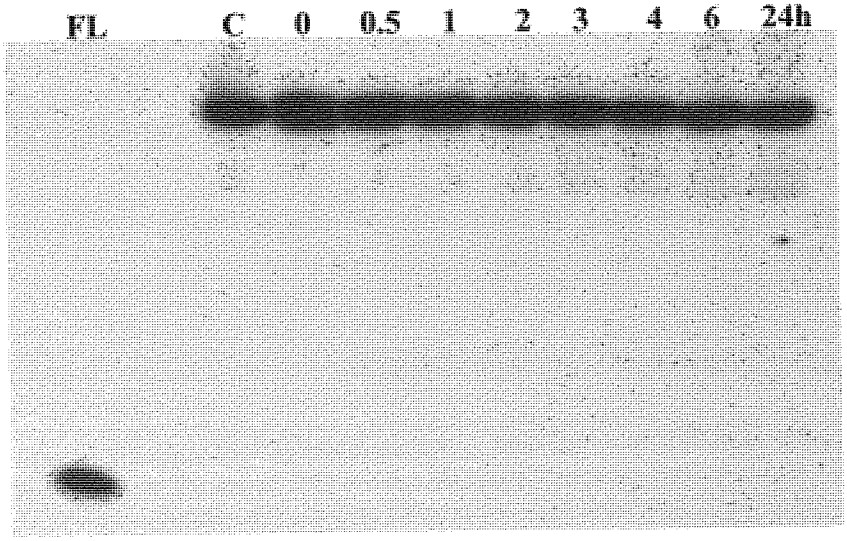

Figure 3.2. *Auto-radiograph demonstrating stability of ribozyme over a time course in serum free medium. The numbers over the bands indicate the time points starting from zero hours to 24 hours and the abbreviation FL indicates free label and C stands for control intact ribozyme. Ribozyme was exposed to the medium and analysed on 20% PAGE (7M urea) gel.*

Therefore it appeared that the ribozyme remained stable during the 24 hours after being incubated for the duration of the experiment in the serum free medium at 37°C. These results show that ribozyme can be used in experiments in which serum free medium is used without risk of adverse effect on the structural integrity of ribozyme.

3.1.1.3. Stability of ribozyme on a monolayer of cells

After investigating the stability of ribozyme in serum and serum free media the stability of ribozyme was investigated on a monolayer of each of the cell lines. This assay was carried out to investigate whether any potential secretions of nucleases or phosphatases by the cellular monolayers can possibly adversely affected the structural integrity of ribozymes. In a case of such possibility existing, the cellular association study results could be spurious as the cellular association observed could be of the degraded shorter fragments of the ribozyme. For this purpose a monolayer of cells was grown as described in section 2.6.2. and the ribozyme was exposed to this monolayer and its stability studied over a time course at 37°C and degradation products analysed on 20% PAGE (7M urea) gel.

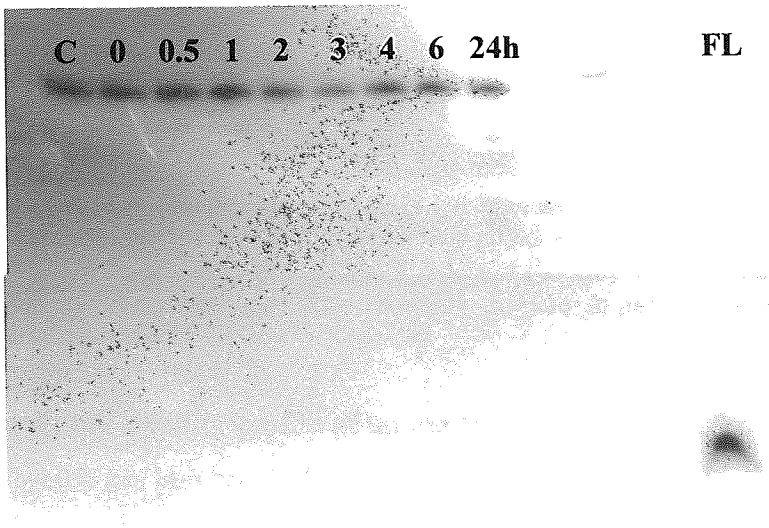

Figure 3.3. *Stability of ribozyme on a monolayer of C6 cells. The numbers over the bands indicate the time points starting from zero hours to 24 hours and the abbreviation FL indicates free label and C stands for control intact ribozyme. Ribozyme was exposed to the medium and analysed on 20% PAGE (7M urea) gel.*

Figure 3.3. shows the stability gel for the ribozyme on a monolayer of rat glioblastoma, C6, cells. The headings on the columns are as explained in the previous sections. The gel shows that from time 0 hours to 6 hours there were no degradation bands visible indicating that there either was no nuclease activity or complete resistance of the ribozyme to any nuclease activity present. It appears that the ribozyme was demonstrably stable and structurally intact. However, at the 24 hour time point column there were some faintly visible bands reflecting slight degradation of the ribozyme despite an intense band at the top of the lane signifying

that majority of ribozyme was still resistant to nuclease degradation and was physically intact.

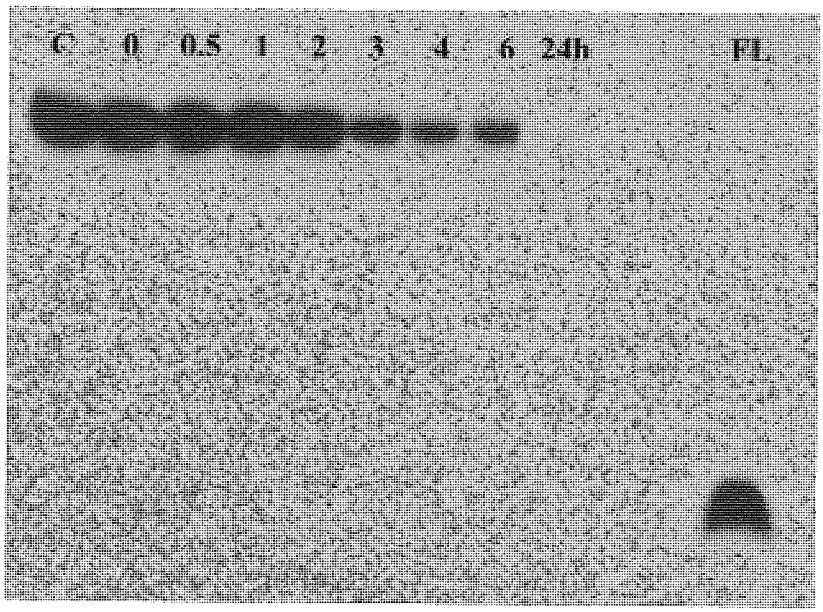

Figure 3.4. *Stability of ribozyme on a monolayer of U87 cells. The numbers over the bands indicate the time points starting from zero hours to 24 hours and the abbreviation FL indicates free label and C stands for control intact ribozyme. Ribozyme was exposed to the medium and analysed on 20% PAGE (7M urea) gel.*

Figure 3.4 shows the stability profile of an internally radiolabelled ribozyme on a monolayer of U87 cells, which are human glioblastoma cells over a time course. As the gel shows there were no degradation bands for any of the time points ranging from 0 to 6 hours confirming the stability of the ribozyme on a monolayer of U87 cells in serum free medium. However at time point 24 hours the ribozyme in the main band is not visible which is probably due to the fact that after 24 hours the ribozyme is completely taken up by cells either intact or in degraded fragments and hence no degradation bands were visualised on the gel to evaluate the stability. From this figure 3.4 it can be safely concluded that the ribozyme remained intact up to 6 hours on a monolayer of U87 cells.

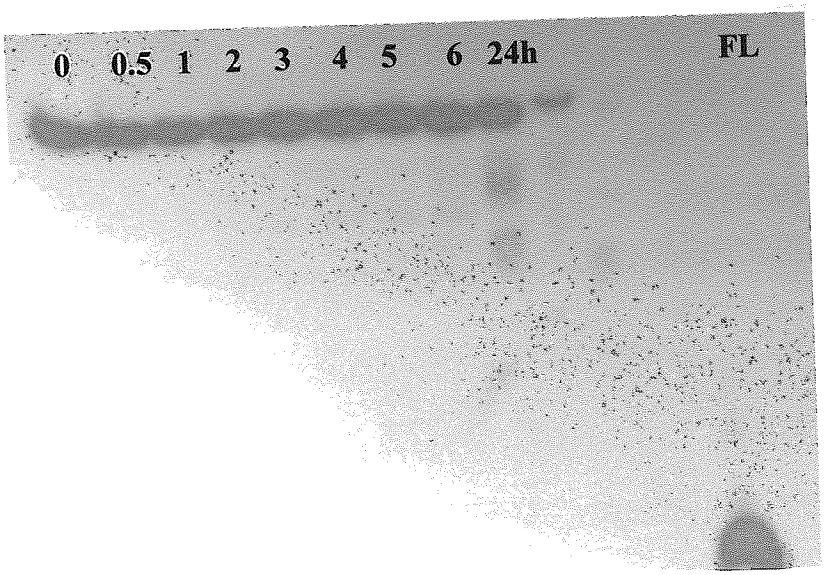

Figure 3.5. *Stability of ribozyme on a monolayer of GT1 cells. The numbers over the bands indicate the time points starting from zero hours to 24 hours and the abbreviation FL indicates free label and C stands for control intact ribozyme. Ribozyme was exposed to the medium and analysed on 20% PAGE (7M urea) gel.*

Figure 3.5 shows the stability profile of ribozyme on a monolayer of GT1 cells, which are rat neuroblastoma cells. The internally labelled ribozyme remained intact up to 6 hours as shown by the absence of any degradation bands on the gel from time intervals 0 to 6 hours. At time point 24 hours the majority of ribozyme was still intact as evidenced by a strong band along with several more degradation bands visible in this lane reflecting nuclease mediated degradation of the ribozyme. These results demonstrate that the ribozyme remained intact up to 6 hours on a monolayer of GT1 cells.

Figure 3.6 shows the stability profile of an internally labelled ribozyme on a monolayer of SY5Y cells, which are human neuroblastoma cells. The band headings are as described in the early section 3.1.1.1. The gel shows that the ribozyme remains intact for up to 6 hours starting from 0 hours as evidenced by the absence of any degradation bands. At time point six hours the majority of the ribozyme was still intact but a reduction in the band intensity in comparison to the bands shows that at this time point a small proportion of the ribozyme underwent degradation whereas the majority of the ribozyme remained intact. At time point 24 hours the ribozyme there were a few visible bands signifying degradation of the ribozyme with a large proportion still intact. This result shows that the ribozyme was intact up to 6 hours.

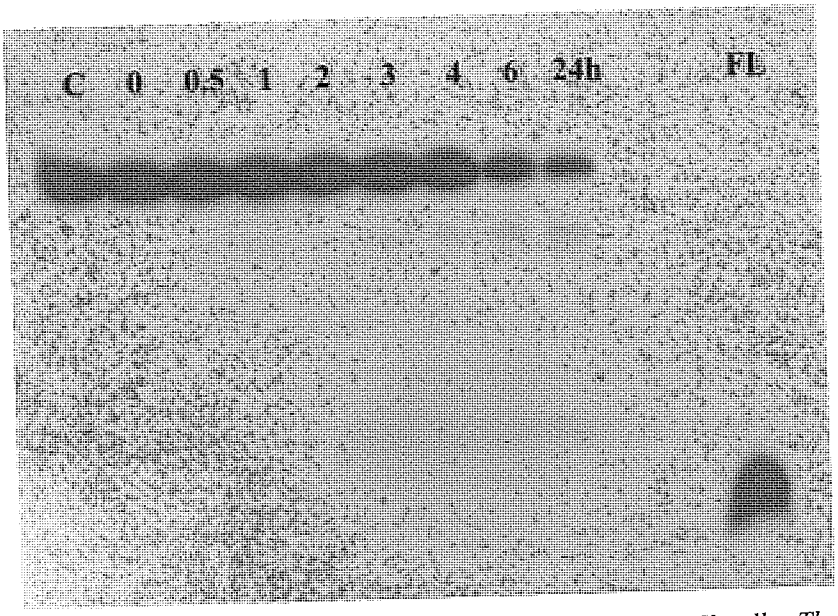

Figure 3.6. *Stability of ribozyme on a monolayer of SY5Y cells. The numbers over the bands indicate the time points starting from zero hours to 24 hours and the abbreviation FL indicates free label and C stands for control intact ribozyme. Ribozyme was exposed to the medium and analysed on 20% PAGE (7M urea) gel.*

These above results in which the stability of the internally labelled ribozyme has been evaluated show that with the exception of serum medium, in all the cellular monolayers and serum free medium studied, the ribozyme was resistant to nuclease activity and maintained complete structural integrity for at least 6 hours. The investigated ribozyme had several chemical modifications to enhance its stability as described by (Beigelman *et al.*, 1995b) and is described in section 1.6. The stability demonstrated in above assays is a substantial improvement in stability in comparison to all RNA nucleic acids when exposed to serum medium which degrades within 0.1 minute (Jarvis *et al.*, 1996). These results allow the ribozyme to be confidently used in subsequent studies of cellular association of ribozyme *in vitro*.

Autoradiographs of stability studies presented in this chapter were only analysed qualitatively to ascertain the stability of ribozyme since stability testing was part of preliminary work to define experimental protocol. A more rigorous approach could have been possible by carrying out densitometry analysis of the bands visible on autoradiographs and qualitative analysis assessments made of the ribozyme stability, which was not possible with these results as some of the autoradiographs were over-exposed.

3.2. Cell growth assays

Cell-growth assays were performed in order to assess the pattern and rate of growth of cultured cell populations as this information was necessary for the design and execution of experiments. Rate of growth of various seeding densities was evaluated to determine optimum concentration for seeding cells on plates for experimental work. Determination of optimum seeding density was important for the design of the experiments as seeding cells at low densities might lead to no cell growth at all or too high seeding density might lead to cells being confluent before the end of the experiment. Patterns of cell growth were also important to obtain valid and rigorous results as cell populations usually grow with a triphasic pattern starting from lag phase (acclimatization) to log phase (exponential growth) to stationery phase (confluency), with all phases having distinctly different growth characteristics. In experimental work such as cell association studies where comparison between cell lines is undertaken, it is important that all cell populations under study have similar growth characteristics.

As a result cell populations which are in lag phase do not provide an ideal basis for comparison as in lag phase populations some cells may be undergoing cellular division whilst others could still be in a stationary G_0 phase. An ideal phase for cell association studies is the log phase in which most cells in a given population are actively dividing and growing. Statinonary phase like lag phase is not an ideal phase for experimentation as cells normally by this point have achieved their full growth potential and are not further growing which is unlike neoplastic cells which are constantly growing. In these assays, cells were seeded in 24 well plates at stated densities as described in section 2.5 and counted after the indicated time interval as described in section 2.4.6 to perform growth assays.

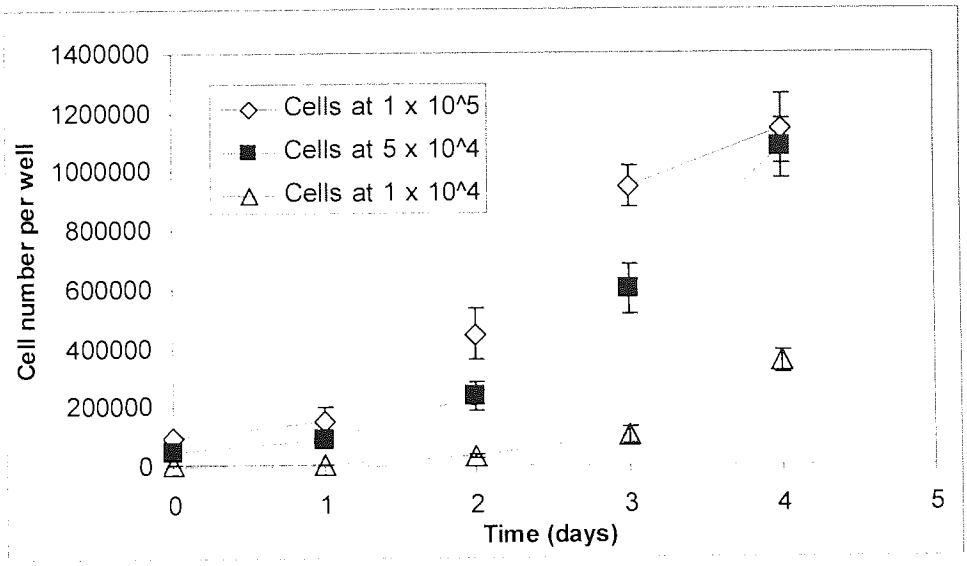

Figure 3.7. *Growth curve for C6 cells after being plated in a 24-well plate at seeding densities of 1×10^5, 5×10^4 and 1×10^4 per well (n=3±SD) and incubated at 37°C for time periods indicated.*

As the graph in figure 3.7 shows all three seeding densities of rat glial cells C6 grow in the wells albeit with different patterns. The 1×10^4 seeding density wells had a very long lag phase (3 days) in comparison to the other two densities, along with a slower growth rate in the log phase.

With the 5×10^4 and 1×10^5 densities there was a 24-hour lag phase after which the cellular growth entered the log phase, which is called the exponential phase. For these two high densities the amount of growth in the log phase was different with the 1×10^5 cells having the highest growth rate (2-fold higher) in comparison to the 5×10^4 seeding density cells and had a population doubling time of 21 hours approximately.

From these curves the 1×10^5 seeding density was chosen for use in future experimental work due to its short lag phase and higher growth rate in the log phase. For future experiments cells were seeded at 1×10^5 cell per well and incubated for 2 days to allow cells achieve log phase at which point the cell number is approximately 4×10^5.

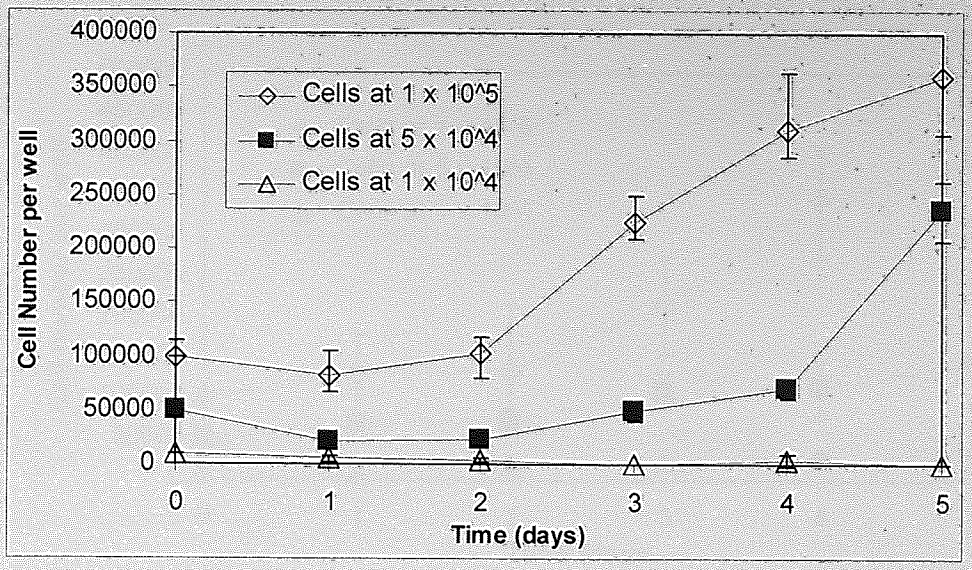

Figure 3.8. *Growth curve for GT1 cells after being plated in a 24-well plate at seeding densities of 1×10^5, 5×10^4 and 1×10^4 per well (n=3±SD) and incubated at 37°C for time periods indicated.*

Figure 3.8 is the graphical representation of the cellular growth curve for GT1 rat neuroblastoma cells. As the curve shows the 1×10^4 cell seeding density did not grow at all whereas the 1×10^5 and 5×10^4 cells per well seeding density showed appreciable growth. The 1×10^5 density had a lag phase of 2 days after which the cellular growth entered the log phase which continued till day 4. After 3 days the 1×10^5 density had 2.25×10^5 cells. Whereas the 5×10^4 cell density had a similar lag phase of 2 days and then entered log phase but the amount of increase in cells was not as high as the 1×10^5 seeding density. After three days the amount of cells on average per well was approximately 5×10^4 cells. At day four a second rapid increase in cell numbers was observed.

The population doubling time for the 1×10^5 seeding density was 21 hours and it was this density which was selected for future experimental work as it had the shortest lag phase and the cells entered optimum growth phase three days post seeding.

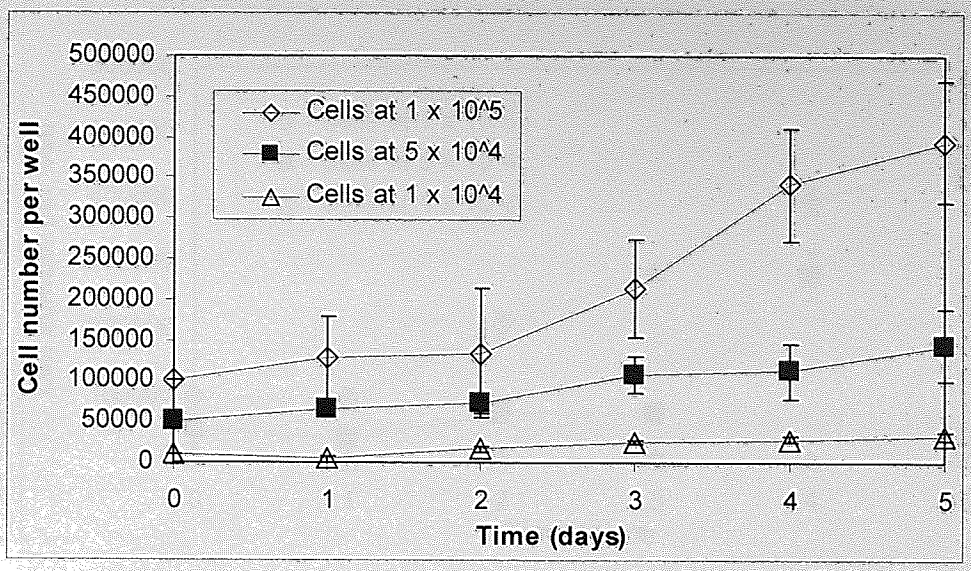

Figure 3.9. *Growth curve for SY5Y cells after being plated in a 24-well plate at seeding densities of 1 × 10^5, 5 × 10^4 and 1 × 10^4 per well (n=3±SD) and incubated at 37℃ for time periods indicated.*

As the graph in figure 3.9 illustrates the 1 × 10^4 and 5 × 10^4 cells do not achieve any notable growth in numbers whereas the 1 × 10^5 density showed an appreciable growth pattern. The cell had a lag phase of two days after which it entered the log phase. In the log phase the cell had linear increase in growth, which continued till day five which was the last time point in the experiment. The cells had a population doubling time of approximately 43.5 hours. From these patterns it was deducted that the appropriate seeding density for future experiments was 1 × 10^5 cells per well.

Figure 3.10 shows the growth curve of human glioblastoma U87 cells over a time period of five days. As the graph shows when cells were seeded at 1 × 10^4 cells per well the cells do not grow until day 5 indicating a very long lag phase. This could be due to the fact that the cells are so far apart to each other and there is not sufficient inter cellular communication in terms of growth hormones secreted by cells and therefore have a very long lag phase. Due to no appreciable cell growth no population doubling times calculation could be done.

For the 5 × 10^4 and 1 × 10^5 cell seeding density, the growth was substantial. As the curve for 5 × 10^4 cells shows there was a lag phase of 3 days after which cells entered the log phase showing exponential growth. The population doubling time was estimated to be 27 hours.

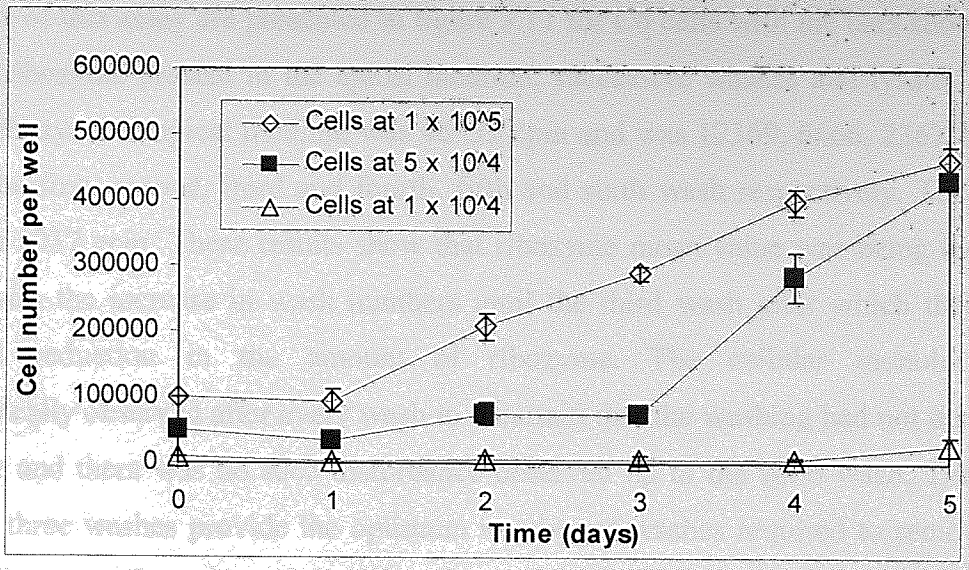

Figure 3.10. *Growth curve for U87 cells after being plated in a 24-well plate at seeding densities of 1 × 10^5, 5 × 10^4 and 1 × 10^4 per well (n=3±SD) and incubated at 37 °C for time periods indicated*

For 1 × 10^5 seeding density the cells showed a lag phase of 24 hours after which the cells entered the log phase. The cells had a population doubling time of 24 hours in the log phase. Cell growth rate started to fall off after the fourth day, which suggests that the cells, due to their high density at this point have exhausted all the available space and nutrients and have entered the stationary phase.

From these curves it was deducted that the best density to use was the 1 × 10^5 cells per well as the cells were in optimal growth phase for experimentation after 48 hours.

3.3. Optimisation of PBS-azide washes

As described in the protocol for cellular association studies, it is important to remove the loosely attached and unbound ribozyme post-incubation with PBS-azide washes and optimisation of these washes is an important step in designing cellular association experiments. As unnecessary washings would damage the cellular monolayer resulting in underestimation of the cellular association and similarly use of less than optimal washes would result in overestimation of cellular association leading to false deductions and less rigorous results. An assay was carried out to determine the optimum number of PBS-azide washes required to remove all loosely bound and unbound labelled ribozyme from cellular monolayers as described in section 2.7.2.

The results of this assay are presented in figure 3.11 for C6 cells with the bars showing mean values of ribozyme present in the apical medium, successive washes and lysate. The mean value of ribozyme in apical medium was 46932 cpm and was 12369, 6666, 2367, 92, 89, 91 cpm for the first, second, third and fourth, fifth and sixth wash respectively. The value for lysate was 3037 cpm. These results show that ribozyme mean value was being increasingly reduced with the increase in wash numbers until the third wash after which there was no significant reduction in the amount of ribozyme. The cellular monolayers were microscopically observed after every wash to ascertain that the washing had not disturbed the monolayer and there was no such disturbance observed up to the sixth wash. These results show that three washes provide the optimum number of washes required to remove loosely attached ribozymes from the cellular monolayers. Results for the other cell lines GT1, SY5Y and U87 were similar to C6 and therefore not shown here. On the basis of these results cellular association protocols used in this thesis include three washes for the cellular association studies when using free ribozyme.

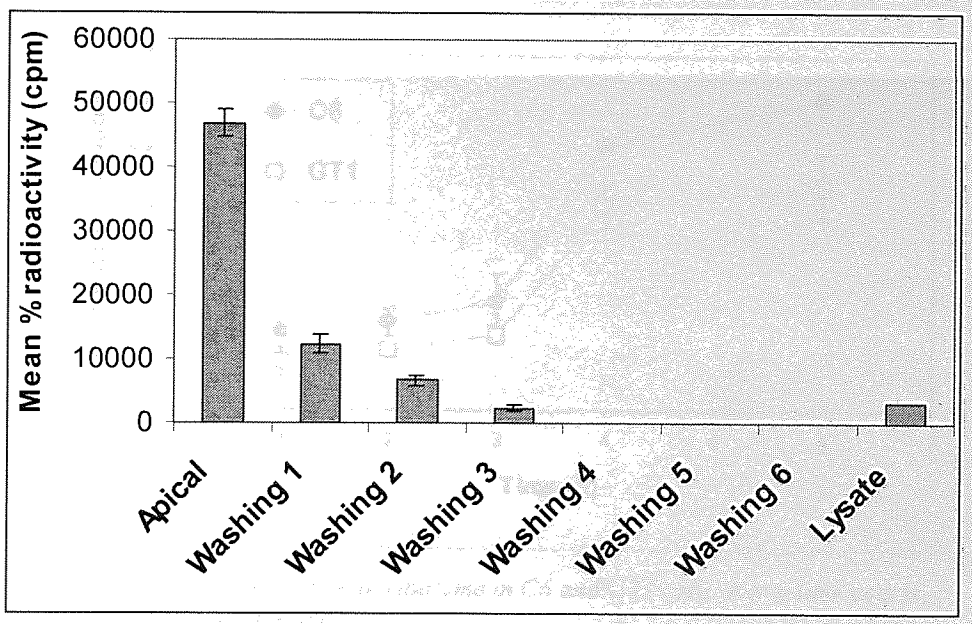

Figure 3.11. *A graph showing the results of an assay to determine the number of PBS-azide washes to remove loosely bound labelled ribozyme from the cellular monolayer of C6 cells. N=3 ± SD*

3.4. Effect of time on the cellular association of ribozyme

In this section the cellular association of exogenously administered ribozyme was investigated over a time course in cultured glioblastoma and neuroblastoma cells from human and rats. The aim of the experiment was to characterise the cellular association with a view to investigate if there was any difference in the pattern and extent of cellular association of ribozyme across type and species of cells.

This investigation was carried out according to the experimental protocol described in section 2.7.3 with the experiment conducted for up to 6 hours by incubating ribozyme in serum-free medium on cellular monolayers. Figure 3.12 shows the results of the cellular association studies of ribozyme for the cell lines, C6 (rat glioblastoma) and GT1 (rat neuroblastoma), carried out over a time course of 6 hours for selected time points, 1, 2, 3, 4 and 6 hours. For all time points the plotted mean values were normalised to cell number across all cell lines to obtain a rigorous comparison between time points and cell lines.

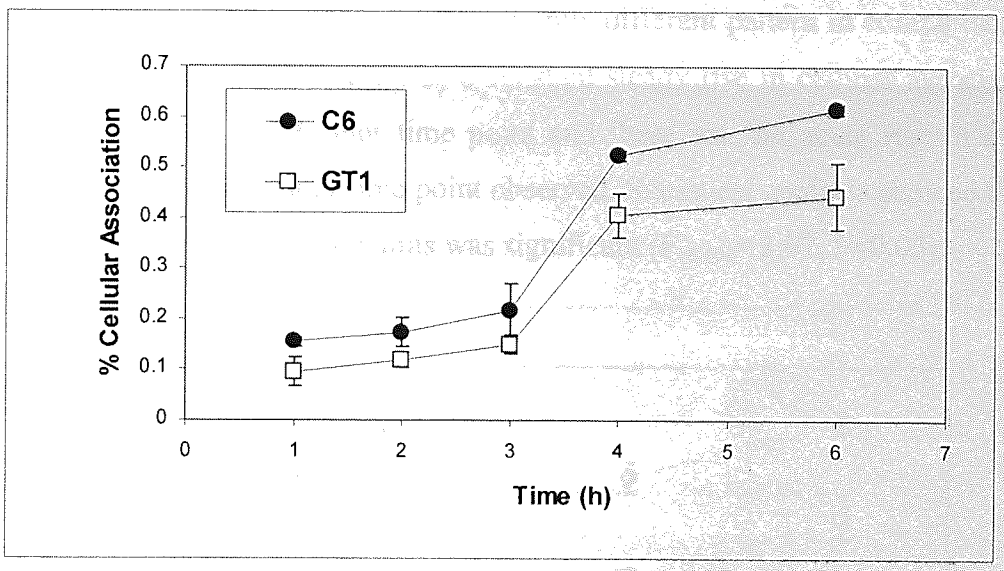

Figure 3.12. *Cellular association of ribozyme in C6 and GT1 cells over a time course. Error bars represent n=3 ± SD.*

The mean percent cellular association values for C6 cells at time points 1 hour, 2 hour, 3 hour, 4 hour, 6 hour were 0.15%, 0.17%, 0.22%, 0.53%, 0.62% respectively. As these figures show the mean cellular association values, overall, were significantly different ($F_{(4,10)}$= 185, $P<0.01$) at different time points. Cellular association increased steadily for the first 3 hours and then rapidly increased by 2.4-fold at the 4 hour time point and then plateaued for the 6 hour time point. For the first 3 hours there was a steady increase in the mean values of

cellular association but this increase was not statistically significant ($P>0.05$) as indicated by post-hoc tests, however at the time points 4 hour and 6 hour, the mean values for cellular association were significantly different from the first three time points ($P<0.05$).

For the rat neuroblastoma cell line, GT1, the mean percent cellular association figures for time points 1, 2, 3, 4 and 6 hour were 0.09%, 0.12%, 0.15%, 0.41% and 0.44% respectively which were statistically significantly different ($F_{(4,10)}= 217$, $P<0.01$). As the pattern of cellular association shows the mean values for the cellular association for the first three time points were rising with time but there was no statistical difference in values as indicated by post-hoc tests. With the remaining two time points, 4 and 6 hour, there was a statistical difference in mean values with each other and also from the first three (1-3 hour) time points ($p<0.05$).

Similarly, as shown in figure 3.13, the ribozyme cellular association values in the human neuroblastoma cell line, SY5Y, for the same time points were 0.10%, 0.13%, 0.21%, 0.34% and 0.51% respectively. With this cell line a slightly different pattern in comparison to other three cell lines was observed. There was a constant steady rise in cellular association from the 1 hour time point up to 6 hour time point and there was no acute rise in association between the third and fourth hour time point observed. Statistical analysis showed that within this cell line the difference in time points was significant ($F_{(4,10)}= 3.97$, $P<0.05$).

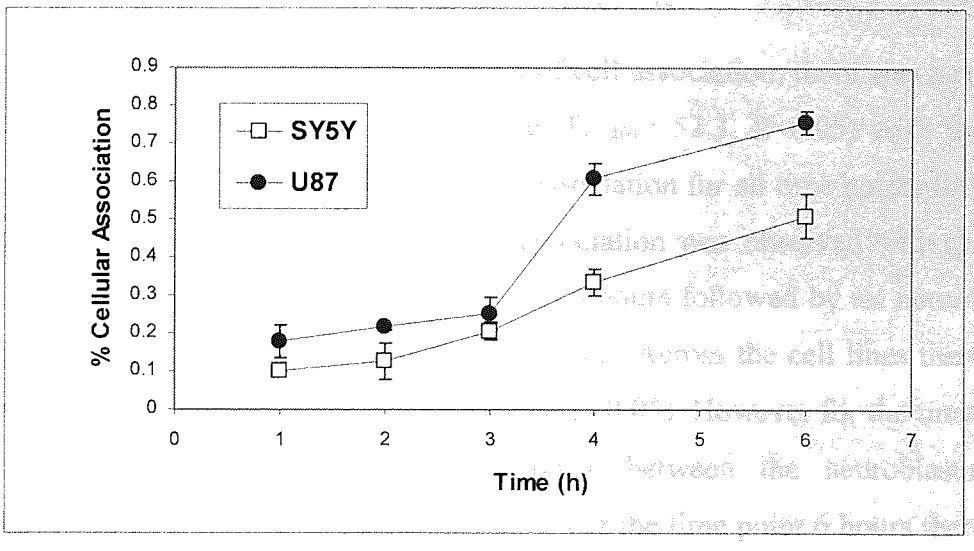

Figure 3.13. *Cellular association of ribozyme in SY5Y and U87 cells over a time course. Error bars represent n=3 ± SD.*

Post-hoc results indicated that first three time points did not have significantly different values whereas with 4 and 6 hour time points the cellular association was significantly different.

Finally for the human glioblastoma cell line U87 (see figure 3.13) the figures were 0.18%, 0.22%, 0.25%, 0.61% and 0.76% for the time points 1, 2, 3, 4 and 6 hour respectively, which were statistically significantly different to each other ($F_{(4,10)}$= 61, P<0.01). However further analysis with post-hoc tests indicated, the first three time points were not significantly different from each other but the last two time points were significantly different to each other and to the first 3 time points. The pattern for association was similar to the above two rat cell lines with a steady rise in cellular association for the first 3 hours and then relatively greater association for the 4 hour time point after which the mean values for cellular association entered a plateau phase. In all the cell lines, generally, the association pattern was similar in all cells with low association observed for the first three hours which probably represents an equilibrium between the association to the cell surface and entrapment in early endosomic vesicles and recycling back to the surface (early efflux phase). After three hours greater ribozyme amount was transported in to the cytoplasm in middle and late endosomic vesicles resuting in increased cellular association as shown in the graph between the three and four time points. After this time period the ribozyme association profile plateaus, representing saturation in the association process.

Overall across the cell lines, in terms of the extent of cell association, there was a significant difference in the cellular association of ribozyme ($F_{(3,40)}$= 52.3, P<0.05) with the human glioblastoma cell line showing the highest cellular association for all time points followed by rat glioblastoma cell line C6. The third highest association was observed with the human neuroblastoma cell line, SY5Y, at time points 3 and 6 hours followed by rat neuroblastoma cell line, GT1, which had the lowest cellular association. Across the cell lines there was no significant difference in time points 1, 2 and 3 hours (p>0.05). However for the time points 4 hour and 6 hour there was significant difference between the neuroblastoma and glioblastoma cell lines within each species (p<0.05). For the time point 6 hours there was no statistical difference between the glioblastoma cells across the species (p>0.05) but there was significant difference between the neuroblastoma cell lines across the species.

It must be noted that the interpretation of existence of differential cellular association in glial and neuronal cells of ribozyme must be viewed with caution as the percentage cell association of ribozyme was poor (less than 1%) and the differences in associations were marginal despite being statistically significantly different in this experiment. Moreover, the liquid scintillation counts obtained for the lysate fractions were very low in these experiments which do not allow strong conclusions to be formulated. In hindsight an experimental design, probably a block design, with replicates greater than three, to take account of variability due to the cellular monolayers, small quantities of ribozyme(picomolar range) and variability in radioactivity counts, would have been appropriate to enable a robust conclusion.

As mentioned in the introduction, to date only two studies have been published to characterise the cellular uptake properties of ribozyme (Fell *et al.*, 1997), (Bramlage *et al.*, 1999), despite successful demonstration of ribozyme efficacy in a variety of experimental and disease models as reported in the literature (see tables 1.3.1, 1.3.2 and 1.3.3). The results of cellular association of ribozyme over a time course obtained in this study are consistent with the findings of (Fell *et al.*, 1997) in which ribozyme uptake was time dependent and reached a plateau phase after four hours. Similar trends in uptake over a time course have been reported with antisense oligonucleotides, molecules which share several properties with ribozymes (Normand-Sdiqui and Akhtar, 1998; Wu-pong *et al.*, 1992; Loke *et al.*, 1989; Shoji *et al.*, 1991; Walker *et al.*, 1995).

However, in contrast to observations with antisense oligonucleotides which were more avidly taken up by neuronal cells (Khan *et al.*, 2000), (Sommer *et al.*, 1996) in comparison to glial cells, the ribozyme *in vitro* had shown a similar affinity for glial and neuronal cells. The absence of a pattern similar to *in vivo* study could be due to *in vitro* nature of the experiment. In summary these results indicate that cellular association of ribozyme was dependent on time and was very limited and furthermore a comparison of cell lines of different species and types suggested that glioblastoma cell lines associate similar ribozyme to neuroblastoma cells.

3.5. Effect of temperature on the cellular association of ribozyme

Evaluation of cellular association of ribozyme over a time course demonstrated that cellular association increases with time up to 4 hours and then reaches a plateau phase. In order to further understand whether this cellular association was an active or passive process the cellular association was investigated at two different temperatures. For this purpose the cellular association of ribozymes was studied for four hours at 37°C and 4°C as described in section 2.7.4. The results of this investigation are shown in the figure 3.14. The mean cellular association for C6 cells at 37°C and 4°C was 0.29% and 0.09% respectively. Giving a difference in cellular association of 3.2 fold and was statistically highly significant ($T_{(8)}$= 3.1, P<0.01). For the rat glioblastoma cell line, GT1, the respective percent cellular association was 0.23% and 0.15% giving rise to a significant difference of 1.5 fold in cellular association ($T_{(8)}$= 0.01, P<0.001). Human neuroblastoma cell line, SY5Y, had a cellular association of 0.15% for 37°C and 0.12% for 4°C, which resulted in a difference of 1.25-fold and which was statistically significant ($T_{(8)}$= 1.45, P<0.05). Finally, the human glioblastoma cell line, U87, had a percent cellular association of 0.29% for 37°C and 0.14% for 4°C having a difference of 2.1-fold which was statistically significant ($T_{(8)}$= 9.3, P<0.01).

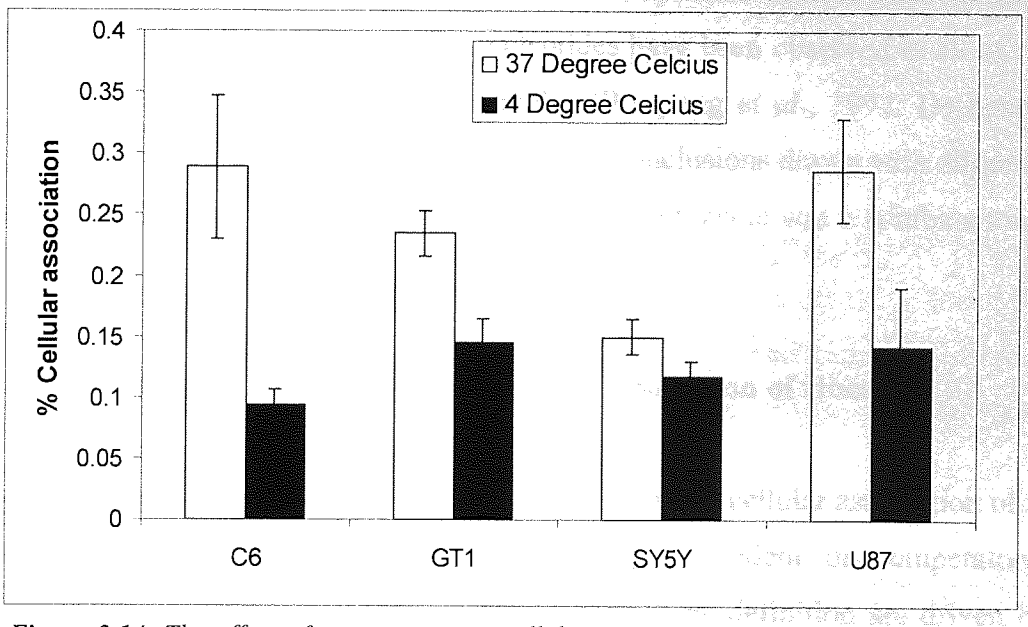

Figure 3.14. *The effect of temperature on cellular association of ribozyme in C6, GT1, SY5Y and U87 cells. The bars in white colour show the cellular association for each cell line at 37℃ and black bars show cellular association at 4℃. Error bars represent n=3±SD.*

As the figures above show all cell lines demonstrated a similar pattern of cellular association at the two temperatures studied reflecting that the cellular association was dependent on

temperature and therefore was an active process. However, at the low temperature despite any significant energy in the cells there was a small cellular association observed which probably suggests that there also may be non-energy dependent component involved in the cellular association as well.

In terms of the extent of cellular association the difference in cellular association at the two temperatures was higher in glial cells in comparison to the neuronal cell lines. This could be explained by the fact that the extent of cellular association in glial cell lines was generally higher as shown in the previous section which led to a more pronounced difference in cellular association at the two temperatures. In contrast the neuronal cell lines, GT1 and SY5Y showed a relatively lower temperature difference in cellular association, which could be explained by the fact that neuronal cells have a relatively less cellular association of ribozyme.

These results are in general agreement with previous studies in which it was shown that cellular association is dependent on temperature (Fell *et al.*, 1997). Similar results were reported in a study by Hudson *et al.*, (1999) in which ribozyme conjugated to a transferrin receptor antibody had a 5 fold lesser uptake at 4°C compared to uptake at 37°C. Reduction in the cellular association of antisense oligonucleotides have been observed in all of the studies of characterisation of uptake of these molecules (Wu-pong *et al.*, 1992; Deshpande *et al.*, 1996). From results obtained in this experiment and conclusions drawn with oligonucleotides studies it can be suggested that that the association of ribozyme was a combination of active and passive processes.

3.6. Effect of metabolic inhibitors on the cellular association of ribozyme

Studies to evaluate the effect of time and temperature on the cellular association of ribozyme demonstrated that cellular association was largely dependent on temperature, which suggested it can be an active process. Active processes by definition are driven by energy and therefore are energy dependent. In order to further evaluate that cellular association seen in these experiments was an active, energy dependent process, cellular association was undertaken after depleting the cells of energy to observe if this manipulation can lead to lesser association. For this purpose cells were depleted of energy by pre-incubation with

10mM NaN_3 (a cytochrome oxidase inhibitor) and 20mM 2-deoxyglucose (a glycolysis inhibitor) for 1 hour prior to the addition of ribozyme to the cells and a cellular association study carried out as described in section 2.7.5.

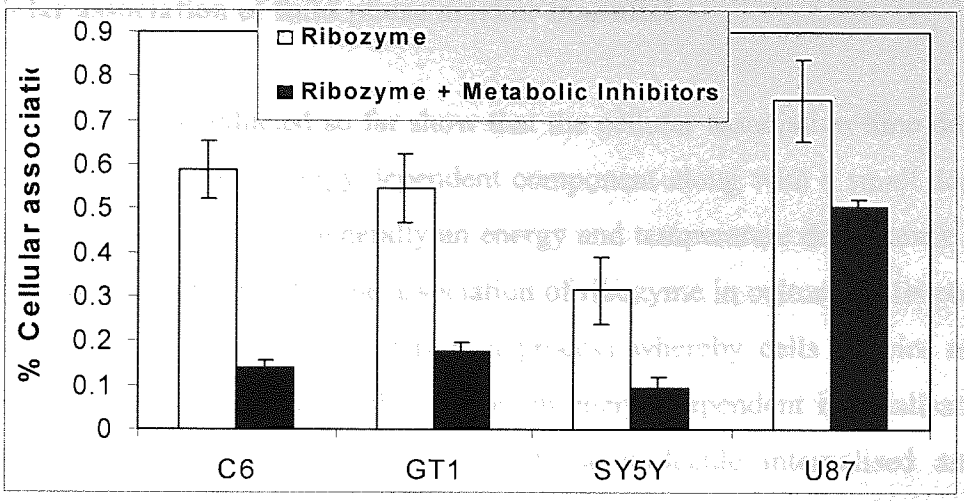

Figure 3.15. *The influence of metabolic inhibitors on the cellular association of ribozyme in C6, GT1, SY5Y and U87 cells. Cells were pre-incubated with metabolic inhibitors at 37℃ for 4 hours in the presence of inhibitors. Error bars represent n=3±SD.*

Figure 3.15 shows the results of ribozyme cellular association in the presence of metabolic inhibitors for all cell lines along with control cells which were cells undergoing normal cellular association and without any metabolic inhibitors pre-incubated with these cells. The rat glioblastoma cell line C6 had a cellular association of 0.59% for control cells whereas experimental cells which were pre-incubated with metabolic inhibitors the association was 0.14% giving rise to a difference of 4.3 fold which was statistically significant ($T_{(4)}$= 1.2, P<0.000). Similar results were seen with GT1 cells in which the cellular association for ribozyme alone was 0.55% and was 0.18% in the presence of metabolic inhibitors giving rise to a significant difference of 3 fold ($T_{(4)}$= 2.3, P<0.000). For the human neuronal cell line, SY5Y, the cellular association was 3.4 fold different and was statistically significant ($T_{(4)}$= 2.8, P<0.05). Finally for the human glial cell line U87 there was a significant difference of 1.5 fold ($T_{(4)}$= 0.8, P<0.05) between the control and experimental cells. In all cell lines studied the pattern of reduction in cellular association of ribozyme after energy depletion was similar, however, in U87 cells despite the absence of any metabolic energy there was a noticeable cellular association which could be due to a non-energy requiring passive process. These results show that generally the cellular association was an energy dependent process with a small component of passive non-energy requiring component. These results are in general agreement with previous studies which have showed similar patterns of reduction in

nucleic acids binding to cells after energy depletion (Wu-pong *et al.*, 1994), (Fell *et al.*, 1997).

3.7. Cellular association of fluid phase marker mannitol

Results from studies conducted so far show that the cellular association time dependent and included a temperature and energy-dependent component along with a small degree of non-energy dependent component. Generally an energy and temperature dependence in a cellular association process indicates that the association of ribozyme in cultured cells could possibly be an endocytotic process. Endocytosis is a process whereby cells acquire metabolically necessary substances from outside the cell by an energy dependent internalisation process. This internalisation depends on the nature of the molecule internalised and could be facilitated by a carrier or a receptor with the mechanism of internalisation being surface adsorption or pinocytosis (cell drinking). In order to investigate whether the cell lines under investigation had any pinocytotic component in their internalisation mechanism, cellular association of a fluid phase marker ^{14}C mannitol was studied over a time course. Mannitol is a glucose dimer which is exclusively taken up by cells via the fluid phase endocytotic process (Besterman *et al.*, 1981) and is used as marker to identify any pinocytosis carried out by cells.

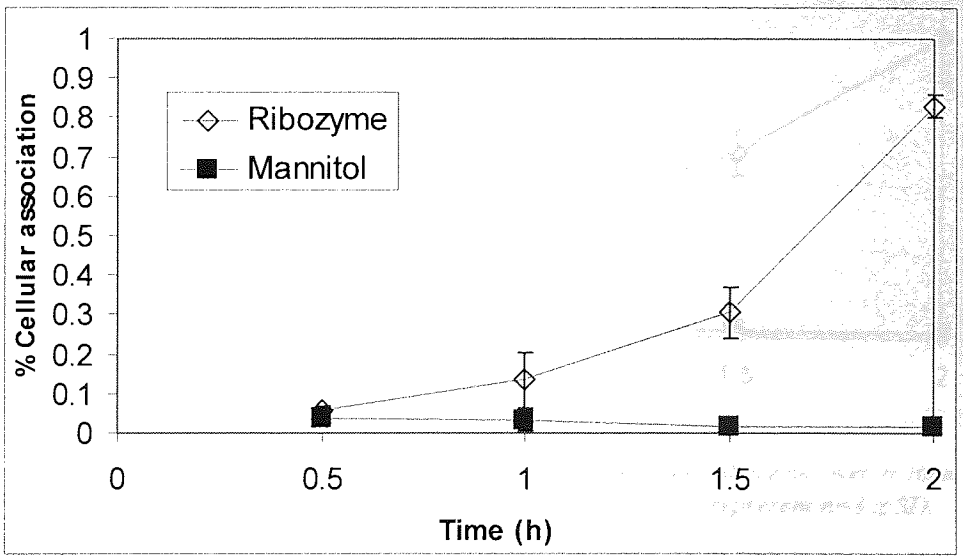

Figure 3.16. *Shows the cellular association of ^{14}C mannitol in comparison with ribozyme over a 2-hour time course in C6 cells. Error bars represent n=3 ± SD.*

Figures 3.16 and 3.17 show the cellular association of mannitol along with ribozyme at 37°C over a time course in rat glial and neuronal cell lines.

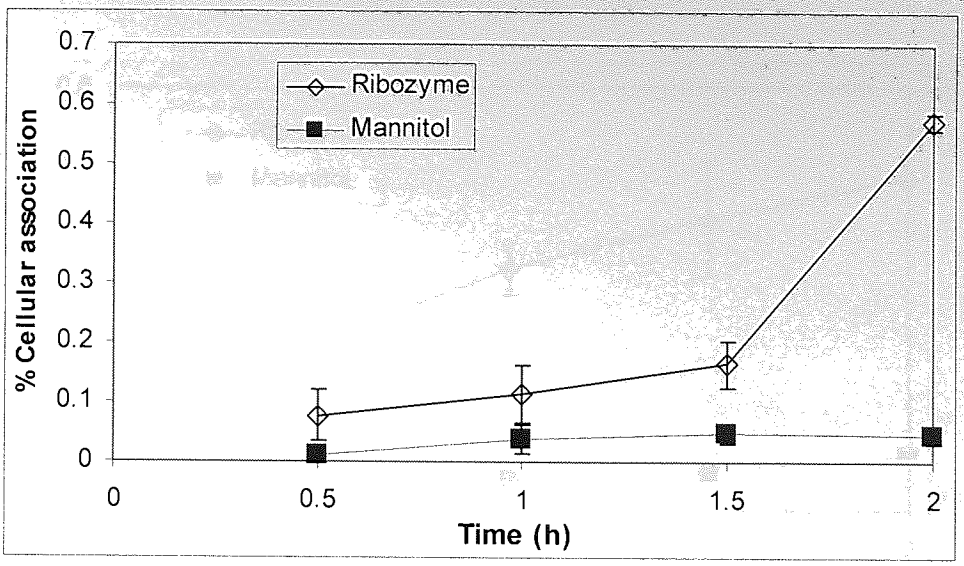

Figure 3.17. *Shows the cellular association of ^{14}C mannitol in comparison with ribozyme over a 2 hour time course in GT1 cells. Error bars represent n=3 ±SD.*

The data from these graphs show that cellular association of mannitol was extremely low and can be considered to be negligible, indicating that these cells do not have any element of pinocytosis in the overall endocytotic process of the cells. Similar results have been seen with the human neuroblastoma and glioblastoma cell lines in respect of the cellular association of mannitol as shown in figure 3.18 and 3.19.

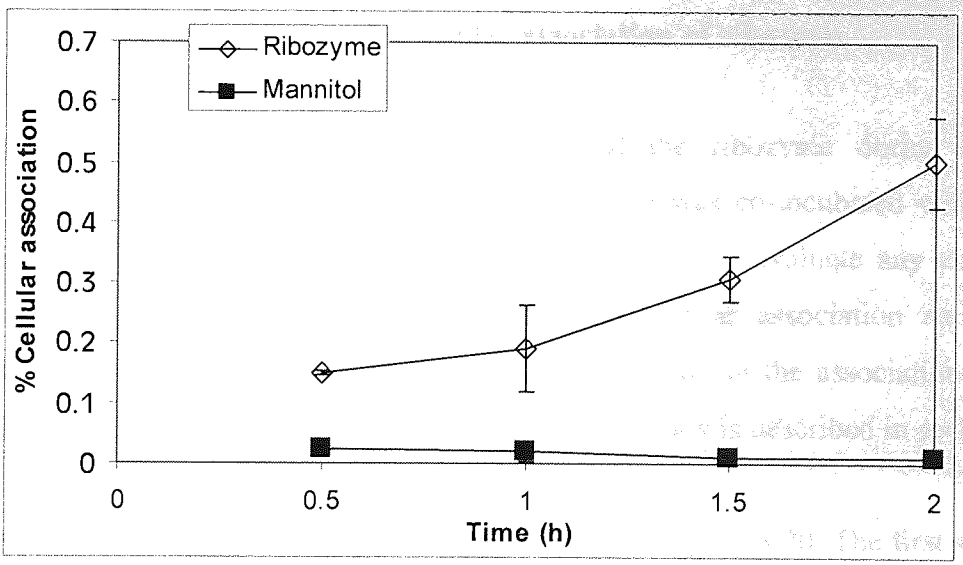

Figure 3.18. *Cellular of association of mannitol along with ribozyme over a time course in SY5Y cells. Error bars represent n=3±SD. Error bars represent n=3 ±SD.*

From this data it can be infered that the cellular association mechanism for ribozyme had no pinocytotic component as there was neglegible constitutive pinocytosis occuring in cells. These results are consistent with other studies (Fell *et al.*, 1997; Islam *et al.*, 2000) in which mannitol was reported to have negligible uptake implying no uptake via pinocytosis.

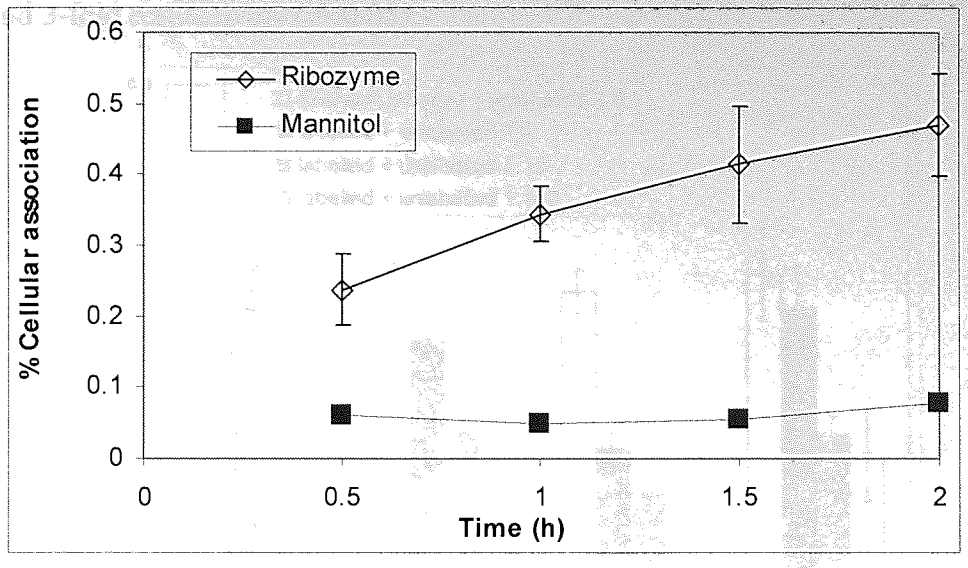

***Figure 3.19**. Cellular of association of mannitol along with ribozyme over a time course in U87 cells. Error bars represent n=3±SD. Error bars represent n=3 ±SD.*

These results support the explanation that the ribozyme association with cells could not be facilitated by a pinocytotic process as there was no constitutive pinocytosis taking place in the cells.

3.8. Effect of self-competition on the cellular association of ribozyme

To further elucidate the binding characteristics of the ribozyme during the cellular association mechanism, the internally labelled ribozyme was co-incubated with increasing concentrations of cold (unlabelled) ribozyme with the aim to evaluate any change in the cellular association of ribozyme. Any reduction in cellular association as a result of competition with a cold ribozyme would indicate specificity in the association mechanism and would exclude non-specificity. The protocol for this study is described in section 2.7.7.

The results for this study for all cell lines are illustrated in figure 3.20. The first set of bars in the chart represent the results for the rat glioblastoma C6 cells. There was a significant reduction in the cellular association of ribozyme as the concentration of cold ribozyme increased ($F_{(3,8)}$= 9, $P<0.05$). Post-hoc tests showed that there was no significant difference observed between the control group and the experimental group in which the hot and cold ribozyme had a one to one ratio ($P>0.05$). However, when the concentration of the cold

ribozyme was 10 and 100 times greater, association of ribozyme was significantly reduced by 2 and 3-fold respectively ($P<0.05$).

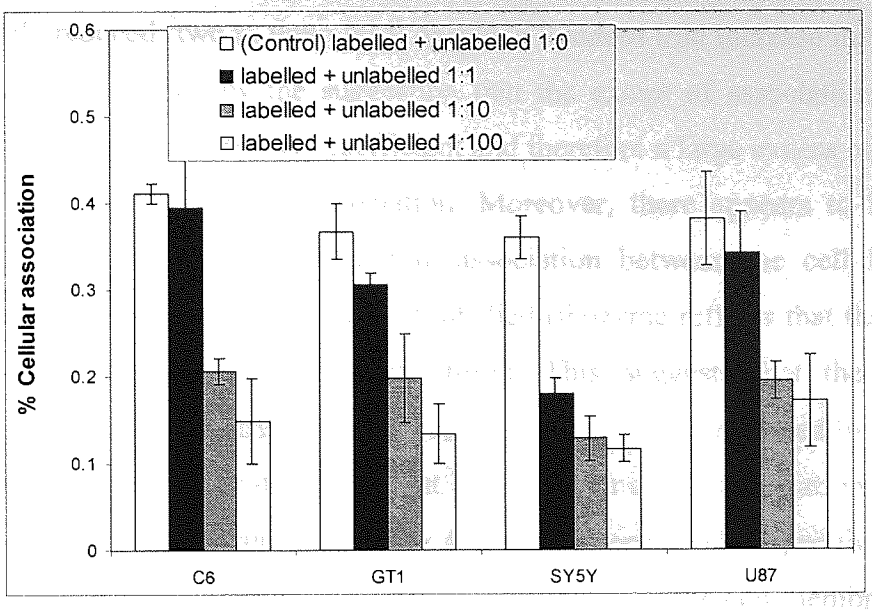

Figure 3.20. *Cellular association of co-incubated labelled ribozyme with increasing concentrations of cold (unlabelled) ribozyme. Data represents n=3±SD.*

Similar results were seen with the rat neuroblastoma cell line, GT1 in which the control was not significantly different to the cells, which had been co-incubated with equal amount of unlabelled ribozyme. However when the concentrations were 10 and 100 times higher the cellular association was significantly reduced ($F_{(3,8)}= 79$, $P<0.000$). This reduction was 2-fold with 10-fold higher concentration group and 3-fold with 100-fold higher group concentration. In contrast to the above two cell lines the rat neuroblastoma cell line, SY5Y, there was significant reduction in cellular association with all experimental groups in comparison to the control ($F_{(3,8)}= 92$, $P<0.001$). This reduction was 2-fold, 3-fold and 3-fold as the competing unlabelled ribozyme concentration ratio increased from 1, 10 and 100 times respectively. Finally for the human glioblastoma cell line, U87, the pattern of reduction of association in the presence of increasing amounts of competing unlabelled ribozyme was similar to the C6 and GT1 cells. There was no significant difference between the control and the first group whereas with the third and fourth group of cells there was significant reduction in the cellular association ($F_{(3,8)}= 5.3$, $P<0.05$). This reduction was approximately 2-fold.

A comparison of the pattern of reduction in cellular association between cell lines with increasing concentrations of cold ribozyme, shows that generally at the high concentrations

(10× and 100× concentrations) there was a similar reduction in the hot riboyzme. In regards to the extent of reduction in the cellular association with self-competition, the cell association is not greatly reduced (two to three fold) despite a hundred fold increase in the concentration. This could be explained by the suggestion that the extent of association of ribozyme, as shown by previous results, is very inefficient and therefore a large excess of cold ribozyme is required to reduce the cellular association. Moreover, there appears to be no significant difference in the pattern of reduction in association between the cell lines. This dose-dependent inhibition in the association of labelled ribozyme reflects that the association was was open to inhibition with self-competition. This suggests that the association was indicative of specific cell surface binding mechanism possibly mediated by binding proteins. These results further demonstrate that that in all cell lines the association of ribozyme was not a non-specific phenomenon but rather a specific process. This specificity in the cellular association indicates the presence of a structure anchored in the cell membrane, which could potentially be a carrier or receptor, which specifically mediates the association process.

3.9. Assessment of cell surface protein binding of ribozyme

Results obtained so far suggest that the association of ribozyme could be mediated by a carrier or receptor macromolecule anchored on the cell membrane. In order to further characterise the nature of the ribozyme-binding molecule, whether it is a lipid or protein, and estimate the amount of ribozyme association to surface proteins post-association trypsin washings experiment was carried out. The rationale for this experiment was that if the ribozyme binding surface molecule was a protein then once the ribozyme was bound to it then this complex will be susceptible to removal with a proteolytic enzyme such as trypsin and if the mediating molecule is a lipid then no bound ribozyme will be able to be washed off with trypsin. The procedure for this experiment is described in section 2.7.10 and the results are described and discussed below.

The results for the post cellular association trypsin washing for human glioblastoma cell line C6 are illustrated in figure 3.21. Total cellular association of ribozyme was taken as control and in comparison to this there was 94% association of ribozyme with the trypsin sensitive cell surface proteins and 4% associated with the lysate fraction which might constitute of non-trypsin sensitive protein sites, lipids or taken up by the cells.

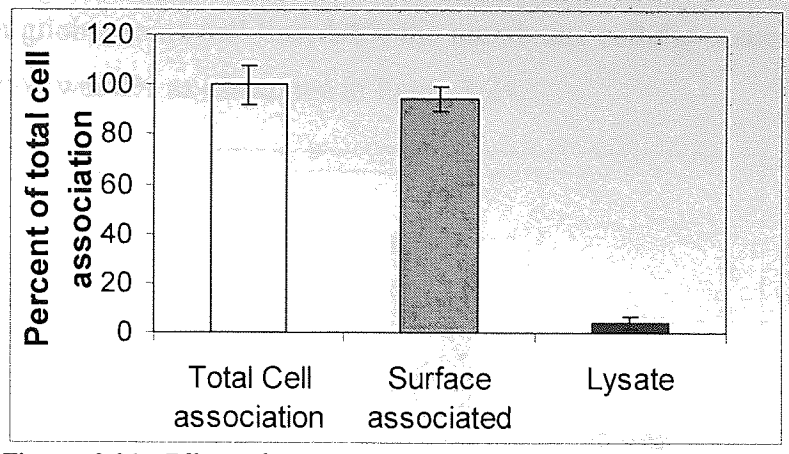

Figure 3.21. *Effect of trypsin washing on cellular association of ribozyme in C6 cells. n=3±SD.*

For the rat neuroblastoma cell line, GT1, the protein associated ribozyme was 78% of the total cellular association as shown in figure 3.22 and for the human neuroblastoma cell line, SY5Y, the membrane associated fraction was 83% (figure 3.23).

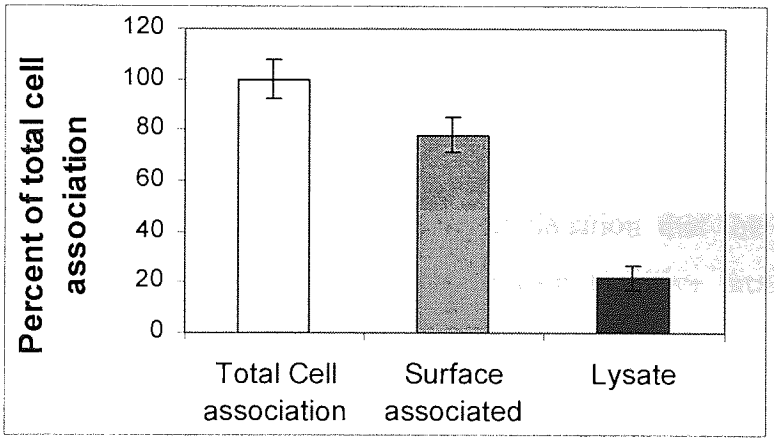

Figure 3.22. *Effect of trypsin washing on cellular association of ribozyme in GT1 cells. n=3±SD.*

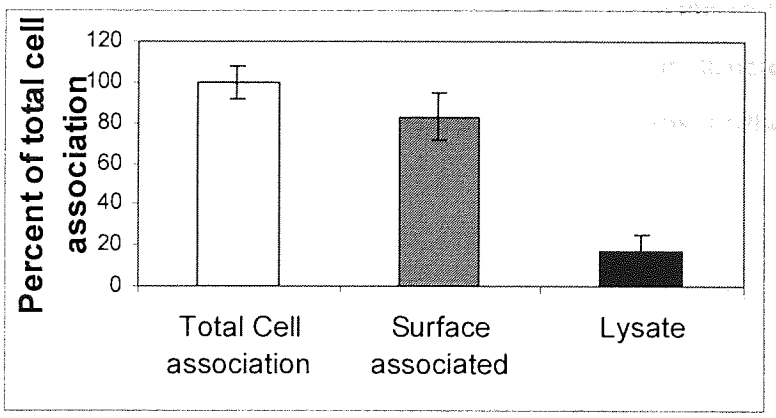

Figure 3.23. *Effect of trypsin washing on cellular association of ribozyme in SY5Y cells. n=3±SD.*

For the human glioblastoma cell line, U87, the membrane cellular association was 93% and the lysate fraction was 8% as illustrated in figure 3.24.

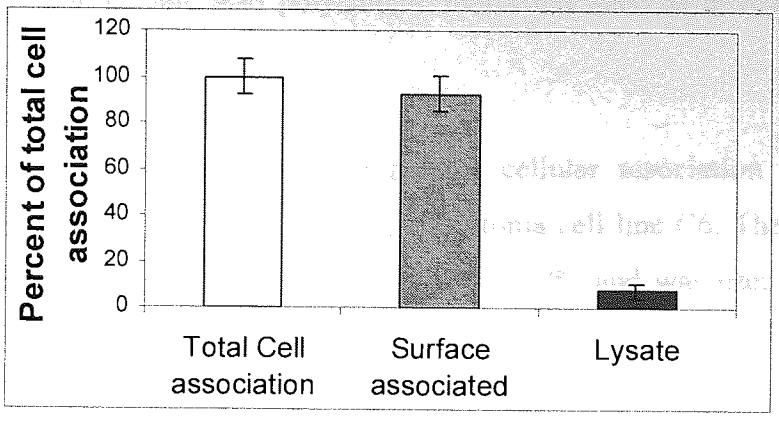

Figure 3.24. *Effect of trypsin washing on cellular association of ribozyme in U87 cells. n=3±SD.*

These results show that a large proportion of ribozyme complexes with cell membrane bound proteins, which are sensitive to trypsin and the remaining fraction could either bind to non-trypsin sensitive protein or cell surface molecules such as lipids, glycoproteins etc or the ribozyme was endocytosed by cells. It can be concluded from these results that ribozyme association in all cells was consistent with the explanation that the large proportion of ribozyme cellular association was mediated by trypsin sensitive proteins present on the surface of cells.

3.10. Effect of competitive inhibitors on cellular association

Investigation of self-competition of cellular association of ribozyme in the previous section implied the presence of a cell membrane anchored lipid or protein structure, which mediates the cellular association process. This cell surface structure was further characterised by trypsin washing experiment and was found to be a protein by nature. To further determine the specificity of this putative protein structure, cellular association of ribozyme was investigated in the presence of large polyanionic nucleic acid molecules such as adenosine triphosphate (ATP), salmon sperm DNA and non-nucleic acid polyanionic molecules such as dextran and heparin as described in section 2.7.8. The rationale for selecting short and long chain nucleic acid molecules such as ATP and salmon sperm DNA was to investigate whether the length of the nucleic acid was of importance for competitively inhibiting ribozyme cellular association. As ATP was a single base monomer and salmon sperm DNA

was a long chain DNA sequence which possessed a large number of anionic charges. To further differentiate the specificity of the association mediating cell surface protein molecules large non-nucleic acid polyanionic molecules such as dextran and heparin were used as competing agents.

Figure 3.25 represents the reduction in percent cellular association of ribozyme in the presence of competitive inhibitors for rat glioblastoma cell line C6. The cellular association of ribozyme in the absence of any inhibitors was 0.28% and was used as a control for the interpretation of the results of this experiment.

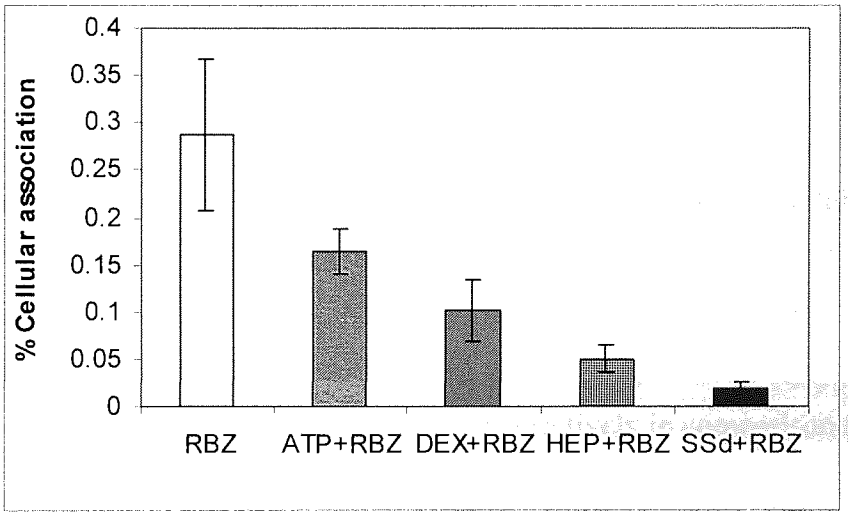

Figure 3.25. *Graph showing percent cellular association of internally labelled ribozyme in the presence of ATP, dextran, heparin and salmon sperm DNA in C6 cells (n=3±SD).*

Co-incubation with competitive inhibitors reduced the cellular association significantly ($F_{(4,20)}$= 19.324, P=0.001). In the case of co-incubation with ATP the cellular association was 0.16%, which was a 57% reduction in comparison to the control. For co-incubation with Dextran the association was 0.10% resulting in a reduction of 36%. For heparin the cellular association of ribozyme had a mean cellular association of 0.05% reducing it to 17%. Salmon sperm DNA co-incubation reduced the association to 0.02% causing it to be reduced to 7% of the control. The effect of cellular association of ribozyme in the presence of competitive inhibitors in rat glioblastoma cell line GT1 is shown in figure 3.26. The cellular association of ribozyme without co-incubation with competitive inhibitors was 0.20% and this value was used as a control for the analysis of the results.

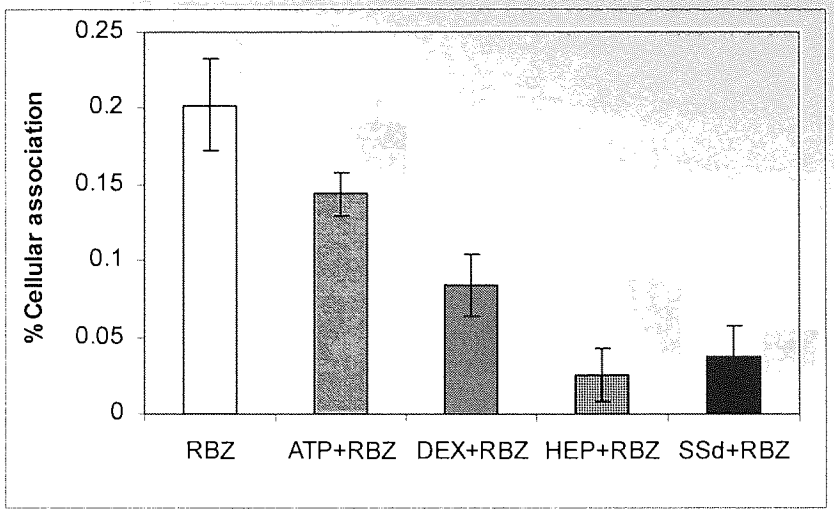

Figure 3.26. *Graph showing percent cellular association of internally labelled ribozyme in the presence of ATP, dextran, heparin and salmon sperm DNA in GT1 cells (n=3±SD).*

As the results show co-incubation of ribozyme with these competitive inhibitors resulted in a significant reduction in cellular association ($F_{(4,20)}$= 10.990, P=0.001). Co-incubation with ATP gave a mean association value of 0.14%, which was a reduction to 70% in comparison to the control. In the case of competition with dextran, heparin and salmon sperm DNA the association was reduced to 40%, 15% and 20% respectively in comparison to the control.

Similarly for the human neuroblastoma cell line SY5Y, co-incubation of ribozyme with competitive inhibitors resulted in significant reduction in cellular association ($F_{(4,11)}$= 17.478, P=0.000) as shown in figure 3.27. Cellular association of ribozyme in the absence of competitive inhibitors was 0.13%. This association was reduced to 84% when the ribozyme was co-incubated with ATP as shown by a cellular association of 0.11%. Co-incubation with dextran gave an association of 0.02% resulting in a reduction to 15%. When heparin and salmon sperm DNA were used the cellular association was 0.04% and 0.02% respectively. These reductions in cellular association were 31% and 15% in comparison to the control.

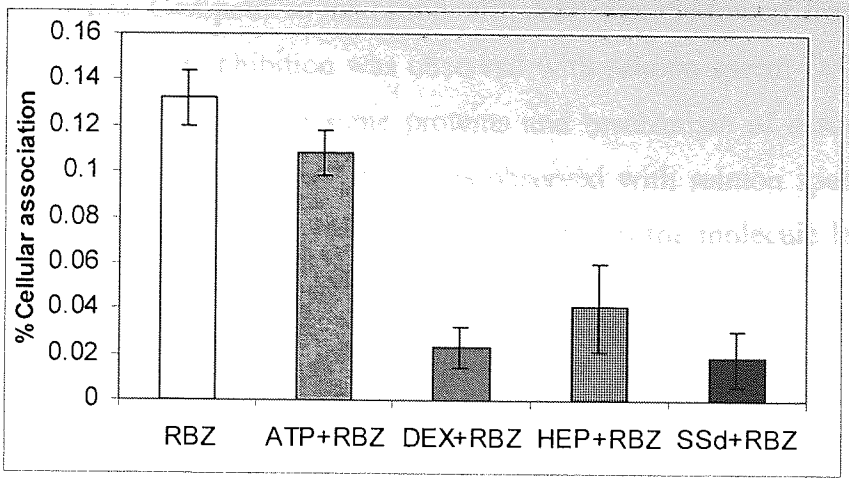

Figure 3.27. *Graph showing percent cellular association of internally labelled ribozyme in the presence of ATP, dextran, heparin and salmon sperm DNA in SY5Y cells (n=3±SD).*

The cellular association of ribozyme in human glioblastoma cell line U87 is illustrated in figure 3.28. As with the other cell lines there was a significant reduction in the cellular association of ribozyme by co-incubation with polyanionic molecules ($F_{(4,10)}$= 20.35, P=0.001). There was a 36, 43, 71 and 86% reduction in the association in comparison to the control cells when cells were co-incubated with ATP, dextran, heparin and salmon sperm DNA respectively.

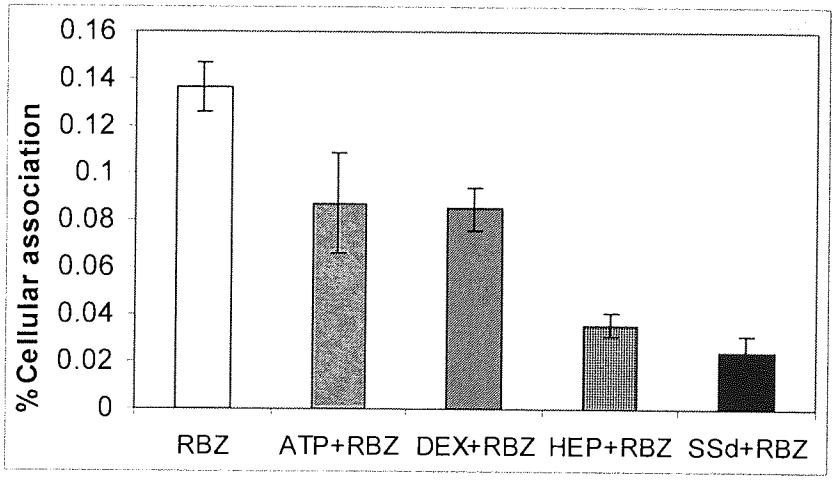

Figure 3.28. *Graph showing percent cellular association of internally labelled ribozyme in the presence of ATP, dextran, heparin and salmon sperm DNA in U87 cells (n=3±SD).*

These results show that the cellular association of ribozyme was inhibited by co-incubation with polyanionic molecules reflecting that the cell surface protein which binds to the ribozyme was not specific for ribozyme association. This putative carrier/receptor surface protein molecule seems to interact with ribozyme in an ionic fashion as shown with the

influence of pH on association (see section 3.11) and is susceptible to competition from other polyanionic molecules. Competitive inhibition with ATP was the lowest from all polyanions and the largest competitive inhibition was observed with salmon sperm DNA reflecting the fact that these molecules share the same proteins and mechanism of association with the ribozyme. Greater inhibition of association was observed with salmon sperm DNA, which has a long sequence and hence greater anionic character in the molecule leading to higher binding with surface proteins.

Beck *et al.*, (1996) has reported that uptake of oligonucleotides is dependent on length of the molecule with increasing length leading to increased uptake. Similar competitive inhibition was seen with heparin and dextran reflecting that ribozyme association was mediated by surface proteins therefore involves a non-specific component. These results are in general agreement with studies of oligonucleotide competition with polyanionic molecules. Loke *et al.*, (1989) reported competitive inhibition of oligonucleotide by single nucleotides such as ATP and also by large molecules such as plasmid DNA. Bennett *et al.*, (1985) had observed a reduction of oligonucleotide uptake by co-incubation with heparin. In another report to assess the effect of polyanions on the uptake of oligonucleotides, Wu-pong *et al.*, (1992) observed a significant reduction in uptake by pre-incubation with 100 molar excess of ATP, random-sequence oligonucleotides, salmon sperm DNA and dextran sulphate. The results shown and discussed in this section demonstrate that that carrier protein molecules mediating the cellular association of ribozyme can be competitively inhibited by large polyanionic molecules. This reflects a non-specific hybridisation element in the interaction of ribozyme with these putative cell surface proteins.

3.11. Effect of pH on cellular association of ribozyme

In order to further understand the nature of cellular association mechanism the cellular association of ribozyme was investigated in growth medium at a range of pH values. Cells were seeded at 1×10^5 cells per well and incubated with internally labelled ribozyme over a range of pH values as described in section 2.7.9.

Figure 3.29 shows the results of the influence of pH on the cellular association of ribozyme on a monolayer of C6 cells. The graphical representation illustrates that cellular association

of ribozyme increases significantly as the pH decreases ($F_{(3,10)}$= 140, P<0.001). At pH 5 there was a 5-fold increase in ribozyme cellular association and a 4-fold increase at pH 6 in comparison to pH 7. Whereas, at basic pH value 8, there is no significant change in cellular association as shown by post-hoc tests (p<0.05).

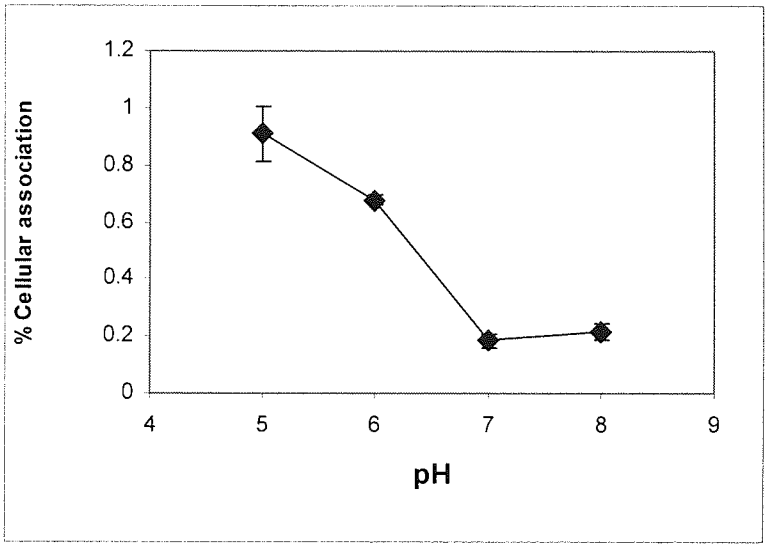

Figure 3.29. *Effect of pH on cellular association of ribozyme on a monolayer of C6 cells. Data represents the means (n=3)±SD.*

The cellular association of ribozyme as function of pH on a monolayer of GT1 cells is represented in figure 3.30. As the results show there was a significant rise in ribozyme cellular association as the pH value decreases ($F_{(3,11)}$= 22, P<0.001). This increase relative to other cell lines is moderate with pH 5 increasing the association by 3-fold. The mean cellular association values at other pH values were different but not significant statistically as shown by post-hoc tests (P<0.05).

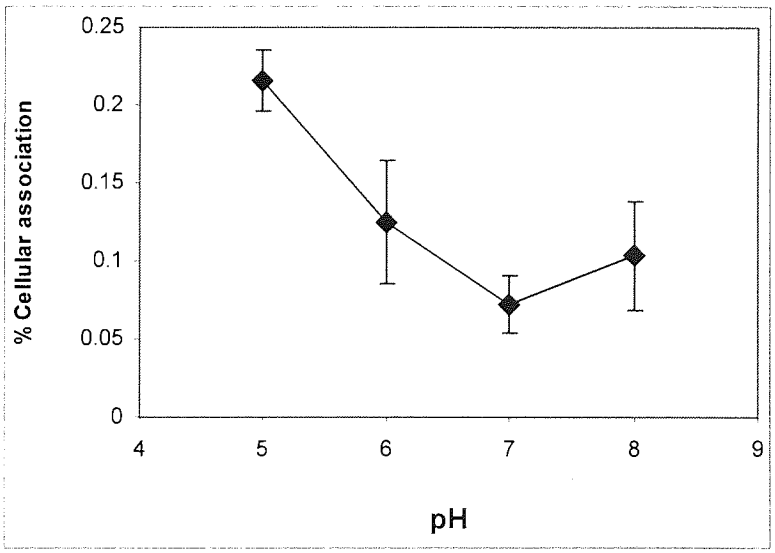

Figure 3.30. *Effect of pH on cellular association of ribozyme on a monolayer of GT1 cells. Data represents the means (n=3)±SD.*

Figure 3.31 illustrates the influence of pH on the cellular association of ribozyme on a monolayer of human neuroblastoma cell line SY5Y. As the graph shows, there was a large and significant increase in the cellular association of ribozyme with a reduction in pH ($F_{(3,10)}$= 111, P<0.000).

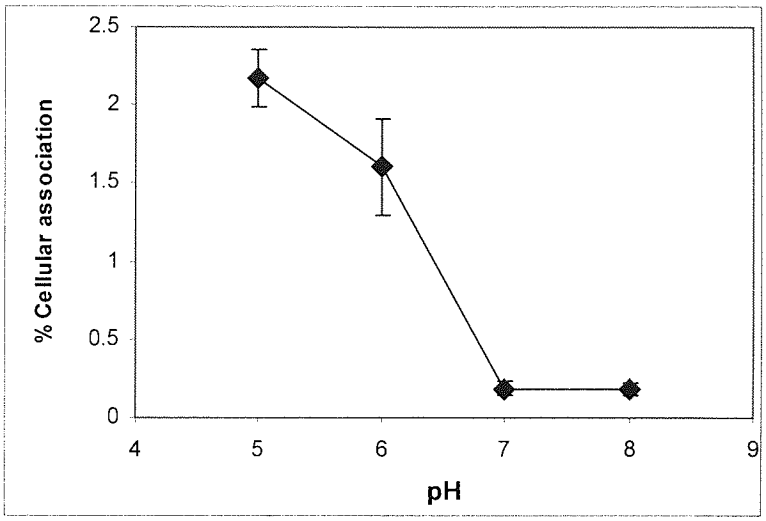

Figure 3.31. *Effect of pH on cellular association of ribozyme on a monolayer of SY5Y cells. Data represents the means (n=3)±SD.*

At pH 5 the cellular association of ribozyme was 12-fold higher in comparison to pH 7 whereas at pH 6 there was a slightly lesser increase of 9-fold. There was no significant change in cellular association observed at pH 8. Post-hoc tests revealed that mean association at pH 5 and 6 were not statistically different to each other but were significantly different to association at pH 7 and 8 (P<0.05).

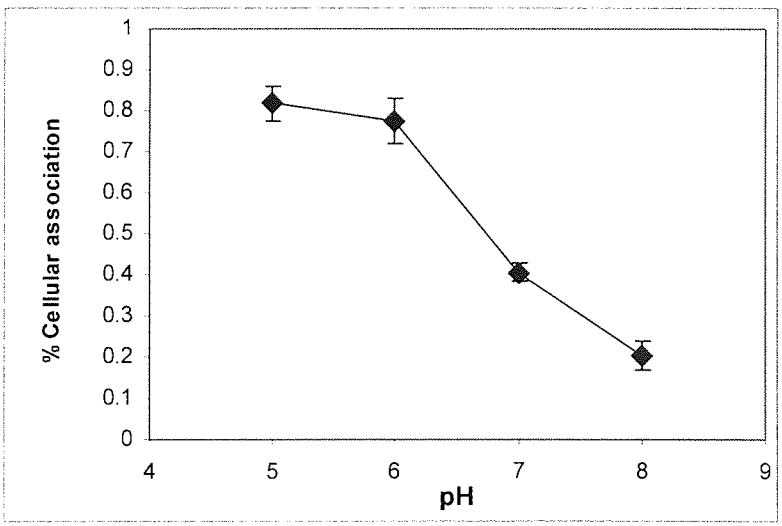

Figure 3.32. *Effect of pH on cellular association of ribozyme on a monolayer of U87 cells. Data represents the means (n=3)±SD.*

Finally, the cellular association of ribozyme on a monolayer of human glioblastoma cells (U87) is represented in figure 3.32. This cell line exhibited a similar pattern to C6 and SY5Y cells with a significantly large increase in cellular association as pH decreases ($F_{(3,11)}$= 14, P<0.001). Post-hoc tests revealed that at lower pH values of 5 and 6 there was a significant difference in association whereas there was no significant difference in the cellular association values between pH 5 and 6 (P<0.05). The difference at pH 5 and 6 was two fold with respect to pH 7. In contrast at pH 8 there was 2-fold reduction in the cellular association of ribozyme, which had not been observed with other cell lines.

In terms of intercellular differences in response to changes in pH, human neuroblastoma cell line, SY5Y, was most sensitive followed by rat glioblastomas C6 and human glioblastoma U87 cells with the rat neuroblastoma cell line SY5Y showing the lowest response to changes in pH. These results are in general agreement with other published work on ribozyme and antisense oligonucleotide (Fell *et al.* 1997), (Beck *et al.* 1996) where a similar increase in uptake of oligonucleotides was observed. The results of this experiment suggest that the putative ribozyme binding cell surface proteins are sensitive to changes in pH by exhibiting a greater affinity for ribozyme at acidic values leading to increased association. It has been postulated previously that enhanced binding observed at low pH could be due to the presence of a 34-kDa membrane protein receptor that functions around pH 4.5 (Goodarzi *et al.*, 1991). This could be due to fact that certain amino acids such as histidine present in proteins, which have a pKa of 6.5 are susceptible to protonation over a pH range of 7.2 to 5.0. In this experiment as the pH of the medium was reduced the binding proteins were protonated at the amino or carboxylic acid terminals of the amino acids leading to greater attraction of oppositely charged ribozymes resulting in greater binding with the polyanionic ribozyme.

3.12. Dissociation of ribozyme from cellular monolayers

Ribozyme cellular association reaches a plateau phase after four to six hours of exogenous administration as shown by time course profiles in figure 3.4. The plateau phase indicates that cellular association is a dynamic process representing both association and dissociation at equilibrium. At the plateau phase if the ribozyme containing external medium is removed and replenished with fresh medium at selected intervals the amount of ribozyme dissociated can be assessed by plotting an dissociation profile. Such a dissociation profile can provide

clues about the sub-cellular distribution of ribozyme in cytoplasmic compartments over a time course.

For this aim a dissociation study of ribozyme was conducted with all cell lines over a time course as described in section 2.7.6. Figures 3.33, 3.34, 3.35 and 3.36 show the dissociation profiles of ribozymes following incubation of ribozyme for 4 hours for all cell lines.

The dissociation pattern of rat glial cell line, C6, is shown in figure 3.33 as reduction in percent associated ribozyme over a time course of six hours. In the first hour, the associated ribozyme was reduced to 70% and further fell to 39% with a constant rate till 3-hour time point. After the 3-hour time point the rate of release of ribozyme from cells was reduced and by 6 hours 26% of associated ribozyme still remained in the cells. This pattern of release can be described as a biphasic release of ribozyme from cells.

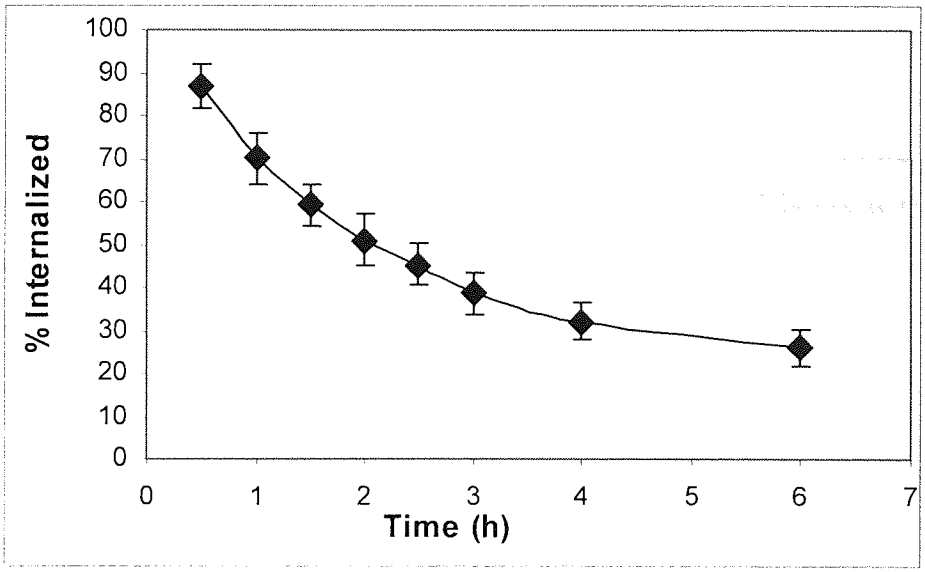

Figure 3.33. *Dissociation profile of internally labelled ribozyme from C6 cells shown by reduction in percent internalised ribozyme over a time course. n=3 ±SD.*

The first phase, which is the fast release period from time points 0 to 3 hours had a higher gradient value of 0.31%/s in comparison to the second slower phase, which had a gradient of value of 0.10%/s.

The dissociation profile of internally labelled ribozyme for rat neuroblastoma cells, GT1, is shown in figure 3.34 and the pattern of release was quite similar to the dissociation profile of C6 cells.

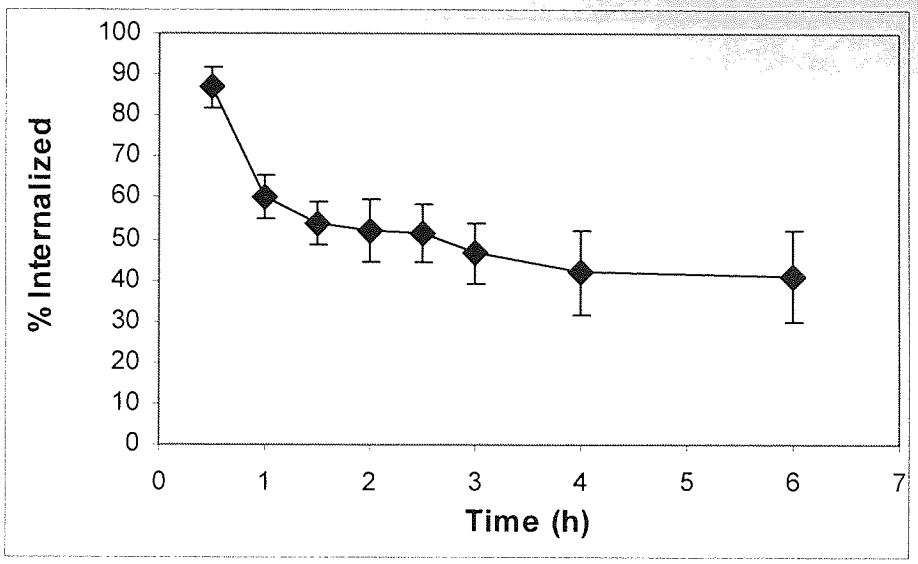

Figure 3.34. *Dissociation profile of internally labelled ribozyme from GT1 cells shown by reduction in percent internalised ribozyme over a time course. Error bars represent n=3 ±SD.*

The release pattern had two different rates of release with the first phase exhibiting a faster reduction in associated ribozyme in comparison to the second phase. In the first phase the associated ribozyme was reduced to 54% which lasted up to 1.5 hours with a rate of 0.74 %/s. The second phase from 2 hours to 6 hours had a slower efflux profile with a rate of associated ribozyme reduction of 0.07%/s. After 6 hours there was still 40% ribozyme associated with the cells.

The dissociation profile for human neuroblastoma cell line SY5Y is shown in figure 3.35, which has a similar pattern of biphasic release as the first two lines described earlier on in the section. The first 'fast' release profile which ends at 2 hour time point has a higher gradient of 0.4%/s in comparison with the second 'slower' phase which had a gradient of 0.07%/s. At 2h time point, which is at the end of the first phase there is a 52% reduction in the total associated ribozyme. In the second as lesser gradient value reflects there is slower reduction in the associated ribozyme with 40% ribozyme remaining associated after 6 hours.

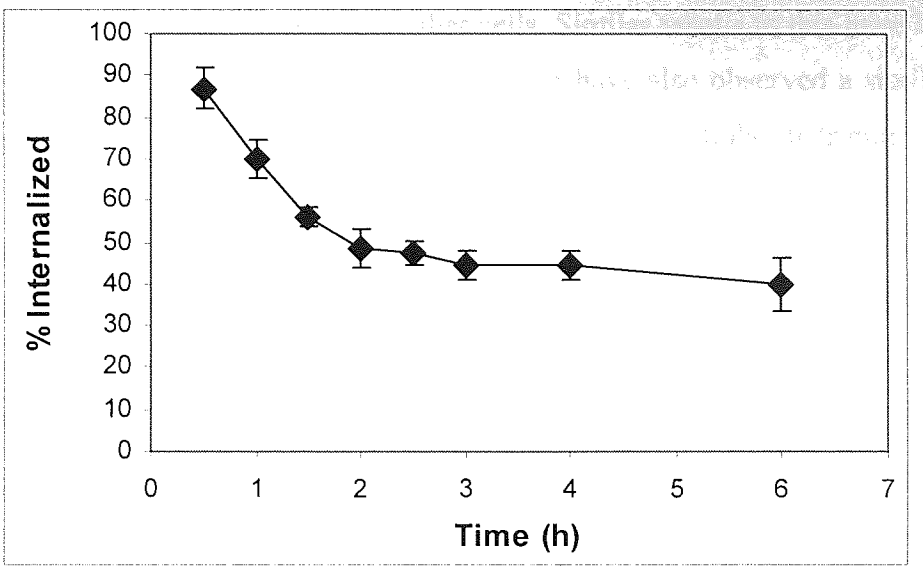

***Figure 3.35**. Dissociation profile of internally labelled ribozyme from SY5Y cells shown by reduction in percent internalised ribozyme over a time course. Error bars represent n=3 ±SD.*

Finally the dissociation profile of ribozyme from human glioblastoma cell line U87 is shown in figure 3.36. The profile exhibited a biphasic pattern with the first phase providing a faster release with a gradient of 0.11%/s and the second phase providing a slower release with a gradient of 0.02%/s. The first phase lasted up to three hours and the second phase, which started from 3 hours and continued to 6 hours. After 6 hours there was still 60% ribozyme remaining associated within cells.

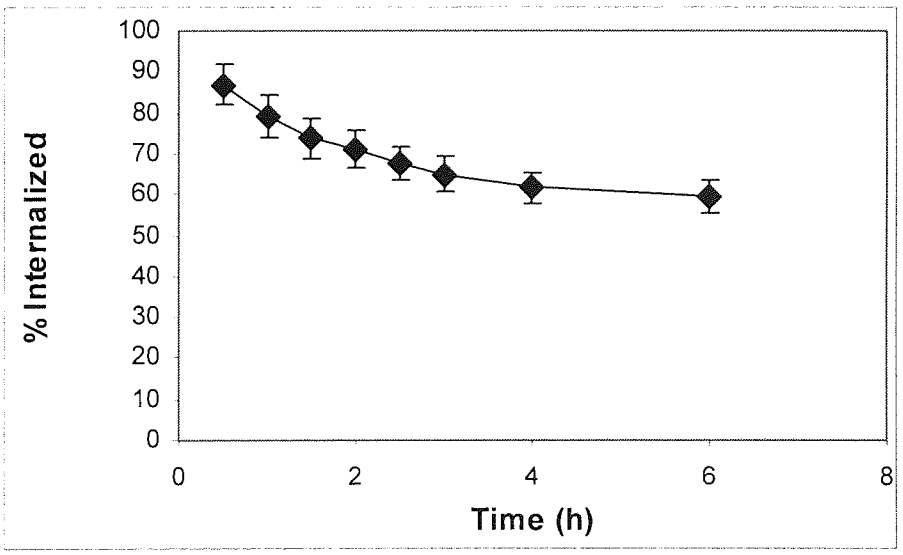

***Figure 3.36.** Dissociation profile of internally labelled ribozyme from U87 cells shown by reduction in percent internalised ribozyme over a time course. Error bars represent n=3 ±SD.*

In terms of comparison of the dissociation profiles of ribozymes between cells the U87 cells transports the associated ribozyme relatively quickly to the deeper compartments as reflected by less steep curve in comparison to the other cells. Similar results to this have been reported by Fell *et al.*, (1997) and Islam *et al.*, (2000) whom have also observed a similar pattern of biphasic release suggesting a two compartment model of sub-cellular distribution.

Release of ribozymes from these two phases may represent release of associated ribozyme from two different cytoplasmic compartments as suggested by (Tonkinson and Stein, 1994). The first compartment being the shallow compartment, which constitutes ribozyme present in the early primary endosomes situated close to the surface or strongly cell surface bound ribozyme. The second slower phase can be described as release form the deeper compartment of cytoplasm, which constitutes the medium to late endosomes, lysosomes or as yet unidentified sites within the cell. This two compartment model of efflux of ribozyme is an inference from the patterns of release as the exact identity of the putative structures is as yet unidentified and these patterns of efflux are thought to be indicative of intracellular trafficking subsequent to endocytosis (Stein *et al.*, 1993).

3.13. Fluorescent localisation studies

Experimental results reported in previous sections have shown that ribozyme cellular association was time and energy dependent process with a component of non-energy dependent cellular association. Results from disassociation studies suggested that ribozyme after being associated by cells could be distributed in different sub-cellular cytoplasmic compartments. In order to confirm the association of ribozyme and to determine the nature of its subcellular distribution, fluorescent localisation studies were carried out with all cell lines. Such information regarding subcellular distribution and cytoplasmic availability at the target sites is necessary for the successful utilization of ribozyme. Ribozyme labelled with fluorescein at the 5'-end was exogenously administered to cells grown in chamber slides as described in the protocol in section 2.7.11 and observed for fluorescence patterns. The results of these studies are presented and analysed in this section. To ensure that auto-fluorescence from cells does not result in spurious results the degree of auto-fluorescence was observed from untreated cells. None of the cells displayed auto-fluorescence ensuring that fluorescence obtained was from subcellular distribution of exogenously delivered flourophores.

The subcellular distribution of ribozyme in rat glioblastoma cell line C6 is shown in figure 3.37. The fluorescence observed from the cells shows that post-cell association, ribozyme was distributed within the cytoplasm with a pattern of fluorescence which can be described as punctate. This punctate pattern suggests that fluorescently labelled ribozyme was sequestered within sub-cellular vesicular structures. Shoji *et al.*, (1991) suggest that such punctate distribution was indicative of entry through endocytosis and subsequent compartmentalisation within vesicles such as endosomes and lysosomes. FITC-dextran which accumulates in endocytic vesicles following cellular association has displayed similar punctate distribution patterns in a number of cell lines (Berlin and Oliver, 1994).

Similar results were seen with the remaining cell lines, rat neuroblastoma cell line, GT1, human neuroblastoma cells, SY5Y, and human glioblastoma cells, U87 (figures not shown). In all these cells the fluorescently labelled ribozyme had a punctate distribution in the cytoplasm reflecting an endocytic association mechanism, with these vesicles possibly being early endosomes, endosomes and lysosomes. In these observations due to the limitations of the equipment it was not possible to confidently state that whether the pattern observed was from within inside the cell or the ribozyme present merely on the surface. From such a statement an investigation of fluorescence with a confocal microscope would have been appropriate. Nonetheless, resutls obtained were consistent with (Fell *et al.*, 1997) in which the distribution of fluorescently labelled ribozyme had displayed punctate distribution within human glioblastoma cells concluding that ribozyme association was an endocytic process. Punctate patterns of distribution have also been observed in studies with oligodeoxynucleotides (Wagner, 1994; Agrawal *et al.*, 2003), and this was considered to be indicative of localisation within endosomal or lysosomal vesicles (Rojanasakul, 1996).

The punctate distribution of the ribozyme due to sequestration in vesicles suggests that ribozyme was taken up by the cells by an endocytic process. In the endocytic model the ribozyme is taken by the cell via a receptor or surface bound protein and internalised in the cytoplasm forming endocytic vesicles such as early endosomes, endosomes and lysosomes and further vesicles of the endocytic process.

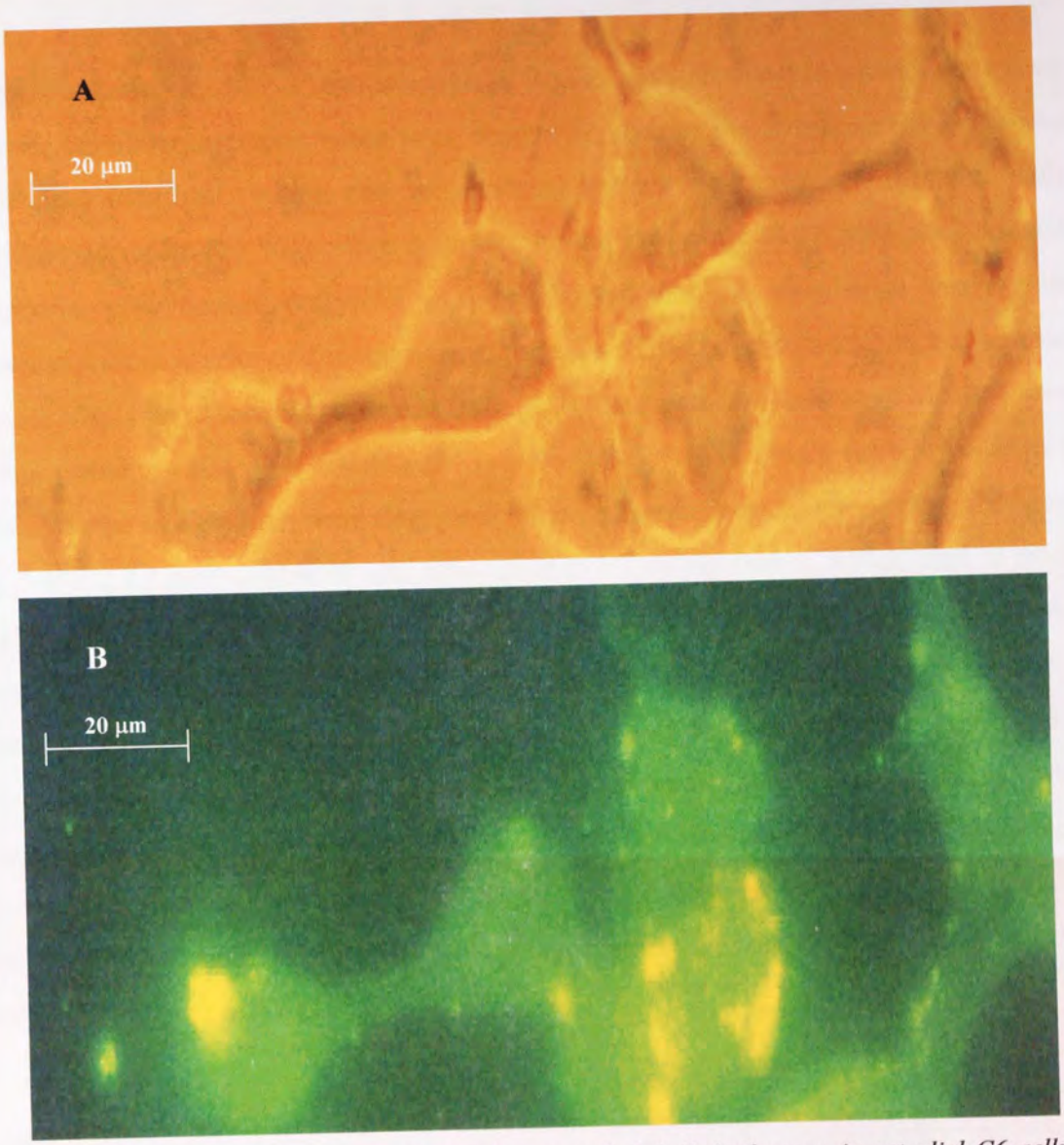

Figure 3.37. *Subcellular distribution of fluorescently labelled ribozyme in rat glial C6 cells (magnification × 400). A is normal light illumination and B is fluorescent illumination.*

These results and the present understanding of the cellular and intracellular trafficking from the published literature shows that ribozymes have a tendency to be trapped in specific intracellular compartments e.g. endosomes and lysosomes and severely limiting their availability at the target sites resulting in no demonstrable efficacy. It is therefore necessary to further delivery systems which can over come this obstacle in the successful application of ribozymes.

3.14. Identification of ribozyme interacting cell surface proteins

Results obtained in the cellular association experiments reported in previous sections show that the cellular association was a time dependent process involving energy and non-energy dependent processes, which can be inhibited by self and cross competition with large polyanionic molecules suggesting a surface bound molecule which mediated association of ribozyme. Post-incubation trypsin washing showed that the association was mediated by proteins present on the cell membrane, which are sensitive to trypsin and bound associated greater ribozyme at low pH values. In order to further elucidate the nature of these membrane bound proteins, cells were fractionated (see section 2.8.1) to obtain cellular proteins present on the membranes, which were then resolved on a South-Western gel as described in section 2.8.2 and 2.8.3 and incubated with ribozymes to identify proteins, which bind to ribozymes. Figure 3.38 illustrates the results of this experiment with the bands from all cells which bind to ribozyme. The gel shown in this figure has five lanes with lane A showing the protein bands for C6 cells and B, C and D showing the surface membrane proteins from GT1, SY5Y and U87 cells respectively. Lane E is the protein ladder run on the gel to make an estimate of the molecular weight of the bands. The ribozyme binding protein bands for rat glial cells C6 are shown in lane A which shows that there are two bands demonstrating hybridisation with ribozyme and comparison with the protein ladder it can be estimated that these proteins have molecular weights of 65 kDa and 58 kDa.

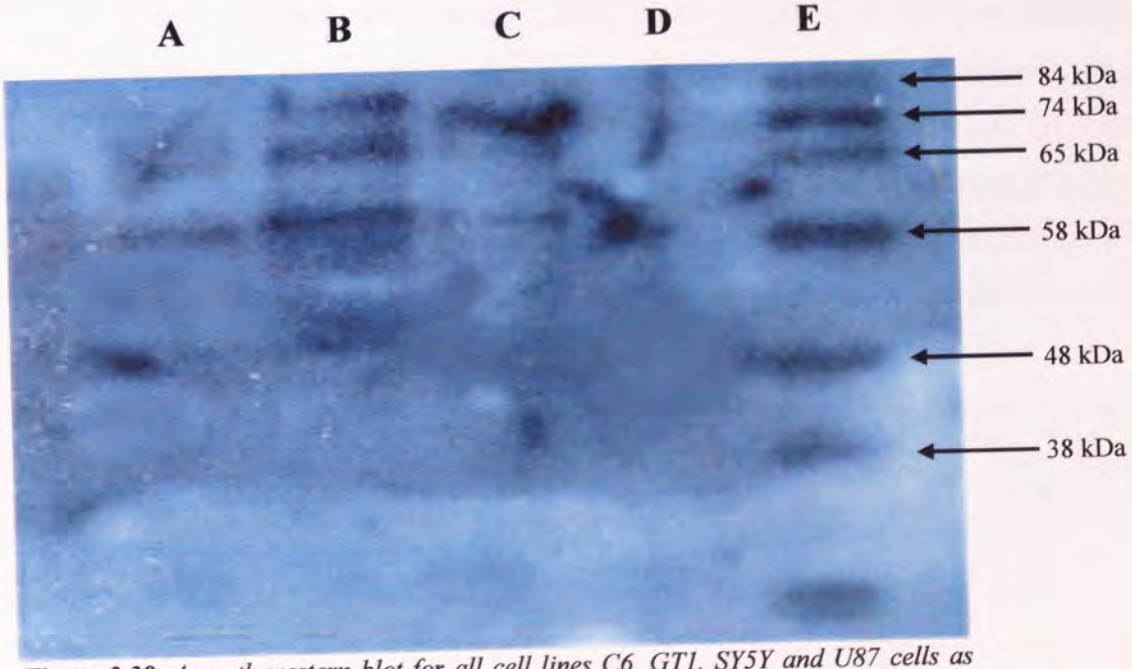

Figure 3.38. *A south-western blot for all cell lines C6, GT1, SY5Y and U87 cells as shown in the lanes A, B, C, and D respectively. With the lane E showing the protein ladder.*

For the rat glioblastoma cells, GT1, there are three distinct bands visible in lane B, which have molecular weights of 84 kDa, 74 kDa and 58 kDa. Lane C shows that for human neuroblastoma cells, SY5Y, there are two proteins, which have hybridised with ribozyme and have estimated molecular weights of 74 kDa and 58 kDa. Finally the human glioblastoma cells U87 (lane D) there was one major band demonstrating high affinity for ribozyme with a molecular weight of 58 kDa. These results show that there is a difference in the type of ribozyme-binding surface proteins in different cells, which may account for the slight differences observed in the extent of cellular association of ribozyme between cell lines. However, there seems to be a protein, 58 kDa, which was present in all cell lines.

Several groups have attempted to identify putative surface proteins, which mediate uptake of nucleic acids whether via an endocytic route or non-endocytic route. Laktionov *et al.*, (1999) have reported that oligonucleotide uptake in keratinocyte cell lines was mediated by a pair of proteins, of 61-63 kDa and 35kDa, present on the surface of cells. A surface protein binding complex of 46 kDa was reported by Akhtar *et al.*, (1996) to be mediating uptake of phosphorothioate and phosphodiester oligonucleotides in Caco-2 cells. In contrast Beltinger *et al.*, (1995) have revealed the existence of five major cell surface phosphorothioate binding proteins ranging in size from ~ 20-143 kDa. In another study Loke *et al.*, (1989) have identified an 80 kDa protein which may mediate the uptake of oligonucleotides. The variability in the reported nucleic acid binding proteins is due to differences in the chemistry of oligonucleotides used for probing these proteins and the type of cells. The exact physiological role of these proteins has not been explained fully yet but it is speculated that internalisation of DNA/RNA with these proteins may represent a salvage pathway for material excreted by apoptotic cells (Bennett, 1993). In contrast to oligonucleotides, to date no such proteins have been identified which mediate the uptake of ribozymes. In this study a ribozyme of same chemistry and equal amounts of cell surface proteins have been used to identify the ribozyme binding proteins in glial and neuronal cells of rat and human brains. The results have shown that there is a difference in the type of proteins which mediate the uptake of ribozyme in the cell lines investigated.

3.15. Concluding remarks

Ribozymes are large polyanionic molecules, typically ranging from 25 to 40 nucleotides in length and with molecular weights in the range of 7500 to 14000 Daltons. Despite such relatively large size and ionic character, ribozymes have been reported to enter cells and exert their action (see table 1.2 and 1.3) but the mechanisms by which ribozymes enter cells have not fully elucidated to date. In this chapter the cellular association properties of an exogenously delivered ribozyme have been investigated and compared in two types of cells namely glial and neuronal from the human and rodent brains. As ribozymes are susceptible to degradation by nucleases and have a serum half life of less than a minute (Jarvis *et al.*, 1996), the ribozyme studied in this thesis was stabilized by several chemical modifications based on the design of Beigelman *et al.*, (1995b) and as shown in section 1.4.1.1. This ribozyme was internally labelled with γ^{32}-P ATP to reduce removal of radiolabel by phosphatases. The stability of ribozyme was evaluated in serum and serum free medium, which showed that the ribozyme was stable up to 1 hour in serum medium beyond which it began to degrade as evidenced by the appearance of degradation bands.

In contrast the ribozyme remained stable up to 24 hours in serum free medium, which was then selected as the medium for use in cellular association experiments. To further investigate the influence of cellular monolayers on the stability of ribozyme it was incubated with cellular monolayers of each cell line and ascertained that up to 6 hours most of the ribozyme was structurally intact. Prior to cellular association studies the number of washes required to remove loosely bound ribozyme to cell surfaces was optimised. The results from optimisation studies showed that a minimum of three washes was required to remove loosely bound ribozyme which is necessary to obtain rigorous results. Following preliminary optimisation work the cellular association of ribozyme was investigated over a time course in each of the cell lines. Results from this study demonstrated that cellular association increased with time in all cells and reached a plateau phase after 6 hours but the magnitude of cellular association was limited and poor. In terms of the pattern of cellular association across the experiments there were slight differences in the extent and pattern of cellular association. However, these differences in cellular association were not consistently observed in the remaining mechanistic experimental results leading to the conclusion that generally there was no difference in cellular association of ribozyme between glial and neuronal cells across

the species. These results are in contrast to oligonucleotides which had shown a greater uptake in neuronal cells *in vivo* (Khan *et al.*, 2000; Sommer *et al.*, 1996).

In order to further elucidate the nature of association mechanism, the association of ribozyme was investigated as a function of temperature and energy. Cells of each cell line were incubated at 37°C and 4°C and observed that the ribozyme cellular association was reduced significantly at low temperature reflecting that the cellular association is an active process. As all active processes are driven by metabolic energy, cellular association was investigated by depleting cells of metabolic energy using metabolic inhibitors. The results obtained from these studies confirmed that ribozyme association was an energy dependent process in all cell lines. However, noticeable cellular association was observed at the low temperature and also after depletion of metabolic energy which suggested the presence of a non-energy dependent component in the cellular association mechanism. In order to further elucidate the mechanism of ribozyme association the extent of pinocytosis carried out by cells was investigated by studying the uptake of mannitol, which is a marker for fluid phase endocytosis. Results obtained in this experiment demonstrated that all of the cell types had negligible uptake of mannitol indicating the absence of pinocytosis from which it is infered that the cellular association mechanism for ribozyme had no pinocytotic component as there was neglegible constitutive pinocytosis occuring. Self-competition with increasing concentration of unlabelled ribozyme reduced the association of ribozyme indicating that there was a specific molecule, which mediated the association of ribozyme. In order to investigate whether this cellar surface ribozyme-binding molecule was a lipid or protein post incubation trypsin washing was carried out. This assessment showed that the majority of ribozyme was bound to trypsin sensitive proteins, which mediate the association of ribozyme in cells.

The specificity of ribozyme association was further investigated by co-incubation with nucleic and non-nucleic acid polyanions all of which reduced the cellular association of ribozyme reflecting the fact that ribozyme cellular association shared the mechanism of association with other polyanionic molecules. The cellular association of ribozyme was increased by reduction of pH suggesting that ionic interactions play a significant role in the hybridisation of ribozyme with surface binding proteins. Finally, fluorescent localisation studies indicated that following cellular association the ribozyme displayed a characteristic

punctate pattern indicating that ribozyme had been sequestered in subcellular vesicles. Ribozyme binding surface proteins were identified using South-Western blotting in each cell line. The results showed that there was difference in the size of proteins in all cell lines, which mediate the cellular association of ribozyme to cells.

From the results presented in this chapter it can be postulated that the cellular association mechanism of ribozyme involves a a combination of energy and non-energy components in which any given molecule binds to cell surface proteins. Cellular association of ribozyme stimulates formation of clathrin coated pits near these ribozyme-protein complexes. These pits facilitate the internalisation of ribozyme and form early endosomes which could either recycle back to the cell membrane or in due course lead to intermediate endosomes, late endosomes and finally lysosomes, which are sequential vesicles of the endocytic pathway (Gruenberg, 2001). In the case of ribozyme this endocytosis results in the entrapment of the ribozyme in the endocytic vesicles creating a further obstacle in the delivery of ribozyme to its target site in the cytoplasm or nucleus. This results in the prevention of ribozyme from carrying out its biological effect as it is unlikely that ribozyme like DNA oligonucleotides, can leave these endosomal compartments by passive diffusion (Akhtar *et al.*, 1991).

This entrapment of the ribozyme in the endocytic vesicles could further lead to either the efflux of the ribozyme from the cell or degradation by nucleases in the harsh acidic environment of the endo-lysosomal vesicles. Endo-lysosomal compartments contain a battery of deoxyribonuclease, ribonuclease, phophatases and pyrophosphatases which together degrade nucleases with $T_{50\%}$ in the range of 30-50 minutes (Hudson *et al.*, 1996b). Loke *et al.*, (1989) and Zhao *et al.*, (1993) have observed similar results of entrapment of most of oligonucleotides in lysosomal-endosomal compartments and it was concluded (Shoji *et al.*, 1991) that endosome to cytoplasm transfer is the critical limiting step for the pharmacological actions of oligonucleic acids.

The fact that oligonucleotides given exogenously exhibit biological activities suggests some molecules escape from these compartments at some point during the endosome to lysosome transport and reach the target sites. However, there is no information available in the literature elucidating the mechanism and extent of this release. In order to overcome this obstacle several strategies have been attempted which include microinjection, permeabilization using pore-forming agents such as *streptolysin-O*, anionic peptides,

electroporation and membrane translocating peptides such as *Tat*, amphipathic model peptides and signal peptides with varying degrees of success (Dokka and Rojanasakul, 2000).

Finally as a caveat it must be noted here that results and conclusions presented in this chapter must be interpreted with a degree of caution as the term cellular association has been loosely used to describe the phenomenon observed in these experiments and it may or may not include cellular uptake. In general, in the antisense and ribozyme literature, the term cellular uptake is used in place of cellular association despite the fact that no conclusive evidence is presented of the internalization of the exogenously administered molecules in most of these studies.

CHAPTER FOUR

EVALUATION AND CHARACTERISATION OF BIODEGRADABLE POLYMER PLGA MICROSPHERES FOR THE CELLULAR DELIVERY OF RIBOZYMES

4.0. Introduction

Successful application of ribozymes for the treatment of clinical conditions is still hampered by several key issues such as instability of ribozyme in serum medium, rapid *in vivo* elimination kinetics, poor cellular delivery and finally minimal target site co-localisation. Resolution of these issues by developing a novel and robust delivery system, which overcomes the above-mentioned limitations, is of paramount importance in order to achieve the eventual utilization of ribozyme therapeutics in clinic.

In previous studies with oligonucleotides such as ribozymes, problems like poor biological stability coupled with rapid elimination kinetics *in vivo* were to some extent overcome by repeated administration of ribozymes to obtain a sustained pharmacological effect. For example, in the case of Peripherin, a neurone specific intermediate filament protein, which has a slow turnover, repeated administration of oligonucleotides for up to 40 days was required for a reduction of protein levels by 90% in cultured PC 12 phaeochromocytoma cells (Troy *et al.*, 1992). The repeated administration of oligonucleotides to achieve a pharmacological response in this study strongly highlights the need for a delivery system for nucleic acid molecules such as ribozymes. A successful and robust delivery system ideally should protect the ribozyme from degradation by nucleases and furthermore should provide a controlled release of ribozyme for a sufficient period of time to ensure optimum pharmacological and therapeutic effect.

One such delivery system, which possesses the above-mentioned required features, is a biodegradable polymer microsphere system prepared from polylactide-co-glycolide (PLGA). The polymer PLGA has been widely studied and extensively applied in many clinical settings as described in section 1.5. Microspheres, which are defined by Davis and Illum,

(1989) as spherical porous structures of micron size range, have been extensively evaluated in various therapeutic settings as sustained release delivery systems (see table 1.4 for a brief review).

Biodegradable polymer microspheres are robust delivery systems, which protect the entrapped biologically labile molecule from hydrolytic degradation, ensuring its pharmacological effects and releasing the entrapped molecule steadily as the polymer matrix degrades. The rate of degradation and the consequent release of the entrapped molecules is dependent on several factors such as relative ratios of monomers in the co-polymer, size of the microspheres, incubation medium, pH and drug loading. These factors can be carefully controlled and selected to obtain a required release profile to suit clinical needs. Further advantage is obtained by the biodegradability of the polymer, for as it degrades and releases the incorporated substance, the polymer and its degradation products are removed by the natural metabolic processes of the body eliminating the need for the surgical removal of the delivery system.

The aim of the experimental work presented in this chapter was to formulate, characterise and evaluate a biodegradable polylactide-co-glycolide polymer microsphere delivery system for ribozymes. Characterisation and assessment of microsphere properties is important as these characteristics have a major influence on the potential use of such systems e.g. on cellular association and potential toxicity (Alonso *et al.*, 1993). Microspheres of two different size ranges were prepared with each of the three co-polymer ratios of lactide to glycolide and were initially characterised in terms of size range, surface morphology, encapsulation efficiency, ribozyme loading and ribozyme release profiles with methods described in section 2.7 and 2.8. Microspheres were prepared using a W/O/W solvent evaporation method, originally used by Ogawa *et al.*, (1988) for the encapsulation of the water-soluble peptide, Leuprolide acetate in to PLGA polymer microspheres.

The method used in our study is described in sections 2.9.1 and 2.9.2 and was an adaptation of the method described by Khan *et al.*, (2000). Briefly, to prepare microspheres by w/o/w double emulsion technique an aqueous solution of the hydrophilic drug was emulsified into an organic solvent to form a w/o emulsion. This emulsion was then homogenised into a second water phase containing stabilisers such as PVA with subsequent removal of the solvent by evaporation and the microspheres collected by centrifugation. The impact of many

formulation and process parameters such as the influence of shear force (Sah *et al.*, 1995a), drug loading, polymer molecular weight (Bodmer *et al.*, 1992), polymer composition (Sah *et al.*, 1995b), volume of inner water phase, volume of DCM, residual solvents (Crotts and Park, 1995), temperature (Herrmann and Bodmeier, 1995), and terminal γ-irradiation (Yoshioka *et al.*, 1995) on various microspheres properties have been investigated intensively.

Following initial characterisation, further release profiles were obtained to investigate the influence of loading on ribozyme release. From this data an appropriate formulation was selected to evaluate cellular delivery in cultured glial and neuronal cells from human and rodent brains. Stability of ribozyme entrapped in microspheres was also assessed to determine whether process parameters adversely affect the structure of ribozyme. Microsphere-entrapped ribozyme stability was investigated in serum medium to assess the degree of protection from nucleolytic degradation of ribozyme. Following characterisation and optimisation studies, the cellular association of microsphere-entrapped ribozyme was evaluated over a time course in cultured glial and neuronal cells. The cellular association mechanism was further characterised to investigate the effect of temperature, metabolic and competitive inhibition.

4.1. RESULTS AND DISCUSSION

4.2. Determination of loading of ribozyme in each formulation

Microspheres of two size ranges 1-5 μm and 10-20 μm were formulated using the protocols described in section 2.9.1 and 2.9.2. For all formulated microspheres the percentage yield, entrapment efficiency, amount of ribozyme loading was calculated. Knowledge of these characteristics is important because these characteristics influence the release kinetics and eventually the efficacy of any microsphere delivery system. These values were calculated by the following mathematical expressions.

$$\% \text{ Yield} = (\text{weight of microspheres/weight of polymer}) \times 100$$

$$\% \text{ Encapsulation efficiency} = (\text{cpm of RBZ solution used/cpm of microspheres}) \times 100$$

$$\text{Actual loading} = (\text{amount of ribozyme entrapped/wt of microspheres}) \times 100$$

The indicative calculated values of percentage yield, encapsulation efficiency and loading are presented in table 4.1 for the two size ranges and each of the three co-polymer ratios.

The percentage yield value shows the amount of polymer, which is finally, present as microspheres and indicates the efficiency of polymer utilisation for a particular formulation.

LA-GA RATIO	% AGE YIELD	ENCAPSULATION EFFICIENCY (%)	LOADING (pmol/mg)
90:10 Small	64	44	0.2
90:10 Large	57	57	0.2
80:20 Small	83	33	0.2
80:20 Large	80	54	0.4
50:50 Small	75	47	0.2
50:50 Large	71	49	0.2

Table 4.1. Summary of encapsulation efficiency and loading of ribozyme in the two size ranges small and large of the three co-polymer ratios 90:10, 20:80 and 50:50.

In all formulations greater than approximately 60% yield was observed, with smaller microspheres exhibiting slightly higher percentage yield than the large ones. The third column in the table summarises the encapsulation efficiency of ribozyme in microspheres. The values of encapsulation for small microspheres were 44, 33 and 47% for 90:10, 80:20 and 50:50 co-polymer ratios respectively. For the large range microspheres these values were 57, 54 and 49% for 90:10, 80:20 and 50:50 co-polymer ratio respectively. Within each co-polymer ratio there was an observation of reduced encapsulation with smaller microspheres in comparison to the large size range microspheres. This lower encapsulation efficiency observed with the smaller size range microspheres could be explained by the fact that a larger surface area of the droplets is formed during emulsification, which results in greater direct contact between the primary emulsion and the external aqueous phase which leads to loss of the ribozyme to the external aqueous phase.

The fourth column in the table lists the values for loading of ribozyme in picomoles per milligram of microspheres. The values of loading between the co-polymer ratios were generally similar. However, like the encapsulation efficiency values the smaller microspheres had lower loading of ribozyme per mg of microspheres in comparison to large microspheres in all of the co-polymer ratios. The small microspheres exhibited a loading of 0.2, 0.2 and 0.2 pmol/mg for 90:10, 80:20 and 50:50 co-polymer ratios respectively. For the large size microspheres these values were 0.2, 0.4 and 0.2 pmol/mg for 90:10, 80:20 and 50:50 co-polymer ratios respectively. To achieve these similar loadings the amount of ribozyme added to the primary emulsion was altered by iteration. Loading within particles is an important factor in microspheres as the amount of ribozyme entrapped in microspheres and its consequent release is essential for efficacy. These results were consistent with previously published results in which small microspheres had an entrapment efficiency of 30% and large size had an entrapment efficiency of 60% (Lewis *et al.*, 1998). There was no effect of the co-polymer ratio on the percentage yield of microspheres, encapsulation efficiency and ribozyme loading whereas the latter two are affected by particle size.

4.3. Characterisation of surface morphology

The surface morphology of the formulated microspheres was observed using scanning electron microscopy (as described in section 2.9.6) in order to investigate physical characteristics of the formulated microspheres such as shape and structure. Figures 4.1, 4.2 and 4.3 show the photomicrograph of the microspheres of two different size ranges small and large with each co-polymer ratio.

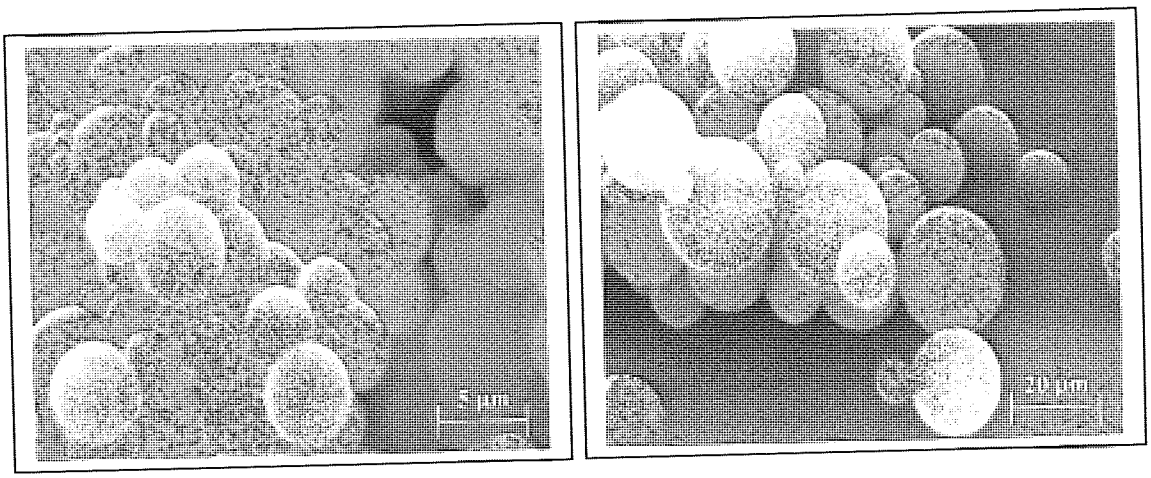

Figure 4.1. *Scanning electron micrograph of 90:10 copolymer microspheres. Microspheres on the left were of the small size range (1-5μm) and the microspheres on the right were of large size range (10-20μm).*

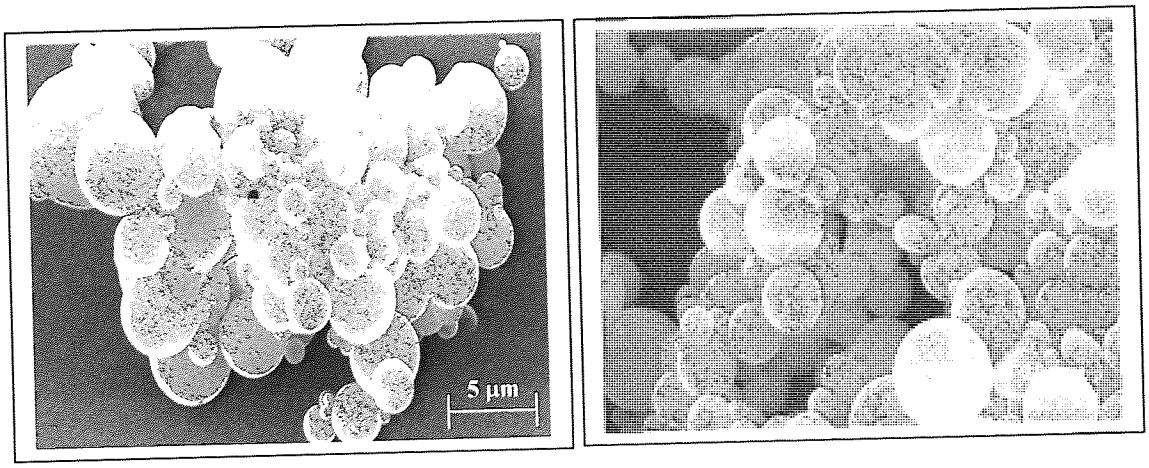

Figure 4.2. *Scanning electron micrograph of 80:20 copolymer microspheres. Microspheres on the left were of the small size range (1-5μm) and the microspheres on the right were of large size range (10-20μm).*

As the figures show all microspheres were successfully formulated and there was no evidence of any irregular, malformed and collapsed microspheres. No polymer debris was visible indicating that all the polymer has been incorporated into the spheres. All spheres

produced from each co-polymer ratio were similar in morphology with regular spherical structures without any visible pores or cracks on the surface displaying a smooth and compact surface. It was obvious from the photomicrographs that there was a range of sphere sizes, which was further confirmed with particle size analyses as presented in the next section.

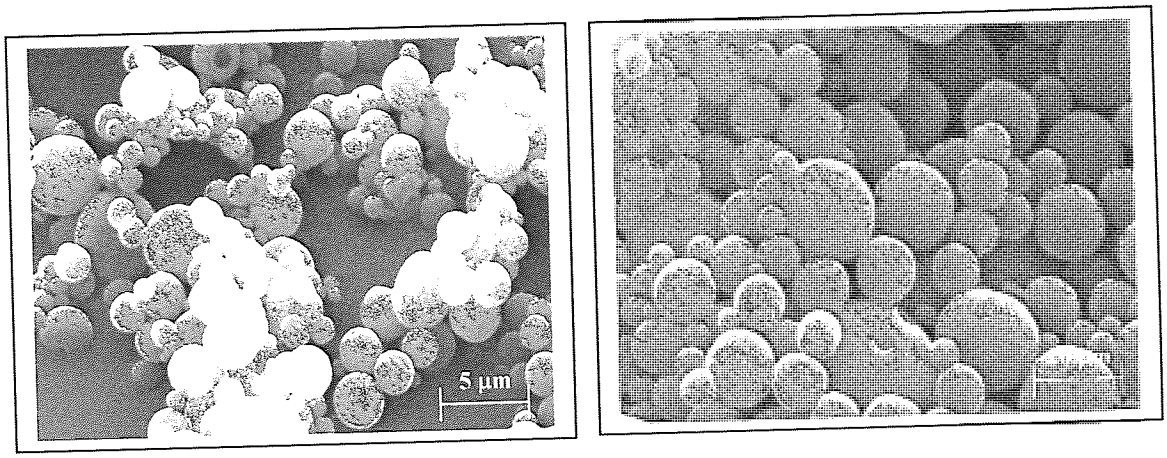

Figure 4.3. *Scanning electron micrograph of 50:50 copolymer microspheres. Microspheres on the left were of the small size range (1-5µm) and the microspheres on the right were of large size range (10-20µm).*

4.4. Evaluation of Particle size

Size range of microspheres has important implications for the release of entrapped microspheres and cellular uptake properties. Therefore an assessment of the range of polydispersity of microspheres is an essential component of microsphere characterisation. The size range of particles was determined using a Malvern Mastersizer as described in section 2.9.5. It was intended to prepare microspheres with mean volume diameters within two size ranges, 1-5µm and 10-20µm, for all co-polymer ratios in order to investigate the influence of size range on formulation characteristics such as release rates. These two ranges were designated small and large microspheres. The results of the sizing experiments are graphically represented in figures 4.4 and 4.5.

Figure 4.4 illustrates the typical particle size distribution observed with the small PLGA microspheres as decribed in section 2.9.2. In the figures the particle size is presented with a logarithmic scale on the x-axis and percent number of particles on the y-axis. For small microspheres the typical mean volume diameter was around 2.77µm (± 1.9µm). Figure 4.5 illustrates the size distribution of typical large microspheres obtained with protocol described

in section 2.9.1. For large microspheres typical mean volume diameter was around 12μm (± 8μm).

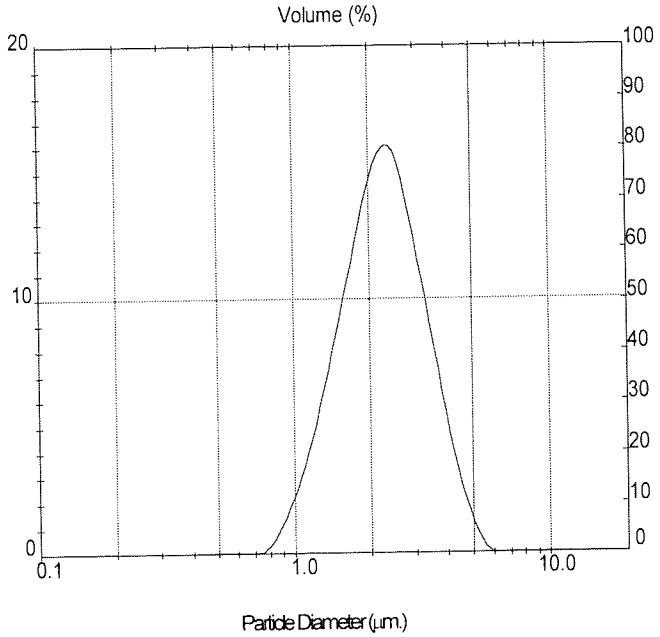

Figure 4.4. *Graphical representation of the typical size distribution range of small PLGA co-polymer microspheres.*

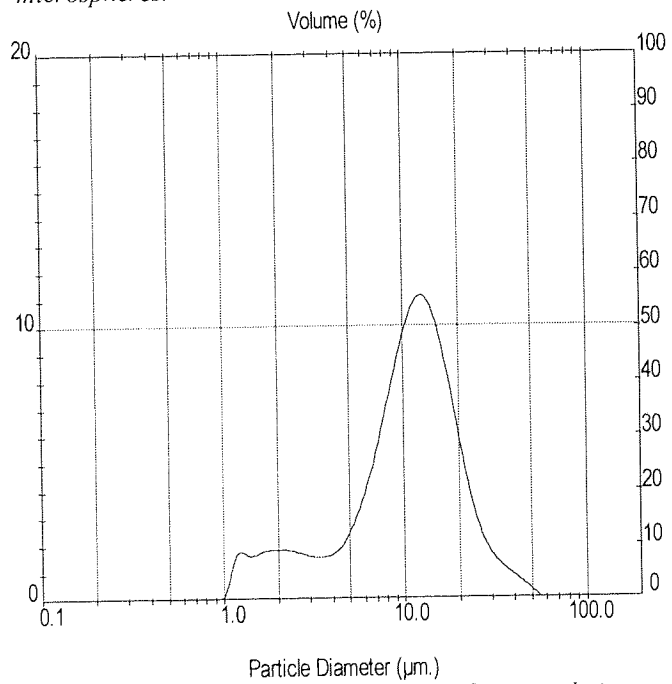

Figure 4.5. *Graphical representation of a typical size distribution range of large PLGA co-polymer microspheres.*

4.5. Evaluation of release profiles of ribozyme

In order to assess whether the ribozymes entrapped within microspheres by the double emulsion method were capable of sustained release of ribozyme from polymer microspheres, *in vitro* release assays were carried out as described in section 2.9.7. In order to further characterise the release profiles the effect of microsphere size and co-polymer ratios on the release of ribozyme was investigated. For this purpose microspheres of two size ranges, small (1-5 μm) and large (10-20 μm), were prepared with each of the three co-polymer ratios, 90:10, 80:20 and 50:50, and their release profile was evaluated in PBS at 37°C for 28 days.

Figure 4.6 illustrates the release of ribozyme from microspheres of two size ranges, small and large, prepared from PLGA 90:10 co-polymer. This co-polymer exhibited a biphasic pattern of release during the 28 days of the investigation for both size ranges. The first phase, which lasted for 24 hours, exhibited an initial rapid release, which was termed the 'burst effect' phase. During this phase 28% of the entrapped ribozyme was released from small microspheres, which was followed by the sustained release phase in which the cumulative drug release was 34, 36, 37 and 38% for days 7, 14, 21 and 28. Up to 28 days there was no observation of any rapid release suggesting no bulk erosion of the polymer microspheres.

In contrast for the large microspheres the burst effect which was rapid release observed during the first 24 hours was 7% which was 4 times lower than the small size range microspheres. This phase was followed by the sustained release phase in which there was steady but small increase in release of ribozyme from 9% at day 7 to 14% at day 14. After this there was even less release with cumulative release values of 12% and 13% for days 21 and 28 respectively. In both size ranges a biphasic pattern of release was observed with a 4 times larger burst effect observed with the small size range microspheres. This can be explained by the fact that increased surface area of smaller microspheres, which is in contact with the release medium causes a relatively greater loss of the ribozyme through diffusion into the release medium from the surface.

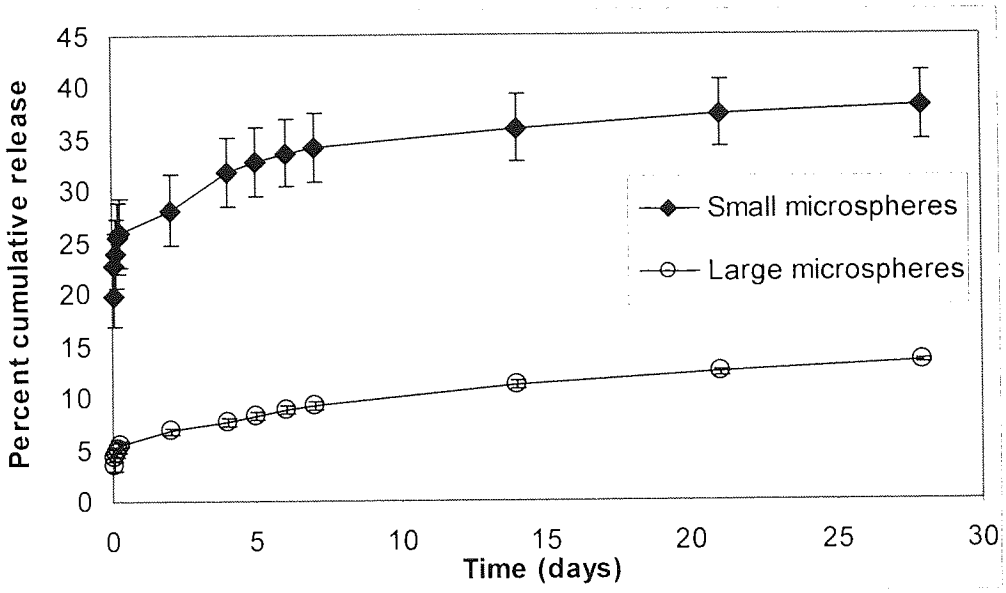

Figure 4.6. Release profile on internally labelled ribozyme in small and large size range 90:10 PLGA microspheres over a time course of 28 days. Error bars represent n=3 ± SD.

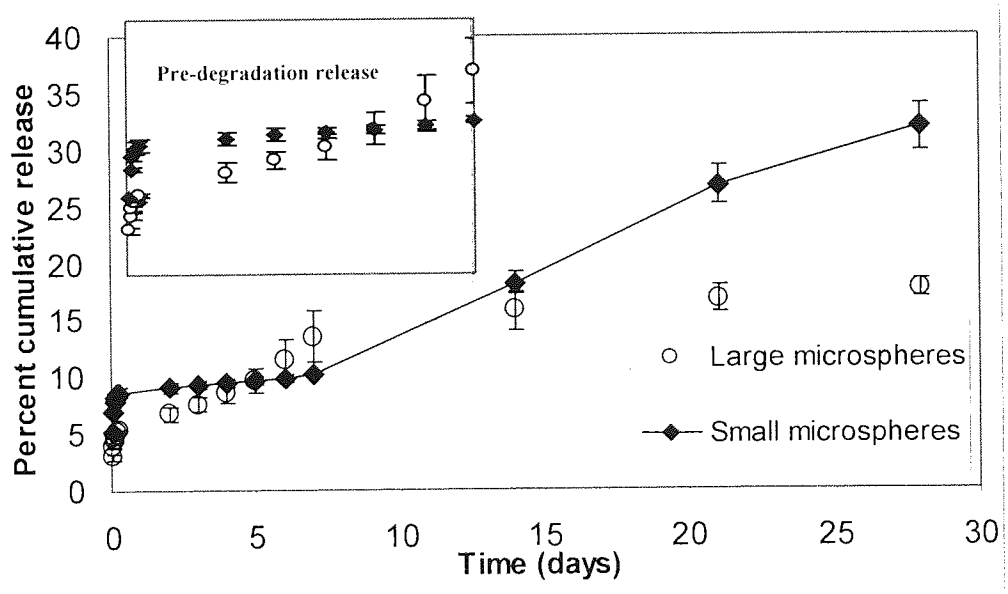

Figure 4.7. Release profile on internally labelled ribozyme in small and large size range 80:20 PLGA microspheres over a time course of 28 days. Error bars represent n=3 ± SD.

The release profile of entrapped ribozyme from both small and large size range microspheres formulated from PLGA 80:20 co-polymer, which consists of 80% lactide and 20% glycolide is illustrated in figure 4.7. In both size ranges the microspheres displayed a tri-phasic pattern of release. The burst effect phase in small microspheres released 9% of the entrapped ribozyme, which lasted till 24 hours after which there was no noticeable release till day 7. This constituted the second phase of the release profile by the end of which only another 1% of the ribozyme was released. This was followed by the third phase, a sustained release phase, during which the mean cumulative ribozyme release increased from 18% at day 14 to 26% at 21 days and finally reaching 31% at day 28, the last time point of the experiment. Overall the release pattern observed was tri-phasic with a lag phase of 7 days between the first phase and sustained release phase. For the large size range microspheres the burst effect was 7%, which lasted for 24 hours. After this phase, in contrast to the small microspheres, ribozyme mean cumulative release increased steadily from 14, 16, 17, and 18% at time points 7, 14, 21 and 28 days respectively forming a sustained release phase. A comparison of the release profiles of small and large microspheres showed that both exhibit a tri-phasic release pattern with small microspheres exhibiting a slightly higher burst phase release, which was due to higher surface area of the microspheres facilitating a greater release.

The release pattern of ribozyme from PLGA 50:50 microspheres is shown in figure 4.8 for two microsphere size ranges small (1-5μm) and large (10-20μm) over a time course of 28 days at 37°C in PBS. Both size ranges displayed a triphasic release profile with smaller microspheres exhibiting a greater release of ribozyme in the first two phases. For the small microspheres there was a mean cumulative release of 6% during burst effect phase of 24 hours. This phase was immediately followed by the sustained release phase in which the ribozyme mean cumulative release increased steadily from 9% to 13% and finally to 16% for time points 7, 14 and 21 days respectively. For the last time point of the experiment at day 28 a large increase in the cumulative mean release value was observed (40%). This sudden increase in the release reflects a third rapid phase of release which possibly might be due to bulk erosion of polymer resulting in rapid release of ribozyme.

A similar pattern of release was observed with the large PLGA 50:50 microspheres demonstrating a burst effect release of 1% which increased although negligibly to 3% after 7 days and remained constant till day 14. There was a further increase to 6% at day 21 and this

phase can be termed as a sustained release phase even though the magnitude of release was quite small. At time 28 day there was a huge increase in mean cumulative release ribozyme value to 60% representing a third phase in the release pattern. Overall in both cases there was a triphasic pattern of release of ribozyme in both microsphere sizes with the small microspheres exhibiting a 6 times greater release at the burst effect phase. The difference in the quantity of release between small and large microspheres has also been seen in other studies as well (Lewis *et al.*, 1998), (Khan *et al.*, 2000).

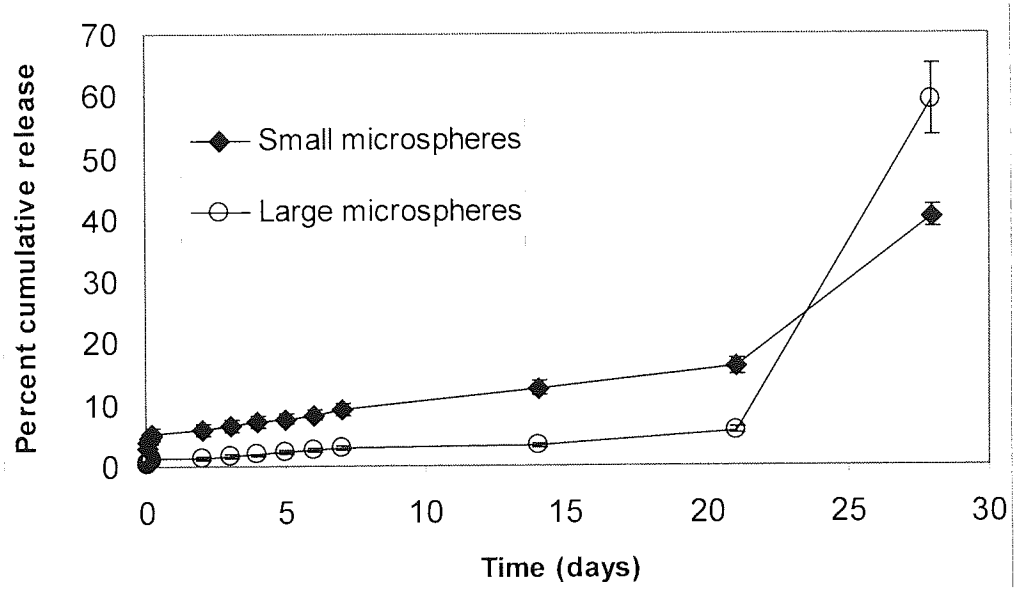

Figure 4.8. *Release profile of internally labelled ribozyme in small and large size range 50:50 PLGA microspheres over a time course of 28 days. Error bars represent n=3 ±SD.*

Release patterns of the ribozyme from each co-polymer illustrates that there are two or three phases of release of ribozyme from microspheres which reflects the fact that release of ribozyme from these microspheres at different phase results from different mechanisms. It is suggested that rapid cumulative release of ribozyme during the initial 'burst effect' is due to the release of ribozyme present or close to the surface of microspheres. During the next phase the release of ribozyme is sustained which is due to the hydration of polymer matrix resulting in degradation of the polymer. Degradation of the polymer is defined as random scission of bonds between the monomers in the polymer backbone resulting in reduction of molecular weight of the polymer but no appreciable weight loss and no soluble monomer products formed (Gopferich, 1997), (Thies and Bissery, 2002). This results in formation of pores and channels, which get filled with the release medium, facilitating steady diffusion of ribozyme through these channels. The third phase, which is only seen in the 50:50 ratio is due to the erosion of the microspheres, which is described as mass loss of polymer matrix

due to loss of monomers, soluble oligomers or even pieces of non-degraded polymer with reduction of molecular weight and release of ribozyme in large amounts. During the second and third phase as the polymer degradation proceeds it generates acidic monomers which results in the pH of the inner core sometimes falling to as low as 1.5 which further enhances the release of ribozyme.

In summary as the microspheres are placed in the incubation medium they are surrounded by the medium and the ribozyme molecules present on or near the surface are washed off which is termed as the burst effect. As more water/medium seeps in to the matrix it causes the scissile bonds of the polymer backbone to break and leading to the creation of pores and channels in the matrix. Entrapped molecules break free from between the polymer chains and diffuse out through these medium/water filled channels and pores. This release is termed the sustained phase as the ribozyme is delivered slowly to the incubation medium. These results are similar to that reported previously for the release of many different drugs including proteins and anti-cancer agents from these and related biodegradable polymers (Crotts and Park, 1998), (Okada and Taguchi, 1995).

Another interesting observation from the comparison of the release profiles across the co-polymer ratios demonstrated that as the glycolide content in the co-polymers increased the burst effect diminished. The reason for this is not entirely clear but may reflect differences in hydrophobicity and degree of crystallinity within the various polymer ratios. As the lactide content in the co-polymer increased the degree of crystallinity increased which results in the lower hydration and the consequent degradation of the co-polymer. The release profile of the 90:10 copolymer exhibits most of the release in the initial burst effect phase and only a limited release of ribozyme in the sustained phase which is release from the degradation of the polymer. As the glycolide content increases as with the 80:20 ratio the proportion of ribozyme release during the degradation phase increases reflecting relatively greater degradation of the polymer. Finally with the 50:50 co-polymer the majority of the released ribozyme is from the degradation and erosion phase with only a small amount released during the burst effect phase.

Analysis of the release profiles with all three co-polymer ratios led to the selection of the 50:50 PLGA co-polymer small size range microspheres as the delivery system of choice for further experimental work. This selection was based on the formulation characteristics of

size, surface morphology and most importantly the release characteristics. This formulation had a triphasic release profile with low initial burst effect, sustained release and finally polymer erosion phase occuring within 28 days which is the required time frame for down-regulation of the of the EGF receptors, the ultimate target molecule of the ribozyme.

4.6. Effect of loading on release profiles

In order to further characterise the factors influencing the release of ribozyme from microspheres the effect of ribozyme loading on the release of ribozyme was evaluated. Ribozyme loading is calculated as shown is section 4.2 and is defined as amount of ribozyme present per mg of formulated microspheres. For this objective microspheres with three different loadings of ribozyme were prepared with loadings values of 2pmol/mg, 10pmol/mg and 20pmol/mg. The results of this study are represented in figure 4.9.

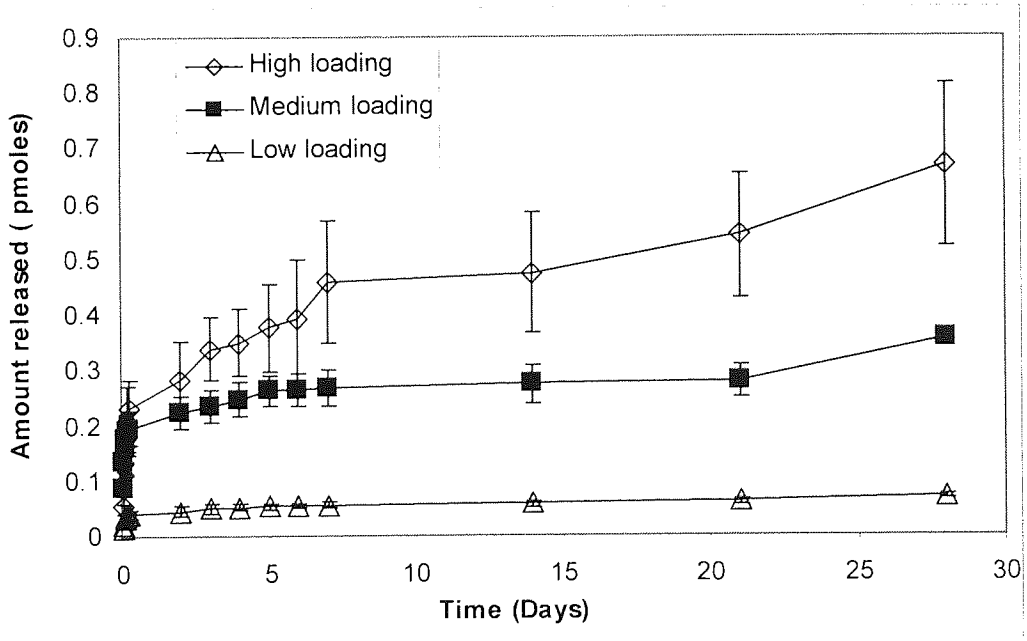

Figure 4.9. *The effect of ribozyme loading on the release of ribozyme from 50:50 small PLGA microspheres. Error bars represent n=3 ± SD.*

A comparison of the release profile of microspheres from each of the three batches, which have three different loadings, demonstrates that the pattern of release was distinctly different amongst them. The high loading microspheres exhibited a triphasic pattern whereas the medium and low loading microspheres exhibited a biphasic pattern of release. Overall the amount of ribozyme released from high loading microspheres was highest followed by release from medium loading microspheres and finally with the low loading microspheres

exhibiting the lowest ribozyme release. Even though there was a similar biphasic pattern of release with medium and low loading microsphere but there was a 5-fold difference in the initial 'burst effect' of ribozyme release. In the low loading microspheres, after the initial phase release, there was no observable ribozyme release up to day 28 with the ribozyme release being 0.03 pmole at day 2 after which the mean cumulative amount released remained constant at 0.04 pmoles till day 28. In contrast for the medium loading microspheres there was an observable release of ribozyme after the burst effect release, which rose from 0.19 pmol at day 2 to 0.22, 0.23, 0.24 and 0.30 pmoles at days 7, 14, 21 and 28 respectively. A comparison of ribozyme release during the initial burst effect phase showed that there was a 2-fold difference in release noticed between the high and medium loading microspheres with the medium loading batch release being 0.16 pmol and high loading release value of 0.30 pmol at 24 hours. In the subsequent phases for the high loading microspheres there was a substantial sustained release of ribozyme in the second phase with mean cumulative release values of 0.34 pmol at day 2, 0.46 pmol at day 7, 0.49 pmol at day 14, 0.59 pmol at day 21 and 0.69 pmol at day 28. The high release of ribozyme observed at days 21 and 28 denote the third phase of release, which could be ascribed to bulk degradation of polymer resulting in increased ribozyme release.

4.7. Stability of the biodegradable microsphere entrapped ribozyme

Results of ribozyme stability in serum medium demonstrated that the chemically modified chimeric ribozyme RPI.4782, like most ribonucleic acid molecules is not stable in serum medium as evidenced by its degradation, which becomes visible at 2 hours (see figure 3.1). This structural instability totally undermines the potential utility of ribozyme strongly reflecting a need for a robust delivery system.

To meet this objective the ribozyme was encapsulated in microspheres as described in section 2.9.2 and characterised as shown in previous sections of this chapter. In order to confirm that polymer-entrapped ribozyme is not physically degraded during the fabrication process and to assess the incubation of polymer entrapped ribozyme in serum medium was not adversely affected a ribozyme stability assay was carried out as described in section 2.9.8. The result of this stability study is represented in figure 4.10.

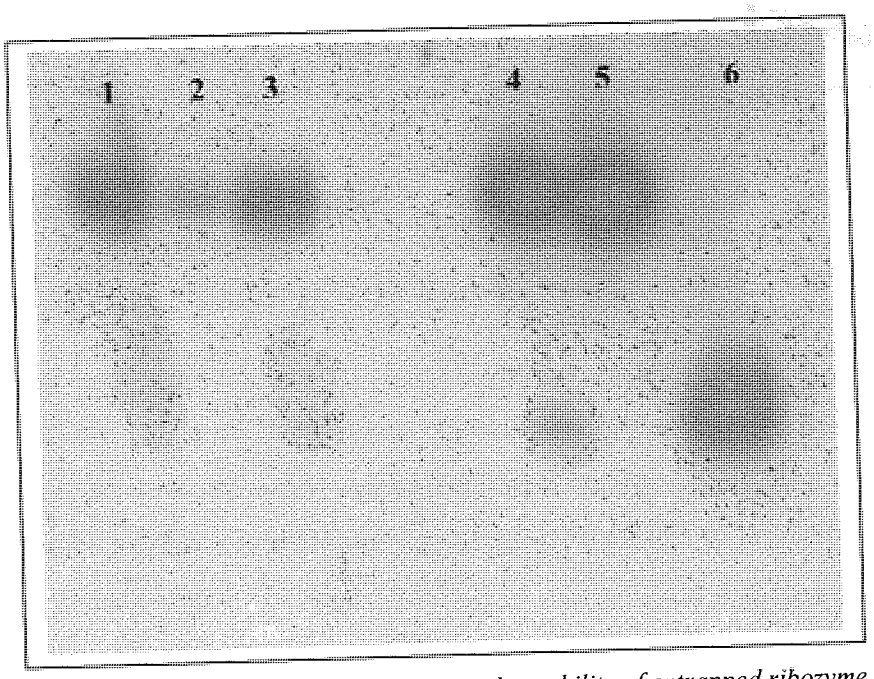

Figure 4.10. *An autoradiograph showing the stability of entrapped ribozyme after 24 hours of shaking on a mechanical shaker. Lane 1-3 shows the entrapped ribozyme extracted from microspheres, which were incubated in ddH_2O, serum free medium, and serum media, respectively, on a mechanical shaker at 37 ℃ for 24 hour. Lane 4-6 shows the internally labelled, 5'labeled full ribozyme and 5'donor half of ribozyme respectively.*

As figure 4.10 shows ribozyme extracted from microspheres incubated in ddH_2O, serum free and serum media as shown in lanes 1 to 3 respectively, remained intact. This shows that ribozyme entrapped in microspheres is protected from nuclease mediated breakdown and remains intact.

Ribozymes, which have not been modified chemically are biologically labile molecules which are susceptible to degradation by nucleases rapidly (Kariko *et al.*, 1994), (Arup *et al.*, 1996), (Elkins and Rossi, 1995). However ribozyme RPI 4782 which is investigated in this study when incubated in all cell lines starts degrading after 6 hours as shown in section 3.1.1. In order to overcome this problem it was encapsulated in microspheres as shown in section 2.9.8. There were two main objectives for this investigation, firstly, whether the ribozymes are protected from degradation by nucleases and secondly to evaluate whether the encapsulation process during which it is exposed to organic solvents, shearing stress and extremes of temperature does not adversely affect its structure.

Results from this study and published literature show that biodegradable polymer matrices can both protect the entrapped nucleic acids from nulcease digestion and also impart

sustained release properties (Lewis *et al.*, 1995; Hudson *et al.*, 1996a). See Hudson *et al.*, (1996b) for further evidence of enhanced ribozyme stability by entrapment in polymers.

4.8. Cellular association properties of microsphere entrapped ribozyme

Cellular delivery of a given drug molecule is an important determinant of its pharmacological efficacy and its optimisation is an important aspect in the development of any therapeutic agent. In the previous chapter the cellular delivery and mechanism of cellular association of ribozyme was investigated. These results showed that showed that association of ribozyme in cellular monolayers was poor and limited, which in turn potentially results in reduced efficacy of the ribozyme. In order to enhance and optimise the cellular delivery of these molecules, ribozymes were entrapped in microspheres prepared from biodegradable polymer PLGA. These ribozyme entrapping microspheres were formulated by employing the double emulsion (w/o/w) and solvent evaporation method and were characterised in the previous sections in terms of surface morphology, particle size range, loading of ribozyme and *in vitro* release kinetics. From the characterisation results the small size range (1-5μm) microspheres of the 50:50 co-polymer ratio of PLGA was selected for cellular work. This selection was based on the fact that this particular formulation provides smooth and compact microspheres with a tri-phasic release profile, suitable for targeting the EGF receptor. Also this size range can be easily administered to cells *in vitro* and also ICV through a 5μL Hamilton syringe for *in vivo* administration (described in chapter 5). In the subsequent sections polymer entrapped ribozyme in the selected formulation was evaluated for cellular association studies. Further studies to elucidate the mechanism of association were carried out by studying the influence of temperature, metabolic inhibition and pH on cellular association of polymer-entrapped ribozyme.

4.9. Optimisation of washes for microsphere work

Prior to cellular association studies an assay was carried out to determine the optimum number of washes to remove loosely attached ribozymes as described in section 2.10.2. The results of this assay are illustrated in figure 4.11.

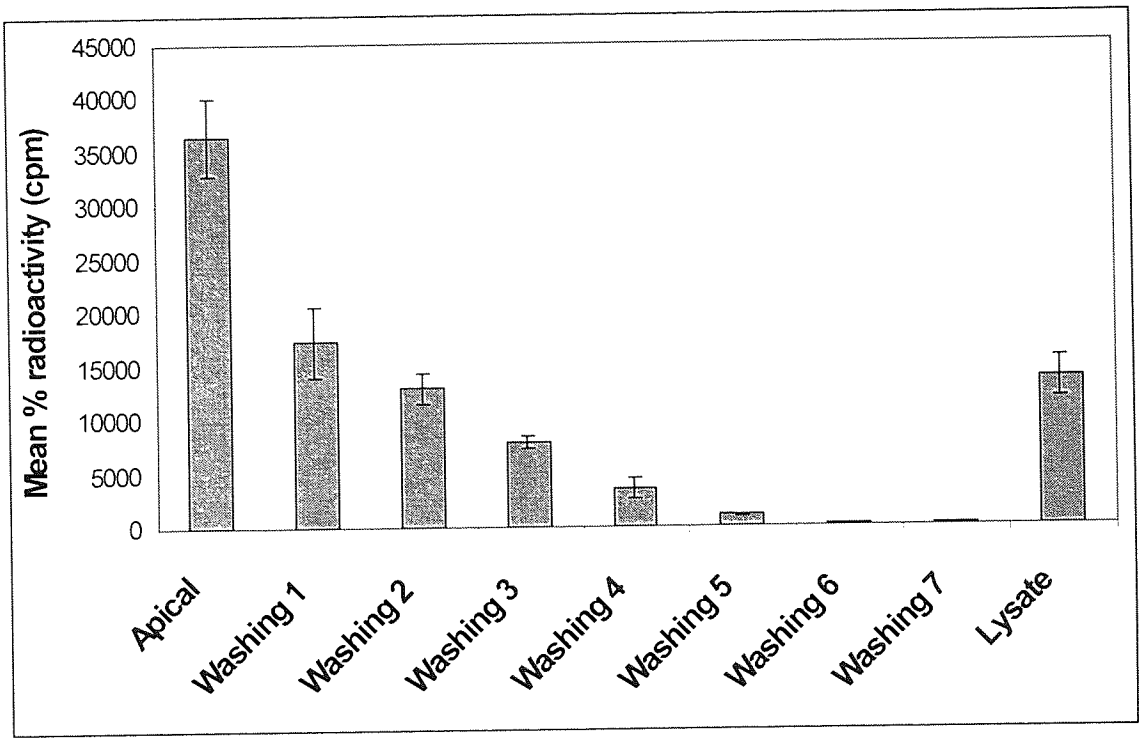

Figure 4.11. *As assay to determine the optimum number of washes to remove loosely attached polymer entrapped ribozyme in C6 rat glial cells. Error bars represent n=3 ± SD.*

The optimisation assay results are shown in figure 4.11 for the number of washes required to remove loosely attached polymer entrapped ribozyme from a monolayer of C6 rat glial cells. The assay shows that a 19% of total radiation was removed with the first wash, 14%, 8%, 4%, 1% with second, third, fourth and fifth washes respectively. The sixth washing only removed a miniscule 0.2% of the radiation. A further seventh wash was carried out but no further significant reduction in radiation was observed. From this data it was decided to use five washes to remove the loosely attached microspheres from the cellular monolayers. Similar results (not shown here) were observed with the remaining cell lines GT1 (rat), SY5Y (human neuronal), U87 (human glial).

4.10. Cellular association over a time course

In order to investigate the extent and pattern of cellular association of ribozyme incorporated in biodegradable polymer PLGA microspheres, cellular association of microspheres over a time course was studied on monolayers of cultured glial and neuronal cells. Microspheres loaded with γ^{32}-P ATP labelled ribozyme were prepared and incubated with cells for various time points up to 8 hours at 37°C as described in section 2.10.2. The cellular association

values were normalised for cell number as with free ribozyme cellular investigations (chapter 3) in order to make a rigorous comparison between cell lines.

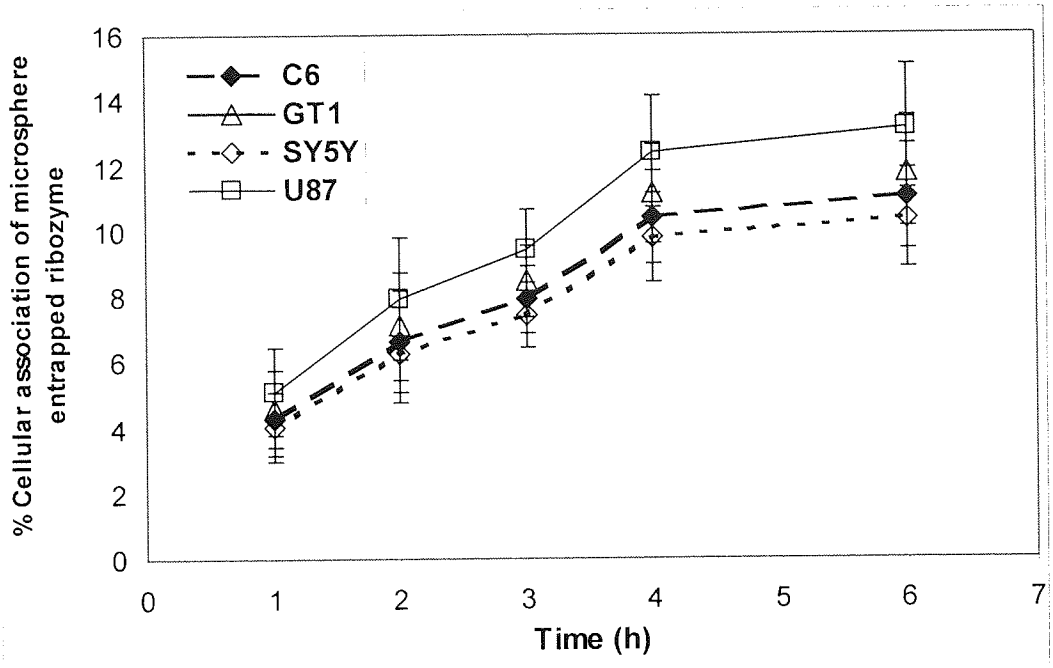

Figure 4.12. *Cellular association of microsphere entrapped ribozyme in C6, GT1, SY5Y and U87 cells over a time course. Error bars represent n=3 ± SD.*

Figure 4.12 illustrates the results of the time course study for cellular association of microspheres containing ribozymes. Generally the pattern of association was similar in all cell lines with a slight difference in the magnitude of association in cells. Human glioblastoma cell line U87, relatively, had the highest mean association value starting with 4.3% at 1 hour and 6.7, 7.9, 10.4, 11.1 and 13.0% for 2, 3, 4, 6 and 8 hours respectively. There was a statistically significant difference between time points ($F_{(5,17)}$= 22.5, P<0.05).

For the rat neuroblastoma cell line, GT1, the association values were 4.6, 7.1, 8.5, 11.2, 11.8 and 13.9% for 1, 2, 3, 4, 6 and 8 hours respectively. There was a significant difference between the time points ($F_{(5,17)}$= 4.9, P<0.05). Cellular association values for the human neuroblastoma cell line (SY5Y) were 4.0, 6.3, 7.4, 9.8, 10.4 and 12.2 % for 1, 2, 3, 4, 6 and 8 hours respectively. There was a significant difference in the association values across the time points ($F_{(5,17)}$ = 9.2, P<0.05). Finally for the human glioblastoma cell line U87 the cellular association values were relatively the highest, 5.1, 7.9, 12.4, 13.2 and 15.5% for 1, 2, 3, 4, 6 and 8 hours respectively. There was significant difference ($F_{(5,17)}$= 11.7, P<0.05) between time points.

These results demonstrate that the association of ribozyme entrapped in microspheres is many fold greater than free ribozyme all cell lines. For the rat glioblastoma C6 cells for the 6-hour time point there was 18-fold increase in association with microspheres in comparison to free ribozyme. For the remaining cell lines, GT1, SY5Y and U87 in comparison to free ribozyme the association of microsphere delivered ribozyme was 27, 20 and 18-fold greater. Within the rat species there was no significant difference between the glial C6 and neuronal GT1 cell lines whereas in the human cultured cells there was 1.9 times greater association in glial U87 cells in comparison to neuronal SY5Y cells. Similar increases (5-fold) in uptake have been reported by Smith, (2000) when oligonucleotides were encapsulated in microspheres and delivered to cells. In another study a 11-fold increase in microsphere delivered oligonucleotide uptake was observed (Khan., 1999). These results suggest that a different mechanism of association of ribozyme could be responsible for the increased association in cultured cells which is not cell type specific as seen by no significant difference in the association of ribozyme in glial and neuronal cells of both species though variations in cell culture conditions need to be considered.

4.11. Effect of temperature on the cellular association of microspheres

In order to further differentiate the association process as active or passive, cellular association of PLGA microspheres was evaluated at two different temperatures, 4 and 37°C, for 4 hours on a monolayer of cultured glial and neuronal cells. The protocol used in this study is described in section 2.10.3 with the results illustrated in figure 4.13.

As the results show, association of microsphere loaded ribozymes was strongly dependent on temperature. In the rat glial cells at the low temperature, 4°C, the cellular association was 4.6% and at the high temperature 37°C it was 13.1%, resulting in a significant ($T_{(6)}$= 0.001, P<0.000) 3-fold difference in the association. Similarly for the rat neuroblastoma, GT1, and human neuroblastoma cell line, SY5Y, it was observed that there was a 3-fold difference between the two temperatures, which was statistically significant ($T_{(6)}$= 0.001, P<0.001). Finally with the human glioblastoma cell line a 3-fold significant difference was observed in the cells ($T_{(6)}$= 0.001, P<0.001). These results strongly demonstrate that the association of ribozyme entrapped in PLGA microspheres was an active process.

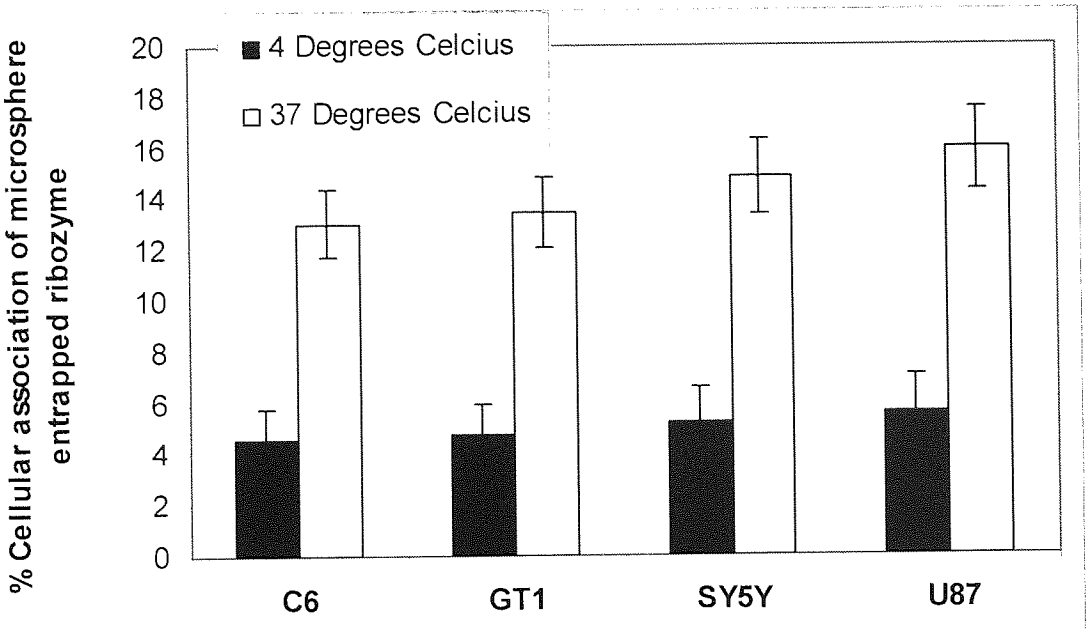

Figure 4.13. *The effect of temperature on cellular association of polymer entrapped ribozyme in C6, GT1, SY5Y and U87 cells. The bars in black colour show the cellular association for each cell line at 4 ℃ and white bars show cellular association at37 ℃. Error bars represent n=3±SD.*

4.12. Effect of metabolic inhibitors on the cellular association of microspheres

Results of the effect of temperature on the cellular association of microsphere-entrapped ribozyme suggest that the association process was an active process and to further confirm this, association of polymer entrapped ribozyme was investigated in the presence of metabolic inhibitors as described in section 2.10.4.

The results of this study are illustrated in figure 4.14 with all four cell lines showing a strong dependence on metabolic energy for association. In the rat glial C6 cells there was a 4.5-fold reduction in the association when cells were devoid of metabolic energy by pre-incubation with α-de-oxyglucose and sodium azide ($T_{(6)}$= 2.4, P<0.000). Similarly there was a 3-fold, 2.6-fold and 2-fold difference in the treated and non-treated normal cell populations in GT1, SY5Y and U87 cells with these differences being statistically significant ($T_{(6)}$= 0.18, 57.7, 2.95, P<0.05). These results confirm that association was an energy dependent process, which can be inhibited by depleting the cells of metabolic energy.

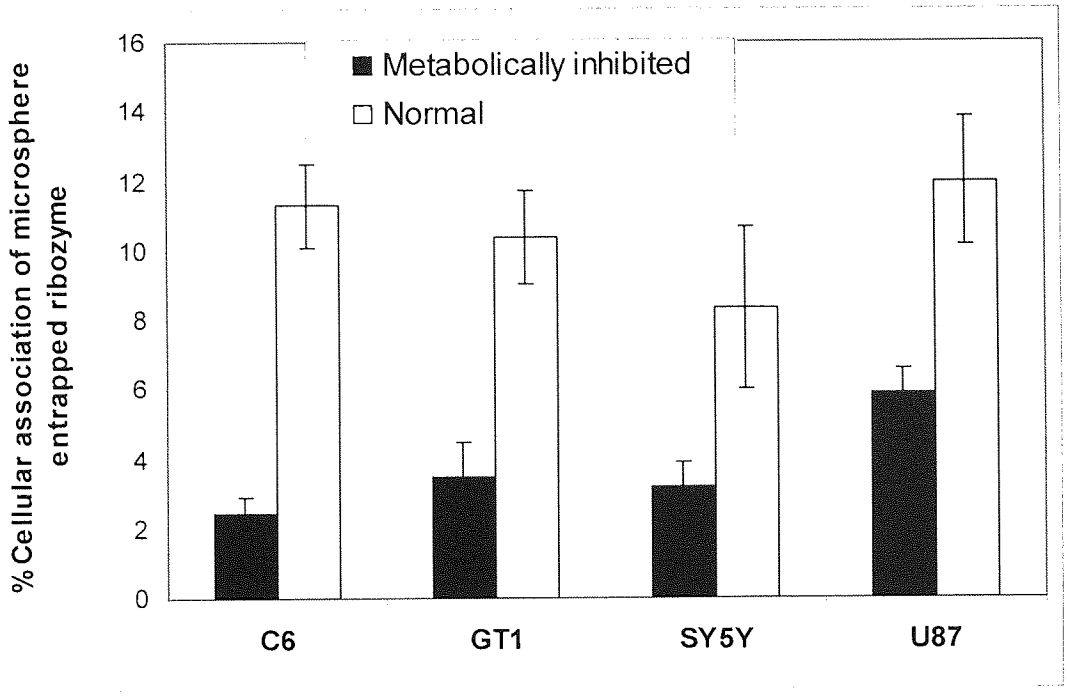

Figure 4.14. *The influence of metabolic inhibitors on the cellular association of polymer entrapped ribozyme in C6, GT1, SY5Y and U87 cells. Cells were pre-incubated with metabolic inhibitors at 37 ℃ for 4 hours in the presence of inhibitors. Error bars represent n=3±SD.*

4.13. Effect of pH on cellular association

In order to further characterise the association of microsphere entrapped ribozyme the effect of pH on the association was investigated using the method described in chapter 2.10.5. The results of this investigation are shown in figures 4.15, 4.16, 4.17 and 4.18.

The effect of pH on the association of microsphere entrapped ribozyme in cultured rat glial cell line C6 is shown in figure 4.15. The values of cellular association of microspheres were 6.1% for pH 5 and 8.3, 7.9 and 8.2% for pH values of 6, 7 and 8 respectively. There was a statistical difference in the mean association values of microspheres ($F_{(3,10)}$= 3.95, P=0.05) with post-hoc test showing that there was no difference between the pH points 6, 7 and 8 where as pH point 5 was significantly different from these points. Overall, the pattern demonstrates that at low pH the mean cellular association was reduced.

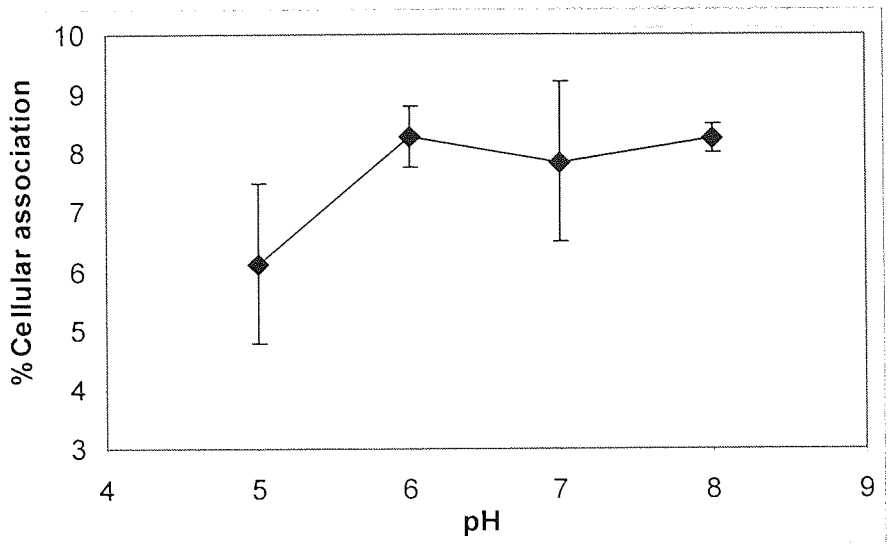

Figure 4.15. *Effect of pH on cellular association of polymer entrapped ribozyme on a monolayer of C6 cells. Data represents the means (n=3)±SD.*

Figure 4.16 illustrates the cellular association of microsphere on cultured neuronal cell line GT1. The cellular association profile shows that there was no effect of pH on the association of low pH with values of 7.6, 7.8 and 8.6% whereas at pH 8 the cellular association was reduced to 5.7%. Overall there was a significant difference in the association ($F_{(3,10)}$= 1.3, P=0.05) with post hoc test showing that pH 8 was significantly different from the lower pH values (P<0.05).

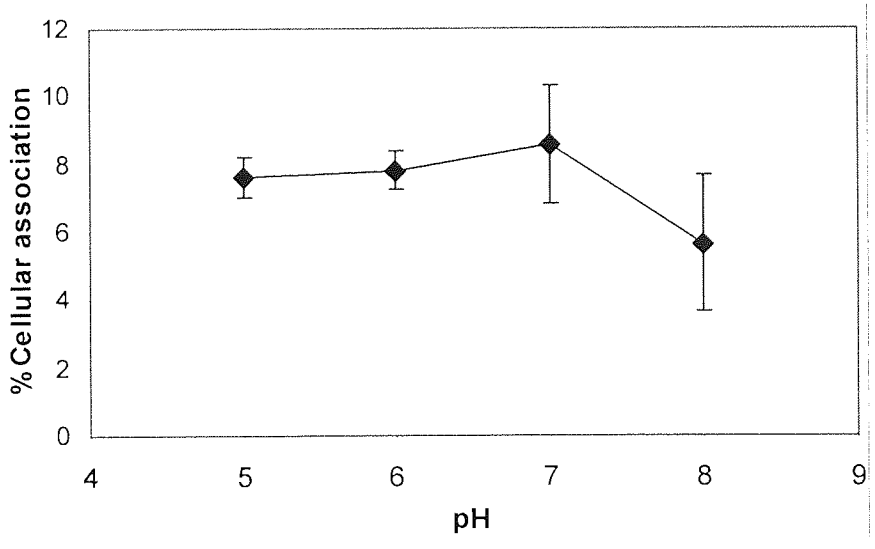

Figure 4.16. *Effect of pH on cellular association of polymer entrapped ribozyme on a monolayer of GT1 cells. Data represents the means (n=3)±SD.*

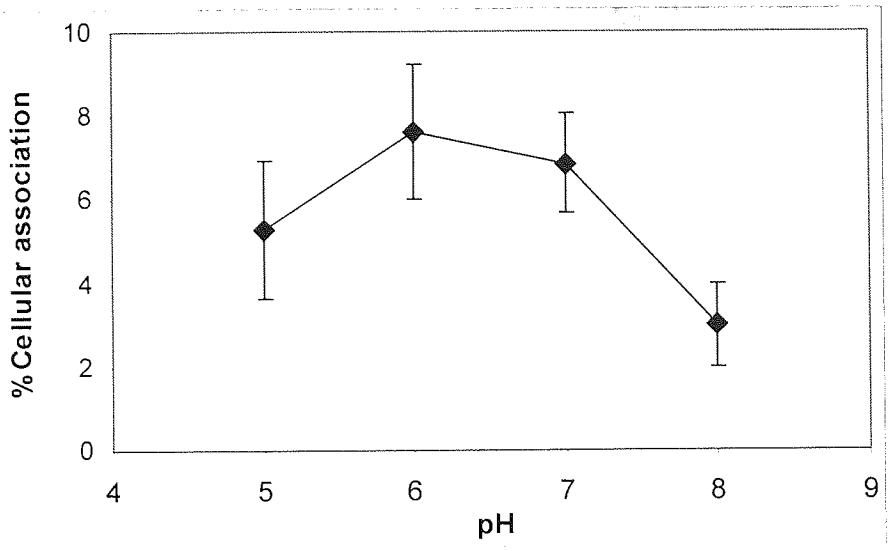

Figure 4.17. *Effect of pH on cellular association of polymer entrapped ribozyme on a monolayer of SY5Y cells. Data represents the means (n=3)±SD.*

Figure 4.17 shows the effect of pH on the cellular association of polymer entrapped ribozymes in cultured human neuronal cells SY5Y. There was significant difference in the cellular association at different pH values ($F_{(3,10)}$= 6.81, P<0.05) with reduced cellular association at pH values 5 and 8 (5.3 and 3.0%) with pH 6 and 7 showing higher values (7.6 and 6.9%).

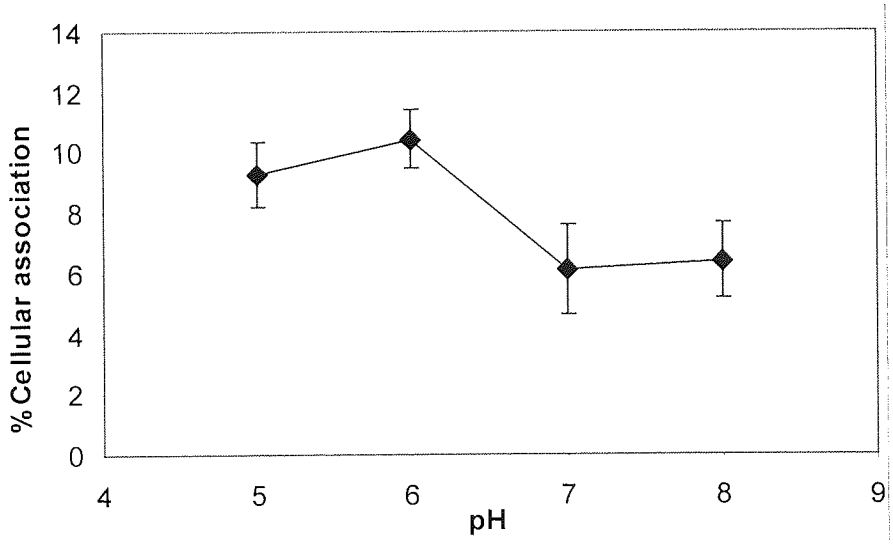

Figure 4.18. *Effect of pH on cellular association of polymer entrapped ribozyme on a monolayer of U87 cells. Data represents the means (n=3)±SD.*

Figure 4.18 shows the effect of pH on the cellular association of microspheres in cultured human glial, U87, cells. The pattern of association at these temperature shows that the association was higher at low pH values (9.2, 10.5% respectively) than higher pH values of 7 and 8 (6.1 and 6.4% respectively) with the differences in the mean association values

significantly different ($F_{(3,10)}$= 13.22, P<0.05). An analysis of the these profiles within each cell line and between cell lines shows that there is no consistent pattern of effect of pH on the mean cellular association of ribozyme loaded microspheres. This data is in contrast to the effect of pH on the association of free ribozymes which increased as the pH value decreased. It seems that a different set of proteins is responsible for the association of microspheres to cells which are not sensitive to pH changes. It was attempted to determine the size of these cell surface proteins with the South-Western blot but due to technical difficulties in optimising the washes required for the procedure (see section 2.8), further work was abandoned in the interests of time.

4.14. Concluding remarks

Cellular delivery of free ribozyme investigated in chapter 3 illustrated that the association of ribozyme in cultured glial and neuronal cells was highly limited. This result highlighted a need to develop a delivery system to enhance cellular delivery of ribozymes. For this aim internally labelled chemically modified ribozyme was encapsulated in microspheres prepared from biodegradable polymer PLGA. Formulated microspheres were characterised for physical and cellular association characteristics in this chapter. Ribozyme was entrapped in microspheres formulated from three different co-polymer ratios, 90:10, 80:20 and 50:50 of the biodegradable polymer PLGA using the double emulsion method. Microspheres of two size ranges (0-5μm and 10-20μm) were prepared by manipulation of the stirring rates during the primary and secondary emulsion preparation phase. Microspheres of high yields were successfully formulated with smaller microspheres exhibiting relatively higher yield than larger microspheres. In contrast the percent encapsulation of ribozyme in the formulation ranged from 34% to 48% for small microspheres and 50% to 57% for large microspheres.

This differential in encapsulation efficiency between small and large size range was further observed in the values of loading of ribozyme per mg of microspheres when higher values with large size range microspheres where observed in comparison to small size range microspheres. The surface morphology of microspheres was observed to ascertain that microspheres were of the desired shape and structure. Scanning electron micrographs illustrated that microspheres were of spherical shape and there was no non-incorporated polymer observed in the micrographs. The surface of formulated microspheres was smooth and there were no collapsed or damaged microspheres. Finally in order to determine the size

range of microspheres the microsphere sizes were evaluated with Malvern Mastersizer the results from which confirmed the size range of microspheres in to two size ranges of 1-5μm and 10-20μm. After successful formulation of microspheres of two size ranges with three different co-polymers of PLGA the release studies of these different microsphere delivery systems were carried out. Release studies evaluated the release of ribozyme from microspheres over a time course. There was a significant difference in the release profiles of ribozyme of three co-polymer ratios with the 50:50 and 80:20 ratio exhibiting a triphasic release profile and the 90:10 ratio of the co-polymer exhibiting a biphasic release profile. Within each co-polymer ratio there was also a significant difference between the large and small microspheres with small microspheres producing a 3 to 4-fold greater ribozyme release at the burst effect. Evaluation of the stability of microsphere entrapped ribozyme was carried out to determine whether the fabrication process does not adversely affect the integrity of ribozyme. Stability study results demonstrated that ribozyme remained intact after the fabrication process and moreover incubation of microsphere-entrapped ribozyme in serum medium protected the ribozyme from degradation from nucleases.

Characterisation of microspheres, in terms of size, shape, yield, loading values, stability and release profiles, was followed by investigation of ribozyme cellular association properties. Cellular association of the selected 50:50 co-polymer ratio small size range microspheres was studied in cultured glial and neuronal cells over a time course. Results from this study showed that cellular association of microsphere entrapped ribozyme was dependent on time and resulting in a cellular association 18 to 27-fold higher than the free ribozyme in the different cell types with no significant difference among the cell lines studied. Further characterisation of the cellular association revealed that the cellular association was a temperature and energy dependent process indicating that it was an active process and was independent of pH of the incubation medium. These results demonstrate that PLGA polymer microspheres can be utilized as a delivery system, which not only protect the ribozyme from degradation but also enhance the cellular delivery of ribozyme and provide sustained release.

CHAPTER FIVE

EVALUATION OF BIODEGRADABLE POLYMER MICROSPHERE SYSTEMS FOR CENTRAL NERVOUS SYSTEM DELIVERY OF RIBOZYMES

5.0. Introduction.

Delivery of drugs to the central nervous system (CNS) remains a challenging area of research despite advances in the understanding of the anatomy and physiology of the central nervous system and parallel new developments of potential therapeutic agents. For many diseases, neurodegenerative and oncogenic, there are still no effective treatment modalities available to deliver drugs into the brain particularly within discrete regions at a controlled rate. This difficulty in CNS delivery arises due to the presence of the formidable blood brain barrier (BBB). The blood brain barrier, which is structurally composed of non-fenestrated brain capillary endothelial cells cemented by tight junctions, block the free exchange of large, poly-ionic and hydrophilic molecules between the blood and brain extracellular fluid. This high degree regulation of CNS permeability by the BBB only allows either small lipophilic drugs to gain access to the CNS cells or molecules which have specific transporters and severely limits penetration of large poly-ionic drug molecules. Unfortunately, recently developed therapeutic agents such as antisense oligonucleotides and ribozymes, which have large sizes and polyanionic character, have insignificant penetration to the CNS. This is highlighted in an editorial in Drug Discovery Today (Pardrige, 2002), which reports that 98% of all new drugs discovered for CNS disorders do not cross the BBB, demonstrating a strong need for a robust and novel CNS delivery system.

However, as described in the introduction of this thesis, several strategies have been employed in order to overcome this problem. These strategies include: osmotic disruption of the blood barrier (Neuwelt *et al.*, 1980), infusion pumps delivering drugs into the cerebrospinal fluid (Harbaugh *et al.*, 1988), catheter systems (Penn *et al.*, 1995), coupling of drugs to a carrier undergoing receptor-mediated trans-cytosis through the blood-brain barrier (Hudson *et al.*, 1999) and implantation of cells in the brain (Gage *et al.*, 1987). One of the

promising strategies for drug delivery to the brain is polymer based drug delivery systems, which have been successfully used to provide delivery of variety of molecules to the brain (see table 1.4). This strategy involves formulation of polymers in to slabs, wafers or microspheres entrapping the drug, which can be stereotactically implanted in discrete regions of the brain to provide sustained and controlled delivery.

Polymer based local treatment strategy entails several advantages including not only delivery of the drug to the desired site at a controlled rate for a required time period but also helps to improve the clinical outcomes by providing a therapeutic concentration at the target site and by preventing debilitating toxicities seen with systemic administration as shown by several studies with polymeric delivery of carmustine (Brem and Gabikian, 2001). Additionally, sustained release of bioactive molecules from polymers obviates the need for repeated administration to the parenchyma or ventricles, which is an inconvenient method and leads to undesirable side-effects such as local tissue damage in the form of non-specific astrocytic proliferation and microglial mediated inflammation. Furthermore the polymeric delivery systems protect biologically labile molecules from degradation and also with biodegradable polymers the need for surgical removal of implanted device is also eliminated once the release of the drug molecule is complete.

Biodegradable polymer microspheres formulated from PLGA potentially constitute a robust delivery system for the site-specific and sustained delivery of ribozyme targeted to neoplastic and neurodegenerative conditions. The biodegradable polymer, PLGA, has a long history of use in experimental and clinical studies with proven biocompatibility of the PLGA microspheres implanted in the brain tissue (Menei *et al.*, 1993). Ribozymes can be entrapped in PLGA polymers by formulating microspheres, which due to their small size can be easily implanted by stereotaxy in precise and functional areas of the brain without damage to the surrounding tissues. This implantation avoids the inconvenient insertion of large implants by open surgery and can be repeated under local anaesthesia if required.

It was the aim of this chapter to investigate the effect of ribozyme containing PLGA microsphere implantation on CNS tissue, characterise distribution of microspheres within the CNS and eventual fate of the microspheres. Despite successful demonstration of microsphere use to achieve delivery of molecules to particular regions of the brain there has been no study reported in the literature which investigates the distribution of characteristics of PLGA

microsphere post ICV injection and also the distribution and fate of released molecules from these microspheres over a time course. The precise distribution of the released molecules in the brain especially in the context of local delivery strategies is important to characterise as it has an significant factor for the selection of optimal injection site and the number of implantations required. Moreover, information regarding distribution as a function of time would be required to develop strategies for short or long half life CNS targets ranging from few days to 6-12 months.

To achieve this aim ribozyme was entrapped in PLGA 50:50 microspheres and following characterisation *in vitro* (chapter 4) microspheres were stereotaxically implanted ICV in male Wistar rat brains. The effect of free ribozyme and microsphere entrapped ribozyme implantation on CNS tissue was investigated by post-injection well being assessment and histological evaluation of the CNS tissue. This was followed by an investigation of the distribution of microspheres, spatially, over a series of time points and compared to free ribozyme in the CNS after ICV injection. Finally, the effect of microsphere size range on the distribution of particles in the CNS.

5.1 RESULTS AND DISCUSSION

5.2. Behavioural assessment of ribozyme treatment

In order to investigate whether the ICV stereotaxic implantation of free and microsphere entrapped ribozyme is safe and does not lead to harmful systemic and/or neurological effects on the animals, a post-injection well being assessment was carried out. In this study, the behaviour of animals was observed after ICV administration, of free and polymer-entrapped ribozyme as described in section 2.11.3 and 2.11.6. The observation of animals included monitoring the animal behaviour for signs of distress such as licking of paws, rising of the fore legs, kicking of hind legs, weight measurement at regular intervals, fur condition and movement of the animals. These observations showed that for the time points studied, 24 hours and 5 days, none of the animals exhibited obvious and noticeable systemic or neurological adverse effects, which would have been evidenced by behavioural changes in comparison to untreated animals.

These results confirmed that free and polymer-entrapped microspheres do not cause behavioural toxicity and are safe and suitable for ICV implantation under anaesthesia in male Wistar rats.

5.3. Histological evaluation

Following assessment of behavioural toxicity after ICV injections of free or polymer-entrapped ribozyme further histological evaluation was carried out to search for histological damage such as neuronal loss and glial cell proliferation. For this purpose rat brain cryosections were prepared as described in section 2.11.2 and 2.11.3 and were examined for histological damage 24 hours and 5 days post ICV implantation using cresyl fast violet staining. The ICV injection was made at co-ordinates 0.8mm caudal to bregma, 0.14mm lateral and 0.36mm ventral to bregma (Paxinos and Watson, 1986).

Coronal sections of the entire brain were microscopically examined for any visible histological damage and illustrative coronal sections of a selection of various parts of the brain are shown in figures 5.1.1 to 5.1.11. In these figures the sections on the left hand side are from an untreated rat and the sections on the right hand side are from polymer treated rat

brain. Certain brain regions were selected for further observation at a higher magnification and these regions contained the areas of: frontal cortex, hippocampus, hypothalamus, cerebellum, striatum, and corpus callosum. The high magnification sections are presented alongside UV photographs in the subseqent distribution study sections. In these areas cresyl violet staining revealed no observed neurological damage, neuronal loss or evidence of glial cell proliferation in any of the two treatment groups as highlighted by the tissue histology. These histological observations at both high and low magnification along with post-implantation behavioural assessments indicate that ICV administration of free or polymer-entrapped ribozyme does not cause any apparent histological and behavioural toxicity.

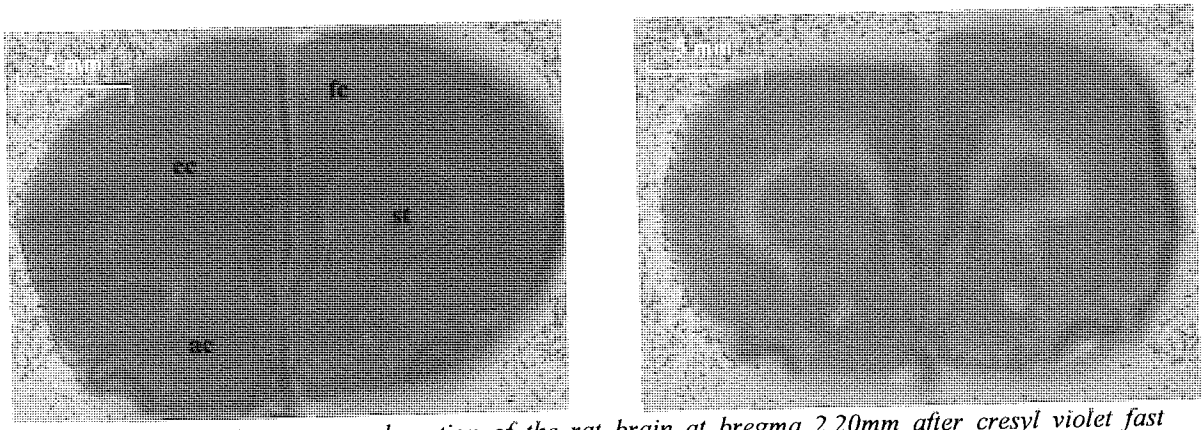

Figure 5.1.1. *Showing a coronal section of the rat brain at bregma 2.20mm after cresyl violet fast staining. Magnification 4×. Fc = Frontal cortex, cc = corpus collusum, st = striatum, ac = anterior commisure.*

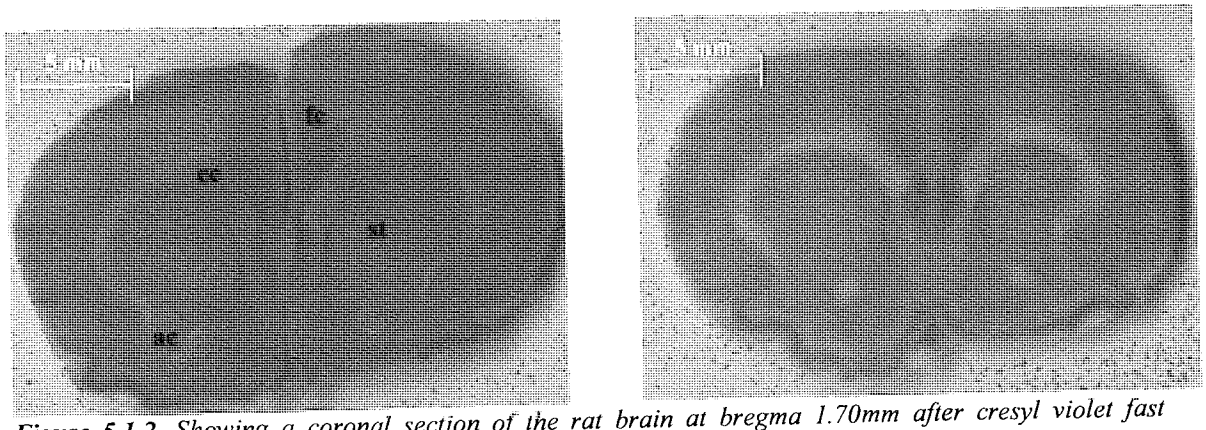

Figure 5.1.2. *Showing a coronal section of the rat brain at bregma 1.70mm after cresyl violet fast staining. Magnification 4×. Fc = Frontal cortex, cc = corpus collusum, st = striatum, ac = anterior commisure.*

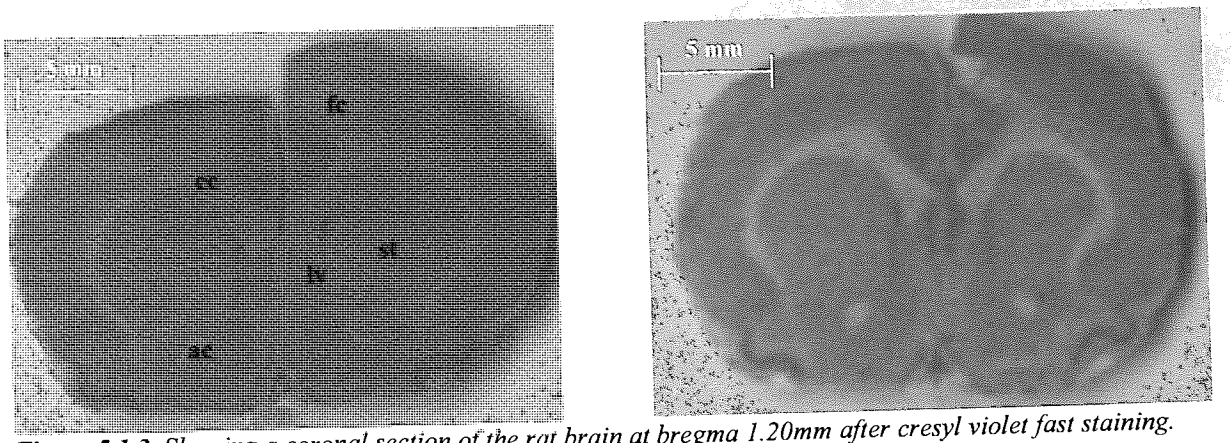

Figure 5.1.3. *Showing a coronal section of the rat brain at bregma 1.20mm after cresyl violet fast staining. Magnification 4×. Fc = Frontal cortex, cc = corpus collusum, st = striatum, ac = anterior commisure, lv = left ventricle.*

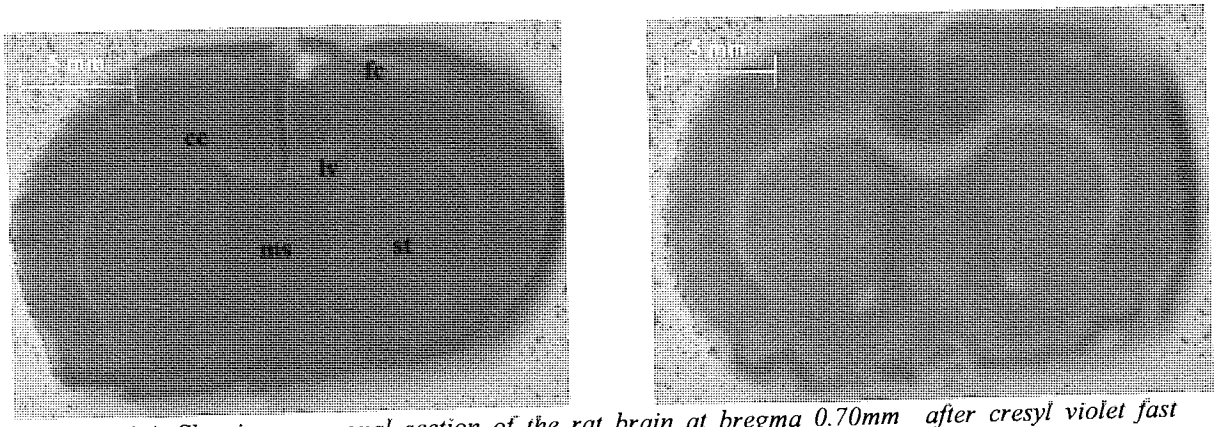

Figure 5.1.4. *Showing a coronal section of the rat brain at bregma 0.70mm after cresyl violet fast staining. Magnification 4×. Fc = Frontal cortex, cc = corpus collusum, st = striatum, ms = medial septal nu, left ventricle.*

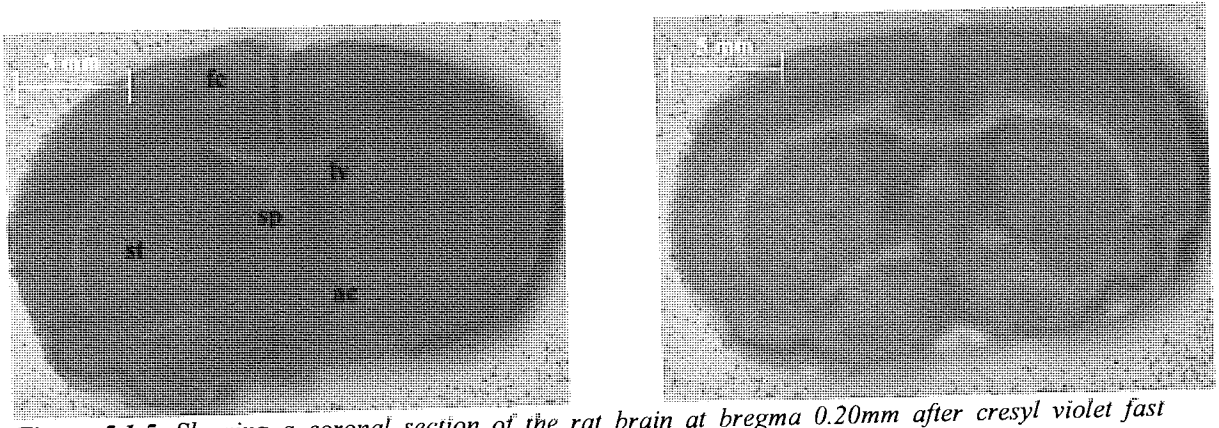

Figure 5.1.5. *Showing a coronal section of the rat brain at bregma 0.20mm after cresyl violet fast staining. Magnification 4×. Fc = Frontal cortex, cc = corpus collusum, st = striatum, ac = anterior commisure, sp = septum, lv = left ventricle.*

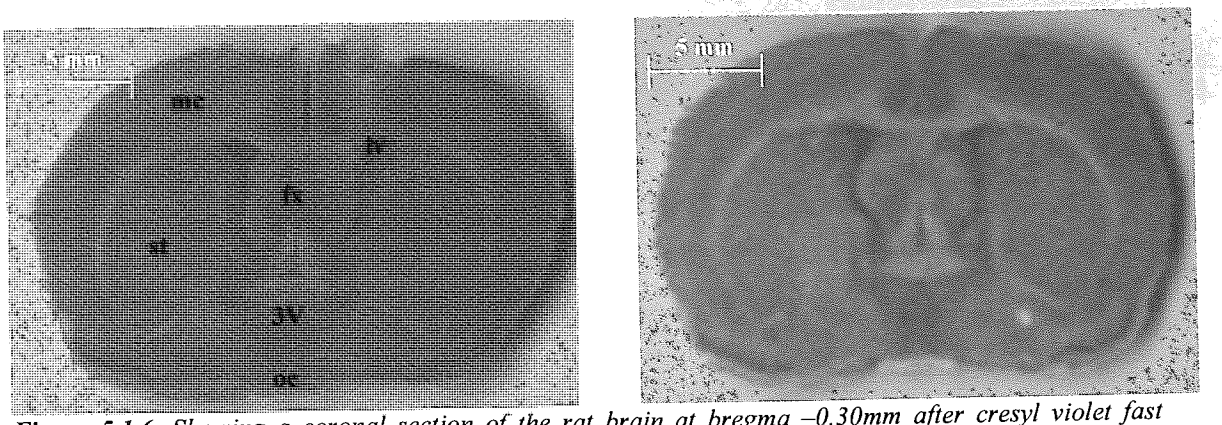

Figure 5.1.6. *Showing a coronal section of the rat brain at bregma –0.30mm after cresyl violet fast staining. Magnification 4×. mc = motor cortex, cc = corpus collusum, st = striatum, oc = optic chiasma, fx = fornix, 3V = third ventricle.*

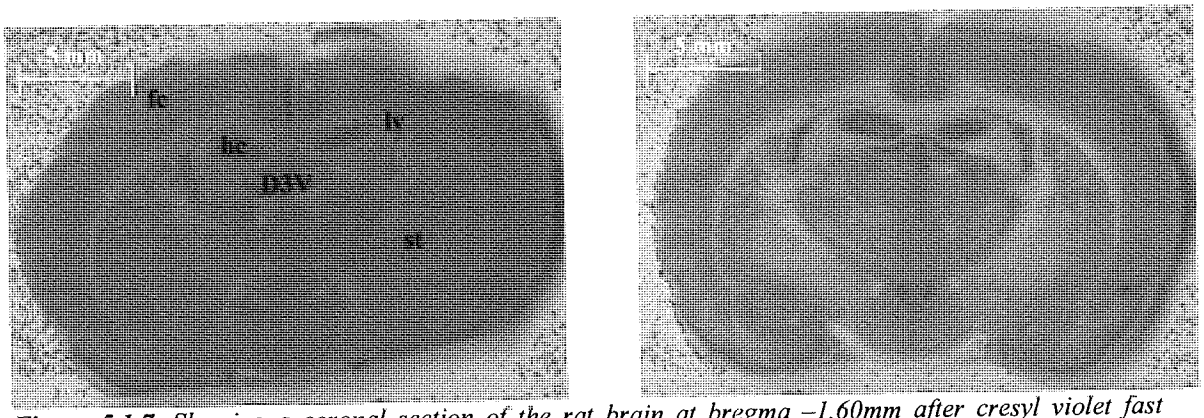

Figure 5.1.7. *Showing a coronal section of the rat brain at bregma –1.60mm after cresyl violet fast staining. Magnification 4×. Fc = Frontal cortex, st = striatum, hc = hippocampus, D3V = dorsal third ventricle, lv = left ventricle.*

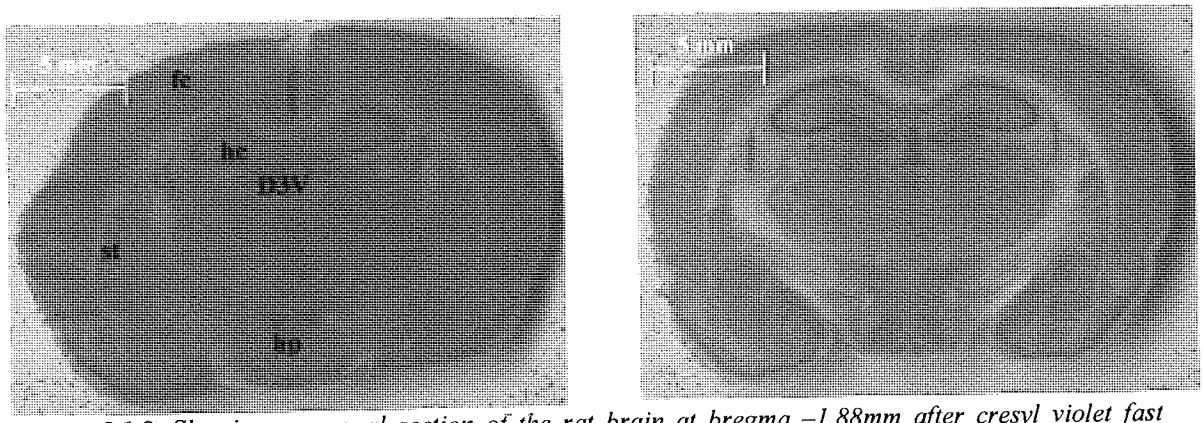

Figure 5.1.8. *Showing a coronal section of the rat brain at bregma –1.88mm after cresyl violet fast staining. Magnification 4×. Fc = Frontal cortex, st = striatum, hc = hippocampus, D3V = dorsal third ventricle, hp = hypothalamic region.*

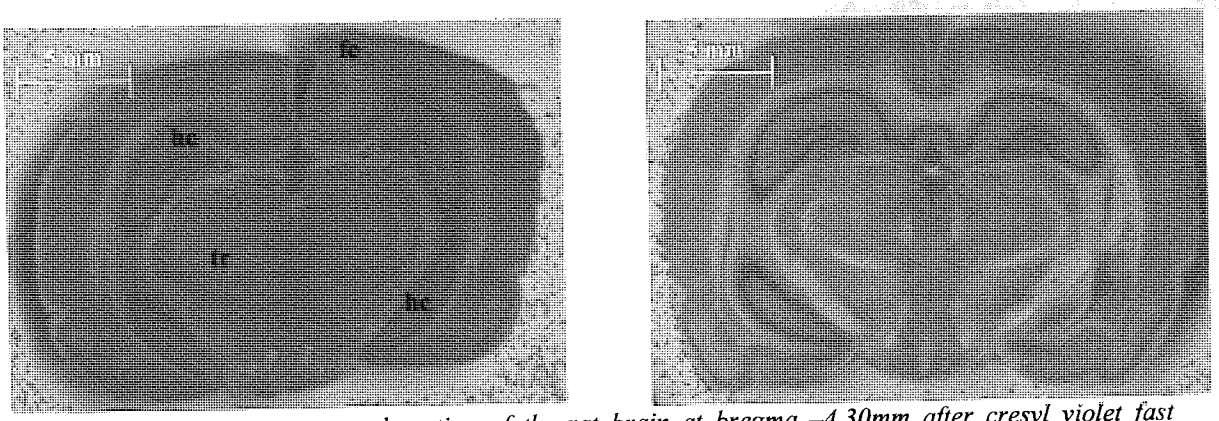

Figure 5.1.9. *Showing a coronal section of the rat brain at bregma –4.30mm after cresyl violet fast staining. Magnification 4×. Fc = Frontal cortex, tr = thalamic region, hc = hippocampus.*

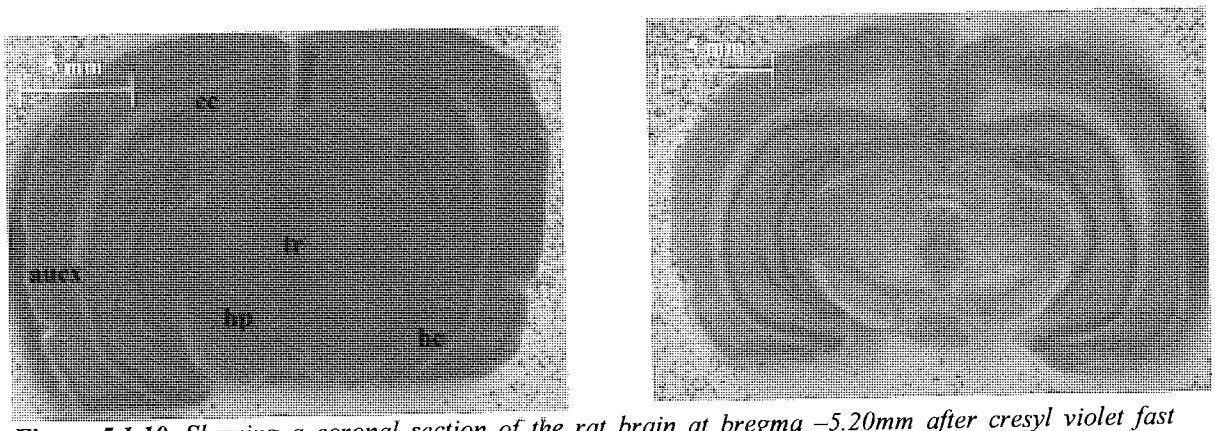

Figure 5.1.10. *Showing a coronal section of the rat brain at bregma –5.20mm after cresyl violet fast staining. Magnification 4×. cc = corpus collusum, aucx = auditory cortex, tr = thalamic region, hp = hypothalamus, hc = hippocampus.*

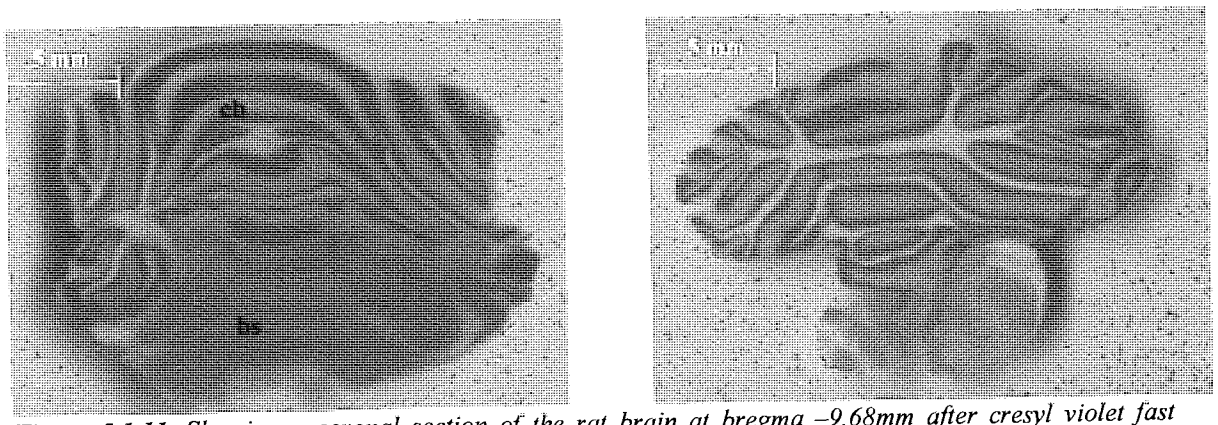

Figure 5.1.11. *Showing a coronal section of the rat brain at bregma –9.68mm after cresyl violet fast staining. Magnification 4×. cb = cerebellum, bs = brain stem region .*

5.4. Stability of ribozyme after *in vivo* CNS injection

The stability of ribozyme after ICV injection *in vivo* was investigated as described in section 2.6.3. As with the *in vitro* studies presented in sections 3.1.1 it is important to evaluate the structural stability of ribozymes *in vivo* as a structurally intact ribozyme which penetrates the cells will be effective in the blocking of target gene expression. The results of this study are presented in figure 5.2. The lane labeled A is the original untreated control ribozyme, lane B is free label γ^{32}P –ATP and lane C is the ribozyme recovered from CNS. As lane C shows all of the ribozyme had degraded after 24 hours. Despite the fact that nuclease activity in the CNS is low (Giannakis *et al.*, 1991), the stability of ribozyme was negligible in the rat brain after 24 hours.

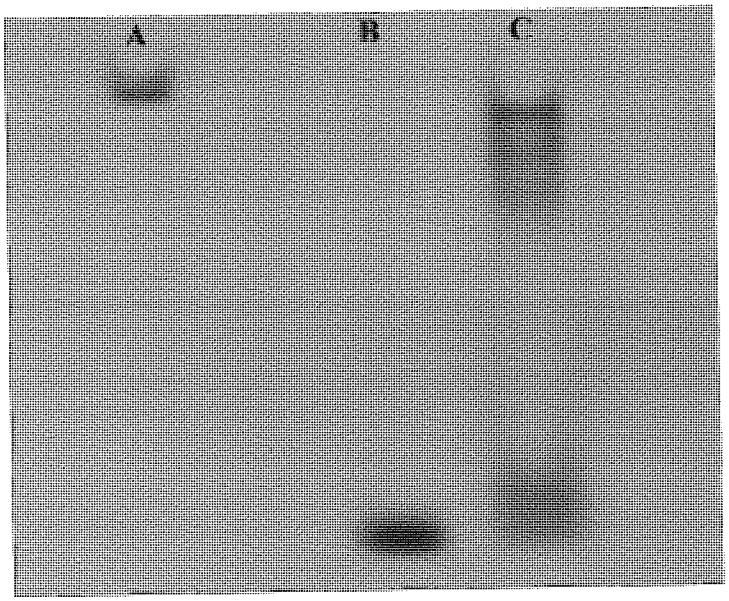

Figure 5.2. *Stability of free ribozyme after ICV administration. Lane A is the control, unexposed ribozyme, whereas lane B is free label γ^{32}-P-ATP and lane C is the free ribozyme recovered from the CNS tissue.*

The stabilty of phosphodiester (PO) and phosphorothioate (PS) ODNs in the CSF after ICV injection has been studied by (Whitesell *et al.*, 1993) and was found that PO were completely degraded within 100 minutes whereas the PS remained stable for this time period. In another report the PS were degraded after 4 hours post ICV infusion (Yee *et al.*, 1994). This poor stability strongly reflects the need for a delivery system which ensures the protection of ribozyme from degradation.

5.5. Distribution of free FITC-Ribozyme in the CNS

After evaluating the potential of toxicity, of free and polymer microsphere entrapped ribozyme via ICV administration, the distribution of free and entrapped ribozyme in the CNS was studied. This information is important for evaluating the potential of novel delivery systems which are being developed for CNS drug targeting. In this section it was aimed to determine the fate and distribution of free and polymer entrapped ribozyme after site-specific lateral ventricular injection. Initially the free ribozyme was studied as described in this section, which was then followed by an investigation of distribution of microsphere entrapped ribozyme (section 5.6). Free riboyzme was injected in to the ventricles of CNS as described in section 2.11.1 and the animal was sacrificed after 3 hours and crysections obtained as described in 2.11.2. These sections were observed under UV light for potential fluouresence from the administered FITC-labelled ribozyme. During these observations no noticeable fluoresence was observed in sections 3 hours post ICV injection indicating that no FITC-ribozyme was present in the CNS.

This could be due to the fact that the free ribozyme was rapidly cleared away from the rat ventricular system present in the brain. The ventricular system in the rat brain, which consists of the two lateral ventricles, third and fourth ventricle, which are interconnected with each other and continous with the sub-arachnoid space and is filled with cerebrospinal fluid (CSF). The CSF is generated at the blood-CSF barrier, which is formed by the tight junctions at the apical membrane surface of the epithelial cells present on the linings of the choroid plexus and other cerebro-ventricular organs (Brightman *et al.*, 1970). Once formed at the lateral ventricles it readily moves by bulk flow to the third and fourth ventricles via channels and enters the sub-arachnoid space by passing through the cisterna magna. At the sub-arachnoid space the CSF flows through the cerebral convexities and is absorbed in to the general circulation at the superior saggital sinus across the arachnoid villi.

It was originally thought that injection of ribozyme at the ventricle will advantageous for two reasons; firstly, it will result in less tissue damage, which is observed with direct parenchmal injection and secondly, it is thought ICV injection is equivalent to slow IV infusion (Aired *et al* 1990) leading to a distribution of the ribozyme in the parenchyma of the cells in a controlled fashion. However, in this case the ribozyme was rapidly cleared away from the CSF by bulk flow and was not present in the ventricles for long enough to diffuse through

the fenestrated, relatively, high permeability ventricular linging composed of ependymal cells at the ventral side of the ventricles and CVOs and permeate in to the parenchyma.

5.6.1. Distribution of polymer entrapped ribozyme 24 hours post ICV injection

In this section the distribution of polymer entrapped fluorescently labelled ribozyme was investigated 24 hours post ICV injection. Microspheres were prepared and characterised as shown in section 2.9 and injected in the lateral ventricles. Animals were sacrificed 24 hours post injection and coronal sections prepared as described in sections 2.11.2 and 2.11.3. Coronal sections of the entire brain were observed for microsphere associated fluoresence and photographs taken of brain areas with visible fluoresence. In the figures presented in this section the photograph on top of each figure were taken under normal light conditions and the photographs at the bottom were taken under UV light conditions.

Figure 5.3.1. *Photographs showing the distribution of microspheres in the ventricles with the normal light photograph at the top and fluorescence photograph at the bottom. Magnification 40×.; Coronal section taken at bregma 0.48mm. CC = corpus collusum, ST = striatum, V = lateral ventricle, MICS = microspheres,SP = septum, arrows show FITC microspheres.*

Figure 5.3.1 shows a coronal section of the brain at bregma 0.48mm which shows the area of ventricles, corpus collusum and caudate putamen. As seen in the figure 5.3.1, micrsopheres remain in the ventricles for 24 hours, unlike free ribozyme and are still fluorescent as shown by the photograph at the bottom. Another interesting observation was that microspheres remained with in the ventricular system and did not diffuse through the walls of the ventricles which are lined by ependymal cells and contain fenestrations, making these walls more permeable in comparison to the blood-brain barrier. The parenchyma was carefully observed at other sites such as the thalamus, hypothalamus, striatum, hippocampus, cerebellum and cortical areas and no fluorescence was observed. All areas of which are continous with ventricles such as the third or fourth ventricles and the subarachnoid space had visible fluoresence indicating the fact that microspheres of the size range used only remain within the ventricular system after 24 hours (figures 5.3.2, 5.3.3, 5.3.4, 5.3.5, 5.3.6, 5.3.7).

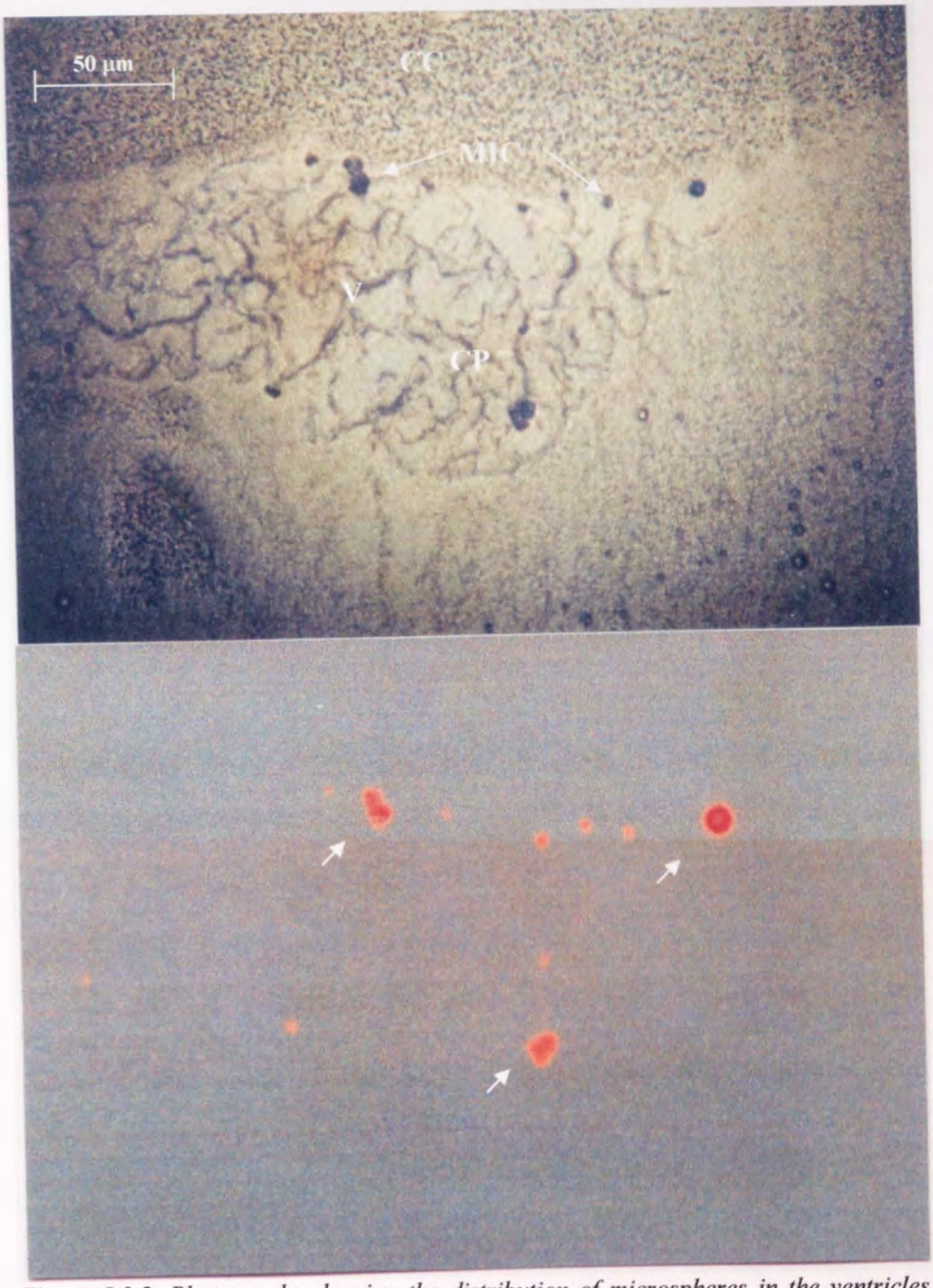

Figure 5.3.2. *Photographs showing the distribution of microspheres in the ventricles with the normal light photograph at the top and fluorescence photograph at the bottom. Magnification 100×.; Coronal section taken at bregma –0.80mm. CC = corpus collusum, V = lateral ventricle, MICS = microspheres, CP = choroid plexus, arrows show FITC microspheres.*

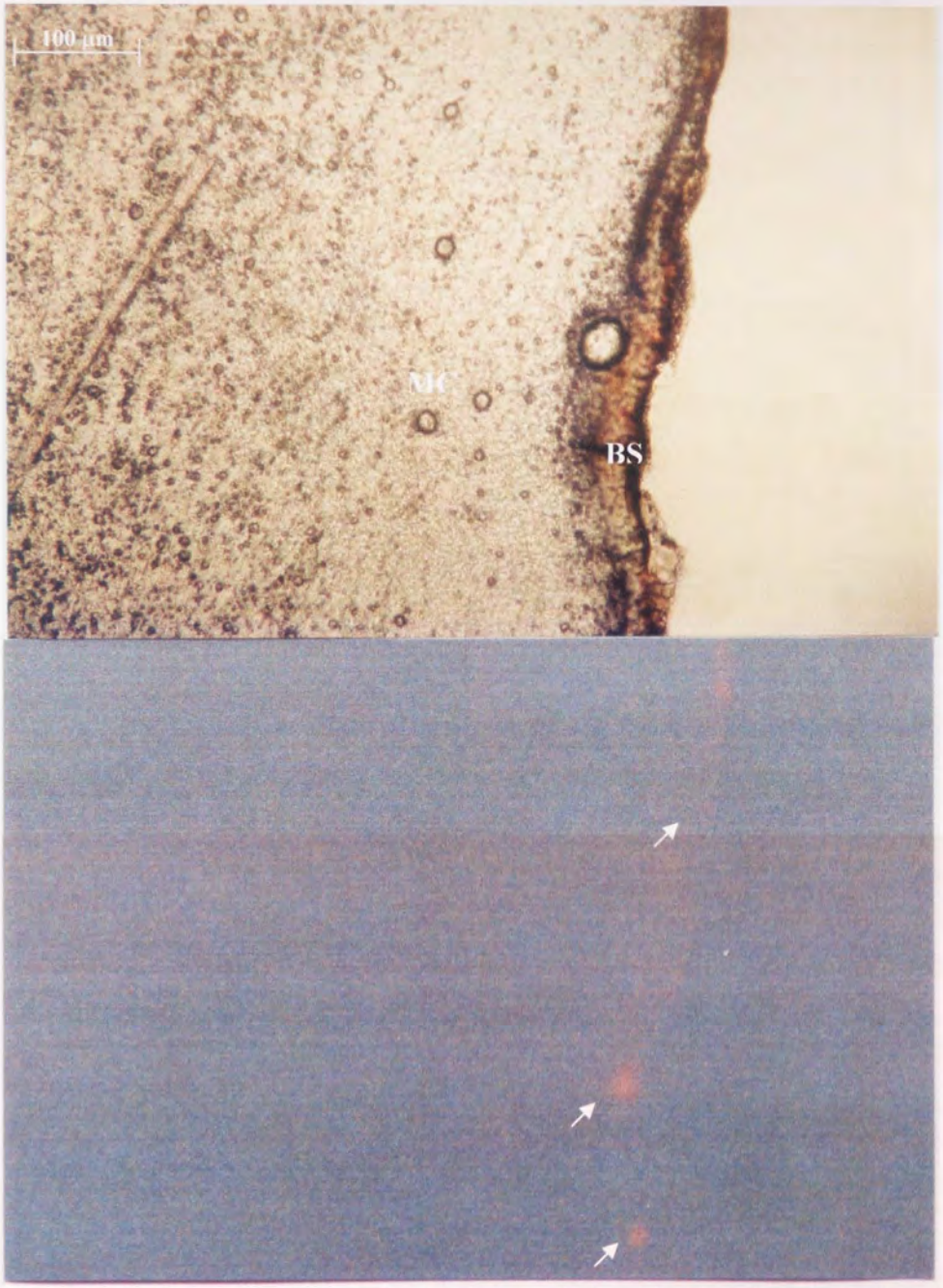

Figure 5.3.3. *Photograph showing the distribution of microspheres at the sub-arachnoid space with the normal light photograph at the top and fluorescence photograph at the bottom. Magnification 40×.; Coronal section taken at bregma –0.92mm. MC = motor cortex, BS = brain surface, arrows show FITC microspheres.*

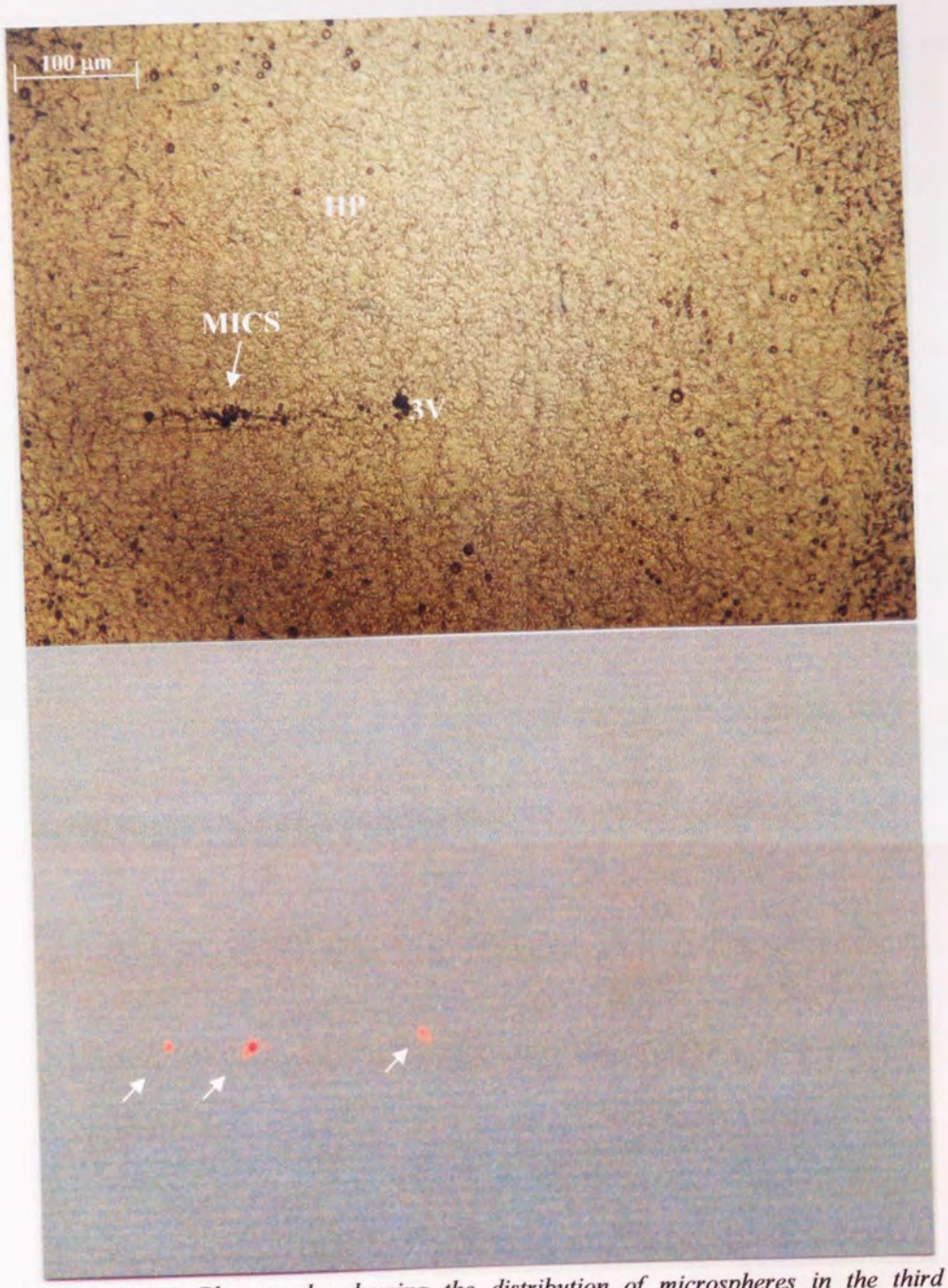

Figure 5.3.4. *Photographs showing the distribution of microspheres in the third ventricle channel with the normal light photograph at the top and fluorescence photograph at the bottom. Magnification 40×.; Coronal section taken at bregma - 1.30mm. HP = hypothalamic region, 3V = third ventricle, MICS = microspheres, arrows show FITC microspheres.*

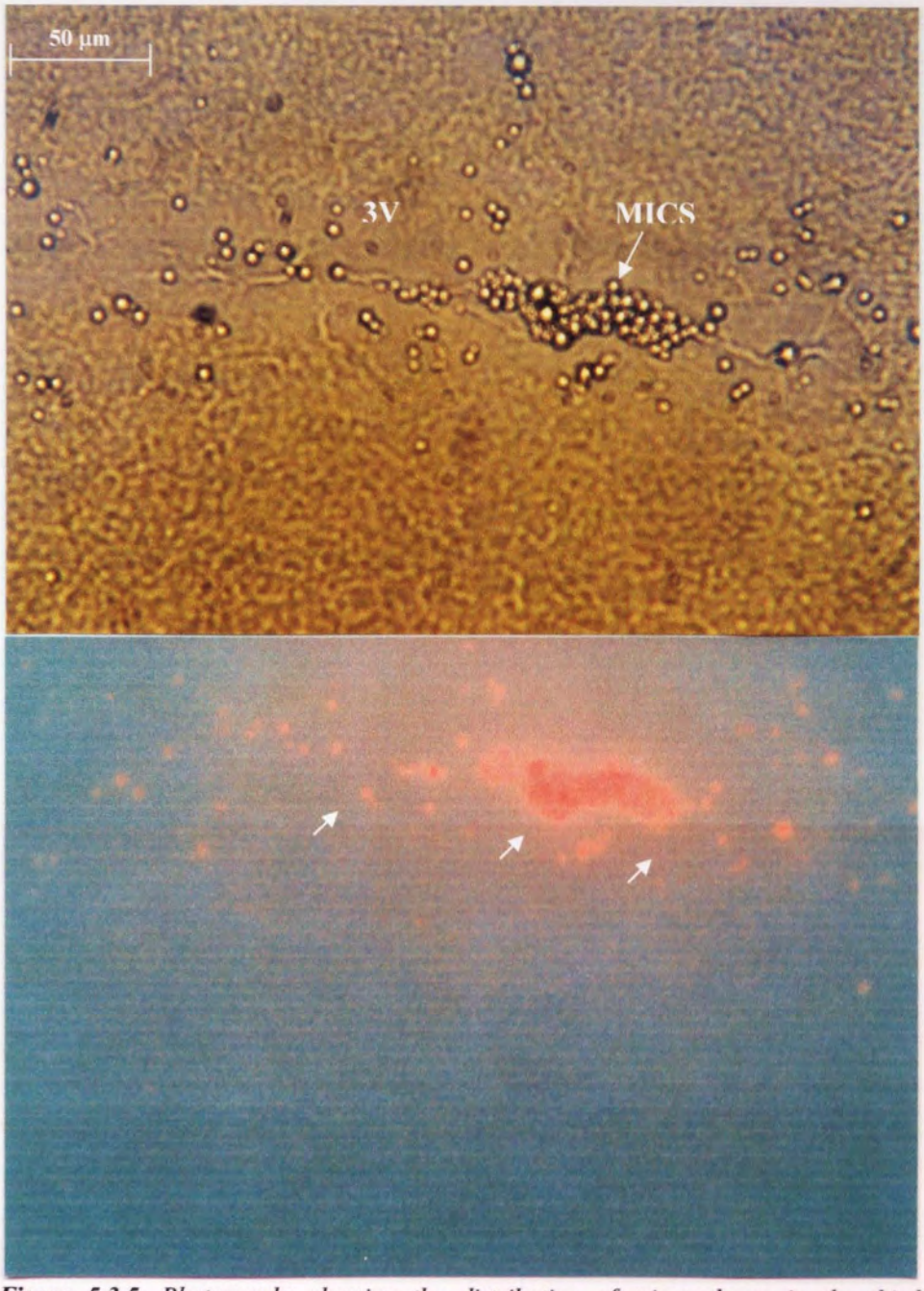

Figure 5.3.5. *Photographs showing the distribution of microspheres in the third ventricle with the normal light photograph at the top and fluorescence photograph at the bottom. Magnification 100×. Coronal section taken at bregma -0.80mm. 3V = third ventricle, MICS = microspheres, arrows show FITC microspheres.*

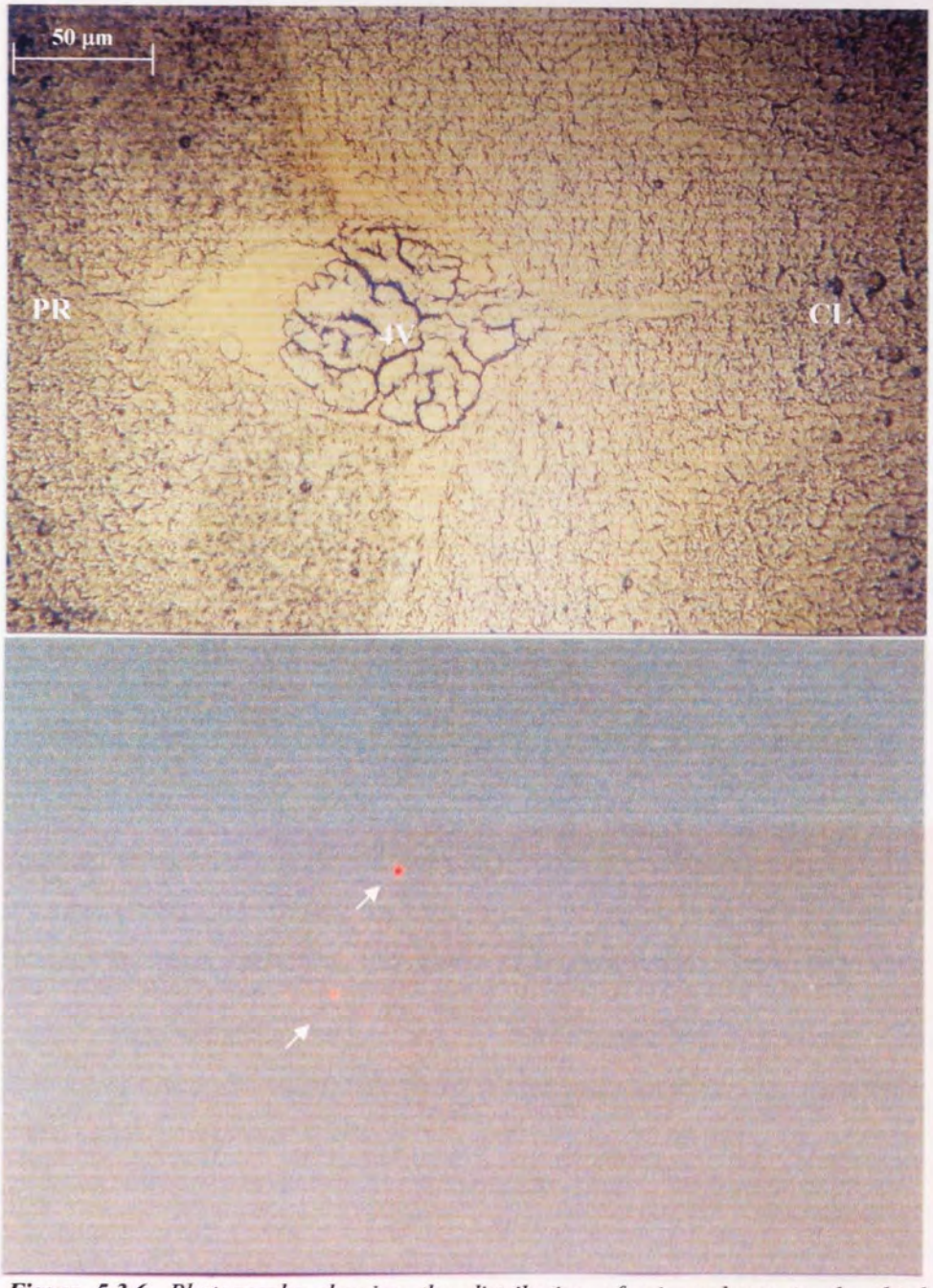

Figure 5.3.6. *Photographs showing the distribution of microspheres in the third ventricles with the normal light photograph at the top and fluorescence photograph at the bottom. Magnification 100×. Coronal section taken at bregma –0.92mm. CL = Cerebellar lobules, PR = pontine region, arrows show FITC microspheres.*

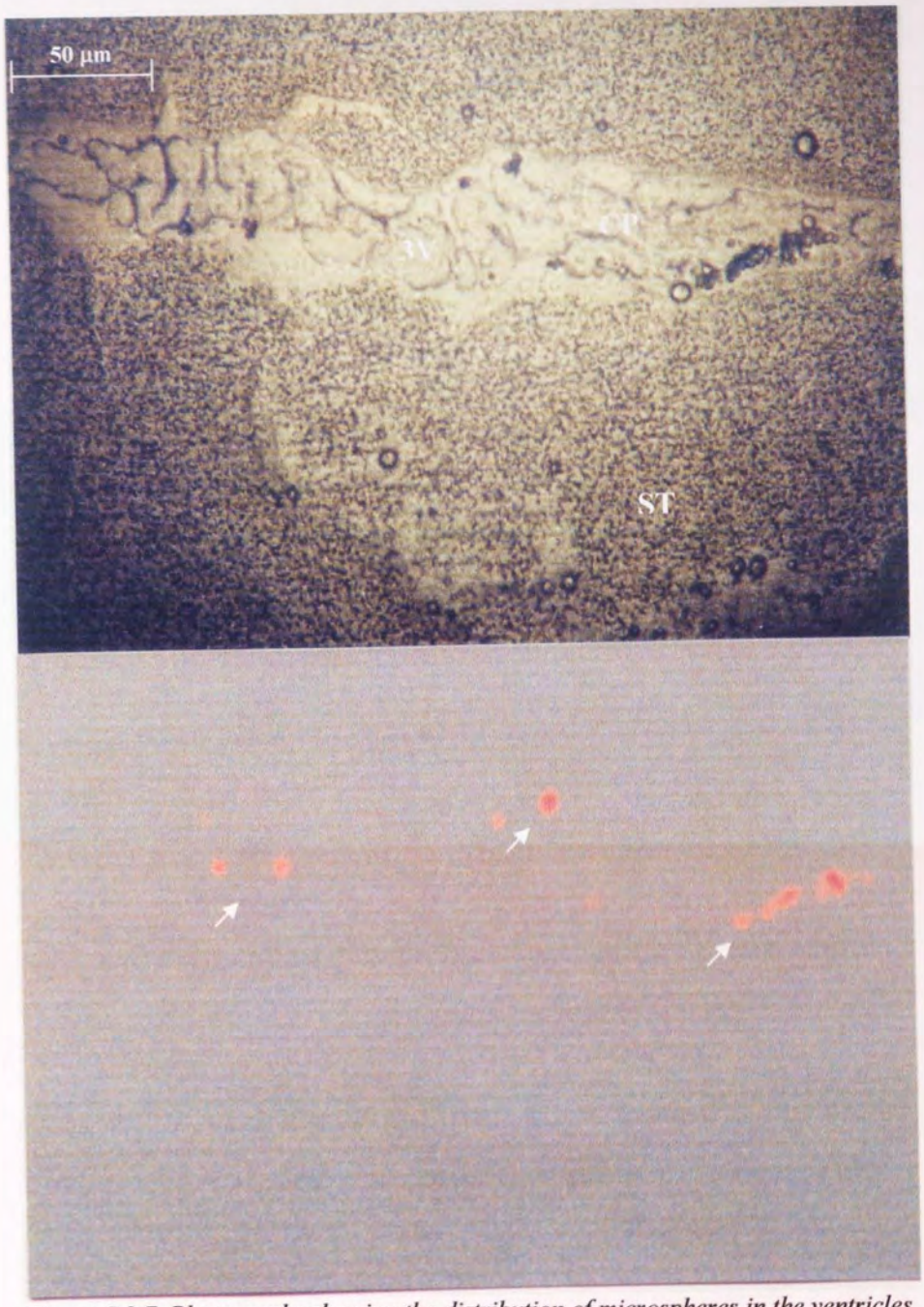

Figure 5.3.7. *Photographs showing the distribution of microspheres in the ventricles with the normal light photograph at the top and fluorescence photograph at the bottom. Magnification 100×. Coronal section taken at bregma –1.31. CP = choroid plexus, 3V = third ventricle, ST = striatum, arrows show FITC microspheres.*

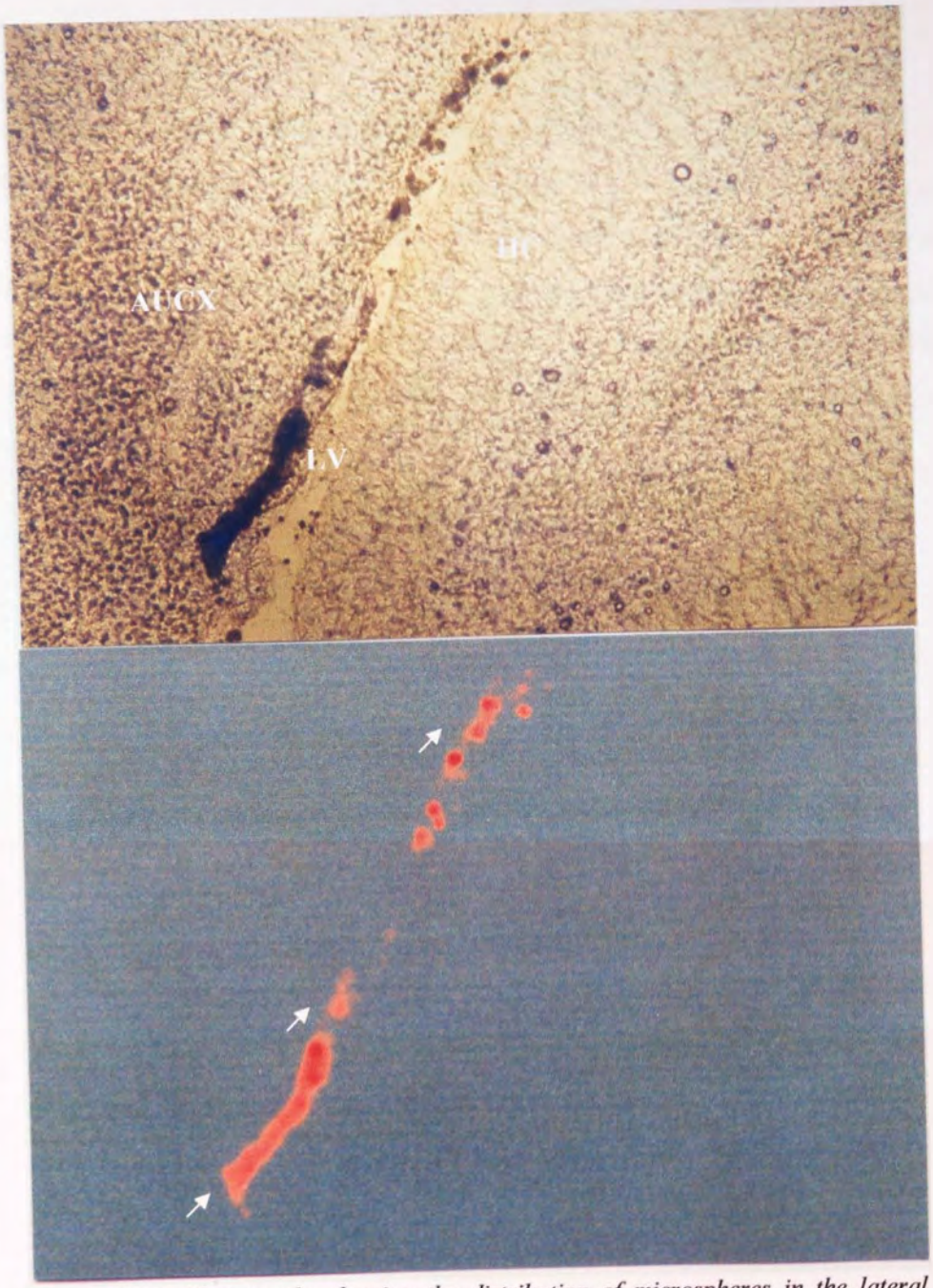

Figure 5.3.8. *Photographs showing the distribution of microspheres in the lateral ventricles with the normal light photograph at the top and fluorescence photograph at the bottom. Magnification 40×. Coronal section taken at bregma –0.280mm. LV = lateral ventricle, HC = hippocampus, AUCX, auditory cortex, arrows show FITC microspheres.*

5.6.2. Distribution of polymer entrapped ribozyme 24 hours post *Intra-Parenchymal* injection

In this section an interesting observation of microsphere depostion in the parenchyma of the brain is presented. During the experimental procedure to investigate the distribution and fate of microspheres 5 days post ICV injection, microspheres were not injected to the ventricles accidently and were instead deposited in the motor cortex region. Preparation of coronal sections after sacrificing of the animal and observation under the microscope (figure 5.4) showed that microspheres remained at the site of deposition and did not spread in the parenchyma.

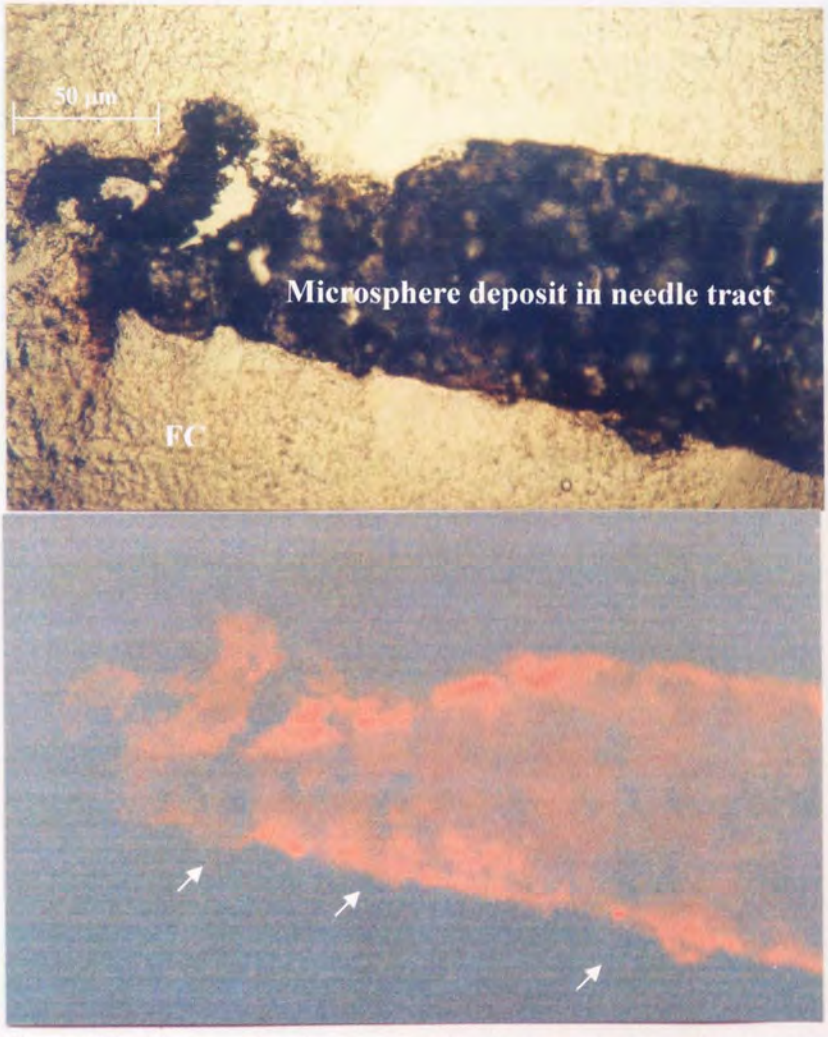

Figure 5.4. *Photographs showing the distribution of microspheres in the ventricles with the normal light photograph at the top and fluorescence photograph at the bottom. Magnification 40×. Coronal section taken at bregma –0.40mm. FC = frontal cortex, arrows show FITC microsphere.*

This was no sign of tissue damage or inflammation around the deposition site apart from the depostion site itself where microspheres displaced nervous tissue.

5.7. Effect of particle size on distribution after 24 hours

Results from previous sections demonstrate that the ribozyme loaded microspheres are mainly located in the CSF ventricular system, mostly in lateral ventricles and do not diffuse to the parechyma of brain. It was hypothesized that this entrapment of microspheres in ventricles is due to their large size range (≈ 5 μm), which renders them unable to pass through the lining of the ventricles. In order to determine whether microsphere size range can be an important factor in CNS distribution of microspheres, particles of two fixed size ranges 2.5 and 0.5 μm were injected in the rat brain ICV and their distribution evaluated by fluorescent localisation.

5.7.1. Distribution of large particles 24-hour post ICV injection in the rat brain

Latex particles of size range 2.5μm (±0.1μm) were injected ICV instead of fluorescently labelled PLGA microspheres because of a sharp, narrow size range and greater fluoresence visibility obtained with these particles. FITC-labelled latex particles were washed with ddH_2O three times to remove solvents before administration. Post-injection behavioural and toxicological assessments were made to determine the safety aspect of latex particles. Coronal sections of the entire brain were prepared and observed for fluoresence and photographs were taken of areas which showed visible fluoresence.

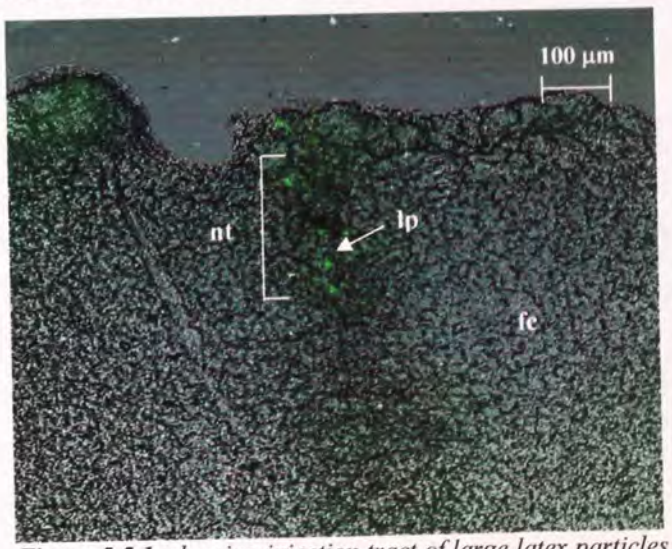

Figure 5.5.1*. showing injection tract of large latex particles at the motor cortex. Bregma –1.25; magnification × 40. fc = frontal cortex, lp = latex particles, nt = needle tract.*

Photographs were taken with axiocam digital camera and Carl Zeiss imaging system. This imaging system allowed light and UV photographs to be stacked above each other. Photographs in this and the next section show both normal and UV pictures stacked above each other allowing greater detail of the sections and visibility of fluoresence together. Figure 5.5.1 shows the injection tract lined with latex particles with the area of motor cortex in the photograph.

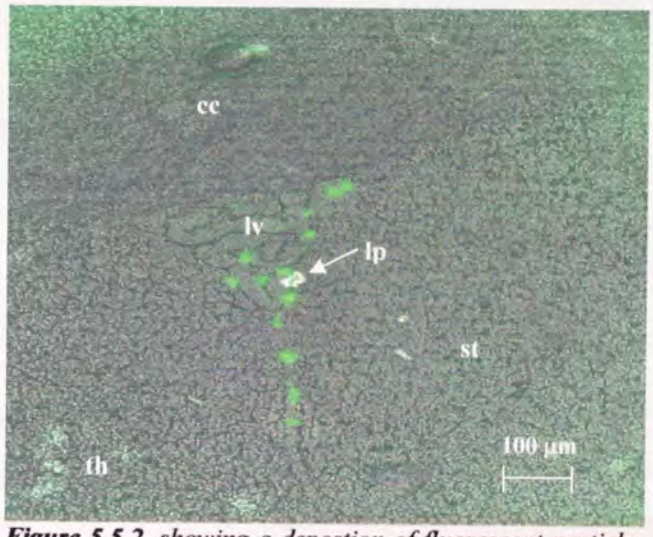

***Figure 5.5.2**. showing a depostion of fluorescent particles in the lateral ventricle 24 hour post ICV injection. Bregma –1.25mm; magnification × 40. lp = latex particles, lv = lateral ventricle, th = thalamus, cc =corpus collusum, st = striatum.*

Figure 5.5.2 shows the presence of latex particles in the lateral ventricle of the brain 24 hours post ICV injection and additionally there was no fluoresence observed in the surrounding areas such as caudate putamen, thalamus and corpus collusum.

This section was further observed with higher magnification (400×) and the fluoresence observed showed that the latex particles remained attached to the ependymal cells of the ventricular lining as shown in Figure 5.5.3.

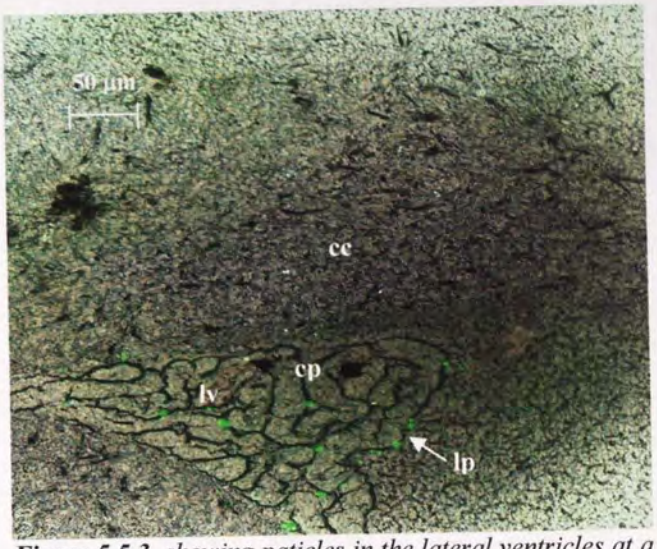

Figure 5.5.3*. showing paticles in the lateral ventricles at a higher magnification × 100. Bregma –1.25mm. lp = latex particles, lv = lateral ventricle, cc =corpus collusum, cp = choroid plexus.*

Figure 5.5.4 shows the distribution of latex particles in the subarachnoid space lining the somatosensory cortex with no fluoresence observed inside the cortical regions.

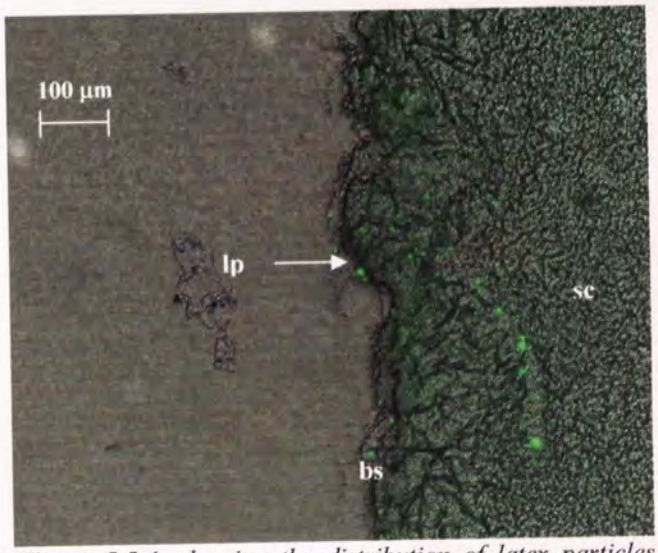

Figure 5.5.4. *showing the distribution of latex particles (lp) at the brain suface (bs) lining the area of somatosensory cortex (sc). Magnification 40×. Bregma – 1.20mm. sc = somatosensory cortex, lp = latex particles, bs = brain surface.*

Further fluorescent particles were observed in the lateral ventricle at bregma –3.45 (figure 5.5.5) and the fourth ventricle near the area of optic chiasma (figure 5.5.6). In all these

ventricular sites there was no sign of fluorescent particles diffusing in to the parenchyma of the brain.

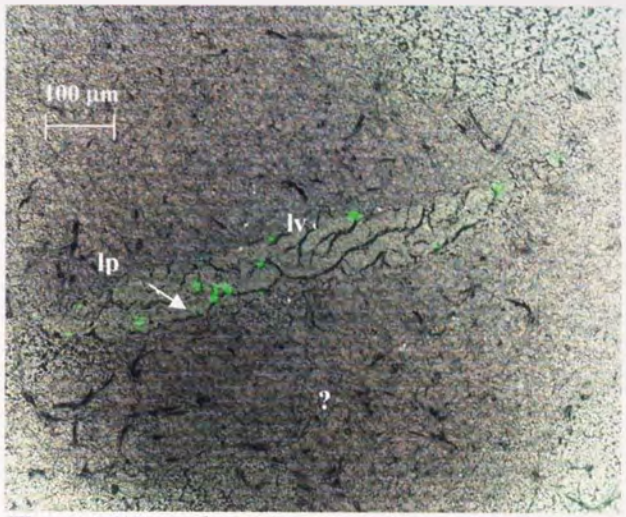

Figure 5.5.5. *A photomicrograph showing the presence of latex particles at the lateral ventricle at bregma – 3.45. Magnification 40×. Lp = latex particles, lv = lateral ventricles.*

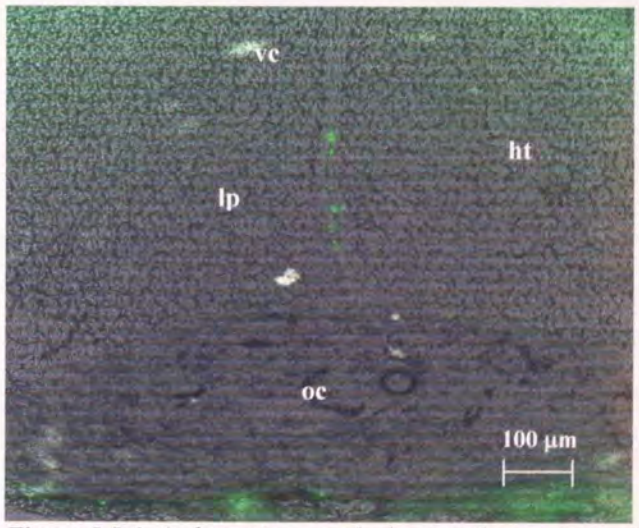

Figure 5.5.6. *A photomicrograph showing the presence of latex particles at the fourth ventricle. Magnification 40×. Bregma –1.20mm. vc = ventricular channel, ht = hypothalamus, oc =optic chiasma, lp = lateral particles.*

5.7.2. Distribution of small particles 24-hour post ICV injection in the rat brain

Investigation of distribution of latex particles of ≈ 2.5μm size range showed that even this size range was incapable of diffusion out of the ventricles in to the parenchyma of the brain. In order to further pursue the effect of particle size on the distribution in the CNS latex particles of the size range 0.5μm were injected ICV and their distribution investigated.

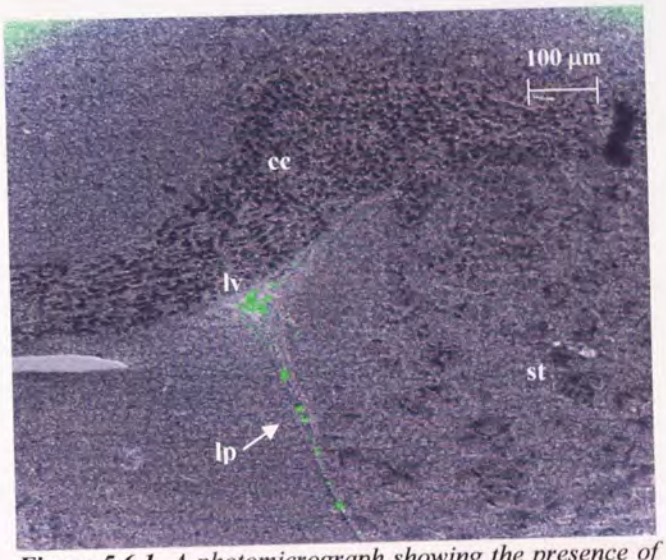

Figure 5.6.1. *A photomicrograph showing the presence of latex particles in the lateral ventricle. Magnification 40×. Bregma –1.20. lv = lateral ventricle, st = striatum, lp = lateral particles, cc = corpus collusum.*

Figure 5.6.1 shows a coronal section of the rat brain at bregma –1.20 with the area of lateral ventricle visible in the photograph. This section shows that latex particles remain located in the ventricles 24 hours post ICV injection and do not seem to be permeating to the parenchyma of the brain. This was further confirmed with an observation of the ventricles at a higher magnification of 100× as shown in figure 5.6.2 which shows that particles remianed attached to choroid plexus and even after 24 hours were unable to penetrate the parenchyma of the brain. From the remaining figures 5.6.3 to 5.6.6 it seems that the distribution of the small latex particles, generally, exhibited a similar distribution in the ventricular system as the large particles.

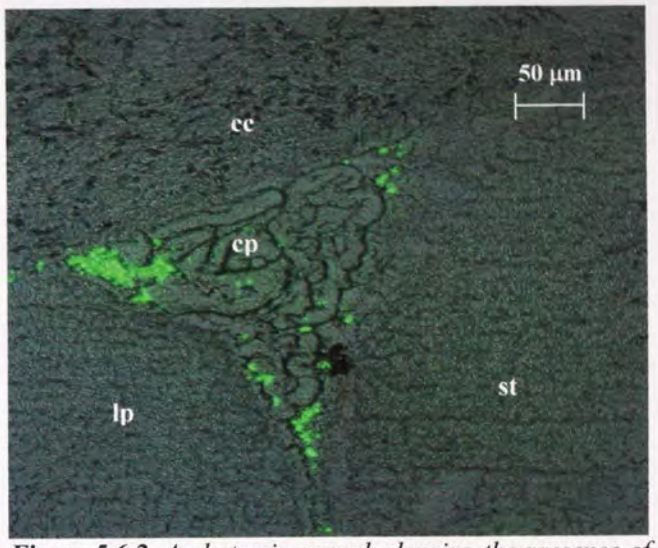

Figure 5.6.2. *A photomicrograph showing the presence of latex particles in the lateral ventricle. Magnification 100×. Bregma –1.20. cc = corpus collusum, st = striatum, lp = latex particles, cp = choroid plexus.*

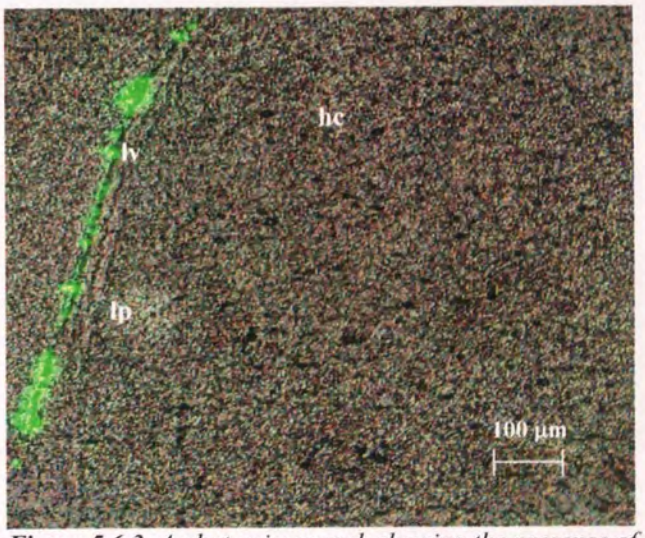

Figure 5.6.3. *A photomicrograph showing the presence of latex particles in the lateral ventricle. Magnification 40×. Bregma –1.20. Lp = latex particles, hc = hippocampus, lateral ventricle.*

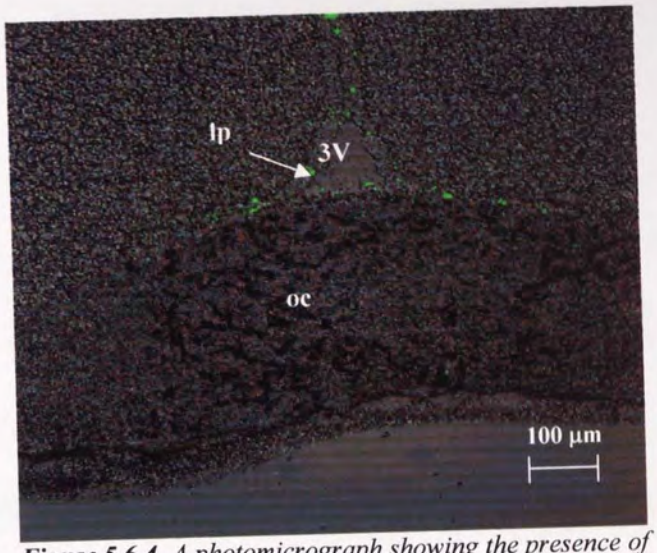

Figure 5.6.4. *A photomicrograph showing the presence of latex particles in the third ventricle. Magnification 40×. Bregma –1.20. oc = optic chiasma, 3V = third ventricle, lp = latex particles.*

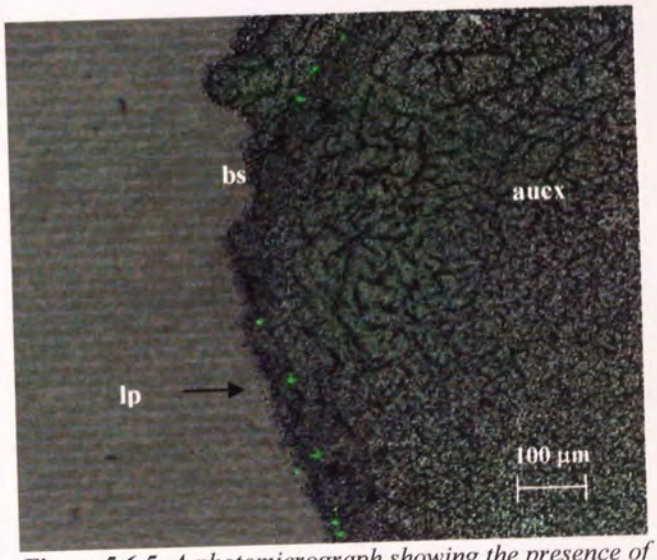

Figure 5.6.5. *A photomicrograph showing the presence of latex particles at the sub-arachnoid space. Magnification 40×. Bregma –1.20. lp = latex particles, aucx = auditory cortex, bs = brain surface.*

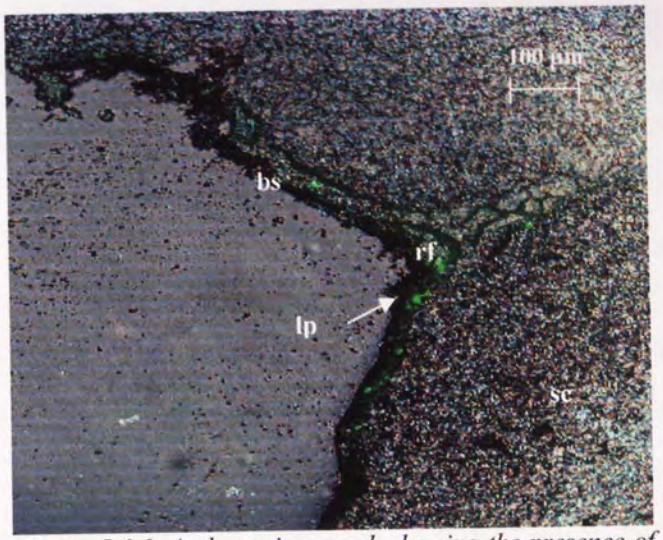

Figure 5.6.6. *A photomicrograph showing the presence of latex particles (lp) near the rhinal fissure (rf) at the brain surface (bs). Magnification 40×. Bregma –1.20. rf = rhinal fissure, lp = latex particles, bs = brain surface, sc = somatosensory cortex.*

5.8. Concluding remarks

In this chapter it was aimed to investigate the potential of biodegradable polymer PLGA microspheres for the CNS delivery of ribozymes.

In order to achieve this aim preliminary investigations were carried out to evaluate the stability and distribution of free ribozyme after ICV injection. The stability investigation of free ribozyme in the CNS demonstrated that most of the free ribozyme had degraded in the CNS after 24 hours. Assessment of distribution of free ribozyme after ICV injection showed no visible distribution of ribozyme in the parenchyma of the cell, which could be explained by the fact that the ribozyme was rapidly cleared by the ventricular system and therefore allowing no riboyzme penetration in to the parenchyma of the brain. These observations of rapid clearance and degradation of free ribozyme underscores the need for a delivery system providing protection from degradation and sustained release of ribozyme. In order to achieve this desired stability and sustained delivery of ribozymes, microsphere delivery systems prepared from biodegradable polymer PLGA incorporating riboyzme were injected ICV to evaluate their *in vivo* CNS delivery potential.

Initially, the toxicological profile of ribozyme containing PLGA microspheres was investigated. This toxicological profiling is important to establish the suitability of biodegradable polymers as an implantable delivery system to the brain after ICV administration. Histological evaluation indicated that there was no toxicity as evidenced by an observation of no local tissue damage or gliosis or any sign of behavioural disturbance in rats. Following these results the distribution of fluorescently labelled ribozyme molecules entrapped in microspheres was investigated 24 hour post ICV injection. The distribution of fluoresence indicated that microspheres of the size range $\approx$ 5μm largely remained entrapped in the ventricular system and did not permeate the parenchyma of the brain. The sites in the brain where microspheres were observed included lateral ventricles, third ventricle, fourth ventricle and sub-arachnoid space. These results indicate that the despite rapid turnover of CSF in the ventricular system the microsphere loaded ribozymes remain in the ventricular system for 24 hours in comparison to free ribozyme which are almost completely removed from the CSF in 24 hours. In an additional result in which microspheres were implanted by mistake in the motor cortex area of the brain for 5 days post ICV injection it was observed

that microspheres remain at the site of injection with no movement of particles to other areas of the brain.

In order to characterize the effect of size of particles on passage through the fenestrated linings of the ventricular system walls and into the parenchyma of CNS, latex particles of two progressively small sizes were studied. It was thought that small particles will be able to pass through the fenestrated ependymal cell lined ventricle walls allowing greated distribution of small particles in the substance of the brain. However, results showed that both particle sizes showed similar distribution profiles in the CNS after ICV injection as the large PLGA microspheres. Due to time constraints, planned experiments to further characterise the uptake of fluorescently labelled ribozymes in the glial and neuronal cells were not carried out.

These results show that micropheres containing ribozymes are capable of and toxicologically safe for stereo-taxic injection in the cerebral ventricles. These microspheres remain at the site of injection without causing any local tissue reaction for 24 hours if injected in the parenchyma of the brain. Injection of microspheres in the lateral ventricles results in localisation of microspheres in the ventricular system for 24 hours. Reduction in particle size distribution form 5μm to 2.5μm and 0.5μm does not result in any visible penetration in the substance of the brain. These results show that microspheres can be effective delivery systems for site-specific delivery of ribozyme in the brain.

CHAPTER SIX

6.0. GENERAL DISCUSSION

Since their discovery in early eighties as naturally occuring RNA molecules with catalytic properties, ribozymes have been extensively investigated as biological tools and potential therapeutic agents but their full realisation as a clinical drug still remains to be achieved. From the published studies it is evident that for successul application of exogenously administered ribozymes in the clinic it is important that certain key issues in the delivery of ribozymes, namely; selective delivery to the target organ and site, uptake by specific cells, transportation to the required sub-cellular compartments and finally hybridisation with the target mRNA for cleavage, are further optimised.

It was the aim of this thesis to characterise and compare the cellular association of ribozyme in glial and neuronal cells *in vivo* and *in vitro*, as this information is important for the optimisation of the cellular delivery of ribozymes and their ultimate use as novel anti-tumour agents for CNS applications. It was further aimed to determine the effect of PLGA polymer microspheres entrapping ribozymes, on the stability and cellular association of ribozymes in these cells with a view to develop a sustained release delivery system for CNS administration of riboyzmes. The ribozyme investigated in this study was targeted to the epidermal growth factor receptor mRNA, as over-expression of EGFR along with a number of other genes has been implicated as a causative factor in the progression of brain tumours such as glioblastomas and neuroblastomas. It is thought that the ribozyme strategy with its high specificity in gene inhibition will provide an effective treatment for brain tumours by down-regulating the expression of tumour causing genes.

The hammerhead ribozyme investigated in this study was administered exogenously as this delivery strategy is more amenable to utilization of chemically synthesized ribozymes and offers many advantages such as repeated administration, titration of the dose to balance risk-benefit ratio, reversibility of treatment and the facility to discontinue treatment if adverse effects become intolerable or severe. However, a major consideration in the exogenous delivery strategy is the evaluation and optimisation of ribozyme stability in biological media

as ribozymes in their unmodified form are highly susceptible to degradation by intra and extra-cellular nucleases as shown in section 1.4.1.1, leading to total loss of ribozyme activity. Therefore it is necessary that steps are taken to enhance the stability of ribozyme by increasing their resistance to nucleases by chemical modifications or by entrapping the ribozyme molecules in a delivery system.

The ribozyme characterised in this thesis has several site-specific chemical modifications involving protecting the 2'-OH groups on pyrimidine bases, terminal ends of the ribozyme and internucleotide bonds to enhance the biological stability (see section 1.6) as these sites are most susceptible to degradation by nucleases (Peyman *et al.*, 1997). Similar modifications have been reported to significantly enhance stability while preserving catalytic activity (Beigelman *et al.*, 1995b; Shimayama *et al.*, 1993). In order to characterise the stability of this 'chimeric' ribozyme molecule evaluated in this experimental work, it was incubated in a range of biological media. In serum medium it was found to be stable for up to 1 hour after which the ribozyme degraded progressively. This degradation of ribozyme structure in serum medium highlights the difficulty experienced with exogenous delivery of nucleic acid molecules as structural integrity is the basis for efficacy. However, ribozyme stability up to 1 hour is a significant development in stability as an all RNA ribozyme molecule degrades within less than a minute (Jarvis *et al.*, 1996).

In contrast, ribozyme remained stable up to 24 hours in serum free medium due to the preclusion of serum from this medium resulting in negligible nuclease activity. This medium was then selected as the incubation medium for use during cellular association experiments, despite the fact that it does not represent the ultimate clinical application, because obtaining information regarding the cellular association characteristics is a key component for the investigation of the cellular delivery of ribozyme. To further investigate the influence of cellular monolayers on the stability of ribozyme it was incubated with cellular monolayers of each cell line and ascertained that up to 6 hours most of the ribozyme was structurally intact which validates the time frame of the association studies.

The ultimate aim in researching ribozyme delivery is to develop ribozyme based therapies for the treatment of brain tumours such as glioblastoma multiforme for which there are no currently satisfactory treatment strategies. It was for this reason cultured glial and neuronal cells were used as a model to investigate the cellular delivery of ribozyme in this thesis. A

parallel interest was to investigate if there was any difference in the association of ribozyme between the glial and neuronal cells of both species as previous work in the laboratory had reported differences in the uptake of oligonucleotides (*in vivo*) (Khan *et al.*, 2000) and ribozymes (*ex vivo*) in different cells (Fell *et al.*, 1997).

In order to characterise the nature and extent of cellular association of ribozymes in both glial and neuronal cells of each species, rat and human, a series of cellular association experiments were carried out. Time course studies indicated that the association of ribozyme increased with time in all cells and reached a plateau phase after 6 hours with the maximum association for rat neuronal cells being 0.44% (GT1) and human neuronal being 0.51% (SY5Y) and for glial cells it was 0.62% (C6, rat) and 0.76% (U87, human). Generally, there was no distinct difference in the overall pattern of association with modest rise in association for the first three hours and with highest association observed between the 3 to 4 hour time points followed by a plateau phase after the 4^{th} hour suggesting saturation in association. Further time points were not investigated as the ribzoyme structure was stable up to 6 hours on the monolayers. These results are consistent with time course uptake reported by (Fell *et al.*, 1997) for ribozyme and with DNA oligonucleotide uptake reported by (Levis *et al.*, 1995). In terms of the extent of ribozyme association, there was no significant difference between the glial and neuronal cells of both, rat and human, species. This is in contrast to reports by (Fell *et al.*, 1997) in which uptake of ribozyme has been found to be cell type specific, with a 3-fold difference observed between the cells of different tissues of non-CNS origin.

The absence of any difference across the cell types and species was consistently observed during the course of mechanistic studies as well. To date there is no study in published literature which compares and evaluates the differences in association of ribozyme in CNS cells only. In contrast there are several studies which have evaluated the uptake of antisense oligonucleotides in CNS cells. These studies show that *in vivo* neuronal cells take up greater oligonucleotides in comparison to glial cells (Khan *et al.*, 2000; Sommer *et al.*, 1996; Ogawa *et al.*, 1995). Due to time constraints it was not possible to investigate the cellular association of ribozyme *in vivo* in order to make an *in vivo* and *in vitro* comparison of cellular association of ribozyme as this could provide useful information for investigating and evaluating various delivery strategies to optimise cellular delivery of ribozyme.

In order to further investigate the nature of the ribozyme association mechanism by cells, mechanistic studies were carried out. Investigation of cellular association of ribozyme at two different temperatures, 37°C and 4°C, indicated that association was an active process, which was temperature dependent and hence required energy to occur. This was confirmed by carrying out association studies in the presence of of metabolic inhibitors which showed that depletion of metabolic energy significantly reduces association. However, a small but noticeable cellular association was observed at the low temperature and also after depletion of metabolic energy which suggested the association mechanism included a non-energy dependent component as well. In an attempt to further characterise the nature of the cellular association process as to whether it was fluid phase mediated or membrane surface carrier molecule mediated the extent of cellular pinocytosis (fluid phase uptake) was determined by studying the association of the fluid phase marker mannitol over a time course. In all cell lines, neuronal and glial, mannitol had no significant uptake indicating that the cells under investigation had negligible pinocytotic activity. From this it is inferred that ribozyme association into cells could not be due to pinocytosis.

To further elucidate the nature of the association mechanism, the specificity of association was investigated by self competition studies. Self-competition studies with increasing concentration of unlabelled ribozyme showed that the association of ribozyme was reduced with higher concentration of unlabelled ribozyme. This indicated that there was a cell surface molecule, which binds to the ribozyme and mediates the association of ribozyme. In order to investigate whether this ribozyme-binding surface molecule was a lipid or protein, post incubation trypsin washings were carried out. This assessment showed that the majority of ribozyme was bound to trypsin sensitive proteins, which mediate the association of ribozyme in cells. The specificity of ribozyme association with this cell surface trypsin-sensitive protein molecule was further investigated by co-incubation with nucleic and non-nucleic polyanions. All of these polyanionic molecules reduced the cellular association of ribozyme reflecting the fact that ribozyme shares the association mechanism with other polyanionic molecules. The association of ribozyme was increased by reduction of pH suggesting that ionic interactions play a significant role in the hybridisation of ribozyme with surface binding proteins. Similar increased uptake in hepatoblastoma cell of oligonucleotide was also reported by (Goodarzi *et al.*, 1991) and it was suggested that this is due to the presence of binding proteins on the cell surface which exhibit greater binding at acidic conditions.

Analysis of the disassociation profile of the associated ribozyme was carried out to obtain information regarding the post-association sub-cellular distribution of ribozyme. The results showed that all cells generally exhibited a biphasic pattern of ribozyme disassociation representing a two compartment sub-cellular distribution of ribozyme in the cytoplasm. The first compartment which accounts for the early rapid release of the ribozyme constitute the early primary endosomes situated close to the surface or ribozyme bound to the cell surface. The second slower disassociation results from the deeper compartments of the cytoplasm such as medium to late endosomes or lysosomes or as yet unidentified sites with cytoplasm.

In order to visualize the sub-cellular distribution and fate of ribozyme post-association fluorescent localisation studies were carried out. The results showed that the associated ribozyme displayed a characteristic punctate distribution pattern indicating that ribozyme had been sequestered in sub-cellular vesicles. Punctate patterns of distribution have also been observed in studies with oligodeoxynucleotides (Wagner, 1994; Agrawal *et al.*, 2003), and this was considered to be indicative of localisation within endosomal or lysosomal vesicles (Rojanasakul, 1996).

Finally, ribozyme-binding cell surface proteins which facilitate the association of ribozyme in cells were separated and identified using South-Western blotting for each cell line. The results showed that rat glioblastoma C6 cells had two proteins of the sizes, 65 kDa and 58 kDa, rat neuroblastoma GT1 cells have three proteins with molecular weights of 84, 74 and 58 kDa. Human neuroblastoma cell line SY5Y had proteins of 74 and 58 kDa and the human glioblastoma cell line expressing a single protein of 58 kDa which binds to ribozyme. It is these molecules which mediate the cellular association of ribozyme. As stated in section 3.14 there are several reports of cell surface proteins of different sizes in the literature from studies in different cells.

The results presented in this chapter show that the cellular association of ribozyme was very poor and limited and it may inolve a combination of internalisation mechanisms which are energy dependent such as endocytosis or non-energy dependent passive processes. Some of the results such as energy and temperature dependence are consistent with an endocytic model of ribozyme association by cells in which, a given molecule binds to cell surface proteins which could be receptors or glycoproteins. Clathrin coated pits are formed in cell

membrane around the ribozyme-protein complexes, which are internalised and form early endosomes. These early endosomes could either recycle back to the cell membrane or in due course lead to endosomes, late endosomes and finally lysosomes, which are the final vesicles of the endocytic pathway (Gruenberg, 2001).

In the case of ribozyme endocytosis results in the entrapment of the ribozyme in the endocytic vesicles creating a further obstacle in the delivery of ribozyme to its target site in the cytoplasm or nucleus. This results in reduced bioavailability of ribozyme in the cytosol and therefore to the prevention of ribozyme from carrying out its biological effect. As it is unlikely that ribozyme like oligonucleotides, can leave these endosomal compartments by passive diffusion (Akhtar *et al.*, 1991). The entrapment of the ribozyme in the endocytic vesicles could further lead to either the efflux of the ribozyme from the cell or degradation by nucleases in the harsh acidic environment of the endo-lysosomal vesicles. Endo-lysosomal compartments contain a battery of deoxyribonuclease, ribonuclease, phophatases and pyrophosphatases which together degrade nucleases with $T_{50\%}$ in the range of 30-50 minutes (Hudson *et al.*, 1996b). Loke *et al.*, (1989) and Zhao *et al.*, (1993) have observed similar results of entrapment of most of oligonucleotides in lysosomal-endosomal compartments and it was concluded (Shoji *et al.*, 1991) that endosome to cytoplasm transfer is the critical limiting step for the pharmacological actions of oligonucleic acids. The fact that oligonucleotides given exogenously exhibit biological activities suggests some molecules escape from these compartments at some point during the endosome to lysosome transport and reach the target sites. However, there is no information available in the literature elucidating the mechanism and extent of this release.

From the discussion so far it is evident that there are three crucial aspects namely, ribozyme stability in serum medium, limited cellular association and entrapment in endo-lysosomal entrapments, which are hampering the successful application of ribozyme in any model system. The first obstacle namely structural stability of ribozyme in serum medium has been addressed by the partial chemical modifications of the ribozyme investigated in this thesis to a limited extent. Further optimisation of the chemistry to enhance stability will lead to unwanted side effects such as seen with serum resistant oligonucleotides. Oligonucleotides with all phosophorothioated linkages lead to non-sequence specific binding to proteins (Stein, 1996). However, as an alternative, utilisation of a pharmaceutical delivery system

which not only protects the ribonucleic acid molecule but also helps in overcoming the remaining two obstacles will be useful.

In this regard several strategies and systems have been investigated which include microinjection, permeabilization using pore-forming agents such as *streptolysin-O*, anionic peptides, electroporation and membrane translocating peptides such as *Tat*, amphipathic model peptides and signal peptides with varying degrees of success (Dokka and Rojanasakul, 2000). Microencapsulation is another strategy which has successfully incorporated nucleic acid molecules in biodegradable polymer microspheres for enhancing the cellular delivery of oligonucleotides (Khan *et al.*, 2000). In order to overcome the above mentioned limitations and obstacles in the cellular delivery of ribozyme it was aimed to microencapsulate ribozyme in PLGA microspheres. PLGA is a copolymer of lactic acid and glycolic acid and is one of the most widely investigated for a range of applications as described in section 1.5.1. Microspheres are porous particles with spherical shape in the micron size range and are emerging as promising delivery systems for site-specific administration of drug molecules.

Information regarding physical characteristics such as microsphere size, size distribution, shape, porosity, loading, encapsulation efficiency is important as these characteristics influence release patterns (Dunne *et al.* 2000). Knowledge of cellular association characteristics is also necessary to deploy microspheres to provide an optimum delivery of drugs in terms of dose and duration to the required site to ensure effective drug concentration for a robust therapeutic effect while at the same time minimising side-effects. These characteristics in turn are greatly dependent on the method selected for formulating microspheres. To date there are several methods available for microencapsulation of drugs in microspheres which include single emulsion process, double emulsion process, coacervation and spray drying (Jain, 2000). From these methods the double emulsion method has been the most widely used technique for manufacturing microspheres which was first reported by (Ogawa, *et al.* 1988).

Ribozyme investigated in this thesis was successfully microencapsulated in to PLGA microsheres and were characterised for physical and cellular association characteristics. Ribozyme was entrapped in microspheres formulated from three different co-polymer ratios, 90:10, 80:20 and 50:50, of the biodegradable polymer PLGA using the double emulsion method. Microspheres of two size ranges (0-5μm and 10-20μm) were prepared by

manipulation of the stirring rates during the primary and secondary emulsion preparation phase. The rationale for investigating three different copolymer ratios and microsphere size range was to select a suitable formulation which not only protects the ribozyme from nucleolytic degradation but also to achieve a sustained release of ribozyme for a sufficiently long period of time to cause down-regulation of the target protein. With all ratios microspheres of high yields were successfully formulated with smaller microspheres exhibiting relatively higher yield than larger microspheres. In contrast the percent encapsulation of ribozyme in the formulation ranged from 34% to 48% for small microspheres and 50% to 57% for large microspheres. This differential in encapsulation efficiency between small and large size range was further observed in the values of loading of ribozyme per mg of microspheres when higher values were observed with large size range microspheres in comparison to small size range microspheres. Similar differences in encapsulation and drug loading between the small and large size range microspheres have also been obeserved in cisplatin loaded PLGA microspheres (Garcia-Contreras *et al.*, 1997).

Scanning electron microscopy showed that microspheres were successfully formulated and had a smooth surface and a compact spherical shape and no collapsed or damaged microspheres were observed. Finally size distribution analysis confirmed the size range of microspheres into two size ranges of 1-5μm and 10-20μm. After successful formulation of microspheres of two size ranges with three different co-polymers of PLGA, the release studies of these different microsphere delivery systems were carried out. Data regarding the kinetics of drug release from microspheres is a critical factor that is directly related to drug availability at the target tissue and hence its therapeutic effect. Release studies evaluated the release of ribozyme from microspheres over a time course with a significant difference in the release profiles of ribozyme of three co-polymer ratios. The 50:50 and 80:20 co-polymer ratios exhibited a triphasic release profile and the remaining 90:10 co-polymer ratio exhibited a biphasic release profile. Within each co-polymer ratio there was also a significant difference between the large and small microspheres with small microspheres producing a 4.3-fold greater ribozyme release at the burst effect than the large microspheres for the 90:10 and 50:50 co-polymer ratios and 1.6-fold difference observed with 80:20 ratio.

Analysis of release patterns showed that in the 90:10 ratio the only significant release of ribozyme was from the microsphere surface which constituted the burst effect after which

there was no significant release. This is due to the fact that the 90:10 ratio due to its high lactide content is more crystalline and is resistant to hydration and degradation which results in entrapment of ribozyme within the polymer matrix. This co-polymer ratio can be used for delivering drug molecules for extended periods of time in the range of 6 to 12 months. The 80:20 ratio in turn displayed triphasic profile with different patterns observed for small and large microspheres. The release incorporated burst effect (release from surface), sustained release (resulting from co-polymer hydration and erosion) and for the small microspheres bulk degradation phase. Finally the 50:50 co-polymer ratio for both microsphere sizes exhibited a triphasic release profile with release of ribzyme from the polymer surface, erosion and bulk degradation. This co-polymer ratio had the lowest burst effect phase and a steady slow release phase which probably results from release of ribzyme from polymer hydration and erosion. After 21 days for both microsphere sizes there was an increased release of ribozyme from bulk degradation. The 50:50 ratio formulation with small microsphere size range was selected for further experimental work due to its 28 day release profile. The initial low burst effect could potentially provide a loading dose and sustained release phase can provide for maintenance of drug concentration at the target site. Bulk degradation of microspheres after 28 days eliminates the need for removal of polymer after completion of drug release.

Evaluation of the stability of microsphere entrapped ribozyme was carried out to determine whether the fabrication process did not adversely affect the integrity of ribozyme. Stability study results demonstrated that ribozyme remained intact after the fabrication process and moreover incubation of microsphere-entrapped ribozyme in serum medium protected the ribozyme from degradation by nucleases.

Characterisation of microspheres, in terms of size, shape, yield, loading values, stability and release profiles, was followed by investigation of ribozyme cellular association properties. Cellular association of the selected 50:50 co-polymer ratio small size range microspheres was studied in cultured glial and neuronal cells over a time course. Results from this study showed that cellular association of microsphere-entrapped ribozyme was dependent on time and had a 5-fold higher cellular association than the free ribozyme with no significant difference among the cell lines studied. Similar increases in the uptake of microsphere entrapped oligonucleotides have been reported by Smith, (2000) and Khan, (1999). This enhanced association observed with microspheres highlighted the potential of microsphere

mediated delivery and warranted further studies to understand the mechanism of microsphere uptake in cells. Further characterisation of the cellular association revealed that the cellular association was a temperature and energy dependent process indicating that it was an active process as the free ribozyme. However, in contrast to free ribozyme microsphere association was independent of the pH of the incubation medium indicating that microsphere is not facilitated by cell surface associated proteins as found with free ribozymes. Due to limitations in time it was not possible to further confirm this with trypsin washings and South-Western blots. The enhanced association seen with microspheres probably results from the altered pharmacokinetics due to increased and sustained release of ribozyme from microspheres acting as a depot in the vicinity of cells. These results demonstrate that PLGA polymer microsphere constitute a robust deliver system, which not only protects the ribozyme from degradation but also enhances the cellular delivery of ribozymes by releasing the ribozyme in a sustained manner.

In recent years nucleic acid molecules have been increasingly used in the CNS as biological tools for understanding gene expression in relation to downstream behavioural consequences, as rapid screens in drug target validation and as potential therapeutic agents (for review see Chiasson, 1996; Wahlestedt, 1994). Despite successfull demonstration of nucleic acid based molecules such as antisense and ribozymes *in vitro* and *in vivo* there are no universal guidelines for their effective application as gene blockers in the CNS. Moreover, the fate of nucleic acid molecules in nervous tissue as well as their mechanism of action are still far from clear, with some studies reporting side-effects and lack of efficacy. This is due to the fact that the CNS presents its own unique challenges with regard to application of this epigenetic technology to the treatment of CNS diseases due to the presence of the biomechanical barrier, the BBB, and the absence of adequate systems for the delivering macromolecules to the brain.

Ribozymes and antisense oligonucleotides have very poor penetration across the BBB as evidenced by a study on *in vivo* pharmacokinetics which showed that only <0.01%/cm^3 tissue of a systemically injected dose of a phosphorothioate antisense oligonucleotide reached the brain where its residence time was as short as 60 minutes (Tavitian *et al.*, 1998). Due to this poor penetration into the CNS shown by large polyanionic molecules after systemic administration, regional therapeutic strategies are particularly becoming an attractive option for this organ system. These strategies include direct intraparenchymal or

intracerebroventricular injections. In the case of direct injection into the ventricles the CSF space provides a practical and physiologically well-defined compartment in which to systemically examine novel drug actions *in vivo*.

As stated earlier the ultimate aim of our research is to apply ribozyme technology to down-regulate oncogenes such as EGFR for the treatment of CNS malignant diseases. Localised delivery strategies such as ICV injection have been applied to assess and investigate the CNS delivery of ribozymes. Results presented in chapter five demonstrate that ICV injections of free and polymer entrapped ribozymes did not have any toxic effects on the CNS tissue as shown by post-injection histological assessments. Fluorescent localisation studies showed that there was no visible fluorescence in the ventricle or surrounding tissue after 24 hours. This could be attributed to either the degradation of free ribozyme in the CNS or to rapid removal of ribozyme from the ventricular system by CSF circulation. This necessitated the use of polymer microspheres from biodegradable PLGA polymer to achieve a stable and sustained delivery of ribozyme in the CNS. Sustained drug release in the central nervous system by the means of implantable polymeric devices has been developed over recent years. The first polymer devices studied were macroscopic implants needing open surgery for implantation, however, newer microencapsulation methods allow the formation of microspheres that can be implanted into the brain by stereotaxy (Camarta *et al.*, 1992), (Howard *et al.*, 1989), (McRae-Deguerce *et al.*, 1988) and (Menei *et al.*, 1993). This stereotaxical method has the additional advantage of multiple and repeated implantations into the brain under local anaesthesia.

The distribution of fluorescently labelled ribozyme molecules entrapped in microspheres was investigated 24 hour post ICV injection. The distribution of fluoresence indicated that microspheres of the size range $\approx$ 5μm largely remained entrapped in the ventricular system and did not permeate the parenchyma of the brain. The sites in the brain where microspheres were observed included lateral ventricles, third ventricle, fourth ventricle and sub-arachnoid space. These results indicate that the despite rapid turnover of CSF in the ventricular system the microsphere loaded ribozymes remain in the ventricular system for 24 hours in comparison to free ribozyme which are almost completely removed from the CSF in 24 hours. In an additional result in which microspheres were implanted by mistake in the motor cortex area fo the brain for 5 days post ICV injection it was observed that microspheres

remain at the site of injection with no movement of particles to other areas of the brain. Similar results have been observed by Liphardt *et al.*, (2001); Smith, (2000) who have reported presence of microspheres at site of injection up to 2 days and also by Khan, (1999) who observed presence of ODN loaded microspheres present in the neostriatum 2 days after the injection.

In order to characterize the effect of size of particles on passage through the fenestrated linings of the ventricular system walls and in to the parenchyma of CNS, latex particles of two progressively small sizes were studied. It was thought that small particles will be able to pass through the fenestrated ependymal cell lined ventricle walls allowing greated distribution of small particles in the substance of the brain. However, results showed that both particle sizes showed similar distribution profiles in the CNS after ICV injection as the large PLGA microspheres. Due to time constraints, planned experiments to further characterise the association of fluorescently labelled ribozymes in the glial and neuronal cells were not carried out.

These results show that micropheres containing ribozymes are capable of and toxicologically safe for stereo-taxic injection in the cerebral ventricles. These microspheres remain at the site of injection without causing any local tissue reaction for 24 hours if injected in the parenchyma of the brain. An ICV injection of microspheres results in localisation of microspheres in the ventricular system for 24 hours. Reduction in particle size distribution form 5μm to 2.5μm and 0.5μm does not result in any visible penetration in the substance of the brain. These results show that microspheres can be developed into effective delivery systems for site-specific delivery of ribozyme in the brain.

SUGGESTIONS FOR FURTHER WORK

- To carry out *in vivo* subcellular distribution studies after ICV injection to determine the extent of free and polymer entrapped microspheres uptake in both glial and neuronal cells in the rat species.

- To carry out efficacy studies using western blotting to determine the extent of EGFr down-regulation and its effect on tumour growth.

- To formulate microspheres with size distribution less than 0.5μm to investigate whether this would allow passage of microspheres through the ependymal lining of the ventricles to achieve greater distribution in the brain parenchyma.

- To carry out south-western blotts with microspheres to determine whether microspheres bind to any cell surface proteins.

REFERENCE LIST

1. RPI (2003) Clinical trial of Angiozyme™ ribozyme. (www.rpi.com/angiozyme).

2. RPI (2003) Clinical trial of Heptazyme™ ribozyme. (www.rpi.com/antihcv).

3. RPI (2003) Clinical trial of Herzyme™ ribozyme. (www.rpi.com/herzyme).

4. Agrawal,S., Sarin,P.S., Zamecnik,M., and Zamecnik,P. (2003) Cellular uptake and anti-HIV activity of oligonucleotides and their analogs. In Erickson,R.P. and Izant,J.G. (eds.) *Gene regulation. Biology of antisense RNA and DNA*. Raven Press Ltd, New York, USA.

5. Akhtar,S., Basu,S., Wickstrom,E., and Juliano,R.L. (1991) Interactions of antisense DNA oligonucleotide analogs with phopholipid membranes (liposomes). *Nucleic Acids Research*, **19**, 5551-5559.

6. Akhtar,S., Beck,G.F., Hawley,P., Irwin,W.J., and Gibson,I. (1996) The influence of polarized epithelial (Caco-2) cell differentiation on the cellular binding of phosphodiester and phosphorothioate oligonucleotides. *Antisense & Nucleic Acid Drug Development*, **6**, 197-206.

7. Akhtar,S., Hughes,M.D., Khan,A., Bibby,M., Hussain,M., Nawaz,Q., Double,J., and Sayyed,P. (2000) The delivery of antisense therapeutics. *Advanced Drug Delivery Reviews*, **44**, 3-21.

8. Akhtar,S. and Lewis,K.J. (1997) Antisense oligonucleotide delivery to cultured macrophages is improved by incorporation into sustained-release biodegradable polymer microspheres. *International Journal of Pharmaceutics*, **151**, 57-67.

9. Alami,R., Gilman,J.G., Feng,Y.Q., Marmorato,A., Rochlin,I., Suzuka,S.M., Fabry,M.E., Nagel,R.L., and Bouhassira,E.E. (1999) Anti Beta ribozyme reduces beta mRNA in transgenic mice: Potential application to the gene therapy of sickle cell anaemia. *Blood Cells, Molecules, and Diseases.*, **25**, 110-119.

10. Ali,M., Lemoine,N.R., and Ring,C.J.A. (1994) The use of DNA viruses as vectors for gene therapy. *Gene Therapy*, **1**, 367-384.

11. Alonso,M.J., Cohen,S., Park,T.G., Gupta,R.K., Siber,G.R., and Langer,R. (1993) Determinants of release rate of tetanus vaccine from polyester microspheres. *Pharmaceutical Research*, **10**, 954-953.

12. Altman,S. (1993) RNA enzyme-directed gene therapy. *Proc.Natl.Acad.Sci.USA*, **90**, 10900-10998.

13. Altman,S., Kiresebom,L., and Talbot,S. (1993) Recent studies of ribonuclease P. *FASEB J.*, **7**, 7-14.

14. Amarzguioui,M. and Prydz,H. (1998) Hammerhead ribozyme design and application. *Cellular and Molecular life Sciences*, **54**, 1175-1202.

15. Amiri,K. and Hagerman,P. (1996) The global conformation of a self-cleaving hammerhead RNA. *Biochemistry*, **33**, 13172-13177.

16. Arup,H., Heidenreich,O., and Eckstein,F. (1996) Stabilized RNA analogues for antisense and ribozyme applications. In Akhtar,S. (ed.) *Delivery strategies for antisense oligonucleotide therapeutics*. CRC press, Boca Raton, Fla., pp 161-76.

17. Avgoustakis,K. and Nixon,J.R. (1991) Biodegradable controlled release tablets: Preparative variables affecting the properties of poly(lactide-co-glycolide) copolymers as matrix forming material. *International Journal of Pharmaceutics*, **70**, 77-85.

18. Ayers,D., Cuthbertson,J.M., Schroyer,K., and Sullivan,S.M. (1996) Polyacrylic acid mediated ocular delivery of ribozymes. *Journal of Controlled Release*, **38**, 167-175.

19. Bassi,G.S., Mollegaard,N.E., Murchie,A.I.H., von Kitzing,E., and Lilley,D. (1995) Ionic interactions and the global conformation of the hammerhead ribozyme. *Nature Structural Biology*, **2**, 45-55.

20. Bassi,G.S., Murchie,A.I.H., and Lilley,D. (1996) The ion-induced folding of the hammerhead ribozyme: core sequence changes that preturb folding into the inactive conformation. *RNA*, **2**, 756-768.

21. Beck,G.F., Irwin,W.J., Nicklin,P.L., and Akhtar,S. (1996) Interactions of phosphodiester and phosphorothioate oligonucleotides with intestinal epithelial Caco-2 cells. *Pharmaceutical Research*, **13**, 1028-1037.

22. Been,M.D. and Wickham,G.S. (1997) Self-cleaving ribozyme of hepatitis delta vireus RNA. *European Journal of Biochemistry*, **247**, 741-753.

23. Beigelman,L., Karpeisky,A., Matulic-Adamic,A., Haeberli,P., Sweedler,D., and Usman,N. (1995a) Synthesis of 2'-modified nucleotides and their incorporation into hammerhead ribozymes. *Nucleic Acids Research*, **23**, 4434-4442.

24. Beigelman,L., McSwiggen,J., Draper,K.G., Gonzalez,C., Jensen,K., Karpeisky,A., Modak,A., Matulic-Adamic,A., DiRenzo,A., Haeberli,P., Sweedler,D., Tracz,D., Grimm,S., Wincott,F.E., Thackray,V., and Usman,N. (1995b) Chemical modifications of hammerhead ribozymes, catalytic activity and nuclease resistance. *The Journal of Biological Chemistry*, **270**, 25702-25708.

25. Beltinger,C., Saragovi,H.U., Smith,R.M., LeSauteur,L., Shah,N., DeDionisio,L., Christensen,L., Raible,A., Jarett,L., and Gewirtz,A.M. (1995) Binding, uptake and intracellular trafficking of phosphorothioate-modified oligodeoxynucleotides. *Journal of Clinical Investigation*, **95**, 1814-1823.

26. Bennett,R.M. (1993) As nature intended? The uptake of DNA and oligonucleotides by eukaryotic cells. *Antisenes Research and Development*, **3**, 235-241.

27. Bennett,R.M., Gabor,G.T., and Merrit,M.M. (1985) DNA binding to human leukocytes. *Journal of Clinical Investigation*, **76**, 2182-2190.

28. Berlin,R.D. and Oliver,J.M. (1994) Characterisation of FITC-Dextran as an indicator of fluid phase pinocytosis. *Journal of Cell Biology*, **85**, 660-671.

29. Besterman,J.M., Airhart,J.A., Woodworth,R.C., and Low,R.B. (1981) Endocytosis of pinocytosed fluid in cultured cells: Kinetic evidence for rapid turnover and compartmentalisation. *The Journal of Cell Biology*, **91**, 716-727.

30. Birikh,K.R., Heaton,P.A., and Eckstein,F. (1997) The sturcture, function and application of the hammerhead ribozyme. *European Journal of Biochemistry / FEBS*, **245**, 1-16.

31. Black, P. Mcl. Brain tumours, parts 1 and 2. New England Journal of Medicine 324, 1471-1476-1555-1564. 1991.

32. Bodmer,D., Kissel,T., and Traechslin,E. (1992) Factors influencing the release of peptides and proteins from biodegradable parenteral depot systems. *Journal of Controlled Release*, **21**, 129-138.

33. Bonen,L. and Vogel,J. (2001) The ins and outs of group II introns. *Trends in Genetics: TIG*, **17**, 322-331.

34. Bramlage,B., Alefelder,S., Marschall,P., and Eckstein,F. (1999) Inhibition of luciferase expression by synthetic hammerhead ribozymes and their cellular uptake. *Nucleic Acids Research*, **27**, 3159-3167.

35. Bramlage,B., Luzi,E., and Eckstein,F. (1998) Designing ribozymes for the inhibition of gene expression. *TIBTECH*, **16**, 434-438.

36. Bratty,J., Chartrand,P., Ferbeyre,G., and Cedergren,R. (1993) The hammerhead RNA domain, a model ribozyme. *Biochemica et Biophysica Acta*, **1216**, 345-359.

37. Brem,H. and Gabikian,P. (2001) Biodegradable polymer implants to treat brain tumours. *Journal of Controlled Release*, **74**, 63-67.

38. Brightman,M.W., Reese,J.S., and Feder,N. (1970) Assessment with the electron microscope of the permeability to peroxidase of cerebral endothelium and epithelium in mice and sharks. In Lassen,N.A. (ed.) *Capillary Permeability*. Copenhagen, p 463.

39. Brown,T. and Brown,D.J. (1991) *Modern machine-aided methods of synthesis. Oligonucleotides and Analogues.* IRL Press, Oxford University Press.

40. Butcher,S.E. (2001) Structure and function of the small ribozymes. *Current Opinion in Structural Biology*, **11**, 315-320.

41. Camarta,P.J., Suryanarayanan,R., Turner,D., Parker,R.G., and Ebner,T.J. (1992) Sustained release of nerve growth factor from biodegradable polymer microspheres. *Neurosurgery*, **30**, 313-319.

42. Cao,X. and Shoichet,S. (1999) Delivering neuroactive molecules from biodegradable microspheres for application in central nervous system disorders. *Biomaterials*, **20** , 329-339.

43. Chetouani,F., Monestie,P., Thebault,P., Gaspin,C., and Michot,B. (1997) ESSA: an integrated and interactive computer tool for analysing RNA secondary structure. *Nucleic Acids Research*, **25**, 3514-3522.

44. Chirmule,N. (2001) Immune responses to adenovirus and adeno-associated virus in humans. *Gene Therapy*, **6**, 1574-1583.

45. Chu,C.C. (1981) The *in vitro* degradation of poly(glycolic acid) sutures, effect of pH. *Journal of Biodmedical Materials Research*, **15**, 795-804.

46. Cobaleda,C. and Sanchez-Garcia,I. (2001) RNaseP: from biological function to biotechnological applications. *Trends in Biotechnology*, **19**, 406-411.

47. Cohen,S., Yoshioka,T., Lucarelli,M., Hwang,L.H., and Langer,R. (1991) Controlled delivery for proteins based on poly(lactic/glycolic acid) microspheres. *Pharmaceutical Research*, **8**, 713-720.

48. Conti,B., Bucolo,C., Giannavola,C., Puglisi,G., Giunchedi,P., and Conte,U. (1997) Biodegradable microspheres for the intravitreal administration of acyclovir: *in vitro/in vivo* evaluation. *European Journal of Pharmaceutical Sciences*, **5**, 287-293.

49. Couvreveur,P. and Puisieux,F. (1992) *Adavanced Drug Deleivery Reviews*, **10**, 141.

50. Crooke,S.T. (1992) Therapeutic applications of oligonucleotides. *Annual Review of Pharmacology and Toxicology*, **32**, 329-376.

51. Crotts,G. and Park,T.G. (1995) Preparation of porous and nonporous biodegradable polymeric hollow microspheres. *Journal of Controlled Release*, **35**, 91-105.

52. Crotts,G. and Park,T.G. (1998) Protein delivery from poly(lactic-co-glycolic acid) biodegradable microspheres: release kinetics and stability issues. *Journal of microencapsulation*, **15**, 699-713.

53. Cutwright,D.E., Beasley,J.D., and Perez,B. (1971) Histological comparison of polylactic and polygycolic acid sutures. *Oral Surgery*, **232**, 165-173.

54. Dahm,S.C., Derrick,W.B., and Uhlenbeck,O.C. (1993) Evidence for the role of solvated metal hydroxide in the hammerhead cleavage mechanism. *Biochemistry*, **32**, 13040-13045.

55. Darr,S.C., Brown,J.W., and Pace,N.R. (1992) The varieties of ribonuclease P. *Trends in Biochemical Sciences*, **7**, 178-182.

56. Davis,S.S. and Illum,L. (1989) Microspheres as drug carriers. *Horiz Biochem Biophys*, **9**, 131-153.

57. Davis,S.S., Illum,L., Moghimi,S.M., Davies,M.C., Porter,C.J.H., Muir,I.S., Brindley,A., Christy,N.M., Norman,M.E., Williams,P., and Dunn,S.E. (1993) Microspheres for targeting drugs to specific body sites. *Journal of Controlled Release*, **24**, 157-163.

58. Dawson, P. A. and Marini, J. C. Hammerhead ribozymes selectively suppress mutant type I collagen mRNA in osteogenesis imperfecta fibroblasts. Nucleic Acids Research 28(20), 4013-4020. 2000.

59. DeOliveira,M.C. (1998) pH sensitive liposomes as a carrier for oligonucleotides a physico-chemical study of the the interaction between DOPE and 15-mer oligonucleotides in quasi-anhydrous samples. *Biochemica et Biophysica Acta*, **1372**, 301-310.

60. DeRose,V.J. (2002) Two decades of RNA catalysis. *Chemistry & Biology*, **9**, 961-969.

61. Deshpande,D., Toledo-Velasquez,D., Thakkar,D., Liang,W., and Rojanasakul,Y. (1996) Enhanced cellular uptake of oligonucleotides by EGF receptor mediated endocytosis in A549 cells. *Pharmaceutical Research*, **13**, 57-61.

62. Dokka,S. and Rojanasakul,Y. (2000) Novel non-endocytic delivery of antisense oligonucleotides. *Adavanced Drug Deleivery Reviews*, **44**, 35-49.

63. Dolzhanskaya,N., Conti,J., Schwenk,V., Merz,G., and Denman,R.B. (2001) Self-cleaving-ribozyme-mediated reduction of betaAPP in human rhabdomyosarcoma cells. *Archives of Biochemistry and Biophysics*, **387**, 223-232.

64. Earnshaw,D.J., Hamm,M.L., Piccirilli,J.A., Karpeisky,A., Beigelman,L., Ross,B.S., Manoharan,M., and Gait,M.J. (2001) Investigation of the proposed interdomain ribose zipper in hairpin ribozyme cleavage using 2'-modified nucleosides. *Biochemistry*, **40**, 7350-7350.

65. Ekstrand,A.J., James,C.D., Cavenee,W.K., Seliger,B., Petterso,R.F., and Collins,V.P. (1991) Genes for EGFR, transforming growth factor, epidermal growth factor and their expression in human gliomas *in vivo*. *Cancer research*, **2164**, 2172.

66. Eldadah,B.A., Ren,R.F., and Faden,A.I. (2000) Ribozyme-mediated inhibition of Caspase-3 protects cerebellar granule cells from apoptosis induced by serum-potassium deprivation. *TheJournal of Neuroscience*, **20**, 179-186.

67. Elder,J., Johnson,M., Milner,K., Mir,K., Sohail,M., and Southern,E.M. (1999) Antisense oligonucleotide scanning arrays. In Schena,M. (ed.) *DNA microarrays: A Practical Approach*. IRL Press, Oxford, pp 77-99.

68. Elkins,D.A. and Rossi,J.J. (1995) Cellular delivery of ribozymes. In Akhtar,S. (ed.) *Delivery strategies for antisense oligonucleotide therapeutics*. CRC Press, Boca Raton, Fla, pp 17-38.

69. Engels,J.W., Scherr,M., Ganser,A., Grez,M., and Wittmann,V. (1998) Modified hammerhead ribozymes as potential therapuetics. *Nucleosides & Nucleotides*, **17**, 9-11.

70. Farhood,H., Bottega,R.M., Epand,L., and Huang,L. (1992) Effect of cationic cholesterol derivatives on gene transfer and protein-kinase C activity. *Biochemica et Biophysica Acta*, **1111**, 239-246.

71. Fay,M.J., Walter,N.G., and Burke,J.M. (2001) Imaging of single hairpin ribozymes in solution by atomic force microscopy. *RNA (New York, N.Y.)*, **7**, 887-895.

72. Fedor,M.J. (2000) Structure and function of the hairpin ribozyme. *Journal of Molecular Biology*, **297**, 269-291.

73. Fedorova,O., Su,L.J., and Pyle,A.M. (2002) Group II introns: highly specific endonucleases with modular structures and diverse catalytic functions. *Methods*, **28**, 323-335.

74. Fell,P.L., Hudson,A.J., Reynolds,M.A., Usman,N., and Akhtar,S. (1997) Cellular uptake properties of a 2'amino/2'-O-Methyl- modified chimeric hammerhead rbozyme targeted to the epidermal growth factor receptor mRNA. *Antisense & Nucleic Acid Drug Development*, **7**, 319-326.

75. Feng,M., Cabrera,G., Deshane,J., Scanlon,K.J., and Curiel,D.T. (1995) Neoplastic reversion accomplished by high efficiency adenoviral mediated delivery of an anti-ras ribozyme. *Cancer research*, **55**, 2024-2028.

76. Feng,Y., Leavitt,M., Tritz,R., Duarte,E., Kang,D., Mamounas,M., Gilles,P., Wong-Staal,F., Kennedy,S., Merson,J., Yu,M., and Barber,J.R. (2000) Inhibition of CCR5-dependent HIV- infection by hairpin ribozyme gene therapy against CC-chemokine receptor 5. *Virology*, **276**, 271-278.

77. Flory,C.M., Pavco,P.A., Jarvis,T.C., Lesch,M.E., Wincott,F.E., Beigelman,L., Hunt III,S.W., and Schrier,D.J. (1996) Nuclease-resistant ribozymes decrease stromelysin mRNA levels in rabbit synovium following exogenous delivery to the knee joint. *Proc.Natl.Acad.Sci.USA*, **93**, 754-758.

78. Floy,B.J., Visor,G.C., and Sanders,L. (1993) Design of biodegradable polymer systems for controlled release of bioactive agents. *Polymeric Delivery Systems*, **10**, 154-167.

79. Fournier,C., Hecquet,B., Bouffard,P., Vert,M., Caty,A., Vilian,M.O., Vanseymortier,L., Merle,S., Krikorian,A., Lefebvre,J., Delobelle,A., and Adenis,L. (1991) Experimental studies and preliminary clinical trial of vinorelbine-loaded polymeric bioresorbable implants for the local treatment of solid tumours. *Cancer Research*, **51**, 5384-5391.

80. Freedland,S.J., Malone,R.W., Borchers,H.M., Zadourian,Z., Malone,J.G., Bennett,M.J., Nantz,M.H., Li,J.-H., Gumerlock,P.H., and Erickson,K.L. (1996) Toxicity of cationic lipid-ribozyme complexes in human prostate tumor cells can mimic ribozyme activity. *Biochemical and Molecular Medicine*, **59**, 153.

81. Fritz,J.J., Lewin,A.S., Hauswirth,W.W., Agarwal,A., Grant,M., and Shaw (2002) Development of hammerhead ribozymes to modulate endogenous gene expression for functional studies. *Methods*, **28**, 276-285.

82. Funato,T., Ishii,T., Kanbe,M., Scanlon,K.J., and Sasaki,T. (1997) Reversal of Ciplatin resistance *in vivo* by an anti-fos ribozyme. *In vivo*, **11**, 217-220.

83. Gage,F.H., Wolf,J.A., Rosenberg.M.B., Xu,L., Yee,J.K., Shults,C., and Friedman,T. (1987) Grafting genetically modified cells to the brain: Possibilities for the future. *Neuroscience*, **23**, 795-807.

84. Garcia-Contreras,L., Abu-Izza,K., and Lu,D.R. (1997) Biodegradable cisplatin microspheres for direct brain injection: Preparation and characterisation. *Pharmaceutical Development and Technology*, **2**, 53-65.

85. Gaspin,C. and Weshof,E. (1995) An interactive framework for RNA secondary structure prediction with a dynamical treatment of constraints. *Journal of Molecular Biology*, **254**, 163-174.

86. Giannakis,C., Forbes,I.J., and Zalewski,P.D. (1991) $Ca^{2+}/Mg^{(2+)}$-dependent nuclease: Tissue distribution relationship to inter-nucleosomal DNA fragmentation and inhibition by Zn^{2+}. *Biochemical and Biophysical Research Communications*, **181**, 915-920.

87. Giannini,C.D., Roth,W.K., Piiper,A., and Zeuzem,S. (1999) Enzymatic and antisense effects of a specific anti-Ki-*ras* ribozyme *in vitro* and in cell culture. *Nucleic Acids Research*, **27**, 2737-2744.

88. Goodarzi,G., Watabe,M., and Watabe,K. (1991) Binding of oligonucleotides to cell membranes at acidic pH. *Biochemical and Biophysical Research Communications*, **181**, 1343-1351.

89. Goodchild,J. (1992) Enhancement of ribozyme catalytic activity by a contigous oligodeoxynucleotide (facilitator) and by 2'-O-methylation. *Nucleic Acids Research*, **20** , 4607-4612.

90. Goodchild,J. and kholi,V. (1991) Ribozymes that cleave an RNA sequence from human immunodeficiency virus: the effect of flanking sequence on rate. *Archives of Biochemistry and Biophysics*, **284**, 386-391.

91. Gopferich,A. (1997) Mechanisms of polymer degradation and elimination. In Domb,A.J., Kost,J., and Wiseman,D.M. (eds.) *Handbook of biodegradable polymers*. Harwood academic publishers, pp 451-71.

92. Gruenberg,J. (2001) The endocytic pathway: A mosain of domains. *Nature Reviews: Molecular Biology*, **2**, 721-730.

93. Gu,J.-L., Nadler,J., and Rossi,J. (997) Use of hammerhead ribozyme with cationic liposomes to reduce leukocyte type 12-lipoxygenase expresson in vascular smooth muscle. *Molecular and Cellular Biochemistry*, **172**, 47-57.

94. Gurerrier-Takada, C., Gardiner, K., March, T., Pace, N., and Altman, S. The RNA moiety of ribonuclease P is the catalytic subunit of the enzyme. Cell 35, 849-857. 1983.

95. Gutman,R.L., Peacock,G., and Lu,D.R. (2000) Targeted drug delivery for brain cancer treatment. *Journal of Controlled Release*, **65**, 31-41.

96. Hampel,A. and Cowan,J.A. (1997) A unique mechanism for RNA catalysis: the role of metal co-factors in hairpin ribozyme cleavage. *Chemistry & Biology*, **4**, 513-517.

97. Hanna,R. and Doudna,J.A. (2000) Metal ions in ribozyme folding and catalysis. *Current Opinion in Chemical Biology*, **4**, 166-170.

98. Harbaugh,R.E., Saunders,R.L., and Reeder,R.F. (1988) Use of implantable pumps for central nervous system drug infusions to treat neurological disease. *Neurosurgery*, **23**, 693-698.

99. Haseloff,J. and Gerlach,W.L. (1998) Simple RNA enzymes with new and highly specific endoribonuclease activities. *Nature*, **334**, 585-591.

100. Hayashi,T. (1994) Biodegradable polymers for biomedical uses. *Progress in Polymer Science*, **19**, 663-702.

101. Heidenreich,O., Benseler,F., Fahrenholz,A., and Eckstein,F. (1994) High activity and stability of hammerhead ribozymes containing 2'-modified pyrimidine nucleosides and phosphorothioates. *The Journal of Biological Chemistry*, **269**, 2131-2138.

102. Hendry,P., Lockett,T.J., and McCall,M.J. (1998) Small efficient hammerhead ribozymes. In Scanlon,K.J. (ed.) *Therapeutic applications of ribozmes*. Humana Press, New Jersey, pp 1-15.

103. Hendry,P. and McCall,M.J. (1996) Unexpected anisotropy in substrate claeavage rates by asymmetric hammerheasd ribozymes. *Nucleic Acids Research*, **24**, 2679-2684.

104. Hendry,P., McCall,M.J., Santiago,F.S., and Jennings,P.A. (1992) A ribozyme with DNA in the hybridising arms displays enhanced cleavage ability. *Nucleic Acids Research*, **23**, 5737-5741.

105. Hendry,P., McCall,M.J., Santiago,F.S., and Jennings,P.A. (1995) In vitro activity of minimised hammerhead ribozymes. *Nucleic Acids Research*, **23**, 3922-3927.

106. Hendry,P., Moghaddam,M., McCall,M.J., Jennings,P.A., Ebel,S., and Brown,T. (1994) Using linkers to investigate the spatial separation of the conserved nucleotides A9 and G12 in hammerhead ribozyme. *Biochemica et Biophysica Acta*, **1219**, 405-412.

107. Henry,S.P., Montieth,D., and Levin,A.A. (1997) Antisense oligonucleotide inhibitors for the treatment of cancer: Toxicological properties of phosphorothioate oligodeoxynucleotides. *Anticancer Drug Discovery*, **12**, 395-408.

108. Herrmann,J. and Bodmeier,R. (1995) Somatastatin containing biodegradable microspheres prepared by a modified solvent evaporation method based on w/o/w-multiple emulsions. *International Journal of Pharmaceutics*, **126**, 129-138.

109. Herschlag,D. (1991) Implications of ribozyme kinetics for targeting the cleavage of specific RNA molecules in vivo: more isn't always better. *Proc.Natl.Acad.Sci.USA*, **88**, 6921-6925.

110. Herschlag,D., Khosla,M., Tsuchihashi,Z., and Karpel,R.L. (1994) An RNA chaperone activity of non-specific RNA binding proteins in hammerhead ribozyme catalysis. *EMBO J.*, **13**, 2913-2924.

111. Hertel,K.J., Pardi,A., Uhlenbeck,O.C., Koizumi,M., Ohtsuka,E., Uesugi,S., Cedergren,R., Eckstein,F., Gerlach,W.L., Hodgson,R., and Symons,R.H. (1992) Numbering system for the hammerhead. *Nucleic Acids Research*, **20**, 3252-3252.

112. Ho,S., Bao,Y., Lesher,T., Malhotra,R., Ma,L.Y., Fluharty,S.J., and Sakai,R.R. (1998) Mapping of RNA accessible sites for antisense experiments with oligonucleotide libraries. *Nature Biotechnology*, **16**, 59-63.

113. Hoffman,A.S. (1977) Medical applications of polymeric fibres. *Journal of Applied Polymer Science.Applied Polymer Symp.*, **31**, 313-334.

114. Holland,S.J. and Tighe,B.J. (1986) Polymers for biodegradable medical devices. The potential of polyesters as controlled macromolecular relaease systems. *Journal of Controlled Release*, **4**, 155-180.

115. Holz,H.M. (1982) *Worthwhile facts about fluorescence microscopy: Filter sets.* Carl-Zeiss Publ. Oberkochen, Germany.

116. Hormes,R., Homann,M., Oeleze,I., Marschall,P., Tabler,M., and Eckstein,F. (1997) The subcellular localisation and length of hammerhead ribozymes determine efficacy in human cells. *Nucleic Acids Research*, **25**, 769-775.

117. Howard,M.A., Gross,A., Grady,M.S., Langer,R.S., Mathiowitz,E., Winn,R., and Mayberg,M.R. (1989) Intracerebral drug delivery in rat with lesion-induced memory deficits. *Journal of Neurosurgery*, **71**, 105-112.

118. Hu,W.Y., Fukuda,N., Kishioka,H., Nakayama,M., Satoh,C., and Kanmatsuse,K. (2001) Hammerhead ribozyme targeting human platelet-derived growth factor A-chain mRNA inhibited the proliferation of human vascular smooth muscle cells. *Atherosclerosis*, **158**, 321-329.

119. Hubinger,G., Wehnes,E., Xue,L., Morris,S.W., and Maurer,U. (2003) Hammerhead ribozyme-mediated cleavage of the fusion transcript NPM-ALK associated with anaplastic large-cell lymphoma. *Experimental Hematology*, **31**, 226-233.

120. Hudson,A.J., Lee,W., Porter,J., Akhtar,J., Duncan,R., and Akhtar,S. (1996b) Stability of antisense oligonucleotides during incubation with a mixture of isolated lysosomal enzymes. *International Journal of Pharmaceutics*, **133**, 257-263.

121. Hudson,A.J., Lewis,K.J., Rao,M.V., and Akhtar,S. (1996a) Biodegradable polymer matrices for the sustained exogenous delivery of a biologically active c-*myc* hammerhead ribozyme. *International Journal of Pharmaceutics*, **136**, 23-29.

122. Hudson,A.J., Normand,N., Ackroyd,J., and Akhtar,S. (1999) Cellular delivery of hammerhead ribozymes conjugated to a transferrin receptor antibody. *International Journal of Pharmaceutics*, **182**, 49-58.

123. Huesker,M., Folmer,Y., Schneider,M., Fulda,C., Blum,H.E., and Hafkemeyer,P. (2002) Reversal of drug resistance of hepatocellular carcinoma cells by adenoviral delivery of anti-MDR1 ribozymes. *Hepatology*, **36**, 874-884.

124. Hughes,M.D., Hussain,M., Nawaz,Q., Sayyed,P., and Akhtar,S. (2001) The cellular delivery of antisense oligonucleotides and ribozymes. *Drug Discovery Today*, **6**, 303-315.

125. Hutchinson,F.G. and Furr,B.G.A. (1985) Biodegradable polymers for sustained delivery of peptides. *Biochemical Society Transactions*, **13**, 520-523.

126. Irie,A., Anderegg,B., Kashani-Sabet,M., Ohkawa,T., Suzuki,T., Halks-Miller,M., Curiel,D.T., and Scanlon,K.J. (1999) Therapeutic efficacy of an adenovirus-mediated anti-H-*ras* ribozyme in experimental bladder cancer. *Antisense & Nucleic Acid Drug Development*, **9**, 341-349.

127. Islam,A., Handley,S.L., Thompson,K.S.J., and Akhtar,S. (2000) Studies on uptake, sub-cellular trafficking and efflux of antisense oligodeoxynucleotides in glioma cells using self-assembley cationic lipoplexes as delivery systems. *Journal of Drug Targeting*, **7**, 373-382.

128. Jabranne-Ferrat,N., Pollock,A.S., and Goetzel,E.J. (2000) Inhibition of expression of thetype I G protein-coupled receptor for vasoactive intestinal peptide (VPAC1) by hammerhead ribozymes. *Biochemistry*, **39**, 9771-9777.

129. Jackson,W.H., Moscoso,H., Nechtman,J.F., Galileo,D.S., Garver,F.A., and Lanclos,K.D. (1998) Inhibition of HIV-1 replication by an anti-tat hammerhead ribozyme. *Biochemical and Biophysical Research Communications*, **245**, 81-84.

130. Jacquier,A. (1996) Group II introns: elaborate ribozymes. *Biochemie*, **78**, 474-487.

131. Jarvis,T.C., DiRenzo,A., Levy,K., Arthur,M., Matulic-Adamic,A., Gonzalez,C., Wolf,T.M., Usman,N., and Stinchcomb,D.T. (1996) Optimising the cell efficacy of synthetic ribozymes. *The Journal of Biological Chemistry*, **271**, 29107-29112.

132. Kariko,K., Megyeri,K., Xiao,Q., and Barnathan,E.S. (1994) Lipofectin-aided delivery of ribozyme targeted to human urokinase receptor mRNA. *FEBS Letters*, **352**, 41-44.

133. Keese,P., Bruening,G., and Symons,R.H. (1983) Comparative sequence and structure of circular RNAs from two isolates of lucerne transient streak virus. *FEBS Letters*, **159**, 185-190.

134. Kennell,J.C., Saville,B.J.M.S., Kuiper,M.T., Sabourinm,J.R., Collins,R.A., and Lambovitz,A.M. (1995) The VS catalytic RNA replicated by reverse trnascription as a satellite of a retroplasmid. *Genes Development*, **9**, 294-303.

135. Khan, A. The sustained delivery of antisense oligodeoxynucleotides using biodegradable polymer microspheres. 67-67. 1999. Aston University.

136. Khan,A., Sommer,W., Fuxe,K., and Akhtar,S. (2000) Site-specific administration of antisense oligonucleotides using biodegradable polymer microspheres provides

sustained delivery and improved subcellular biodistribution in the Neostriatum of the rat brain. *Journal of Drug Targeting*, **8**, 319-334.

137. Khazaie,K., Schirrmacher,V., and Lichtner,R.B. (1993) EGF receptor in neoplasia and metastasis. *Cancer and Metastasis Review*, **12**, 255-274.

138. Kisich,K.O., Malone,R.W., Feldstein,P.A., and Erickston,K.L. (1999) Specific inhibition of Macrophage TNF-α expression by in vivo ribozyme treatment. *The Journal of Immunology*, **163**, 2008-2016.

139. Kitajima,I., Hanyo,N., Soejima,Y., Hirano,R., Arahiro,S., Yamaoka,S., Yamado,R., Marayumo,I., and Kaneda,Y. (1997) Efficient transfer of synthetic ribozymes into cells using Hemagglutinating virus of Japan (HVJ)-cationic liposomes. *The Journal of Biological Chemistry*, **272**, 27099-27106.

140. Klibanov,A.O. (1990) Amphipathic polyethleneglycols effectively prolong the circulation time of liposomes. *FEBS Letters*, **268**, 235-237.

141. Kondo,H., Mori,S., Takino,H., Kijima,H., Yamasaki,H., Ozaki,M., Tetsua,I., Urata,Y., Abe,T., Sera,Y., Yamakawa,K., Kawasaki,E., Yamaguchi,Y., Kondo,T., and Eguchi,K. (2000) Attenuation of expression of gamma-Glutamylcysteine synthetase by ribozyme transfection enhance insulin secretion by pancreatic beta cell line MIN6. *Biochemical and Biophysical Research Communications*, **278**, 236-240.

142. Konopka,K., Rossi,J., Swiderski,P., Slepushkin,V.A., and Duzgunes,N. (1998) Delivery of an anti-HIV-1 ribozyme into HIV-infected cells via cationic liposomes. *Biochemica et Biophysica Acta*, **1372**, 55-68.

143. Kotani,M., Ando,H., Hu,W., Kunimoto,S., Saito,S., Kanmatsuse,K., and Fukuda,N. (2003) Chimeric DNA-RNA hammerhead ribozyme targeting PDGF A-chain mRNA specifically inhibits neointima formation in rat carotid artery after ballon injury. *Cardiovascular Research*, **57**, 265-276.

144. Kruger, K, Grabowski, P, Zaug, A. J., Sands, J, Gottschling, D. E., and Cech, T. R. Self-splicing RNA: autoexcision and autocyclization of the ribosomal RNA intervening sequence of *Tetrahymena*. Cell 31, 147-157. 1982.

145. Kulkarni,R., Pani,K., Newman,C., and Leonard,F. (1966) Polylactic acid for surgical implants. *Archives of Surgery*, **93**, 839-843.

146. Kumar,G.S. (1987) Biodegradable polymers: Prospects and progress. *Marcell Dekker, NY.*,44-45.

147. Kung,H.J., Chang,C.M., and Pelley,R.J. (1994) Structural basis of oncogenic activation of epidermal growth factor receptor. In Pretlow,T.G. and Pretlow,T.P. (eds.) *Biochemical and molecular aspects of selected cancers.* Academic Press, San Diego, pp 19-45.

148. Kurz,J.C. and Fierke,C.A. (2000) Ribonuclease P: a ribonucleoprotein enzyme. *Current Opinion in Chemical Biology*, **4**, 553-558.

149. L'Huillier,P.J., Soulier,S., Stinnarke,M., Lepourry,L., Davis,S., Mercier,J., and Vilotte,J. (1996) Efficient and specific ribozyme-mediated reduction of bovine alpha-lactalbumin expression in double transgenic mice. *Proc.Natl.Acad.Sci.USA*, **93** , 6698-6703.

150. Lafontaine,D.A., Norman,D.G., and Lilley,D. (2002) Folding a catalysis by the VS ribozyme. *Biochimie*, **84**, 889-896.

151. Laktionov,P.P., Dazard,J., Vives,E., Rykova,E., Piette,J., Vlassov,V.V., and Lebleu,B. (1999) Characterisation of membrane oligonucleotide-binding proteins and oligonucleotide uptake in keratinocytes. *Nucleic Acids Research*, **27**, 2315-2324.

152. Langer,R. and Folkman,J. (1976) Polymers for the sustained release of proteins and other macromolecules. *Nature*, **263**, 797-800.

153. Langer,R. and Pappas,N.S. (1981) Presentations and future applications of biomaterials in controlled drug delivery systems. *Biomaterials*, **2**, 201-214.

154. Langlois,M., Lee,N.S., Rossi,J., and Puymirat,J. (2003) Hammerhead ribozyme-mediated destruction of nuclear foci in myotonic dystrophy myoblasts. *Molecular Therapy*, **0**, 1-11.

155. Lansing-Taylor,D. and Salman,E.D. (1998) *Basic Fluorescence Microscopy.* Academic Press Inc., San Diego USA.

156. Lavrovsky,Y., Tyagi,R.K., Chen,S., Song,C.S., Chatterjee,B., and Roy,A.K. (1999) Ribozyme-mediated cleavage of the estrogen receptor messenger RNA and inhibition of receptor function in target cells. *Molecular Endocrinology*, **13**, 925-934.

157. Le Ray,A.M., Vert,M., Gautier,J.C., and Benoit,J.P. (1994) Fate and [^{14}C]poly(DL-lactide-co-glycolide) nanoparticles after intravenous and oral administration to mice. *International Journal of Pharmaceutics*, **106**, 201-211.

158. Lenslag,J.W., Pennongs,A.J., Bos,R.R.M., Rozena,F.R., and Boering,G. (1987) Resorbable materials of poly(L-lactide). Plates and screws for internal fracture fixation. *Biomaterials*, **8**, 70-73.

159. Levis,J.T., Butler,W.O., Tseng,B.Y., and Tseng.P.O.P. (1995) Cellular uptake of oligodeoxyribonucleoside methlphosphonates. *Antisenes Research and Development*, **5**, 251-259.

160. Lewin,A.S. and Hauswirth,W.W. (2001) Ribozyme gene therapy: applications for molecular medicine. *Trends Mol Med*, **7**, 221-228.

161. Lewis,D.H. (1990) Controlled release of bioactive agents from lactide/glycolide polymers. In Chasin,M. and Langer,R. (eds.) *Biodegradable Polymers as Drug Delivery Systems.* Marcel Dekker, New York, pp 1-42.

162. Lewis,K.J., Irwin,W., ., and Akhtar,S. (1995) Biodegradable ploy(L-lactic acid) matrices for the sustained delivery of antisense oligonucleotides. *Journal of Controlled Release*, **37**, 173-183.

163. Lewis,K.J., Irwin,W.J., and Akhtar,S. (1998) Development of a sustained-release biodegradable polymer delivery system for site-specific delivery of oligonucleotides: Characetrisation of P(LA-GA) copolymer microspheres *in vitro*. *Journal of Drug Targeting*, **5**, 291-302.

164. Lieber,A. and Strauss,M. (1995) Selection of efficient cleavage sites in target RNAs by using a ribozyme expression library. *Molecular and Cell Biology*, **15**, 540-551.

165. Liphardt,J., Onoa,B., Smith,S.B., Tinoco, and Bustamante,C. (2001) Reversible unfolding of single RNA molecules by mechanical force. *Science*, **292**, 733-737.

166. Liu,F. and Altman,S. (1995) Inhibition of viral gene expression by the catalytic RNA subunit of RNaseP from Eschericia coli. *Gene Dev.*, **9**, 471-480.

167. Loke,S.L., Stein,C.A., Zhang,X.H., Mori,K., Nakanishi,M., Subasinghe,C., Cohen,J.S., and Neckers,L.M. (1989) Characterisation of oligonucleotide transport into living cells. *Proc.Natl.Acad.Sci.USA*, **86**, 3474-3478.

168. Long,D.M. and Uhlenbeck,O.C. (1994) Kinetic characterisation of intramolecular and intermolecular hammerhead RNAs with stem II deletions. *Proc.Natl.Acad.Sci.USA*, **91**, 6977-6981.

169. Lorens,J.B., Sousa,C., Bennett,M.F., Molineuax,S.M., and Payan,D.G. (2001) The use of retroviruses as pharmaceutical tools for target discovery and validation in the field of functional genomics. *Current Opinion in Biotechnology*, **12**, 613-621.

170. Lyngstadaas,S.P., Risnes,S., Sproat,B.S., Thrane,P.S., and Prydz,H.P. (1995) A synthetic, chemically modified ribozyme eliminates amelogenin, the major translation product in developing mouse enamel in vivo. *EMBO J.*, **14**, 5224-5229.

171. Macejak,D.G., Lin,H., Webb,S., Chase,J., Jensen,K., Jarvis,T.C., Leiden,J.M., and Couture,L. (1999) Adenovirus-mediated expression of a ribozyme to c-*myb* mRNA inhibits smooth muscle cell proliferation and neointima formation in vivo. *Journal of Virology*, **73**, 7745-7751.

172. MacKay,S.L.D., Tannahill,C.L., Auffenberg,T., Ksontini,R., Copeland,E.M., and Moldawer,L.L. (1999) Characterization in vitro and in vivo of hammerhead ribozymes directed against murine tumor Necrosis Factor α. *Biochemical and Biophysical Research Communications*, **260**, 390-397.

173. Makino,K., Arakawa,M., and Kondo,T. (1985) Preparation and the in vitro degradation properties of polylactide microcapsules. *Chemical and Pharmaceutical Bulletin*, **33**, 1195-1201.

174. Maniotis,D., Wood,M.J.A., and Phylactou,L.A. (2002) Hammerhead ribozymes reduce central nervous system (CNS)-derived neuronal nitric oxide synthase messenger RNA in a human cell line. *Neuroscience Letters*, **329**, 81-85.

175. Marcote,N. and Goosen,M.F.A. (1989) Delayed release of water soluble macromolecules from polylatide pellets. *Journal of Controlled Release*, **9**, 75-85.

176. Maysinger,D., Filipovic-Grcic,J., and Cuello,A.C. (1993) Effects of coencapsulated NGF and GM1 in rats with cortical lesions. *NeuroReport*, **4**, 971-974.

177. McRae-Deguerce,A., Hjorth,S., Dillon,D.L., Mason,D.W., and Tice,T.R. (1988) Implantable microencapsulated dopamine (DA): a new approach for slow-release DA delivery into brain tissue. *Neuroscience Letters*, **92**, 303-309.

178. McRae,A. and Dahlostrum,A. (1994) Transmitter-loaded polymeric microspheres induce regrowth of dopaminergic nerve terminals in striata of rats with 6-OH-DA induced parkinsonism. *Neurochem.Int.*, **25**, 27-33.

179. McRae,A., Hjorth,S., Dahlostrum,A., Dillon,D.L., Mason,D.W., and Tice,T.R. (1992) Dopamine fiber growth induction by implantation of synthetic dopamine-containing microspheres in rats with experimental hemi-parkinsonism. *Mol.Chem Neuropathol*, **16**, 123-141.

180. Menei,P., Benoit,J.P., Boisdron-Celle,M., Fournier,D., Mercier,P., and Guy,G. (1994) Drug targeting into the central nervous system by stereotactic implantation of biodegrdable microspheres. *Neurosurgery*, **34**, 1058-1064.

181. Menei,P., Boisdron-Celle,M., Croue,A., Guy,G., and Benoit,J.P. (1996) Effect of stereotactic implantation of biodegradable 5-fluorouracil-loaded microspheres in healthy and C6 glioma-bearing rats. *Neurosurgery*, **39**, 117-123.

182. Menei,P., Daniel,V., Montero-Menei,C., Brouillard,M., Pouplard-Barthelaix,A., and Benoit,J.P. (1993) Biodegradation and brain tissue reaction to poly(D,L-lactide-co-glycolide) microspheres. *Biomaterials*, **14**, 470-478.

183. Menei,P., Pean,J.M., Nerriere-Daguin,V., Jollivet,C., Brachet,P., and Benoit,J.P. (2000) Intracerebral implatation of NGF-releasing biodegradable microspheres protects striatum against excitotoxic damage. *Experimental Neurology*, **161**, 259-272.

184. Menei,P., Venier,M.-C., Gamelin,E., Saint-Andre,J.-P., Hayek,G., Jadaud,E., Fournier,D., Mercier,P., Guy,G., and Benoit,J. (1999) Local and sustained delivery of 5-Fluorouracil from biodegradable microspheres for the radiosensitization of glioblastoma. *Cancer*, **86**, 325-330.

185. Michel,F. and Ferat,J.L. (1995) Structure and activities of group II introns. *Annual review of Biochemistry*, **64**, 435-461.

186. Miller,R.D., Brady,J.M., and Cutwright,D.E. (1977) Degradation rates of oral resorbable implants (polylactates and polyglycolates): Rate modification with changes in PLA/GA copolymer ratios. *Journal of Biomedical Materials Research*, **11**, 711-719.

187. Miller,W.A., Hercus,T., Waterhouse,P.M., and Gerlach,W.L. (1991) A satellite RNA of barley yellow dwarf virus contains a novel hammerhead structure in the self-cleaving. *Virology*, **183**, 711-720.

188. Modjtahedi,H. and Dean,C. (1994) The receptor for EGF and its ligands: Expression prognostic value and target for therapy in cancer. *International Journal of Cancer.*, **4**, 277-296.

189. Morris,M. and Lucion,A.B. (1995) Antisense oligonucleotides in the study of neuroendocrine systems. *Journal of Neuroendocrinology*, **7**, 493-500.

190. Nakada,Y., Fattal,E., Foulquier,M., and Couvreur,P. (1996) Pharmacokinetics and biodistribution of oligonucleotide adsorbed onto poly(isobutylcyanoacrylate) nanoparticles after intravenous administration in mice. *Pharmaceutical Research*, **13**, 38-43.

191. Neuwelt,E.A., Frenkel,F.P., Diehl.L.H., Vu,S., Rapoport,S., and Hill,S. (1980) Reversible osmotic blood-barrier disruption in humans: implications for the chemotherapy of malignant brain tumors. *Neurosurgery*, **7**, 44-52.

192. Normand-Sdiqui,N. and Akhtar,S. (1998) Oligonucleotide delivery: Uptake of rat transferr receptor antibody (OX-26) conjugates into an in vitro immortalised cell line model of the blood-brain barrier. *International Journal of Pharmaceutics*, **163** , 63-71.

193. Ogawa,S., Brown,H.E., Okano,H.J., and Pfaff,D.W. (1995) Cellular uptake of intracerebrally administered oligodeoxynucleotides in mouse brain. *Regulatory Peptides*, **59**, 143-149.

194. Ogawa,Y., Yamamoto,M., Okada,H., Yashiki,T., and Shimamoto,T. (1988) A new technique to efficiently entrap leuprolide acetate into microcapsules of poly(lactic acid) or copoly(lactic/glycolic acid). *Chemical & Pharmaceutical Bulletin*, **36**, 1095-1103.

195. Ogris,M., Brunner,S., Schuller,S., Kircheis,R., and Wagner,E. (1999) PEGylated DNA/transferrin-PEI complexes: reduced interaction with blood components, extended circulation in blood and potential for systemic gene delivery. *Gene Therapy*, **6**, 595-605.

196. Okada,H. and Taguchi,H. (1995) Biodegradable microspheres in drug delivery. *Critical Review Therapeutic Drug Carrier System*, **12**, 1-99.

197. Oshika,Y., Nakamura,M., Tokunaga,T., Ohnishi,Y., Abe,Y., Tsuchida,T., Tomii,Y., Kijima,H., Yamazaki,H., Ozeki,Y., Tamaoki,N., and Ueyama,Y. (2000) Ribozyme approach to downregulate vascular endothelial growth factor (VEGF) 189 expression in non-small cell lung cancer (NSCLC). *European Journal of Cancer*, **36**, 2390-2396.

198. Ostrowski, L. E., Bigner, Sandra H., Humphrey, P. A., and Bigner, D. D. Genetic alterations and gene expression in human malignant glioma. In: Pretlow, T.G.and Pretlow, T.P.(eds) Biochemical and molecular aspects of selected cancers. 143-168. 1994. San Diego, Academic Press.

199. Paolella,G., Sproat,B.S., and Lamond,A.I. (1992) Nuclease resistant ribozymes with high catalytic activity. *The EMBO Journal*, **11**, 1913-1919.

200. Pardrige,W.M. (2002) Crossing the blood-brain barrier: are we getting it right? *Drug Discovery Today*, **6**, 1-2.

201. Park,T.G. (1994) Degradation of poly(D,L-lactic acid) microspheres: Effect of molecular weight. *Journal of Controlled Release*, **30**, 161-173.

202. Parker,S.L., Tong,T., and Bolden,S. (1996) Cancer statistics. *CA Cancer J Clin.*, **46** , 5-27.

203. Parry,T.J., Cushman,C., Gallegos,A.M., Agrawal,A.B., Richardson,M., Andrews,L.E., Maloney,L., Mokler,V.R., Wincott,F.E., and Pavco,P.A. (1999) Bioactivity of anti-angiogenic ribozymes targeting *Flt*-1 and KDR mRNA. *Nucleic Acids Research*, **27**, 2569-2577.

204. Parthasarthy,R., Cote,G.J., and Gagel,R.F. (1999) Hammerhead ribozyme-mediated inactivation of mutant RET in medullary thyroid carcinoma. *Cancer research*, **59**, 3911-3914.

205. Paxinos,G. and Watson,C. (1986) *The rat brain stereotaxic co-ordinates*. New York: Academic Press, USA..

206. Pean,J.M., Menei,P., Morel,O., Montero-Menei,C., and Benoit,J.P. (2000) Intraseptal implantation of NGF-releasing microspheres promote the survival of axotomized cholinergic neurons. *Biomaterials*, **21**, 2097-2101.

207. Penn,R.D., York,M.M., and Paice,J.A. (1995) Catheter systems for intrathecal drug delivery. *Journal of Neurosurgery*, **83**, 215-217.

208. Perlman,H., Sata,M., Krasinski,K., Dorai,T., Buttyan,R., and Walsh,K. (2000) Adenovirus-encoded hammerhead ribozyme to Bcl-2 inhibits neointimal hyperplasia and induces vascular smooth muscle cell apoptosis. *Cardiovascular Research*, **45**, 570-578.

209. Peyman,A., Helsberg,M., Kretzschmar,G., Mag,M., Ryte,A., and Uhlmann,E. (1997) Nuclease stability as dominant factor in the antiviral activity of oligonucleotides directed against HSV-1 IE110. *Antiviral Research*, **33**, 135-139.

210. Phylactou,L.A. (2000) Ribozyme and peptide-nucleic acid-based gene therapy. *Adavanced Drug Deleivery Reviews*, **44**, 97-108.

211. Pieken,W.A., Olsen,D.B., Benseler,F., Aurup,H., and Eckstein,F. (1991) Kinetic characterization of Ribonuclease-resistant 2'-Modified hammerhead ribozymes. *Science*, **253**, 314-316.

212. Pierce,M. and Ruffner,D.E. (1998) Construction of a directed hammerhead ribozyme library: towards the identification of optimal target sites for antisense-mediated gene inhibition. *Nucleic Acids Research*, **26**, 5093-5101.

213. Pley,H.W., Flaherty,K.M., and McKay,D.B. (1994) Three dimensional structure of a hammerhead ribozyme. *Nature*, **372**, 68-74.

214. Prasmickaite,L., Hogset,A., Maelandsmo,G., Berg,K., Goodchild,J., Perkins,T., Fodstad,O., and Hovig,E. (1998) Intracellular metabolism of a 2'-O-methyl-stabilised ribozyme after uptake by DOTAP transfection or as free ribozyme. A study by capillary electrophoresis. *Nucleic Acids Research*, **26**, 4241-4248.

215. Propsting,M.J., Kubicka,S., Genschel,J., Manns,M.P., Lochs,H., and Schmidt,H.J. (2000) Inhibition of transtherytin-met30 expression using Inosine15.1 hammerhead

ribozymes in cell culture. *Biochemical and Biophysical Research Communications*, **279**, 970-973.

216. Puerta-Fernandez,E., Romera-Lopez,C., Barroso-delJesus,A., and Berzal-Herranz,A. (2003) Ribozymes: Recent advances in the development of RNA tools. *FEMS Microbiology Reviews*, **767**, 1-23.

217. Rak,J., Ford,J.L., Rosron,C., and Walters,V. (1985) The preparation and characterisation of poly(D,L-lactic acid) for use as a biodegradable drug carrier. *Pharm Acta Helvetiae*, **60**, 162-169.

218. Rhoades,K. and Wong-Staal,F. (2003) Inverse Genomics™ as a powerful tool to identify novel targets for the treatment of neurodegenerative diseases. *Mechanisms of Ageing and Development*, **124**, 125-132.

219. Rojanasakul,Y. (1996) Antisense oligonucleotide therapeutics. *Adavanced Drug Deleivery Reviews*, **18**, 115-131.

220. Rosen,H.B., Chang,J., Wnek,G.E., Linhardt,R.J., and Langer,R. (1983) Bioerodible polyanhydrides for controlled drug delivery. *Biomaterials*, **4**, 131-133.

221. Rossi,J. (1998) Therapeutic Ribozymes: Principles and applications. *BioDrugs*, **9**, 1-10.

222. Ruffner,D.E. and Uhlenbeck,O.C. (1990) Thiophosphate interference experiments locate phosphates important for the hammerhead RNA self-cleavage reaction. *Nucleic Acids Research*, **18**, 6025-6029.

223. Sah,H., Toddywala,R., and Chien,Y.W. (1995a) Biodegradable microspheres prepared by a w/o/w technique: effects of shear force to make a primary w/o emulsion on their morphology and protein release. *Journal of microencapsulation*, **12**, 59-69.

224. Sah,H., Toddywala,R., and Chien,Y.W. (1995b) Continuous release of proteins from biodegradable microcapsules and in vivo evaluation of their potential as a vaccine adjuvant. *Journal of Controlled Release*, **35**, 137-144.

225. Sakakura,C., Takahasi,T., Hagiwara,A., Itoh,M., Sasabe,T., Lee,M., and Shobayashi,S. (1992) Controlled release of Cisplatin from lactic acid oligmer microspheres incorporating cisplatin: *In vitro* studies. *Journal of Controlled Release*, **22**, 69-74.

226. Salmi,P., Sproat,B.S., Ludwig,J., Hale,R., Avery,N., Kela,J., and Wahlestedt,C. (2000) Dopamine D_2 receptor ribozyme inhibits quinpirole-induced stereotypy in rats. *European Journal of Pharmacology*, **388**, R1-R2.

227. Saltzman,W.M., Mak,M., Mahoney,M.J., Duenas,E.T., and Cleland,J.L. (1999) Inracranial delivery of recombinant nerve growht factor: release kinetics and protein distribution for three delivery systems. *Pharmaceutical Research*, **16**, 232-240.

228. Sambrook,J., Fritsch,E.F., and Manniatis,T. (2002) *Molecular cloning: A laboratory Manual.* Cold Spring Harbour Laboratory Press, Cold Spring Harbour, NY, USA.

229. Sandberg,J.A., Parker,V.P., Blanchard,K.S., Sweedler,D., Powell,J.A., Kachensky,A., Bellon,L., Usman,N., Rossing,T., Borden,E., and Blatt,L.M. (2000) Pharmacokinetics and tolerability of an antiangiongenic ribozyme (ANGIOZYME) in healthy volunteers. *Journal of Clinical Pharmacology*, **40**, 1462-1469.

230. Scherr,M., LeBon,J., Castanotto,D., Cunliffe,H.E., Meltzer,P.S., Ganser,A., Riggs,A.D., and Rossi,J. (2001) Detection of antisense and ribozyme accessible sites on native mRNAs: Application to NCOA3 mRNA. *Molecular Therapy*, **4**, 454-460.

231. Scherr,M. and Rossi,J. (1998) Rapid determination and quantitation of the accessibility to native RNAs by antisense oligodeoxynucleotides in murine cell extracts. *Nucleic Acids Research*, **26**, 5079-5085.

232. Scott,W.G. and Klug,A. (1996) Ribozymes: structure and mechanism in RNA catalysis. *TIBS*,220-224.

233. Shelburne,C.P. and Huff,T.F. (1999) Inhibition of kit expression in P815 mouse matocytoma cells by a hammerhead ribozyme. *Clinical Immunology*, **93**, 46-58.

234. Shimaya,T., Nishikawa,S., and Taira,K. (1995) Generality of the NUX rule: Kinetic analysis of the results of systematic mutations in the trinucleotide at the the cleavage site hammerhead ribozymes. *Biochemistry*, **34**, 3649-3654.

235. Shimayama,T., Nishikawa,M., and Taira,K. (1993) Nuclease resistant chimeric ribozymes containing deoxynucleotides and phosphorothioates linkages. *Nucleic Acids Research*, **21**, 2605-2611.

236. Shoji,Y., Akhtar,S., Periasamy,A., Herman,B., and Juliano,R.L. (1991) Mechanism of cellular uptake of modified oligodeoxynuleotides containing methylphosphonate linkages. *Nucleic Acids Research*, **19**, 5543-5550.

237. Sigurdsson,S.T. and Eckstein,F. (1995) Structure-function relationships of hammerhead ribzoymes:from undertanding to applications. *TIBTECH*, **13**, 286-289.

238. Sioud,M. and Leirdal,M. (2000) Therapeutic RNA and DNA enzymes. *Biochemical Pharmacology*, **60**, 1023-1026.

239. Sioud,M., Natvig,J.B., and Forre,O. (2002) Preformed ribozyme destroys tumour necrosis factor mRNA in human cells. *Journal of Molecular Biology*, **223**, 831-835.

240. Smith, D. L. CNS delivery of antisense oligodeoxynucleotides using biodegradable microspheres. 50-50. 2000. Aston University.

241. Sohail,M., Akhtar,S., and Southern,E.M. (1999) The folding of large RNAs studied by hybridisation to arrays of complementary oligonucleotides. *RNA*, **5**, 646-655.

242. Sommer,W., Rimmondi,R., O'Connor,W., Hannsson,A., Ungerstedt,U., and Fuce,K. (1996) Intrastrially injected c-fos antisense oligonucleotide interferes with striatonigral but not striatopallidal GABA transmission in the conscious rat. *Proc.Natl.Acad.Sci.USA*, **93**, 14134-14139.

243. Spenlehauer,G., Vert,M., Benoit,J.P., and Boddaert,A. (1989) In vitro and in vivo degradation of poly(D,L-lactide/glycolide) type microspheres made by solvent evaporation method: Morphology and release characteristics. *Biomaterials*, **10**, 557-563.

244. Sporn,M.B. and Robert,A.B. (1985) Autocrine growth factors and cancers. *Nature*, **313** , 745-747.

245. Stein,C.A. (1996) Exploiting the potential of antisense: beyond phosphorothioate oligdeoxynucleotides. *Chemistry & Biology*, **3**, 543-584.

246. Stein,C.A., Tonkinson,J.L., Zhang,L.M., Yakubov,L.A., Gervasoni,J., Taub,R., and Rottenberg,S.A. (1993) Dynamics of the internalization of phosphodiester oligodeoxynucleotides in HL60 cells. *Biochemistry*, **32**, 4855-4861.

247. Su,J., Fukuda,N., Hu,W., and Kanmatsuse,K. (2000) Ribozyme to human TGF-Beta 1 mRNA inhibits the proliferation of human vascular smooth muscle cells. *Biochemical and Biophysical Research Communications*, **278**, 401-407.

248. Sullenger.B.A. and Cech,T.R. (1994) Ribozyme-mediated repair of defective mRNA by targeted , trans-splicing. *Nature*, **371**, 619-622.

249. Sullivan,S.M. (1994) Development of ribozymes for gene therapy. *The journal of Investigative Dermatology*, **100**, 85s-89s.

250. Sun,L.Q., Cairns,M.J., Saravolac,E.G., Baker,A., and Gerlach,W.L. (2000) Catalytic nucleic acid: from lab to applications. *Pharamcological Reviews*, **52**, 325-347.

251. Symons,R.H. (1992) Small catalytic RNAs. *Annual review of Biochemistry*, **61**, 641-671.

252. Symons,R.H. (1994) Ribozymes. *Curr.Opin.Struct.Biol.*, **4**, 322-330.

253. Tabler,M., Homann,M., Tzortzakaki,S., and Sczakiel,G. (1994) A three nucleotide helix I is sufficient for full activity of a hammerhead ribozyme: Advanatages of an asymmetric design. *Nucleic Acids Research*, **22**, 3958-3965.

254. Tamargo,J.R. and Brem,H. (1992) Drug delivery to central nervous system: a review. *Neurosurgery*, **2**, 259-279.

255. Tanabe, T., Kuwabara, T., Warashina, M., Tani, K., Taira, K., and Asano, S. Oncogene inactivation in a mouse model. Nature 406, 473-474. 2000.

256. Tanaka,K., Yamada,T., Ohyagi,Y., Asahara,H., Horiuchi,I., and Kira,J. (2001) Suppression of transthyretin expression by ribozymes: a possible therapy for familial amyloidotic polyneuropathy. *Journal of the Neurological Sciences*, **183**, 79-84.

257. Tanner, N. K. Ribozymes: the characteristics and properties of catalytic RNAs. FEMS Microbiology Reviews 23, 257-275. 1999.

258. Tari,A.M. (2000) Preparation and application of liposome-incorporated oligodeoxynucleotides. *Methods Enzymol.* , **313**, 372-388.

259. Tavitian,B., Terrazzino,S., Kuhnast,B., Marzabal,S., Stettler,O., Dolle,F., Deverre,J.R., Jobert,A., Hinnen,F., Bendriem,B., Crouzel,C., and Di Giamberardino,L. (1998) *In vivo* imaging of oligonucleotides with positron emission tomography. *Nature Medicine*, **4**, 467-471.

260. Taylor,N.R., Kaplan,B.A., Swiderski,P., Li,H., and Rossi,J. (1992) Chimeric DNA - RNA hammerhead ribozymes have enhanced in vitro catalytic efficiency and increased stability in vivo. *Nucleic Acids Research*, **20**, 4559-4565.

261. Teng,J., Fukuda,N., Hu,W., Nakayama,M., Kishioka,H., and Kanmatsuse,K. (2000) DNA-RNA chimeric hammerhead ribozyme to transforming growth factor-β_1 mRNA inhibits the exaggerated growth of vascular smooth muscle cells from spontaneously hypertensive rats. *Cardiovascular Research*, **48**, 138-147.

262. Thies,C. and Bissery,M.C. (2002) Biodegradable microspheres for parenteral administration. In Lim,F. (ed.) *Biomedical applications of microencapsulation.* CRC Press, Florida, pp 53-74.

263. Thybusch-Bernhardt,A., Aigner,A., Beckmann,S., Czubayko,F., and Juhl,H. (2001) Ribozyme targeting of HER-2 inhibits pancreatic cancer cell growth in vivo. *European Journal of Cancer*, **37**, 1688-1694.

264. Tonkinson,J.L. and Stein,C.A. (1994) Patterns of intacellular compartmentalization, trafficking and acidification of 5'-fluorescein labeled phosphodiester and phosphorothioate oligodeoxynucleotides in HL60 cells. *Nucleic Acids Research*, **22**, 4268-4275.

265. Trang,P., Kilani,A., Lee,J., Hsu,A., Liou,K., Kim,J., Nassi,A., Kim,K., and Liu,F. (2002) RNaseP ribozymes for the studies and treatment of human cytomegalovirus infections. *Journal of Clinical Virology*, **25**, S63-S74.

266. Troy,C.M., Greene,L.A., and Shelanski,M.L. (1992) Neurite outgrowth in peripherin depleted PC12 cells. *Journal of Cell Biology*, **117**, 1085-1092.

267. Tsuchida,T., Kijima,H., Oshika,Y., Tokunaga,T., Abe,Y., Yamazaki,H., Tamaoki,N., Ueyama,Y., Scanlon,K.J., and Nakamura,M. (1998) Hammerhead ribozyme specifically inhibits mutant K-ras mRNA of human pancreatic cancer cells. *Biochemical and Biophysical Research Communications*, **253**, 368-373.

268. Tsuchihashi,Z., Khosla,M., and Herschlag,D. (1993) Protein enhancement of hammerhead ribozyme catalysis. *Science*, **262**, 99-102.

269. Tsukioki,K., Suzuki,J., Fujimori,M., Wada,Y., Yamauro,K., Ito,K., Morishita,R., Kaneda,Y., Isobe,M., and Amano,J. (2002) Expression of matrix metalloproteinases in cardiac allograft vasculapothy and its attenuation by anti MMP-2 ribozyme gene transfection. *Cardiovascular Research*, **56**, 472-478.

270. Tuschl,T. and Eckstein,F. (1993) Hammerhead ribozymes: Importance of stem-loop II for activity. *Proceedings of the National Academy of Sciences of the United States of America*, **90**, 6991-6994.

271. Tuschl,T., Golkhe,C., Jovin,T., Westhof,E., and Eckstein,F. (1995) A three dimensional model of for the hammerhead ribozyme based on fluoresence measurements. *Science*, **266**, 785-789.

272. Uhlenbeck,O.C. (1987) A small catalytic oligoribonucleotide. *Nature*, **328**, 596-600.

273. Usman,N. and Cedergren,R. (1992) Exploiting the chemical synthesis of RNA. *Trends in Biochemical Sciences*, **17**, 334-339.

274. Usman,N. and Stinchcomb,D.T. (1996) Design, synthesis and function of therapeutic hammerhead ribozymes. *Nucleic Acids Molecular Biology*, **10**, 243-264.

275. Usman, Nassim and Blatt, Lawrence. M. Nuclease-resistant synthetic ribozymes: developing a new class of therapeutics. The Journal of Clinical Investigation 106, 1197-1202. 2000.

276. Vert,M., Mauduit,J., and Li,S. (1994) Biodegradation of PLA/GA polymers: increasing complexity. *Biomaterials*, **53**, 85-92.

277. Veziers,J., Lesourd,M., Jollivet,C., Montero-Menei,C., Benoit,J.P., and Menei,P. (2001) Analysis of brain biocompatibilty of drug-releasing biodegradable microspheres by scanning and transmission electron microscopy. *Journal of Neurosurgery*, **95**, 489-494.

278. Wada,R., Hyon,S., and Ikada,Y. (1991) Salt formation of lactic acid oligomers as matrix for sustained release of drugs. *Journal of Pharmacy and Pharmacology*, **43**, 605-608.

279. Wagner,R.W. (1994) Gene inhibition using antisense oligodeoxynucleotides. *Nature*,333-335.

280. Walker,I., Irwin,W.J., and Akhtar,S. (1995) Improved cellular delivery of antisense oligonucleotides using transferrin receptor antibody-oligonucleotide conjugates. *Pharmaceutical Research*, **12**, 1548-153.

281. Walter,N.G. and Burke,J.M. (1998) The hairpin ribozyme: structure, assembly and catalysis. *Current Opinion in Chemical Biology*, **2**, 24-30.

282. Wang,C., Tsai,L., Tsao,Y., Hsieh,J., Chien,W., Liao,C., Wang,H., Liu,H., and Chen,S. (2002) Recombinant adenovirus encoding H-ras ribozyme induces apoptosis in laryngeal cancer cells through caspase- and mitochondria-dependent pathways. *Biochemical and Biophysical Research Communications*, **298**, 805-814.

283. Wang,H.T., Palmer,H., Lindardt,R.L., Flanagan,D.R., and Schmitt,E. (1990) Degradation of polyester microspheres. *Biomaterials*, **11**, 679-685.

284. Wang,P.P., Frazier.J., Brem,H. (2002) Local delivery to the brain. *Advanced Drug Delivery Reviews*, **54**, 987-1013.

285. Westphal,M., Delavault,P., Hilt,D., Olivarus,R., Belin,V., Daumas-Duport,C. (2000) Placebo controlled multicentre double-blind randomized prospective phase III trial of

local chemotherapy with biodegradable carmustine implants (Gliadel™) in 240 patients with malignant gliomas: final results, Abstract. *Neuro-Oncol*, **2**, 301.

286. Whitesell,L., Geselowitz,D., Chavany,C., Fahmy,B., Walbridge,S., Alger,J.R., and Neckers,L.M. (1993) Stability, clearance and disposition of intraventricularly administered oligodeoxynucleotides: Implications for therapeutic application within the central nervous system. *Proc.Natl.Acad.Sci.USA*, **90**, 4669.

287. Wincott,F.E., DiRenzo,A., Shaffer,C., Grimm,S., Tracz,D., Workman,C., Sweedler,D., Gonzalez,C., Scaringe,S., and Usman,N. (1995) Synthesis, deprotection, analysis and purification of RNA and ribozymes. *Nucleic Acids Research*, **23**, 2677-2684.

288. Wong,A.J., Zoltick,P.W., and Moscatello,D.K. (1994) The molecular biology and molecular genetics of astrocytic neoplasms. *Seminars in Oncology*, **21**, 139-148.

289. Wu-pong,S., Weiss,T.L., and Hunt,C.A. (1992) Antisense c-*myc* oligonucleotide cellular uptake. *Pharmaceutical Research*, **9**, 1010-1017.

290. Wu-pong,S., Weiss,T.L., and Hunt,C.A. (1994) Calcium dependent cellular uptake of a c-myc antisense oligonucleotide. *Cellular and Molecular Biology*, **40**, 843-850.

291. Wuthrich,P., Ng,S.Y.R.R.V., and Heller,J. (1992) *Journal of Controlled Release*, **21**, 191.

292. Xing,Z. and Whitton,J.L. (1992) Ribozymes which cleave arenavirus RNAs: identification of susceptible target sites and inhibition by target site secondary structure. *Journal of Virology*, **66**, 1361-1369.

293. Xu,R., Liu,J., Chen,X., Xu,F., Xie,Q., Yu,H., Guo,Q., Zhou,X., and Jin,Y. (2001) Ribozyme-mediated inhibition of caspase-3 activity reduces apoptosis induced by 6-hydroxydopamine in PC12 cells. *Brain Research*, **899**, 10-19.

294. Yang,J.H., Usman,N., Chartrand,P., and Cedergren,R. (1992) Minimum ribonucleotide requirement for catalysis by the RNA hammerhead domain. *Biochemistry*, **31**, 5005-5009.

295. Yee,F., Ericson,H., Reis,D.J., and Wahlestedt,C. (1994) Cellular uptake of intracerebroventricular administered biotin- or digoxigenin-labeled antisense oligodeoxynucleotides in the rat. *Cell and Molecular Neurobiology*, **14**, 475-486.

296. Yokoyama,Y., Takahasi,Y., Shinohara,A., Wan,X., Takahashi,S., Niwa,K., and Tamaya,T. (2000) The 5'-end of hTERT mRNA is a good target for hammerhead ribozyme to suppress telomerase activity. *Biochemical and Biophysical Research Communications*, **273**, 316-321.

297. Yokoyama,Y., Wan,X., Takahasi,Y., Shinohara,A., Liulin,T., and Tamaya,T. (2002) Divalent hammerhead ribozyme targeting template region of human telomerase RNA has potent cleavage activity, but less inhibitory activity on telomerase. *Archives of Biochemistry and Biophysics*, **405**, 32-37.

298. Yoshikawa,H., Nakao,Y., Takada,K., Muranishi,S., Wada,R., Tabat,Y., Hyom,S.H., and Ikada,Y. (1998) Targeted and sustained delivery of aclarubicin to the lymphatics by lactic acid oligomer microspheres in rat. *Chemistry and Pharmacy Bulletins.*, **37**, 802-804.

299. Yoshioka,S., Aso,Y., and Kojima,S. (1995) Drug release from poly(dl-lactide) microspheres controlled by γ-irradiation. *Journal of Controlled Release*, **37**, 263-267.

300. Yu,Q., Pecchia,D., Kingsley,S., Heckman,J.E., and Burke,J.M. (1998) Cleavage of highly structured viral RNA molecules by combinatorial libraries of hairpin ribozymes. *Journal of Biological Chemistry*, **73**, 5381-5387.

301. Zamel,R. and Collins,R.A. (2002) Rearrangement of substrate secondary structure facilitates binding to the *Neurospora* VS ribozyme. *Journal of Molecular Biology*, **324**, 903-915.

302. Zhang,X., Yamado,R., Shimaya,T., Imada,K., and Hattori,T. (1996) Phosphorothioate ribozyme against the conserved sequence in V3 loop of HIV-1. *Biochemical and Biophysical Research Communications*, **229**, 466-471.

303. Zhao,J.J. and Lemke,G. (1998) Selective disruption of neuregulin-1 function in vertebrate embryos using ribozyme-tRNA transgenes. *Development*, **125**, 1899-1907.

304. Zhao,Q., Matson,S., Herrera,C.J., Fisher,E., Yu,H., and Krieg,A.M. (1993) Comparison of cellular binding and uptake of antisense phosphodiester, phosphorothioate and mixed phosphorothioate and methylphospnate oligonucleotides. *Antisenes Research and Development*, **3**, 53-66.

305. Zoumadakis, M. and Tabler, M. Comparative analysis of cleavage rates after systematic permutation of the NUX consensus target motif for hammerhead ribozymes. Nucleic Acids Research 23(7), 1192-1196. 1995.

306. Zuker,M. (1989b) On finding all suboptimal foldings of an RNA molecule. *Science*, **244**, 48-52.

307. Zuker,M. (1989a) Prediction of RNA secondary structure by energy minimisation. *Methods in Molecular Biology (Clifton, N.J.)*, **25**, 267-294.

APPENDIX

LIST OF PUBLICATIONS

1. **Nawaz, Q**. and Akhtar, S. (2000) Evaluation and characterisation of biodegradable Polylactide-co-glycolide microspheres for sustained release of ribozymes. *Journal of Pharmacy and Pharmacology*, **52**, 28

2. **Nawaz, Q**. and Akhtar, S. (2001) Comaparison and characterisation of ribozyme uptake in cultured neuronal and glial cells. *28th Annual Meeting and Exposition of the Controlled Release Society,* San Diego, California.

3. Hughes, M.D., Hussain, M., **Nawaz, Q.**, Sayyed, P. and Akhtar, S. (2001) The cellular delivery of antisense oligonucleotides and ribozymes. *Drug Discovery Today*, **6**, 303-315.

4. Akhtar, S., Hughes, M.D., Khan, A. Bibby, M., Hussain, M., **Nawaz, Q**., Double, J., Sayyed, P. (2000) The delivery of antisense therapeutics. *Advanced Drug Delivery Reviews*. **44**, 3-21.